# THE MAGNETIC DEPOSITION RECORD IN SOME SCANDINAVIAN PEAT PROFILES

Thesis submitted in accordance with the requirements of the University of Liverpool for the degree of Doctor in Philosophy, by

Mervyn David Hywel Jones
May, 1986

# THE MAGNETIC DEPOSITION RECORD IN SOME SCANDINAVIAN PEAT PROFILES

M.D.H. JONES

**Abstract**

This study uses a range of magnetic parameters, eg. Susceptibility (X), Saturation Isothermal Remanence (SIRM), Anhysteretic Remanence (ARM), interparametric ratios (ARM/X, SIRM/X, SIRM/ARM) and coercivity of remanence data ($IRM_{-n}$/SIRM, $(B_0)_{CR}$), coupled with various dating methods (eg. moss increment counting and radiometric dating) to estimate the magnetic deposition onto some Scandinavian peat bogs. The sites available included 4 from southern Finland, 5 from northern Finland, 2 from northern Norway and 1 from southern Denmark. In addition to the magnetic techniques, a range of chemical determinations (iron, copper, zinc, lead, nickel and, where available, manganese) have been made, or are utilised, for all the peat cores.

The reproducibility of the primary magnetic deposition record at Kaurastensuo, southern Finland has been examined. The rise in magnetic particulate concentrations, termed the magnetic 'take-off', was consistently dated to about 1931 for 7 of the 8 cores used, regardless of hummock-hollow microtopography.

The persistence of magnetic minerals over timescales of $10^1$-$10^3$ years has been examined by means of long core profiles from 4 southern Finnish bogs. The mineral magnetic and heavy metal profiles (iron, copper, zinc, lead and nickel) were in reasonable accord with the development of the individual bogs above different mineral soils. The development of peat profiles is dated from between 8000-9000 years BP using $^{14}C$ dates spanning both the ombrotrophic and minerotrophic phases.

The availability of moss increment counts for the northern Scandinavian sites and $^{210}Pb$ determinations for Draved Moss, southern Denmark and Mo-I-Rana, northern Norway, has allowed estimates of variation in the magnetic deposition to be made. The northern Scandinavian sites all show increasing deposition from 1900, although maximum surface deposition varies from site to site, between 1.24-22.6 $10^{-6}Am^2yr^{-1}$. The magnetic deposition at Draved Moss was estimated to be 21.6 $10^{-6}Am^2yr^{-1}$ at a sub-surface maximum dated to between 1967-1978. The increase in lead deposition at Draved Moss is in reasonable agreement with that of published lead deposition profiles from the same site, using earlier attempts at $^{210}Pb$ determinations. At Mo-I-Rana, northern Norway, the maximum magnetic deposition value is estimated to be 8.65 $10^{-6}Am^2yr^{-1}$ for the surface slice, spanning the last 21 years.

Any spatial variation in deposition within the Scandinavian sites appears to be partly masked by site-specific features, for example the close proximity of industrial sources at 2 of the Finnish sites and the iron and steel works at Mo-I-Rana. Magnetic deposition at the latter site is in good agreement with the history of iron and steel production within the region since the turn of the century.

# CONTENTS

Page No.

## Tables

(contd...)

## Figures

(contd...)

(contd...)

(contd...)

## Plates

## Acknowledgements

There is inevitably a large number of people to whom I owe my thanks for their encouragement and advice throughout my research. I am especially grateful to Prof. F. Oldfield for his timely and well chosen comments.

Special thanks are due to my friends Harri Vasander and Mikko Liukkonen of the Department of Botany at Helsinki University for their help whilst in Finland, and to Kimmo Tolonen for the use of his data, both published and unpublished. Thanks are also due to Bent Aaby of the Danish Geological Survey for allowing me to core Draved Moss.

I owe much to the patience of Jenny Jones who has kindly donated much of her time to proof-read this thesis. Thanks are also due to my colleagues Nigel and Sandra for their assistance in the $^{210}Pb$ dating, Andrew Hunt for his SEM work, and Simon Robinson for invaluable assistance with XRD analysis.

I would also like to thank Ian and Suzanne for the photographic work, Sandra and Paul for cartographic advice and Ingrid for her scissors.

Finally, thanks are due to Pete, John and Richard for the occasional light sporting relief.

The work has been carried out whilst in receipt of a Liverpool University Postgraduate Scholarship. The fieldwork was carried out with the aid of sponsorship from: the Department of Geography, Liverpool University; the Violet Cressy Marcks-Fisher Travelling Scholarship Fund ; and the Maj and Tor Nessling Foundation.

## The Raised Bog

Ein Stamm ist es von ungeheurer Dicke;

Die langste Tanne misst die Dicke nicht;

Die Krone aber kurz, unglaublich kurz;

Der Dornstrauch uberschaut sie schon.

Vom Regen nur und Thau des himmels ist es ausgewachsen.

Die erde narht es nicht.

Und wenn das Wasser sonst den Abhang eilends flieht, -

Hier siehst du es auf Hoh'und Abhang weilen!

**Dau, J.H.C., 1823**

# 1. Introduction

## 1.1 Introduction

Peat is the accumulated remains of dead plants. Usually there is no clear break in the continuum between a mineral soil with organic matter in it, for example in the surface of a podsol, and an almost pure Sphagnum peat of which more than 99% is organic matter. Most peats contain less than 20% of unburnable inorganic matter, although some soil scientists allow up to 35% and industrial standards permit as much as 55% (Clymo, 1983).

Ombrotrophic bogs are those built up over periods of time above the groundwater table, so that the surface is remote from any ground or surface water influence. Under these conditions, the surface is nutrient deficient, relying exclusively on a supply of nutrients from the atmosphere via rainwater, snow and atmospheric fall-out (wet and dry deposition processes). These conditions of growth often afford an excellent opportunity for the preservation of a record of atmospheric deposition, and in recent years, the potential of such peat accumulation for the historical monitoring of pollutant deposition has been explored.

Chemical inputs to the ombrotrophic bog surface derive from natural and anthropogenic sources. Similarly, particulate inputs may also be broken down under these two main headings, with the advent of new technologies permitting the identification of iron oxides from fossil fuel combustion and other industrial processes. The accumulation of metals within the ecosystem to potentially toxic levels is almost exclusively a post-industrial legacy that has only recently been appreciated.

The use of depositional environments, for example lake sediments, peatlands and icefields for industrial monitoring, has become increasingly significant in recent decades, with the advent of an 'environmental impact

assessment philosophy' (Jones, 1985). The nature of such studies encompasses the understanding of the transfer of particulates and heavy metals within and between terrestrial ecosystems, the atmosphere and the hydrosphere (Hughes et al., 1980). The need to reconcile a multidisciplinary approach with a realistic range of variables is exemplified by Jones (op. cit.). The incorporation of mineral magnetic studies within the framework of historical pollution studies is an alternative being increasingly explored in the past decade.

This chapter provides the necessary methodological base upon which the subsequent work is based. The rationale for using the sites chosen in Scandinavia, primarily those in Finland and Denmark is a simple one. The sites in southern and northern Finland all have some form of recent chronological control available. The majority of cores have been dated by the Moss Increment Dating Method (Chapter 4, sub-section 4.2.2) by Dr. K. Tolonen of the University of Helsinki. Two further sites, Kaurastensuo and Laaviosuo are dated by means of growth rate equations from each site (Chapter 2, sub-section 2.2.4). The author gratefully acknowledges the provision of these data by the Department of Botany, University of Helsinki and Dr. K. Tolonen. The Danish site, Draved Moss, is dated by means of 210-Lead (Chapter 5, sub-section 5.2.3) for comparison with the 210-Lead data provided in Aaby et al. (1979).

## 1.2 Environmental Applications of Magnetic Measurements

The use of palaeomagnetic techniques concerned with the measurement of natural properties reflecting the Earth's magnetic field, for example natural remanent magnetisation (NRM), is well documented (cf. Thompson & Oldfield, in press). The measurement of remanent and non-remanent properties within lake sediments, peat cores, soils and

atmospheric particulates, is a recent innovation based on advances in instrument microelectronics (sub-section 1.7.1). Thompson et al. (1980) cite examples of environmental applications of magnetic measurements to problems in geophysics, meteorology, climatology, hydrology, limnology, oceanography, sedimentology, geomorphology, soil science, ecology and land-use studies. In view of previous reviews, for example Thompson et al. (op. cit.), Bloemendal (1982), Maher (1984) and Jones (1985), the outline of such applications in some of the major environmental contexts is deliberately brief.

### 1.2.1 Soil Studies

The study of soil magnetism was pioneered by Le Borgne (1955, 1960), who was the first to observe the phenomenon of magnetic enhancement within the surface layers of soils, as indicated by distinctly raised values of magnetic susceptibility. This work was taken up by the Russian school of soil magnetists,for example Vodyunitskiy (1981), who observed the apparent ordered variation of magnetic susceptibility within soil profiles. The characterisation of magnetically enhanced topsoils, typically consisting of mixtures of ultrafine (<0.03μm) and fine (0.03-0.05μm) grains, has been undertaken by Mullins (1977) and Longworth & Tite (1977). Mullins (op. cit.) provides a comprehensive review of the application of magnetic techniques to soil science up to that time.

The most recent studies of soil magnetic properties have derived from the application of magnetic measurements to environmental studies, for example, the magnetic characterisation of soils (Maher, op. cit.), the construction of source-sediment linkages in specific case studies (Olfdield et al., 1979c), and the association of different soil regimes and observed magnetic characteristics in studies of catchment-based particulate influx (Dearing, 1979; Rummery, 1981). Finally, quantitative identification of soil

magnetic mineralogies has been attempted by, for example Longworth & Tite (op. cit.) and Maher (op. cit.), who used Mössbauer analysis to independently assess the magnetic characteristics of soils.

### 1.2.2 Lake Sediment Studies

Lake sediments provide a natural record of the lake and catchment processes through time. The advent of increased dating resolution through techniques such as laminae counting and radiometric dating, has provided insights into process changes thus allowing inferences about the impact of human interference within the catchment.

The use of mineral magnetism in an environmental context, in contrast to a palaeomagnetic context, initially centred on the use of susceptibility measurements on long core profiles (Molyneux & Thompson, 1973). Subsequent work comprised the correlation of Holocene lake sediments from Lough Neagh by volume magnetic susceptibility. The synchroneity of the susceptibility-based correlations was independently confirmed by relative diatom frequency analysis (Thompson et al., 1975). Bloemendal (op. cit.) used this approach on sediments from Llyn Goddionduon, North Wales, further characterising the main horizons by detailed mineral magnetic and elemental analyses of key cores. A similar approach was used by Dearing (op. cit.) based on a detailed $^{210}Pb$ chronology.

Banerjee et al. (1981) extended the principle that SIRM/X can distinguish chemical species such as magnetite and haematite, and approached the problem of grain size variation in magnetite in some detail (cf. sub-section 1.5.6). By plotting susceptibility (abscissa) against anhysteretic remanent magnetisation, ARM (ordinate), for sediment samples comprising magnetite minerals, they demonstrated changes in average grain size by changes in the slope of the regression line. This

approach is similar to the use of ARM/X described in sub-section 1.6.4. A more recent example is the measurement of weakly diamagnetic sediments from Mirror Lake, USA (Oldfield & Appleby, 1984a). Inter-core correlations are used to identify sediment focussing and to reflect the changing types and impact of human activity within the catchment. Further examples of the sediment-based approach are cited in Thompson & Oldfield (op. cit.).

1.2.3 Atmospheric Studies

Less is known about the presence of magnetic minerals in the atmosphere than about their presence in any other major environmental system. Once the magnetic particles formed during combustion are emitted, they become incorporated in the local atmospheric aerosol mass. Their subsequent deposition depends on a variety of factors including particle size, meteorology and topography (Jones, op. cit.).

Until the comparatively recent introduction of direct methods of air sampling, for example the Hi-Vol air filters and particle cascade impactors, atmospheric particulates have been studied indirectly using lake sediments, peat cores and snow samples. Preliminary results given in Hunt et al. (1984) demonstrate that characterisation of power station and automotive emissions may be achieved by a combination of mineral magnetic tecniques, including isothermal remanence. Preliminary results from a study of oceanic dusts collected over Barbados suggested that they may be characterised by coercivity of remanence and isothermal remanence, into 'summer' and 'winter' groups (Jones, 1982). Subsequent work by Oldfield et al. (1985) extended this characterisation to other oceanic locations, allowing differentiation between those particulates of anthropogenic origin and those derived from deflation processes.

The work of Hunt (in prep.) concerned with the direct sampling of the atmosphere, suggests that the capacity to differentiate the magnetic

'fingerprint' of particulate emissions is of considerable value in pollution monitoring studies. The work of Jones (1985) observed the indirect approach by evaluating heavy metal and mineral magnetic linkages within the deposition at ombrotrophic peat sites in heavily industrialised areas (South Yorkshire) and more 'remote' sites (Cumbria and Central Scotland). Current research is in progress to evaluate the contribution of magnetic measurements in 'acid rain' situations.

1.2.4 Peat Studies

As mentioned in sub-section 1.2.3, peat studies are an indirect method of measuring the past mineral magnetic content of the atmosphere. Initial studies recorded the changes in atmospheric fall-out of magnetic particulates at sites in northern England (Oldfield et al., 1978a). The results demonstrated that the influx of these minerals has increased by 2 to 3 orders of magnitude since the beginnings of the widespread use fossil fuel in combustion processes associated with the start of the Industrial Revolution. In all cases, the maximum SIRM values came after the initial rise in values, often referred to as the 'take-off'. Subsequent work, for example Oldfield et al. (1979a) has examined the effects of microtopographical variations (hummock-hollow complexes) and changes in the vegetation cover on the mineral magnetic record. The hummock cores from Cumbrian peat sites all appeared to trap an order of magnitude more particles. Recent examples provided in Thompson & Oldfield (op. cit.) have revealed that this differential capacity between hummocks and hollows (or pools), is consistent throughout a range of sites in Britain and North America. The ability of magnetic measurements to discern variations in particle deposition as a result of changes in microtopography, may aid studies of the dynamics of particle deposition to vegetated surfaces (Jones, op. cit.).

Recent mineral magnetic studies in peat have been concerned with temporal variations in particulate pollution. Using a moss increment derived chronology Oldfield et al. (1981) estimated the magnetic deposition, as approximated by SIRM, in four southern Finnish sites. This work is examined in detail in Chapter 2.

### 1.2.5 Other Studies

Magnetic measurements have been carried out in numerous environmental situations to date. Among other areas is the enhancement of stream bedload material in hydrological studies. For example, Arkell et al. (1983) have observed the supply and transport of coarse sediments from an upland catchment in North Wales, using enhanced bedload material. Other studies, again related to atmospheric and peat studies, have evaluated linkages between the pollen record in peat and lake sediments and the mineral magnetic record. Richardson (1986) has examined the relationships between critical pollen and magnetic horizons in an evaluation of human impact at sites in England and North America.

The role of mineral magnetics in other fields, such as archaeology, has become increasingly important in recent times. The role of magnetic measurements in archaeological surveys has been noted by Mullins (1974) and Oldfield et al. (1984) with specific reference to the enhancement of topsoils by localised burning, for example hearths and burnt ramparts.

## 1.3 Sources of Magnetic Minerals in the Atmosphere

Within the time-space continuum the atmosphere consists of a heterogenous mix of gases and particulates derived from a number of sources. Variations in the relative proportions of the atmospheric constituents differ at local, regional and global scales. Removal of particulates from the atmosphere is a function of meteorological

conditions, particle size and height of injection. Meteorological conditions determine the form of removal or deposition, for example dry deposition (sedimentation, impaction and diffusion) or wet deposition (rain-out and wash-out), as well as determining the atmospheric residence time along with the particle size and height of injection. For example, large particles (>10μm) are subject to rapid sedimentation and hence short atmospheric residence times, whilst smaller particles respond to local turbulence, and therefore, are subject to extended transport mechanisms, and longer residence times.

The magnetic minerals in the present day atmosphere may be divided into two broad groups: **natural** and **anthropogenic.** According to Thompson & Oldfield (op. cit.) these two groups comprise four main sources at global regional and local scales. The sources are **volcanic eruptions, wind erosion, industrial** and **combustion** processes and finally, **extra-terrestrial** particles.

Magnetic measurements of lake and marine sediments in volcanic areas show that tephra layers incorporated into the sediments are often marked by peaks in magnetic suceptibility, especially with basic tephra, rich in ferro-magnesium minerals (Thompson & Oldfield, op. cit.). Deposition of volcanic dusts occurs at all scales, depending on particle size. Volcanic sources contribute a significant proportion to the total particulate content of the atmosphere, and more specifically, to the stratosphere, in particular the Junge Aerosol Layer at about 20-25km altitude. The long residence time of sub-micron particles in both the troposphere and stratosphere has led to the estimation of the Dust Veil Index, the density of which is known to have varied over time (eg. Lamb, 1970). Deposition of volcanic dusts is thought by some authors to be a major contributor to the magnetic mineral assemblages in deep sea sediments (cf. Thompson & Oldfield, op. cit.).

A second natural source is wind erosion, providing significant loadings of the atmosphere at the local scale and occasionally regional and global scales. Soil magnetic studies (eg. Mullins, 1977) have noted the strong ferrimagnetic nature of surface soils as a result of enhancement mechanisms such as fire, which is also a significant factor in wind erosion. Particles formed by attrition are usually quite large with diameters >1μm, therefore, residence time in the atmosphere is short and deposition close to the source. The natural dust loadings in the lower atmosphere over the Atlantic, as a result of deflation, are a significant contributor to the dusts over Barbados (Oldfield et al., 1985). These natural processes of deflation have been increased in recent times by increased pressure on the land through human activity. One example on the local scale is the increase in mechanised cultivation leading to greater 'field' erosion and increases in the inorganic content of local peat formations (eg. Vuorela, 1983; Tolonen, 1984). On an increased timescale and over global scales, loess deposits suggest that the pattern of Pleistocene climatic change have been important in controlling the exposure of fine surface materials to wind erosion and the atmospheric transport of deflation products. Jones (op. cit.) gives a detailed review of the contribution of wind erosion to the global heavy metal cycles of copper, nickel, zinc and lead.

The main atmospheric sources of anthropogenic particulates are threefold: fossil fuel combustion (coal and oil) for power generation and automobiles, iron and steel manufacture, and non-ferrous metal smelting. These come under the 'umbrella' of industrial and combustion processes. The increase in spherule concentrations since the beginning of the Industrial Revolution is referred to in sub-section 1.2.4.

The final source of magnetic particulates in the atmosphere is the contribution of extra-terrestrial particles. The significance of this source

is only likely to become important on a local scale, associated with meteorites, and in those areas remote from any form of terrigenous input, for example the Central Pacific. Evidence cited by Jones (op. cit.) suggests that dusts of meteoric origin contain high concentrations of nickel. These dusts are estimated to have an atmospheric residence time of about two years and a global surface contribution of approximately $1.4 \times 10^7$ tons annually. Other minor sources of contribution include the localised loadings from forest fires.

## 1.4 Magnetic Mineral and Heavy Metal Linkages

The term 'heavy metal' is used throughout this study to describe the elements iron, copper, nickel, lead and zinc collectively. The term derives from those elements whose specific gravity is greater than 4 or 5. The present study follows the definition most frequently applied in ecological studies, and includes those elements with a specific gravity of greater than 5. The five elements listed above, and additionally manganese, all have specific gravities greater than 7.

Within studies of the anthropogenic component of atmospheric particulates there is growing evidence that the deposition of heavy metals and fly ash particles are linked. Trace elements within coal, for example, may account for 2-40% of the total weight, although a content of 5-15% is more common (Jones, op. cit.). The products of fossil fuel combustion include enriched heavy metals such as cadmium, chromium, nickel, lead and zinc (eg. Davison et al., 1974) and also magnetic spherules (eg. Griffin & Goldberg, 1981; McCrone & Delly, 1973). The emissions from electric powered steel furnaces include chromium, lead, copper, zinc and manganese, which were preferentially enriched on particle surfaces (Van Craen et al., 1983), whilst the particulate emissions from an iron foundry

were found to contain magnetic spherules (Puffer et al., 1980). This indirect evidence, by association, is discussed in more detail in Chapter 5, section 5.6.

Recent research has also indicated a more direct link between particulate form and elemental enrichment. For example, in terms of enrichment on fly ash particles, Davison et al. (op. cit.) have noted that certain trace elements increase in specific concentration with decreasing particle size in particles emitted to the atmosphere from high temperature combustion or conversion processes. Cadmium, chromium, nickel, lead and zinc among others, all showed pronounced concentration trends with particle size, whilst iron, among others, showed limited concentration trends.

Hulett et al. (1980) observed that chromium, copper, manganese, nickel, vanadium and zinc were concentrated in the magnetic phase of coal fly ash from several power stations. The authors concluded that these elements were probably in the form of substituted spinels, $Fe_{3-n}M_nO_4$.

In urban studies, authors have separated dusts and urban soils into magnetic and non-magnetic fractions. The evidence from these studies (eg. Linton et al., 1980) suggests that lead in particular is concentrated in high density magnetic particles especially in kerb-side samples. The implication here is that the magneto-chemical association was a function of automotive sources, for example the tetraethyl-lead additives found in high octane fuels.

It is acknowledged that these are just a few examples of the growing body of research on anthropogenic particulate form and chemical composition. The examples do, however, illustrate that there is substantial evidence which suggests that during combustion processes iron oxides and heavy metals may become associated. A comprehensive outline of the

theories of formation, trace element composition and enrichment in the magnetic fraction is given in Jones (op. cit.).

## 1.5 Concepts of Mineral Magnetism

### 1.5.1 Mineral Magnetism

Since rocks consist of mineral grains and crystals, their magnetisation arises from those mineral constituents present which are measurably magnetic. These magnetic mineral constituents often represent only a few percent of the total rock. Since it is this small proportion and its physico-chemical state which determines bulk magnetic properties and magnetisation, there are two consequences. The first is that magnetic properties can be quite variable within a given rock body or structure due to chemical inhomogeneity, depositional or crystalline conditions and post-formational geologic history (Carmichael, 1982). The second consequence is that the magnetic characteristics are not necessarily closely predictable by the lithology, because it is the minor fraction, commonly iron oxides, which control magnetisation. When the gross mineralogy of the rock is broken down into its constituents by, for example deflation, particle-size influences and sorting occur in the atmospheric transport and sediment deposition in the case of the latter can become less important in an environmental context.

'Mineral magnetism' is the term given to the investigation of inherent magnetic mineralogy and granulometry of natural samples, as distinct from the more established fields of rock magnetism and palaeomagnetism. It may be summarised briefly as the investigation of magnetic mineralogies, concentrations and grain sizes in natural samples by the measurement of both their in-field and remanent response to a series of externally applied and artificially induced magnetic fields. Most of the mineral magnetic

parameters are, however, derived from palaeo- and rock magnetic studies (section 1.6). The mineral magnetic approach is based on well-established but newly applied physical principles.

The following three sub-sections outline the basic types of intrinsic magnetisation found within a lattice. Detailed reviews of the theory of rock magnetism may be found in, for example, Stacey & Banerjee (1974), O'Reilly (1976) and Carmichael (1982). Passing mention is made of the work of rock magnetists only where it is felt that this will aid the understanding of environmental mineral magnetism. The concept of magnetic hysteresis is briefly described in sub-section 1.5.5, and finally, the magnetic behaviour relating to effects of crystal size, shape and structure is outlined in sub-section 1.5.6. Superparamagnetism is one such effect. As it is also a form of intrinsic magnetisation, however, it is outlined along with diamagnetism and paramagnetism in the following sub-section.

### 1.5.2 Diamagnetism, Paramagnetism and Superparamagnetism.

**Diamagnetism** is a fundamental magnetic property present in all materials (Carmichael op. cit.). The effect is very weak and exists only in the presence of an applied field, hence it tends to be masked by all other types of magnetic behaviour. Diamagnetism arises from the interaction of an applied field with the orbital motion of electrons resulting in a net magnetic moment aligned in the opposite direction of the field. The result is a very weak negative magnetisation of the order $10^{-9}m^3kg^{-1}$. Diamagnetism is for all practical purposes independent of temperature. Naturally occurring minerals such as quartz, feldspar, calcite, and water exhibit diamagnetic behaviour. In addition, organic matter such as the peat/carbon matrix within peat bogs is known to exhibit diamagnetic behaviour.

**Paramagnetism** exists where the magnetic induction is slightly

greater than the externally applied magnetic field. There is a partial alignment of the atomic dipole moments to augment the net magnetisation in the direction of the applied field. Paramagnetism results from the electron spin of unpaired electrons. The effect is weak and exists only in the presence of an applied field. The resulting magnetic susceptibility is of the order $10^{-8}$-$10^{-9}m^3kg^{-1}$. Naturally occurring minerals known to exhibit paramagnetism include garnet, pyroxene, biotite, olivene and carbonates of iron and manganese.

**Superparamagnetism** is similar to, but much stronger than paramagnetic behaviour. It is exhibited by ultrafine ferro- or ferrimagnetic grains, about 0.001μm to 0.03μm in diameter, which exhibit thermal vibrations at room temperature. The co-operative alignment of atomic dipole moments of these grains are overcome by the disordering effect of thermal energy of the same magnitude as the magnetic energy. These ultrafine magnetic materials do not possess a stable remanent magnetisation or exhibit hysteresis as their magnetisation are continually undergoing thermal reorientation. In the presence of an applied field they will, however, possess an overall magnetic alignment or 'apparent' magnetisation. The susceptibility of superparamagnetic grains is much higher than that of an equivalent amount of mineralogically comparable stable single domain or multidomain grains. This means that the presence of a small proportion of superparamagnetic grains in a natural sample can have an important effect on its susceptibility.

### 1.5.3 Ferromagnetism

**Ferromagnetism** results when the atomic magnetic moments tend strongly to align parallel to one another because of exchange interaction energy, including when no external field is applied (Carmichael, op. cit.). Spontaneous or intrinsic magnetisation occurs because the moments are all

orientated in the same direction. This results in the ability to retain a remanent magnetisation.

Ferromagnets such as iron are characterised by magnetic properties with a long range interaction ordering of the moments that is lost at a critical temperature - the Curie temperature, $T_C$, due to thermal energy disorientation. Above the Curie temperature the material is paramagnetic, with the effect being strong and residual.

### 1.5.4 Ferrimagnetism and Antiferromagnetism

The main naturally occurring magnetic minerals encountered in environmental studies have been variants of ferromagnets, known as ferrimagnets, and imperfect antiferromagnets (Thompson & Oldfield, in press). **Ferrimagnetism** is essentially very similar to ferromagnetism, being difficult to distinguish between the two even using magnetic measuring techniques. Ferrimagnetism results when the atomic magnetic moments are antiparallel although an appreciable net magnetisation results. The magnetic sublattices do not have balancing moments, either because of unequal numbers of spins or unequal dipole moments. Ferrimagnetism is commonly exhibited by iron oxides, for example magnetite.

**Antiferromagnetism** occurs when the atomic magnetic moments assume an ordered antiparallel arrangement in the absence of an applied field, however, the magnetic moments are identical, so the material exhibits zero bulk intrinsic magnetisation. The susceptibility of antiferromagnets is comparable to that of paramagnetic materials.

A variant of antiferromagnetism is **spin-canted antiferromagnetism** which occurs when the antiparallel magnetic moments are deflected from the antiferromagnetic plane, resulting in a weak 'parasitic' magnetism. This magnetism disappears at the material's Curie temperature. An example of a spin-canted antiferromagnet is haematite.

On removal from an applied field, both ferrimagnets and antiferromagnets (including spin-canted variants) will retain a remanent magnetisation. Ferrimagnetic and (canted) antiferromagnetic materials may be characterised by the gradients in remanent magnetisation acquired through the application of increasingly stronger external fields - hysteresis.

### 1.5.5 Hysteresis

The majority of natural samples contain a mixture of magnetic mineral types within their assemblage. These vary in both mineralogy and magnetic granulometry. The resultant **hysteresis** is therefore a composite picture of magnetic response. Hysteresis is the increasing magnetisation of a sample with the increasing strength of an applied external field. Saturation magnetisation occurs when magnetisation no longer increases with the increase in applied field. A hysteresis loop is obtained by cycling the magnetic field from an extreme in one direction to an extreme in the opposite direction and back again.

Figure 1.1 taken from Bloemendal (1982) shows the hysteresis loop for an assemblage of randomly orientated ferrimagnetic grain sizes varying from ultrafine superparamagnetic grains (0.001-0.03μm) to coarse multidomain grains, >17μm (Stacey & Banerjee, 1974). The intensity of magnetisation (M) is plotted on the ordinate and the field strength ($B_0$) on the abscissa.

Some of the magnetic properties used in later chapters to characterise materials can be classed as hysteresis parameters and the inter-relationships between these properties may be best be understood in terms of hysteresis loops (fig. 1.1). There are five main parameters connected with the hysteresis loop. First is **Saturation Magnetisation,** $M_S$, the magnetisation induced in the presence of a large (ca.1T) magnetic field. On removal of this field the magnetisation follows the path marked

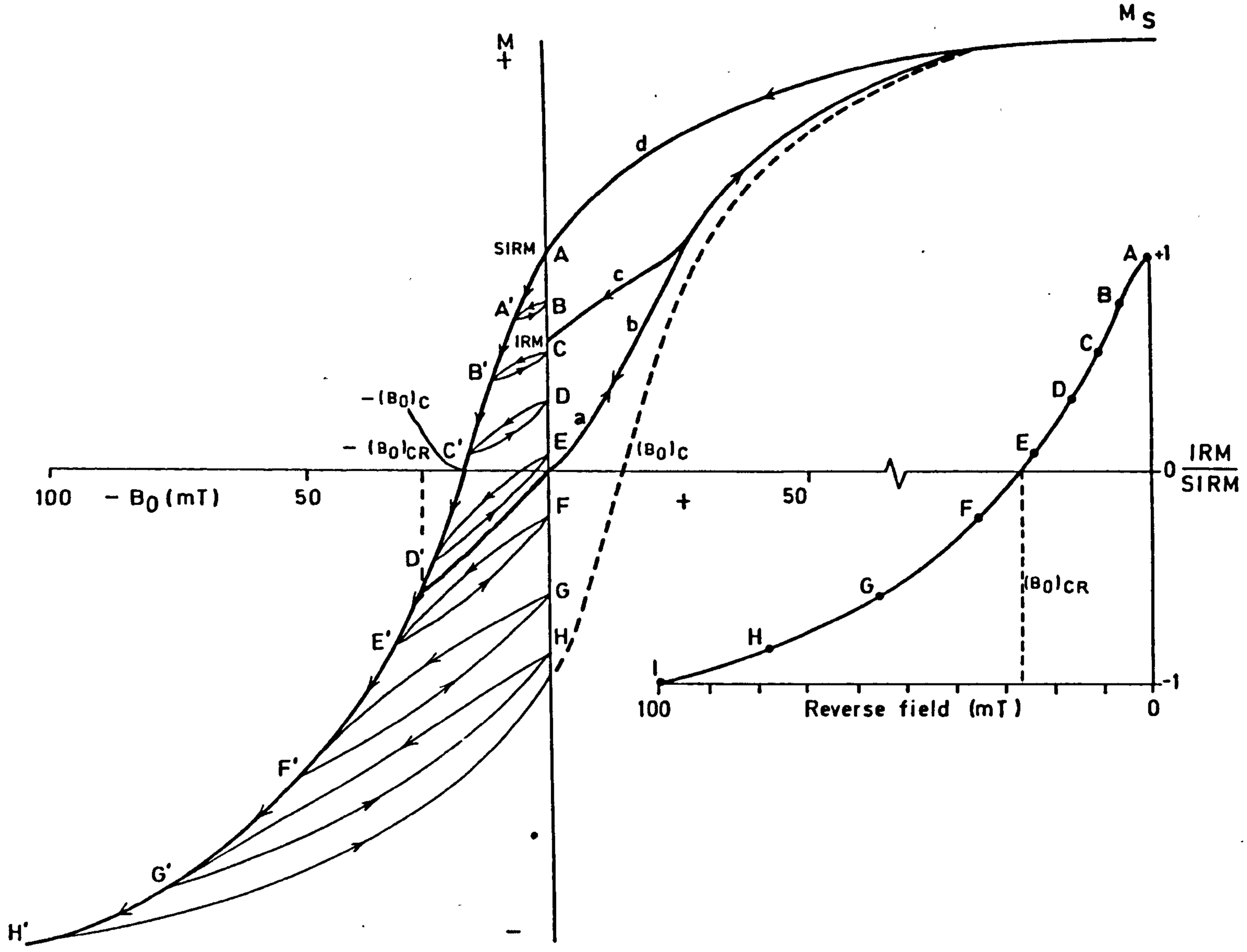


**Figure 1.1** The hysteresis loop. Showing the five main hysteresis parameters (see text for explanation). Inset: the coercivity of remanence curve produced from the reverse fields A-I (after Bloemendal, 1982).

'd' in fig. 1.1. The remanent magnetisation is termed **Saturation Isothermal Remanent Magnetisation,** SIRM, the second parameter. By the application of a reverse field, usually in a stepwise series, A-A'(B), B-B'(C)... (fig. 1.1), the induced magnetisation can be reduced to the point C' (fig. 1.1). The reverse field which actually produces this is the third parameter, called **Saturation Coercivity,** $(B_0)_C$. The fourth, the application of a larger field termed the **Coercivity of Remanence,** $(B_0)_{CR}$, leaves zero magnetisation when the sample is withdrawn from the field. Finally, the fifth is the initial (low field) reversible susceptibility which follows the path marked 'a' in fig. 1.1. Along this path, all the apparent in-field effects are reversible on withdrawal of the field ie. there is no remanent magnetisation. The gradient of the path 'a' gives the ratio between induced magnetisation and the intensity of the magnetising field, or the **Magnetic Susceptibility,** $\chi$, of the sample.

Hysteresis properties are closely related to composition and grain size, for example, Day et al. (1977) found no grain size dependence of hysteresis parameters ($(B_0)_C$ < 5mT) in coarse particles of titanomagnetite (>150μm). In contrast fine particles (ca.0.1μm) revealed systematic grain size dependence of parameters with $(B_0)_C$ as high as 200mT. The nature of grain size and domain theory is outlined in the following sub-section. A comprehensive description of the hysteresis loop and its related parameters is given in Bloemendal (op. cit.) and Thompson & Oldfield (op. cit.).

### 1.5.6 Magnetic Behaviour

Magnetic behaviour of minerals is governed to an extent by the effects of crystal size, shape and structure. Shape-related factors involve anisotropic effects which all materials possess, that is, the variation of magnetic properties within a sample with varying direction. Thompson & Oldfield (op. cit.) note three types: magnetocrystalline-, shape- and strain-

anisotropy.

The hysteresis properties of ferromagnets are largely related to the arrangements of magnetic domains. Consequently magnetic domains play an important role, along with anisotropy, in controlling the magnetic properties of natural magnetic materials (Dunlop, 1981). For example, increased magnetic 'hardness' may result from, among other things, the subdivision of grains to form monodomain regions (O'Reilly, 1976).

Domains and domain walls are present in magnetic grains, in an attempt to remain in a self-demagnetised state. When a large magnetic grain is magnetised, the internal demagnetising field, which is orientated opposite to the direction of the spins, produces a strong magnetostatic energy and a large external field. In an attempt to produce a state of lower total energy the grains may divide into domains. The number of domains and domain walls is controlled by establishing a balance between the various competing energies. The most advantageous balance is achieved by domains of about 1μm in size (Thompson & Oldfield, op. cit.).

An obvious control on domain status is volume since domains will not form in grains which have critical grain sizes too small to contain a domain wall. These grains are termed **single domain** as they only contain one domain. The magnetic properties of single domain grains are in marked contrast to **multidomain** grains since the domain wall motions play no part in their magnetisation cycle. The magnetic remanence of single domain grain assemblages is much higher and more stable than that of multidomain grain assemblages resulting in clear differences in the hysteresis properties (eg. Dunlop, 1969). The hysteresis loops of two extremes are presented in fig. 1.2, depicting the narrow loop of 'soft' magnetic materials, for example magnetite, and the wide loop of 'hard' magnetic materials, for example haematite.

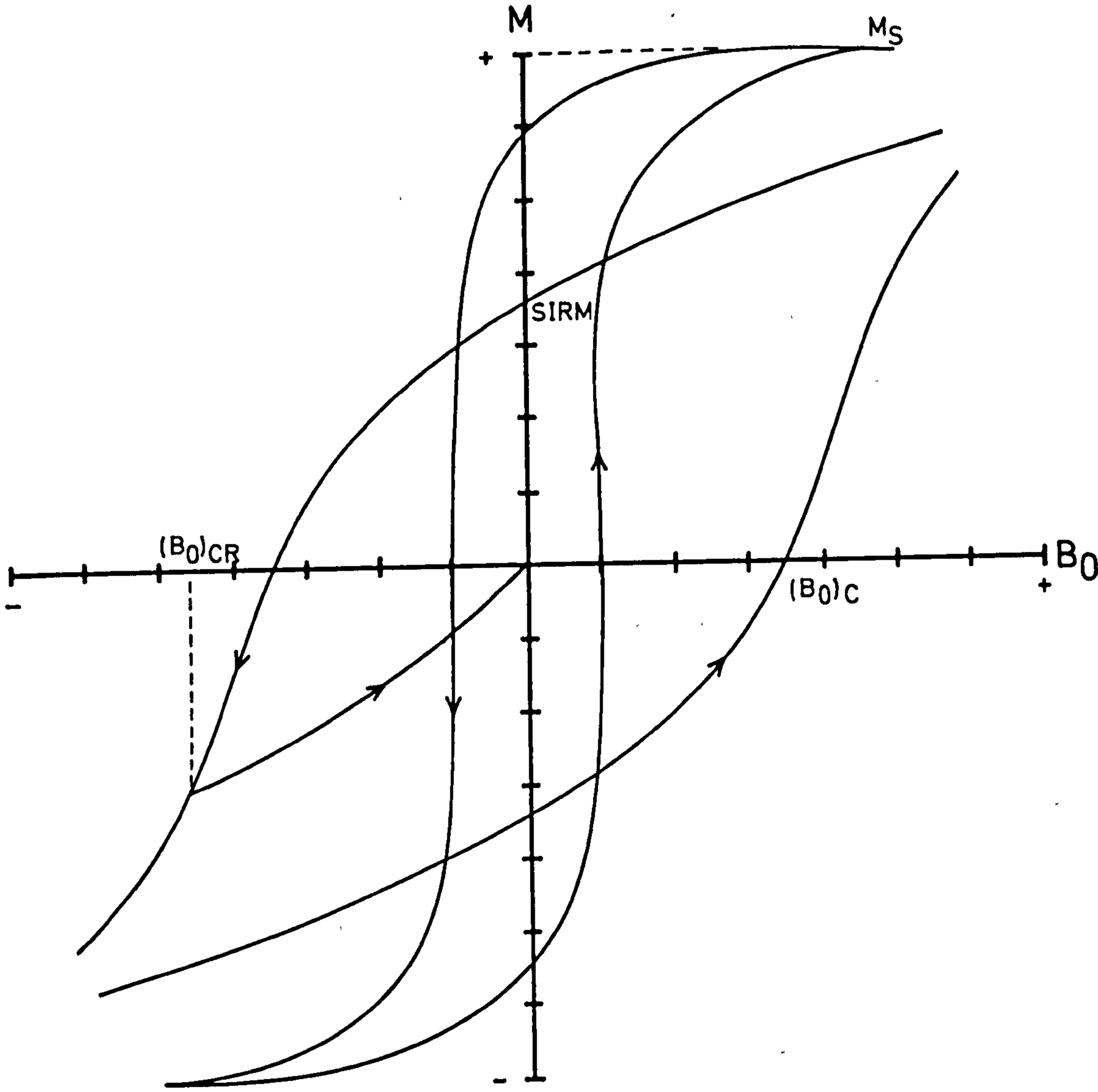


**Figure 1.2** Variation in hysteresis loops for 'soft' and 'hard' magnetic materials. The 'soft' material loop is denoted by the narrow field ($B_0$) band and the 'hard' material loop by the wide field band (redrawn from Bloemendal, 1982).

There are two critical boundaries between the three main grain types: superparamagnetic, (stable) single domain and multidomain. The critical size at the transition between superparamagnetic and stable single domains is termed $d_s$, and is about 0.03μm for equidimensional magnetite grains according to Dunlop (1972, 1973). Some variation must, however, result from the presence of variable, extrinsic sources of anisotropy (O'Reilly, op cit). The upper limit of the stable single domain grain size, $d_o$, is less well defined, being calculated by Dunlop (1972) to be about 0.06μm and subsequently 0.05μm (Dunlop, 1973) for equidimensional magnetite grains. Evidence from the latter (Dunlop, op. cit.) suggested that in elongated single domain particles the transition may be higher. The size range between the upper limit of true single domain behaviour (ca.0.05μm) and true multidomain behaviour (ca.0.17μm) is occupied by elongated single domain grains and small multidomain grains with **pseudo-single domain** characteristics (Dunlop, op. cit.).

The response to both magnetisation and demagnetisation of magnetic grains is therefore influenced by their domain status. Large multidomain grains will respond to relatively low magnetic fields by, for example, reversible domain wall or translation, producing enlargement of those domains with magnetic moments closest to the direction of the applied field. The application of stronger fields produces a rotation of the magnetic moments in the direction of the field. In contrast, the parallel alignment of spins in single domain grains produces spontaneous magnetisation along the easiest axes, the a-axis in the case of prolate elipsoids. To overcome, and reverse this, the application of a relatively higher magnetic field is required. Single domain grains thus have greater magnetic stability, or are magnetically 'harder', than multidomain grains.

### 1.5.7 Other Magnetic Effects

There are two further magnetic principles that are worth noting. One is time-dependence of magnetisation and the other temperature-dependence. Changes in magnetisation with time are known as **viscous** changes, and may arise through a variety of causes. From the environmental mineral magnetic viewpoint the most important is probably thermal activation. Magnetic viscosity can lead to either the growth or loss of magnetisation. A viscous sample stored in a magnetic field will increase its magnetisation and may even acquire a viscous remanent magnetisation, VRM. Loss of VRM can be brought about by leaving a viscous sample in a zero-field environment. In many cases, viscous magnetisation changes have been found to be proportional to the logarithm of time (cf. Thompson & Oldfield, op. cit.).

Temperature dependence of magnetic minerals relates to the variation in magnetic properties, for example, $M_S$, X and remanence observed with changes in temperature. Ferromagnetic and ferrimagnetic materials have characteristic temperatures above which their ordered magnetic structure is destroyed through increased thermal derangement, resulting in paramagnetism (cf. sub-sections 1.5.3 and 1.5.4). This temperature, the Curie point ($T_C$), is analogous to the Néel point, $T_N$, below which the atomic moments of antiferromagnets and ferrimagnets are arranged alternately parallel and antiparallel. The Curie point for magnetite is 580°C, and the Néel point for haematite, 680°C.

## 1.6 Magnetic Parameters and Interpretation

The response of the mixed magnetic mineral assemblages contained within the peat samples may be rapidly characterised by a series of forward and reverse field parameters generated and measured on currently

available instrumentation (cf. sub-section 1.7.1). This range of isothermal parameters provides a variety of information about a given mineral assemblage. Interpreting this information is dependent on an assessment of the relative sensitivity of each of the parameters, and their associated interparametric ratios, to the individual factors of assemblage composition, concentration and grain size distribution.

1.6.1 Magnetic Susceptibility

Low field **Magnetic Susceptibility,** usually represented by the Greek letter, Chi ($\chi$), is given the notation, X (mass specific) and K (volume) throughout. Susceptibility expresses the ratio between the magnetisation induced in a sample and the magnetising field. It is usually indicative of the volume concentration of magnetic minerals in a sample, where the assemblage is predominantly ferrimagnetic. Susceptibility is relatively independent of magnetic grain size. The intrinsic susceptibility of, for example, the canted antiferromagnetic oxides is usually masked by the ferrimagnetic contribution. Magnetite need amount to only 1% of the haematite content in a sample for the two minerals to contribute equally to X. However, in ferrimagnetic-deficient samples, canted antiferromagnetic, diamagnetic and paramagnetic components may make a significant contribution to the measured susceptibility as, for example, in the case of the diamagnetic properties of the plastic 10cc sample pots and the organic component of the peat itself. Table 1.1 summarises the diamagnetic components of the plastic containers, with and without foam packing, and the organic peat matter from the various sites. This diamagnetic component of the peat ($-0.51\pm0.39\ 10^{-8}m^3kg^{-1}$) is 1.9 times higher than that calculated for the 10cc pots ($-0.27\pm0.08\ 10^{-8}m^3kg^{-1}$), although both are noticeably lower than the value for pots and packing foam ($-1.06\pm0.23\ 10^{-8}m^3kg^{-1}$). The diamagnetic components of the pots

**Table 1.1** Diamagnetic Properties of Peats. Including the diamagnetic properties of plastic containers and packing foam.

| Site* | Mass Specific Susceptibility $10^{-8}m^3kg^{-1}$ | Volume Susceptibility dimensionless | Number of Samples |
|---|---|---|---|
| **Kaurastensuo, hollows** | -0.55±0.26 | - | 28 |
| **Kaurastensuo, hummocks** | -0.51±0.28 | - | 11 |
| **KAC (0-540cm)** | -0.51±0.12 | - | 70 |
| **KAX (0-462cm)** | -0.45±0.09 | - | 79 |
| **Laaviosuo, Site X** | -0.56±0.46 | - | 103 |
| **Varrassuo, Site X** | -0.40±0.33 | - | 86 |
| **Varrassuo, hollow** | -0.41±0.45 | - | 18 |
| **Haukilampi (0-230cm)** | -0.79±0.32 | - | 48 |
| **N. Scandinavian Sites** | -0.42±0.49 | - | 7 |
| **Draved Moss, S. Denmark** | -0.49±0.18 | - | 45 |
| **Mo-I-Rana, N. Norway** | -0.16±0.03 | - | 8 |
| **10cc Sample Pots** | -0.27±0.08 | -2.9±0.8 | 83 |
| **Sample Pots & Foam** | -1.06±0.23 | -5.2±2.1 | 10 |

* Located in southern Finland unless otherwise stated

(and foam) and peat have been added to the sample values throughout, where applicable.

**Frequency Dependent Susceptibility** ($X_{fd}$), analogous to quadrature susceptibility ($X_q$) used in earlier research (eg. Bloemendal, 1982), is displayed by magnetic minerals within a specific range of grain sizes. These **viscous** grains ca.0.03μm in diameter, span the transition between superparamagnetic and stable single domain grains. By raising the frequency of the measuring field within the susceptibility bridge (cf. section 1.7.1), a proportion of the grains with magnetic relaxation times exceeding the experimental measurement time will no longer contribute to the signal as superparamagnetic grains. By raising the frequency of the ($X_{HF}$), the superparamagnetic boundary is effectively reduced to a smaller volume, encompassing those grains of increasingly fast relaxation times. By measuring the susceptibility of a sample at both low and high frequencies, a decrease in the $X_{HF}$ compared to the $X_{LF}$ will indicate the presence of magnetic grains with a relaxation time between 0.5 and 0.05 seconds. The percentage frequency dependent susceptibility, used throughout, is calculated by the following formula:

$$X_{fd}(\%) = \frac{X_{LF} - X_{HF}}{X_{LF}} \cdot 100 \qquad [1.1]$$

### 1.6.2 Anhysteretic Remanent Magnetisation

If a sample is subjected to a decreasing alternating field (100mT to 0mT), with a small steady field superimposed (0.04mT), it acquires a remanent magnetisation approximately proportional to the steady field. This **Anhsysteretic Remanent Magnetisation,** ARM, is indicative of the volume concentration of the finer magnetic grains (fine grained stable single domain) within the sample (King et al., 1982).

ARM is a close analogue of thermoremanent magnetisation (TRM). Its advantage over TRM is the non-destructive nature of the technique; ie. the peat sample does not have to be combusted. There is also the ease and speed of measurement. When plotted against SIRM, the discriminating nature of ARM is particularly sensitive to grain size changes (cf. sub-section 1.6.4).

1.6.3 Saturation Isothermal Remanent Magnetisation

**Isothermal Remanent Magnetisation** (IRM) refers to the relaxation which occurs anywhere along the pathway 'b' in fig. 1.1 after magnetisation. **Saturation Isothermal Remanent Magnetisation** (SIRM) is the remanent magnetisation of the point $M_S$ on the hysteresis loop (fig. 1.1). SIRM is, like susceptibility, indicative of the volume concentration of magnetic minerals within the sample. In contrast to X, SIRM is a remanence and, therefore, is not affected by diamagnetic or paramagnetic components of the assemblage. However, the SIRM will reflect changes in magnetic grain size and mineralogy where SIRM and X are not proportional. Where SIRM and X can be shown to be directly proportional, the use of SIRM as a concentration parameter is acceptable (Jones, 1985). The evidence from Scandinavian peat bogs suggests that, even with microtopographical variations, SIRM is proportional to X. For example, at Kaurastensuo the Pearson Product Moment Correlation (r) for all hummocks is r= 0.98 and for all hollows r= 0.99, both significant at the 0.01 level (fig. 1.3). This strong statistical correlation holds regardless of site location or microtopraphy (and therefore vegetation).

The minimum (saturating) field required to induce SIRM is indicative of magnetic mineral type composition within a sample. Magnetite will saturate in fields of less than 200mT, whilst fine grain haematite, for example, may require fields greater than 1500mT (Bloemendal, op. cit.).

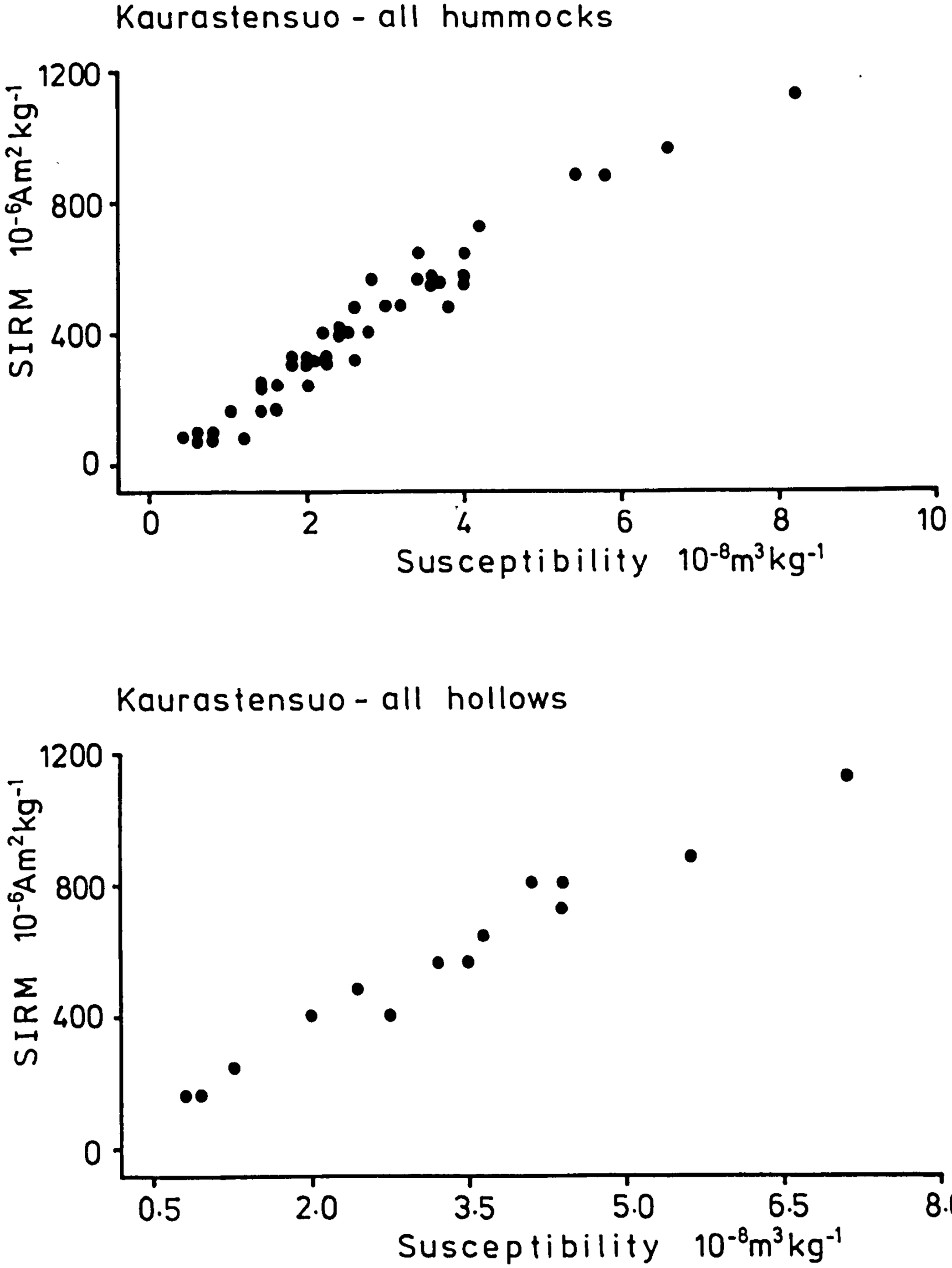


**Figure 1.3** Relationship between susceptibility and SIRM for hummock and hollow cores at Kaurastensuo. The correlation (Pearson's r) for all hummocks is r= 0.98 (n= 44) and for all hollows, r= 0.99 (n= 14). Both correlation coefficients are significant at the 0.01 level.

Figure 1.4 in summary, presents a schematic view of the relationship between the concentration-based parameters and the magnetic grain size variable.

### 1.6.4 Interparametric Ratios

The relative sensitivities and discriminatory nature of the concentration-based parameters is added to, and supported by, the interparametric ratios. Four ratios are considered in interpretations throughout this study; $IRM_{300mT}$/SIRM, ARM/SIRM, SIRM/X and SIRM/ARM.

The ratio of the forward field 300mT and SIRM is considered a useful support of SIRM in determining magnetic mineral types within a sample. Samples containing a large proportion of magnetite will have a ratio value approaching unity. In contrast, relatively lower proportions of magnetite-type minerals will lower the ratio, indicating the presence of 'harder' minerals.

ARM/X is interpreted as being sensitive to changes in the concentration of fine-grain minerals. Where the concentration of fine grain minerals is high, the ARM will be higher relative to the X. Conversely, where there are low concentrations of fine grain minerals present, the X value will be proportionally larger in comparison to the ARM.

Since SIRM exhibits a significantly greater variation with ferrimagnetic grain size than does susceptibility, SIRM/X is indicative of grain size variations (Bloemendal, op. cit.). If grain volume is the only variable, minimum SIRM/X values will occur in stable single domain grains, whilst low values occur in both superparamagnetic and coarse multidomain grains. However, where mineral variations play a role, samples dominated by a ferrimagnetic assemblage will have SIRM/X values less than, or equal to $100kAm^{-1}$. Samples with high concentrations of paramagnetic minerals,

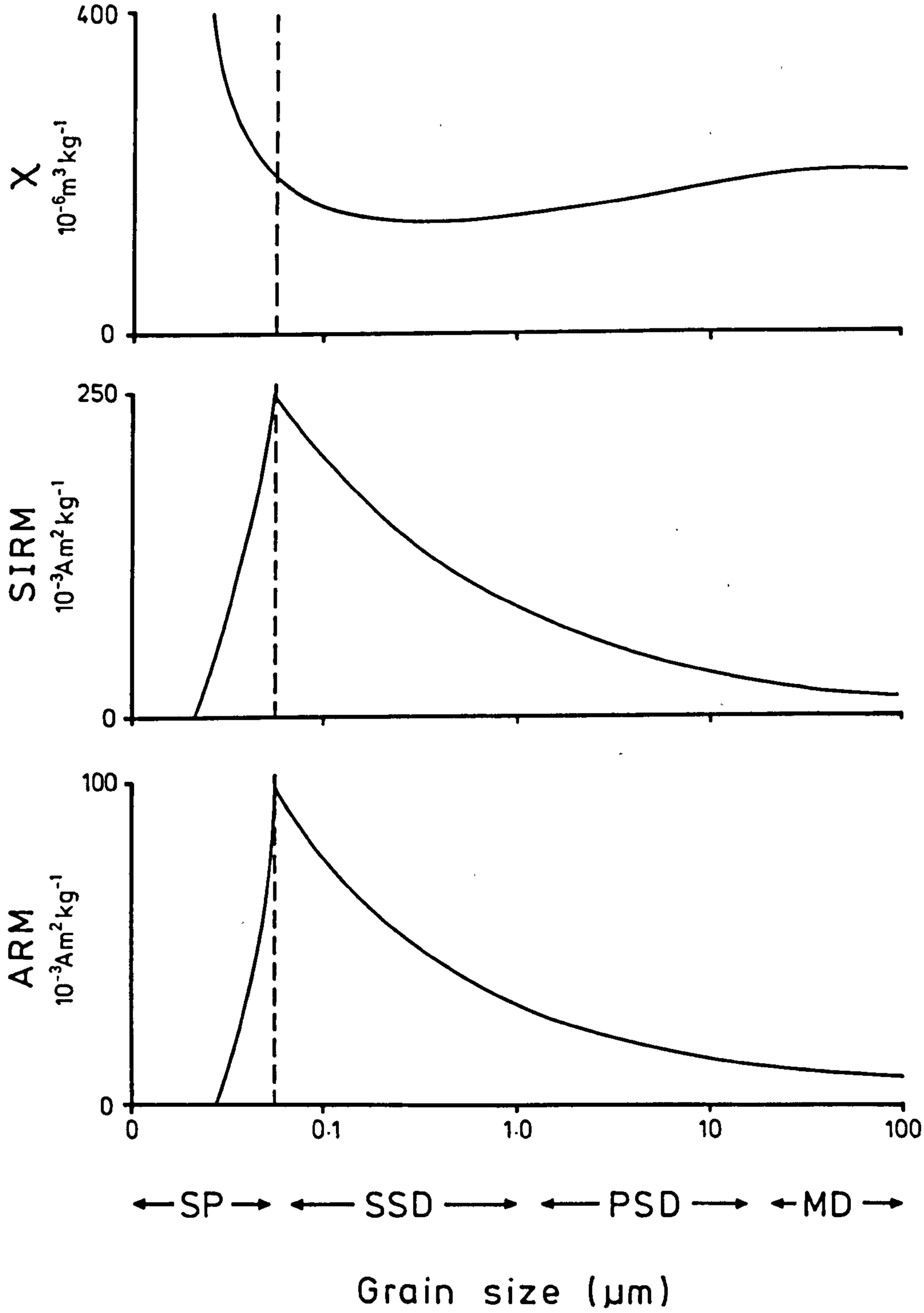


**Figure 1.4** Schematic diagrams of concentration-based parameters against grain size (redrawn from Maher, 1984).
SP = Superparamagnetic
SSD = Stable single domain
PSD = Pseudo single domain
MD = Multidomain

with weak positive X but no remanence, and low concentrations of ferrimagnetic minerals may have SIRM/X values of $<1kAm^{-1}$.

The ratio of SIRM/ARM may be used to indicate stable single domain versus coarse multidomain contrasts in ferrimagnetic grain assemblages. For example, high SIRM/ARM values are interpreted as reflecting a larger multidomain content. Evidence to date, for example Hunt et al. (1984), suggests that anthropogenic magnetic particles can produce SIRM/ARM values in excess of 100.

1.6.5 Demagnetisation Parameters

The use of stepwise demagnetisation is, in theory, independent of concentration being controlled by mineral type and grain size. This affects the ability of the sample to demagnetise in increasing reverse fields. The term 'reverse field' is used interchangeably with backfield throughout. For example, assemblages dominated by multidomain and superparamagnetic grains exhibit 'soft' demagnetisation behaviour. The result is a characteristically concave coercivity of remanence curve. The point along this curve, at which IRM/SIRM equals zero is the coercivity of remanence, $(B_0)_{CR}$ (cf. sub-section 1.5.5). Coercivity has been shown to be a sensitive discriminator between natural samples, even where the curves are the composite result of multimineralic assemblages (cf. Maher, op. cit.). Figure 1.5 depicts the various curve shapes for monomineralic assemblages ranging from a fine grain, canted antiferromagnetic type, displaying maximum resistence to demagnetisation, to a coarse multidomain type displaying little or no resistence to demagnetisation. $(B_0)_{CR}$ values for canted antiferromagnetic minerals are high (>60mT) and the curve shape markedly convex, indicating extreme 'hardness' of the material. In contrast, the $(B_0)_{CR}$ values of coarse multidomain minerals are less than 30mT. The coercivity of remanence curves presented throughout this study

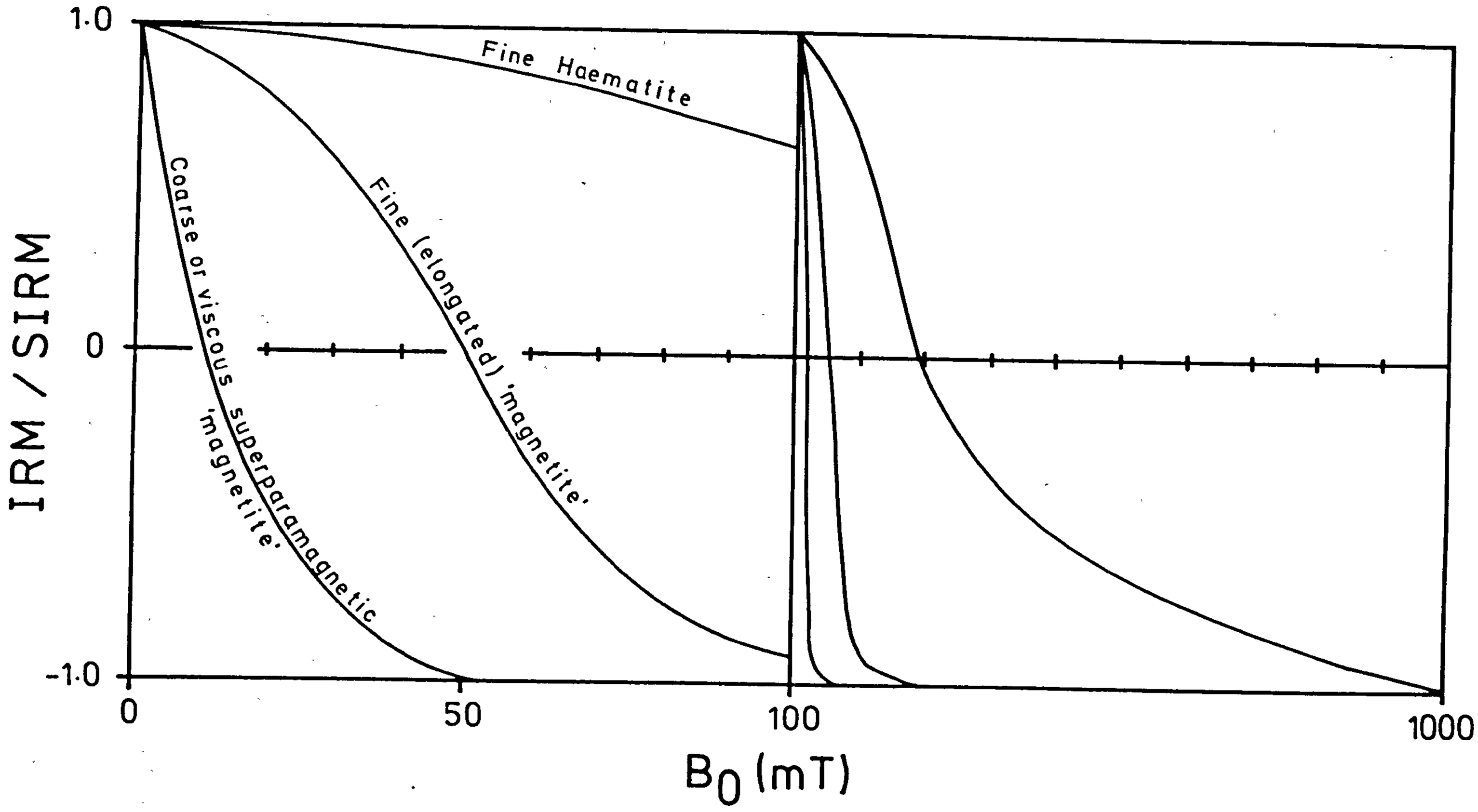


**Figure 1.5** Coercivity of remanence curves (linear plot) for monomineralic assemblages

comprise a number of backfield measurements (cf. inset, fig. 1.1) in order to fit a curve. All the plots are accompanied by the sample name and $(B_0)_{CR}$ value (mT), followed by the SIRM of the sample (cf. fig. 2.14). A summary of the characteristics of the curves presented in fig. 1.5 is given in Table 1.2 (after Maher, op. cit.).

The reverse field data of which the coercivity curves comprise arealso presented for selected backfields: $IRM_{-20mt}$/SIRM, $IRM_{-40mT}$/SIRM, $IRM_{-100mT}$/SIRM and $IRM_{-300mT}$/SIRM, in the enclosed plot at the end of all the magnetic profile diagrams (cf. fig. 2.6). Calculation of the ratio of IRM at a particular backfield to SIRM facilitates evaluation of the mineral magnetic assemblages. In earlier work the ratio $IRM_{-100mT}$/SIRM, termed the 'S' ratio, has been particularly useful in discriminating assemblages with varying proportions of ferrimagnetic to antiferromagnetic minerals (eg. Bloemendal, op. cit.). 'S' values enable some rapid indication of the contrasts between ferrimagnetic and canted antiferromagnetic assemblages within a suite of samples.

## 1.7 Instrumentation and Units of Measurement

### 1.7.1 Instrumentation

A detailed description of the magnetic instrumentation is given in Maher (op. cit.), and since the instrumentation is now becoming commercially available, only passing reference is made of their components. Apparatus for magnetic remanence measurements has been greatly simplified in terms of convenience, sample preparation and speed of operation as a result of electronic and technical innovations in the fields of integrated circuitry and micro-computers.

The in-field susceptibility measurements ($X$, $X_{fd}$) were carried out using a dual frequency susceptibility sensor (MS.1.B) connected to a digital

**Table 1.2** Summary of Coercivity of Remanence Curve Characteristics* (after Maher, 1984)

| $(B_0)_{CR}$ mT | Reverse Resaturation Field (RRF) | Low-Field Curve Shape | General Curve Shape | Mineralogy | Grain Size |
|---|---|---|---|---|---|
| <30 | 60-100 | Concave | 'J'-shaped | Ferri-magnetic | Coarse, multidomain. (± admixed superpara-magnetic) |
| 35-60 | 80-100 | Convex | 'S'-shaped | Ferri-magnetic | Single domain |
| >100 | >200 | Strongly Convex | 'S'-shaped | Canted antiferro-magnetic | - |

* cf. Figure 1.5

display meter. The sensors are pre-calibrated by means of paramagnetic salts such as ferrous ammonium sulphate. Readings are obtained by placing the sample within the air core of the coil and values calculated by means of 4 separate readings (A,B,C,D) per sample:

$$\text{Reading } (R_1) = \frac{(B+C) - (A+D)}{2} \qquad [1.2]$$

The readings were replicated not less than 10 times per sample where $R_1<10$, as in the majority of cases. The diamagnetic component of the pre-measured pots was subtracted and the value expressed as specific susceptibility on a unit sample-weight basis. The diamagnetic component of the peat was also estimated from the deeper 'clean' peat, and taken into account.

$X_{fd}$ was measured simply by altering the pre-set field strength of the sensor from low frequency to high frequency. Values were calculated using formula [1.1]. In all cases, the measurements were conducted at constant temperatures of between 12-15°C in order to achieve minimal environmental instability. The sensitivity of the sensor was estimated to be of the order $10^{-9}$-$10^{-10}m^3kg^{-1}$ using replicates.

ARM, IRM and SIRM were measured using a combination of portable pulse magnetisers to generate the field and a portable low speed spinning fluxgate magnetometer with a sensitivity of ca.0.2 $10^{-6}Am^2kg^{-1}$. The ARM was grown in a portable anhysteretic remanent magnetiser with a peak alternating field of 100mT and a superimposed d.c. field equivalent to the UK geomagnetic field (0.04mT). The sensitivity of the ARM measured on the fluxgate magnetometer was approximately 1.0 $10^{-6}Am^2kg^{-1}$.

IRM was grown in a peak d.c. field of up to 850mT. The maximum field generated, 850mT, is referred to as the SIRM throughout this study. It

is recognised, however, that samples dominated by extremely hard materials (eg. fine grain haematite) will not be fully saturated in a forward field of less than 1T. The evidence from earlier work, however, suggests that such assemblages are extremely rare in peat-based studies (eg. Oldfield et al., 1981). The smaller d.c. fields were precisely controlled and uniformly generated on another pulse magnetiser with a maximum field of 300mT.

The fluxgate magnetometer may be calibrated regularly throughout the sample runs by means of a known standard specimen (commercial tape). The mass specific value is calculated by means of two sample measurements, North and East vectors:

$$\text{ARM, (S)IRM} = \frac{\sqrt{N^2 + E^2} \times 12.9}{\text{sample mass}} \qquad [1.3]$$

The constant, 12.9, is the volume of a 25.4mm x 25.4mm (1 inch x 1 inch) cylinder.

### 1.7.2 Units of Measurement

The magnetic units of measurement used throughout this study are S.I. units. Table 1.3 outlines the S.I. and c.g.s. units for magnetic studies, as well as the units of measurement for chemistry. An important point to note is that all susceptibility measurements are in $10^{-8}$ S.I. units whereas the magnetic remanence follows the more frequently used $10^{-6}$ S.I. units.

### 1.7.3 Data Quality

The ease and rapidity of the magnetic measurements have allowed a fair degree of resolution and sensitivity through the use of replicate samples. This is true of total element determinations as well. Samples have been packed in clean, acid washed pots (Appendix 1) for the measurement by means of a purpose built peat press (Appendix 2). The ability to

**Table 1.3** Units of Measurement. Magnetic and chemical units (S.I.).

Magnetics- General

| Parameter | Symbol | S.I. Unit | C.G.S. Unit | Conversion to c.g.s |
|---|---|---|---|---|
| **Volume Susceptibility** | K | dimensionless | $GOe^{-1}$ | x0.0796 |
| **Specific Susceptibility** | X | $m^3kg^{-1}$ | $Gcm^3g^{-1}Oe^{-1}$ | x79.6 |
| **Volume Magnetisation** | M | $Am^{-1}$ | $Gcm^{-3}$ | x0.001 |
| **Specific Magnetisation** | - | $Am^2kg^{-1}$ | $Gcm^3g^{-1}$ | x1.0 |
| **Magnetic field Strength** | $B_0$ | T | Oe | x10,000 |

Magnetics- This study

| | | |
|---|---|---|
| **Specific Susceptibility** | X | $10^{-8}m^3kg^{-1}$ |
| **Frequency Dependent Susceptibility** | $X_{fd}$ | % |
| **ARM, (S)IRM** | | $10^{-6}Am^2kg^{-1}$ |
| **ARM/X** | | $Am^{-1}$ |
| **SIRM/X** | | $kAm^{-1}$ |
| **SIRM/ARM** | | dimensionless |
| **'S', $IRM_n$/SIRM** | | % |
| **$SIRM_{VS}$** | | $10^{-6}Am^2$ |
| **$SIRM_{DR}$** | | $10^{-6}Am^2yr^{-1}$ |

Chemistry

| | |
|---|---|
| **Specific Total Concentration** | $\mu g.g^{-1}$ |
| **Annual Flux** | $mg.m^{-2}yr^{-1}$ |

determine magnetic fields on the pulse magnetisers is controlled by a dial-display meter configuration. Any inaccuracies in determining the fields will have been internally consistent throughout the data set. These however, are envisaged to be minimal.

The data quality of the elemental determinations has been maintained by the use of nitric acid blanks and replicate measurements throughout (Appendix 3). The data quality of the chronologies presented in Chapters 2-5 is dependent on, and a function of, the assumptions used to derive that chronology. These various assumptions, related to specific chronologies, are discussed in the respective chapters. It is felt, however, that the chronologies used, in the absence of independent calibration, are reasonable approximations given their cautious use within the defined limits of each particular case example.

## 1.8 Objectives of the Study

The present study arises from the recent development of mineral magnetic techniques and their particular application in atmospheric- and peat-based studies. The empirical approach, used in previous work and throughout this study, is based on a conceptual model of relationships between environmental processes and the formation of a primary deposition record in peat. This approach, similar to that of other mineral magnetic studies (eg. Oldfield et al., 1981), is based on two assumptions. The first is that the inorganic component within the peat layers contains one or more mineral magnetic assemblages of sufficient magnitude to allow diagnostic inferences to be made. The second assumption is based on the requirement that the form and distribution of mineral magnetic assemblages in peat are persistent in both spatial and temporal terms. The latter assumption implies a persistence from formation, through the

transportation processes, to deposition and residence time in peat. This exceeds the timespan covered by industrialisation and its effects in Scandinavia (ca.100-150 years) but is within the timescale of microtopographical stability, specifically hummock-hollow regeneration, ca.2500 -1000 years (cf. Aaby, 1976; Barber, 1978).

The aims of the present study are:

i) To examine the reproducibility of the primary magnetic deposition record in a raised bog, taking account of changes in vegetation and hummock-hollow microtopography;

ii) To examine the persistence of the magnetic record over timescales of $10^1$-$10^3$ years, from a number of Scandinavian raised bogs;

iii) To examine the magnetic mineral-heavy metal linkages in minerotrophic and ombrotrophic peat layers overlying contrasting mineral soils;

iv) To use recent chronologies, where available and applicable, to estimate post-industrial influences on the heavy metal and mineral magnetic constituents within the inorganic component of surface peats;

v) Following on from iv), to attempt to identify any possible spatial and temporal variation in magnetic mineral and heavy metal deposition within and between Scandinavian countries, given the limitations of the study sites and their location;

vi) To examine the empirical evidence from a range of supportive techniques to characterise the sources of magnetic particulates within the surface layers of specific Scandinavian sites.

## 2. A Reproducible Record from Kaurastensuo, South Finland

### 2.1 Introduction

The spatial variation in magnetic profiles from the crown of an ombrotrophic bog, Kaurastensuo (61°02'N 24°59'E), is examined in this chapter. The effect of variations in plant species composition, fluctuations in the water table and variations in microtopography are also discussed. The evidence presented here is intended to provide the basis for a more confident and reliable interpretation of data from Norway, Finland and Denmark in subsequent chapters. The establishment of a reproducible record will complement pre-existing data from other sites in Finland, for example, Harpar Lilltrask, Karpansuo, Munasuo and Kunnoniemensuo in South and East Finland (Oldfield et al., 1981).

The contribution of magnetic particulates to the total inorganic fraction is estimated, indirectly, by means of statistical correlations (sub-section 2.3.5). The results are discussed and interpreted in sections 2.4 - 2.9.

### 2.2 Methods

#### 2.2.1 Study Site

Kaurastensuo Bog is located in South Finland about 3km south of Lammi Biological Station (University of Helsinki) in the parish of Lammi. The bog lies within the transition between the concentric mires of coastal Finland and the eccentric mires of the inland (fig. 2.1, inset) as defined by Eurola & Ruuhijärvi (1961). There has been a small amount of drainage to the west of the bog and also on the eastern margin. The majority of the raised bog surface including the ombrotrophic crown remains virgin peatland (fig. 2.1). The centre of the raised bog overlies ancient lake sediments, dated at between 8120±110 $C^{14}$ years BP, for the bottom of

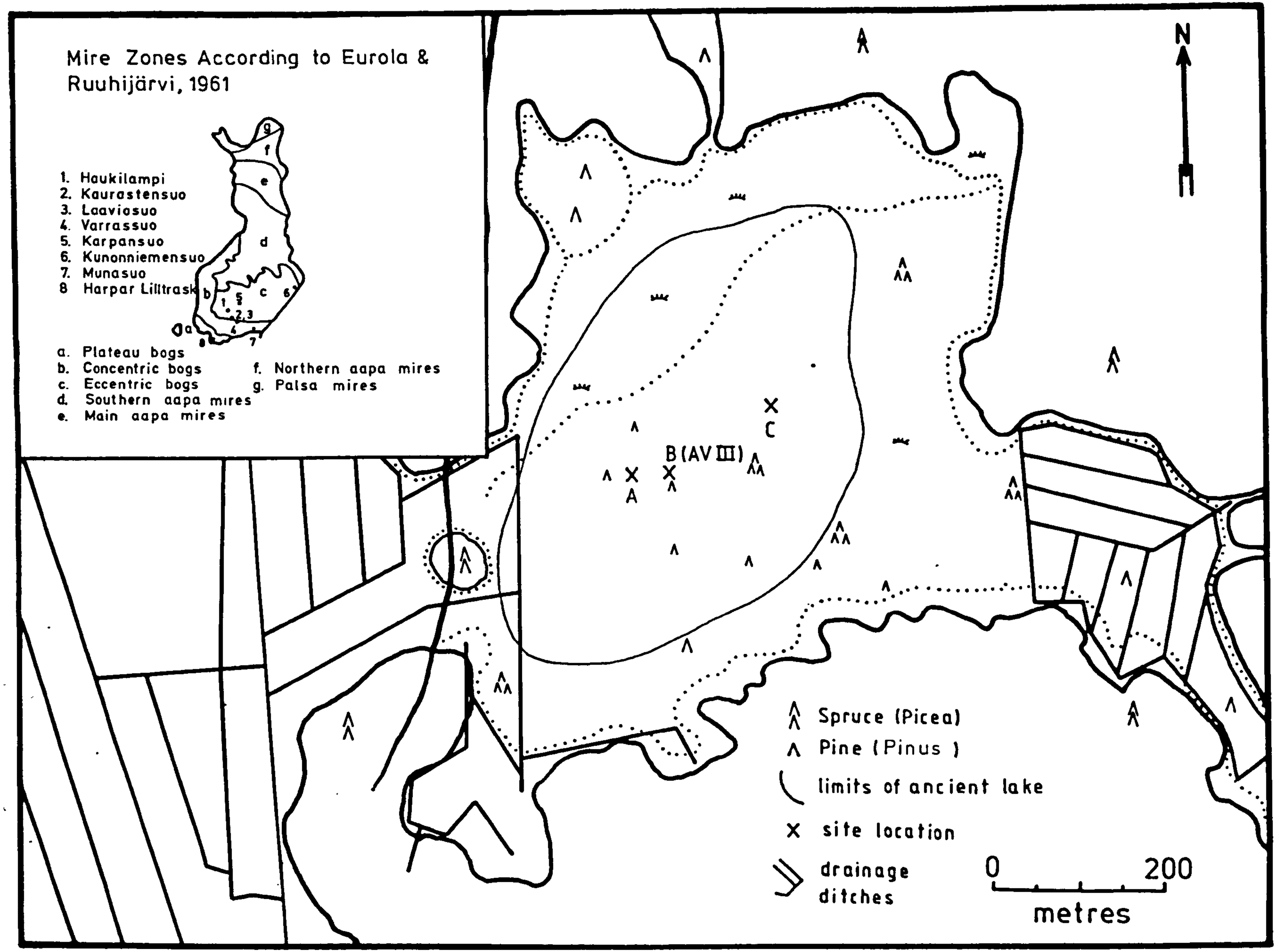


**Figure 2.1** Kaurastensuo peat bog, Lammi, southern Finland. The inset shows the location of sites in southern Finland in relation to the mire zones according to Eurola & Ruuhijärvi, 1961.

KAX (site-X[B][1]), and 8950±120 years BP (Appendix 4).

2.2.2 Sampling Methods

A total of eight surface cores were used from three sites (A, B and C) on the ombrotrophic crown (fig. 2.1). Six cores were taken as hummock-hollow pairs, one set from each site. The two remaining cores are the surface sections (top 50cm) of the long profiles at site B and site C. Cores C5 (hummock) and C6 (hollow) come from site A; C3 (hummock), C4 (hollow) and KAX (hummock) come from site B; whilst C1 (hummock), C2 (hollow) and KAC (hummock) come from site C (fig. 2.1). Cores KAX and KAC are additional material used primarily in the estimation of growth rates and particulate influx to the bog (sections 2.5 and 2.9).

All the surface cores were extruded by means of a partial-vacuum, 12cm diameter stainless steel corer. The extruded cores were sliced at 2.5cm intervals, and in some cases, at lower depths, 5cm intervals. In cores C1 and C6 the surface slices were 3cm and 1cm respectively. The length and slice intervals of each core are presented in Table 2.1.

2.2.3 Core Stratigraphy

The surface vegetation constituents are noted in Table 2.2. All 5 hummock cores comprised primarily Sphagnum fuscum. All cores, with the exception of C6 contained some S. fuscum in the 'live' layer. KAX and KAC consist of loosely compacted S. fuscum with little or no humification, between H1 and H3 on the Von Post scale (Von Post, 1922).

2.2.4 Core Chronology

Published work by Tolonen (1982) and unpublished data (Tolonen, pers. comm.) have investigated the relationship between the net vertical

---

1. Site-X is the location of the long core profile, KAX, given in Chapter 3, section 3.4.4. This is adjacent to the site used for $C^{14}$ dating (Tolonen, 1979, unpubl. data). This site has been called site B in the present chapter.

**Table 2.1** Core data for Kaurastensuo, southern Finland

| Core | Length (cm) | Slice Interval (cm) | |
|---|---|---|---|
| | | **2.5cm** | **5cm** |
| C1, Hummock | 49 | 0-20* | 20-45 |
| C2, Hollow | 37 | 0-15 | 15-35 |
| C3, Hummock | 45 | 0-20 | 20-45 |
| C4, Hollow | 34 | 0-34 | - |
| C5, Hummock | 52.5 | 0-25 | 35-50 |
| C6, Hollow | 39 | 0-37.5** | - |
| KAX, Hummock | 50 | 0-50 | - |
| KAC, Hummock | 50 | 0-50 | - |

* Surface slice = 0-3cm

** Surface slice = 0-1cm

**Table 2.2** Surface Vegetation of Kaurastensuo Cores

| Core | Depth (cm) | Vegetation (main constituents) | Depth of Water Table (cm) 22-8-83 | Surface | Site Notes |
|---|---|---|---|---|---|
| Site C, C1 | 0-3 | **Polytrichum strictum, Sphagnum fuscum, Calluna vulgaris, Empetrum nigrum, Vaccinium oxycoccus** | 35 | Hummock | Open virgin peatland with some Spruce<br>Wind direction: westerly<br>Distance between cores: 30cm<br>Amplitude: 11cm<br>Other vegetation: **E. vaginatum, C. vulgaris, S. balticum** |
| Site C, C2 | 0-3.5 | **Myalia anomalia, S. fuscum, Vaccinium microcarpum** | 24 | Hollow | |
| Site C, KAC | 0-2.5 | **S. fuscum** | 30.5 | Hummock | |
| Site B, C3 | 0-5 | **S. fuscum, S. angustifolium, Andromeda polifolia, V. oxycoccus, Eriophorum vaginatum** | 28 | Hummock | Edge of open virgin peatland<br>wind direction: westerly<br>Distance between cores: 31cm<br>Amplitude: 11cm<br>Other vegetation: **Rubus chamaemorus, E. vaginatum, S. balticum & Mycea spp.** |
| Site B, C4 | 0-2.5 | **M. anomalia, S. fuscum, S. angustifolium, E. nigrum, C. vulgaris** | 17 | Hollow | |
| Site B, KAX | 0-2.5 | **S. fuscum, S. angustifolium, C. vulgaris** | 32.5 | Hummock | |
| Site A, C5 | 0-4.5 | **P. strictum, S. fuscum** (dead), **S. rubellum, S. angustifolium, E. vaginatum** | 25.5 | Hummock | Within stunted Spruce zone<br>Wind direction: westerly<br>Distance between cores: 30cm<br>Amplitude: 14.5cm |
| Site A, C6 | 0-1 | **Cladonia rangiferina (lichens), C. vulgaris** | 11 | Hollow | |

height increase (growth) of peat and nine variables: bulk density, pyrophosphate index, fibre content, decomposition (Von Post), carbon percentage of organic matter, moisture, dielectric constant, humification percentage (Pyavchenko) and humification by centrifuge (Gost). The data are based on samples from a fairly loose S. fuscum core taken at site C, Kaurastensuo (fig. 2.1). Growth rates are calibrated against actual measurements of S. fuscum annual productivity in the live layers, which give reliable figures for the surface samples (Lindholm, 1981).

Using the bulk density data for the Kaurastensuo cores, growth rates, expressed as $mm.yr^{-1}$ have been obtained from the log. linear equation (Tolonen, unpubl. data):

$$\ln.y = 8.267 - 2.0463 \ln.x_1 \qquad (n= 9) \quad [2.1]$$

where: $y$ = vertical growth rate ($mm.yr^{-1}$)

$x_1$ = bulk density ($gdm^{-3}$)

ln = natural logarithm

The correlation coefficient, $r= -0.926$, is significant at the 0.01 level.

The absence of any other dating method for this study precludes any comparison and testing of this equation. Clymo (1970) noted that although precision of any one method of measurement may be estimated with standard statistical techniques, a highly precise estimate is not necessarily highly accurate. Close agreement between the mean results is therefore the best evidence of accuracy. The more diverse the methods, the better their mutual support. The growth rates are used tentatively in sections 2.5 and 2.8 to establish the effects of growth rates on the magnetic record, and to estimate, quantitatively, the influx of magnetic particulates to the bog surface.

## 2.3 Results

### 2.3.1 Cumulative Dry Mass and Estimated Growth Rates

Growth rates in peat bogs vary spatially across the bog surface, and temporally, through the peat profile. Changes in microhabitat conditions and species affect both factors (Clymo, 1965, 1973). Variations in growth rates over time may be measured indirectly by plotting the cumulative dry mass per unit area against depth within the profile. These measurements are based on the variations in bulk density of consecutive slice increments within the profile. Bulk density values for cores C1-C6 are presented in fig. 2.2 reflecting variations in species composition, compaction, hummock-hollow microtopography and relationship to the water table. Surface bulk density values are consistently higher in the hollows than in the hummocks. Maximum bulk density values for all cores, hummock and hollow, occur towards the base of the short profiles, with the exception of occasional anomalously high values, for example, the 2.5-5cm slice in C4 (hollow). Ash residues are also presented in fig. 2.2 in relation to the bulk density values (sub-section 2.3.4).

Cumulative dry mass curves against depth for cores C1-C6 are presented in fig. 2.3. The gradients of the hummock cores are steeper than their respective hollows at all three sites. The gradients of the hummock and hollow cores at site C are also steeper than the respective cores at site B, which in turn, are steeper than those of their respective cores at site A.

Using the bulk density equation [2.1] given in sub- section 2.3.4, the net vertical height increases have been calculated for cores C1-C6, and in addition, KAX and KAC. A summary of these growth rates is presented in Table 2.3, along with the pre-existing data from the original hummock (Tolonen, op. cit.). The values for all cores increase gradually towards the surface from a minimum depth of 22.5cm, with the exception of C6. The

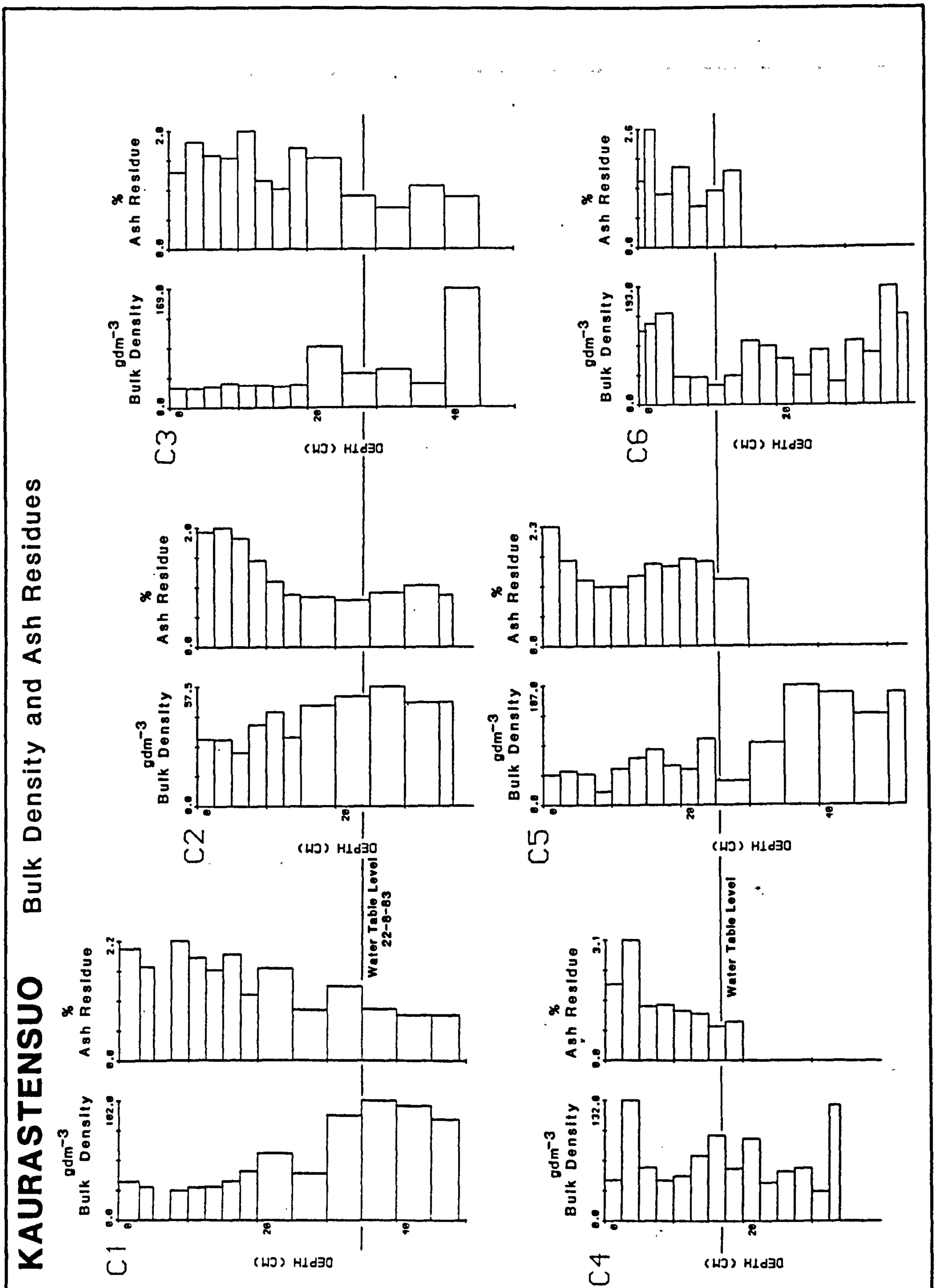


Figure 2.2 Bulk density and ash residues of cores C1-C6, Kaurastansuo

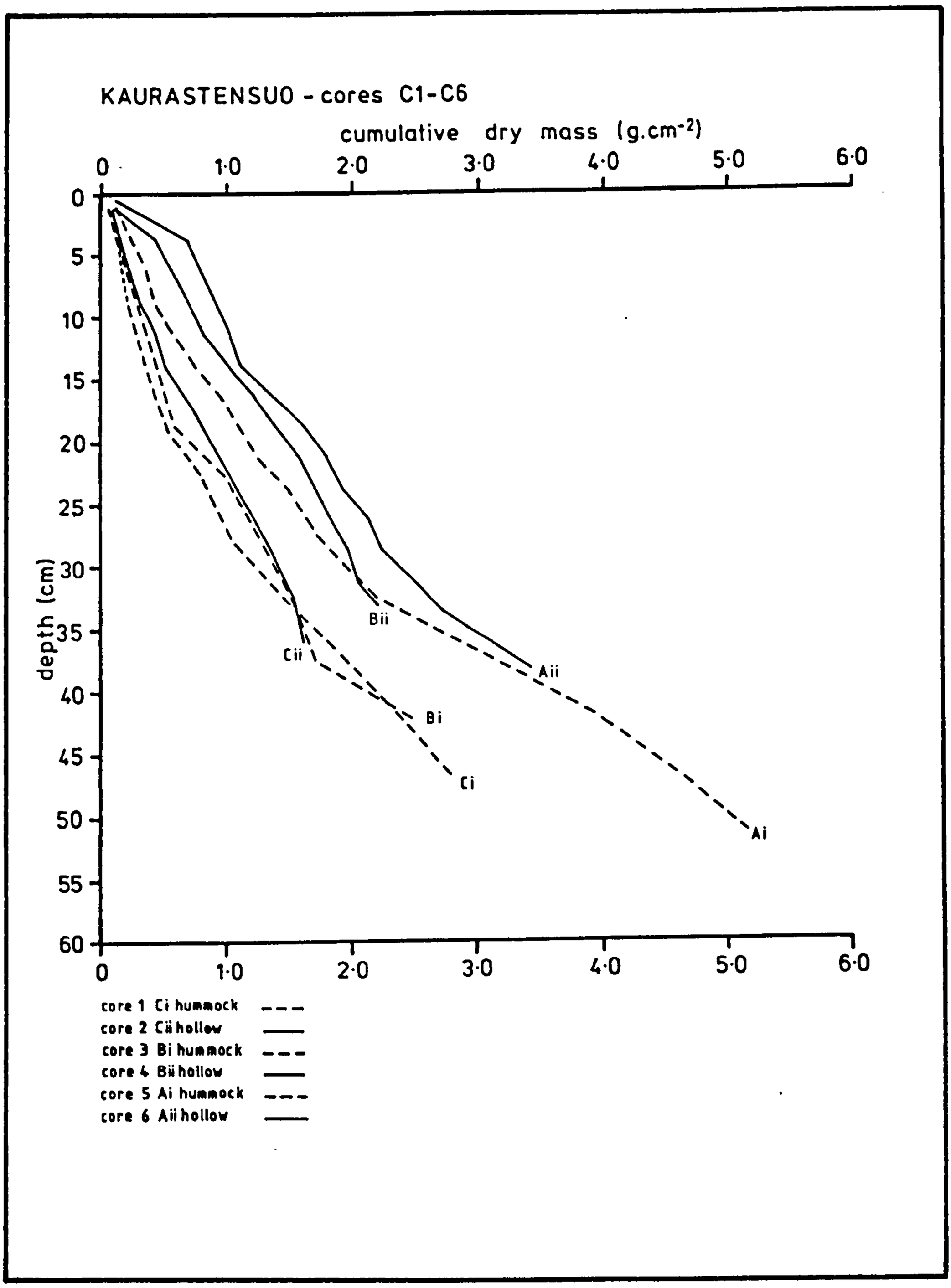


**Figure 2.3** Cumulative dry mass curves for cores C1-C6, Kaurastensuo

**Table 2.3** Summary of Net Vertical Height Increase.
The average growth rate (r), is given ± standard deviation for all cores at varying depth intervals; the mean growth rate for the whole of the core is given underneath. The data for site AVII (Tolonen, 1984; pers. comm.). refers to site C in this study (fig. 1).

| C1, Hummock | | C2, Hollow | | C3, Hummock | | C4, Hollow | |
|---|---|---|---|---|---|---|---|
| Depth (cm) | r $mmyr^{-1}$ | Depth (cm) | r $mmyr^{-1}$ | Depth (cm) | r $mmyr^{-1}$ | Depth (cm) | r $mmyr^{-1}$ |
| 0-17.5 | 4.01±0.78 | 0-15 | 3.02±1.08 | 0-20 | 3.70±0.52 | 0-12.5 | 1.32±0.28 |
| 17.5-30 | 1.67±0.48 | 15-37 | 1.22±0.14 | 20-40 | 1.02±0.36 | 12.5-25 | 0.59±0.24 |
| 30-49 | 0.37±0.05 | | | | | 25-34 | 1.46±0.91 |
| x r | 2.35±1.7 | | 2.20±1.2 | | 2.8±1.35 | | 1.16±0.74 |
| n | 13 | | 11 | | 12 | | 14 |

| C5, Hummock | | C6, Hollow | | KAX, Hummock | | KAC, Hummock | |
|---|---|---|---|---|---|---|---|
| Depth (cm) | r $mmyr^{-1}$ | Depth (cm) | r $mmyr^{-1}$ | Depth (cm) | r $mmyr^{-1}$ | Depth (cm) | r $mmyr^{-1}$ |
| 0-12.5 | 2.49±2.50 | 0-5 | 0.18±0.03 | 0-10 | 5.20±0.5 | 0-15 | 6.00±1.20 |
| 2.5-52.5 | 0.57±0.63 | 5-15 | 1.96±0.77 | 10-20 | 3.70±0.6 | 15-35 | 4.10±1.70 |
| | | 15-39 | 0.67±0.68 | 20-30 | 7.70±2.7 | 35-50 | 2.67±0.44 |
| | | | | 30-45 | 3.30±1.5 | | |
| | | | | 45-60 | 5.30±1.3 | | |
| x r | 1.17±1.78 | | 0.86±0.9 | | 5.07±1.9 | | 4.2±1.8 |
| n | 16 | | 17 | | 24 | | 20 |

**Site AVII**

| Depth (cm) | r $mmyr^{-1}$ | Age* yrs BP | Bulk Density $g.dm^{-3}$ |
|---|---|---|---|
| 0-72.5 | 2.42 | 0-300 | 40.4±8.6 |

* Estimated by means of several moss increment dated cores from adjacent hummocks

average growth rate (r) for core C6 decreases from 1.96 mm.yr$^{-1}$ (5-15cm) to 0.18 mm.yr$^{-1}$ (0-5cm). This corresponds with an increase in bulk density values from ca.45 gdm$^{-3}$ (5-10cm) to 115-145 gdm$^{-3}$ (0-5cm).

The age (years before 1983 [BP]) of each slice in the eight cores is calculated by means of the growth rates. These results are presented in Table 2.4. Core C6 has been omitted from the table since the surface layer, 0-1cm, contained no live S. fuscum, comprising mainly the lichen Cladonia rangiferina. The hollow cores, C2 and C4, have been included due to the abundance of S. fuscum throughout the core, including the surface sample. The age versus depth curves for the cores are presented in fig. 2.4. The relationship between the gradient of the curve, and microtopography and site location evident above 20cm, is similar to that expressed by the cumulative dry mass curves (fig.2.3). This is evident from the linear relationship between cumulative dry mass and age for KAX in fig. 2.5.

### 2.3.2 Magnetic Measurements

The magnetic profiles for cores C1-C6 are presented in figs. 2.6-2.11. Cores KAX and KAC are presented in figs. 2.12 and 2.13 respectively. The concentration dependent parameters, X, SIRM and ARM and their respective interparametric ratios, ARM/X, SIRM/X and SIRM/ARM are presented for all cores. In addition, the backfield ratios ($IRM_{-20mT}$/SIRM, $IRM_{-40mT}$/SIRM, $IRM_{-100mT}$/SIRM and $IRM_{-300mT}$/SIRM) are also given. The profiles for cores C1-C6 (figs. 2.6-2.11) are plotted against depth in the upper part of the diagrams and against cumulative dry mass in the lower part. Variations in the thickness of each slice increment represent variations in dry mass (g.cm$^{-2}$) through the profile. The variations in dry mass down-profile for KAX and KAC are negligible, therefore the magnetic profiles for these two cores are plotted only against depth.

An obvious feature in all the core profiles is the inflection point in

**Table 2.4** Age-Depth Relationships for Kaurastensuo
Core C6 (site A) is omitted (see text) and KAX has been calculated using data provided by Tolonen (pers. comm.). All the calculations are based on the log. linear bulk density equation [2.1]. Age BP refers to age before 1983.

| C1, Hummock | | C2, Hollow | | KAC, Hummock | | C3, Hummock | | C4, Hollow | | KAX, Hummock | | C5, Hummock | |
|---|---|---|---|---|---|---|---|---|---|---|---|---|---|
| Depth (cm) | Age BP (yrs) | Depth (cm) | Age BP (yrs) | Depth (cm) | Age BP (yrs) | Depth (cm) | Age BP (yrs) | Depth (cm) | Age BP (yrs) | Depth (cm) | Age BP (yrs) | Depth (cm) | Age BP (yrs) |
| 3 | 10 | 2.5 | 8 | 2.5 | 3 | 2.5 | 6 | 2.5 | 15 | 2.5 | 10 | 2.5 | 17 |
| 5 | 14.5 | 5 | 16 | 5 | 8 | 5 | 11 | 5 | 38* | 5 | 21 | 5 | 39 |
| 7.5 | 20 | 7.5 | 21 | 7.5 | 12 | 7.5 | 18 | 7.5 | 65 | 7.5 | 31 | 7.5 | 57 |
| 10 | 24.5 | 10 | 32 | 10 | 17 | 10 | 27 | 10 | 80 | 10 | 41 | 10 | 60 |
| 12.5 | 30.5 | 12.5 | 48 | 12.5 | 22 | 12.5 | 34 | 12.5 | 99 | 12.5 | 52 | 12.5 | 85 |
| 15 | 36.5 | 15 | 57 | 15 | 26 | 15 | 41 | 15 | 139 | 15 | 62 | 15 | 127 |
| 17.5 | 44.5 | 20 | 93 | 17.5 | 34 | 17.5 | 48 | 17.5 | 209 | 17.5 | 72 | 17.5 | 188 |
| 20 | 27.5 | 25 | 136 | 20 | 39 | 20 | 55 | 20 | 234 | 20 | 83 | 20 | 218 |
| 25 | 108 | 30 | 187 | 22.5 | 46 | 25 | 174 | 22.5 | 298 | 22.5 | 93 | 22.5 | 242 |
| 30 | 132 | 35 | 226 | 25 | 64 | 30 | 209 | 25 | 312 | 25 | 103 | 25 | 329 |
| 35 | 256 | 37 | 265 | 27.5 | 71 | 35 | 254 | 27.5 | 334 | 27.5 | 114 | 30 | 350 |
| 40 | 418 | | | 30 | 79 | 40 | 299 | 30 | 360 | 30 | 124 | 35 | 502 |
| 45 | 569 | | | 32.5 | 84 | | | 32.5 | 368 | 32.5 | 134 | 40 | 1057 |
| 49 | 689 | | | 35 | 88 | | | 34 | 442 | 35 | 145 | | |
| | | | | 37.5 | 101 | | | | | 37.5 | 155 | | |
| | | | | 40 | 110 | | | | | 40 | 165 | | |
| | | | | 42.5 | 117 | | | | | 42.5 | 176 | | |
| | | | | 45 | 126 | | | | | 45 | 186 | | |
| | | | | 47.5 | 135 | | | | | 47.5 | 196 | | |
| | | | | 50 | 146 | | | | | 50 | 207 | | |

* Calculated from the mean growth rates given in Table 2.3

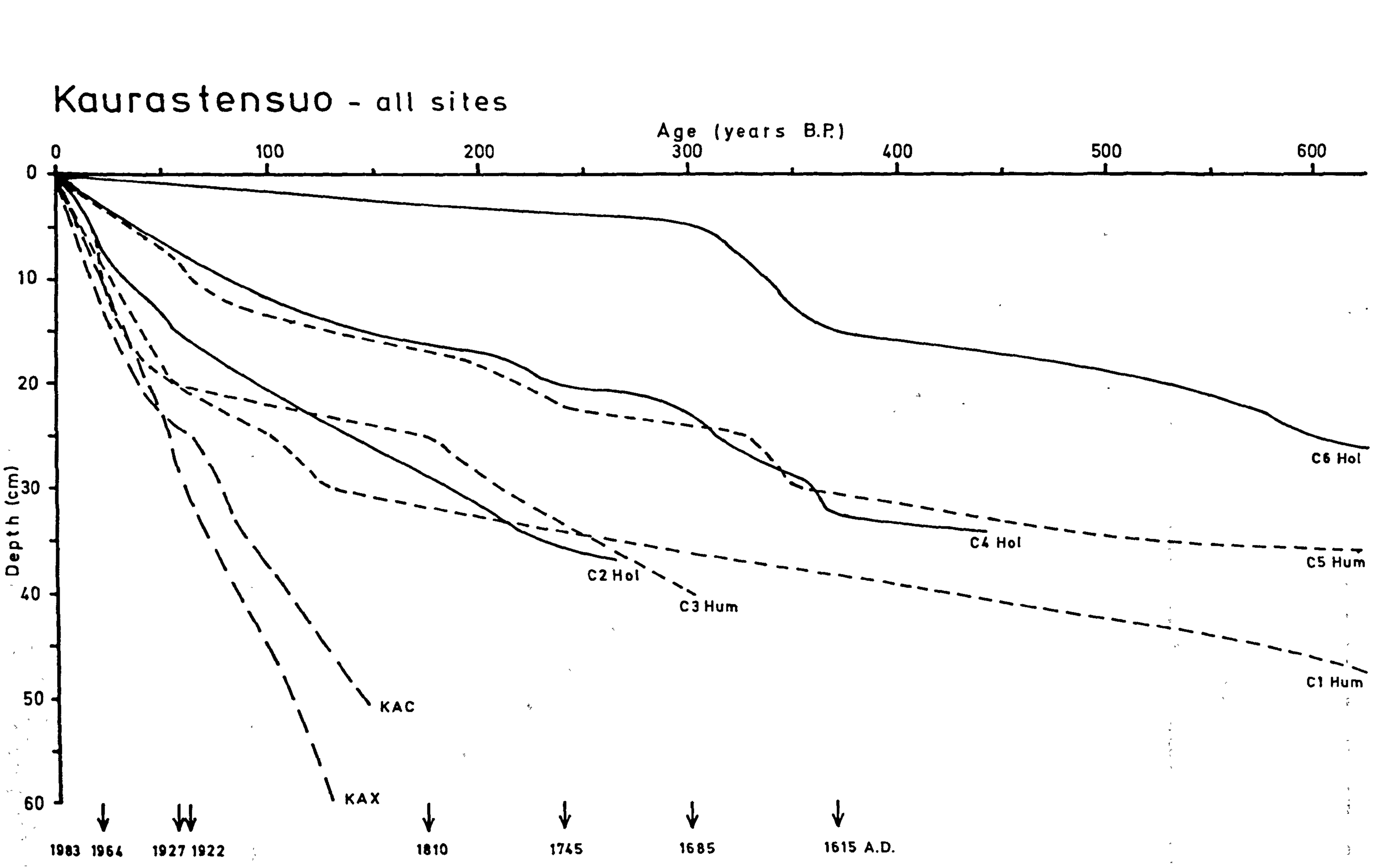


**Figure 2.4** Age/depth curves for cores C1-C6, KAC and KAX, Kaurastensuo

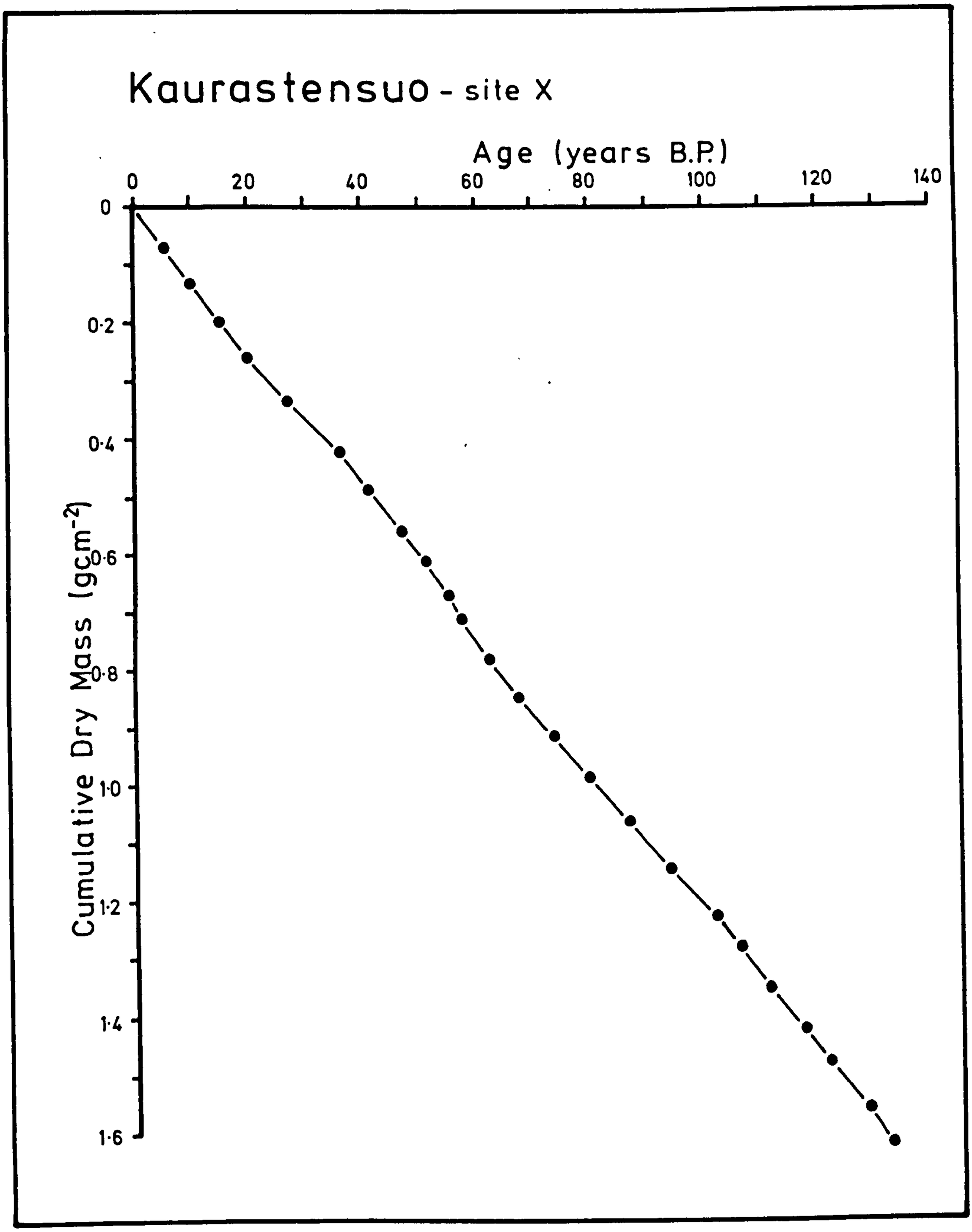


**Figure 2.5** Cumulative dry mass as a function of age for KAX, Kaurastensuo

the SIRM and ARM profiles. This point of inflection is usually coincident with the lower limits of positive, measurable X. For convenience this point has been termed the 'take-off' point. At Kaurastensuo the take-off point is seen as a relatively unambiguous horizon throughout the cores (section 2.8). The depth of this feature varies from core to core, based on the SIRM, $SIRM_{VS}$ and X data. It is consistently deeper in the hummock profiles than in their respective paired hollows. The relative depths of the take-off point within the eight cores are presented in Table 2.5.

Small variations in the SIRM values are evident between the hummock and hollow cores at each site. With the exception of site A the peak values are found within the hummocks. The highest values are at site B, 1115 $10^{-6}Am^2kg^{-1}$ and 1084 $10^{-6}Am^2kg^{-1}$ for sub-surface peaks within cores C3 and C4 respectively. Conversely, the lowest peak value is found within KAX (230 $10^{-6}Am^2kg^{-1}$), also at site B. An explanation of this variation within cores from the same site is given in sub-section 2.4.1. Cores C2 and C6 (hollows) display peak SIRM values at the surface, C3 and KAX (hummocks) both at site B display the peak value at 2.5-5cm whilst the remaining cores all display deeper sub-surface peaks, the deepest being in C5 (site A) at 12.5-15cm.

Below the take-off point the X values become negative, displaying the diamagnetic properties of the samples. The diamagnetic properties of the peat/carbon matrix are typically between -0.39 $10^{-8}m^3kg^{-1}$ and -0.76 $10^{-8}m^3kg^{-1}$. Where bulk X is very low and SIRM/X values are relatively constant, as at Kaurastensuo, then SIRM may be used as a crude indicator of concentrations of ferrimagnetic minerals within the sample. At Kaurastensuo there is a strong statistical relationship between X and SIRM, with a coefficient of r= 0.96. Based on this assumption, pre-take-off susceptibility samples exhibit very low concentrations, typically 20 times

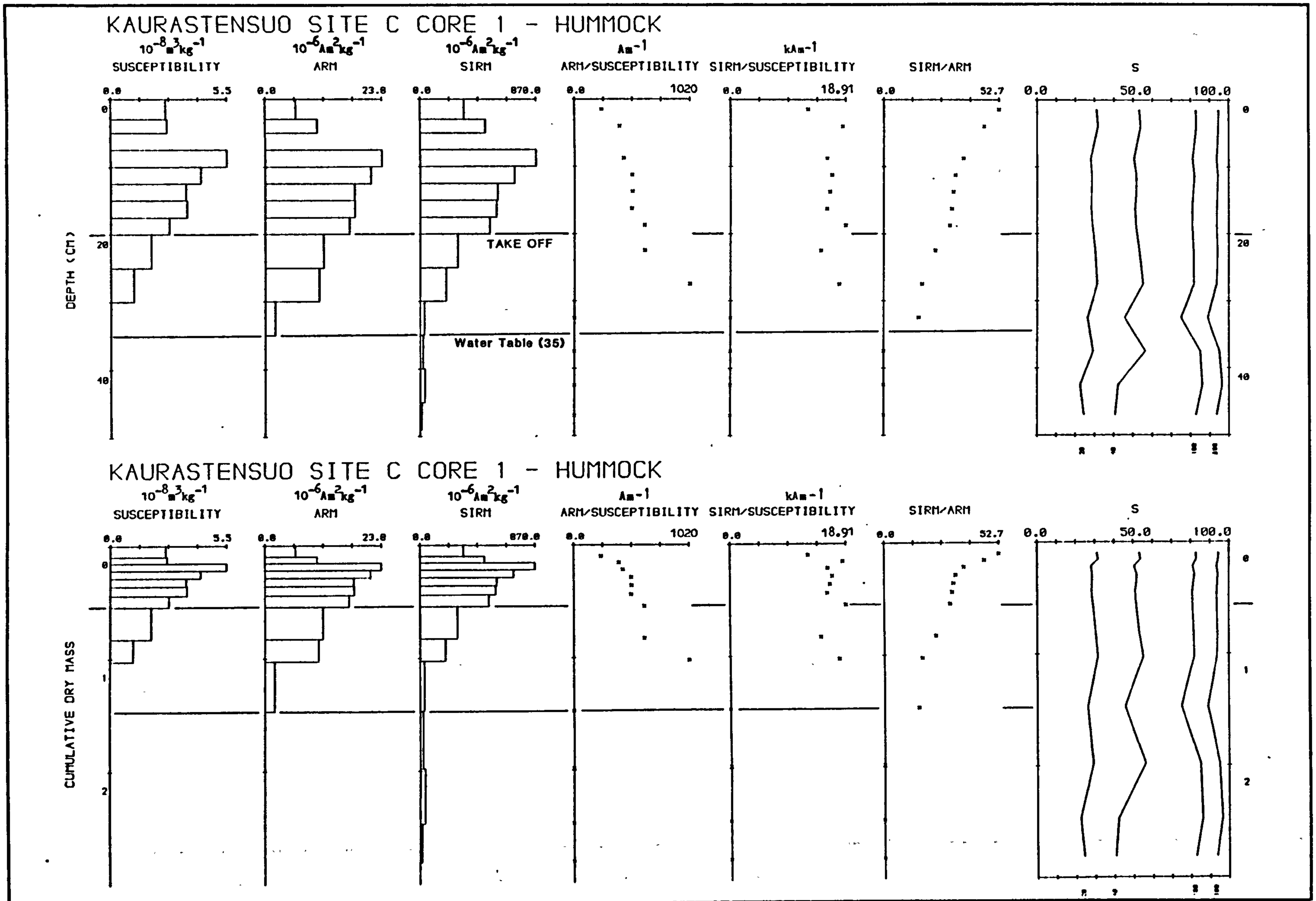


**Figure 2.6** Magnetic measurements of hummock core C1, site C (Ci), Kaurastensuo

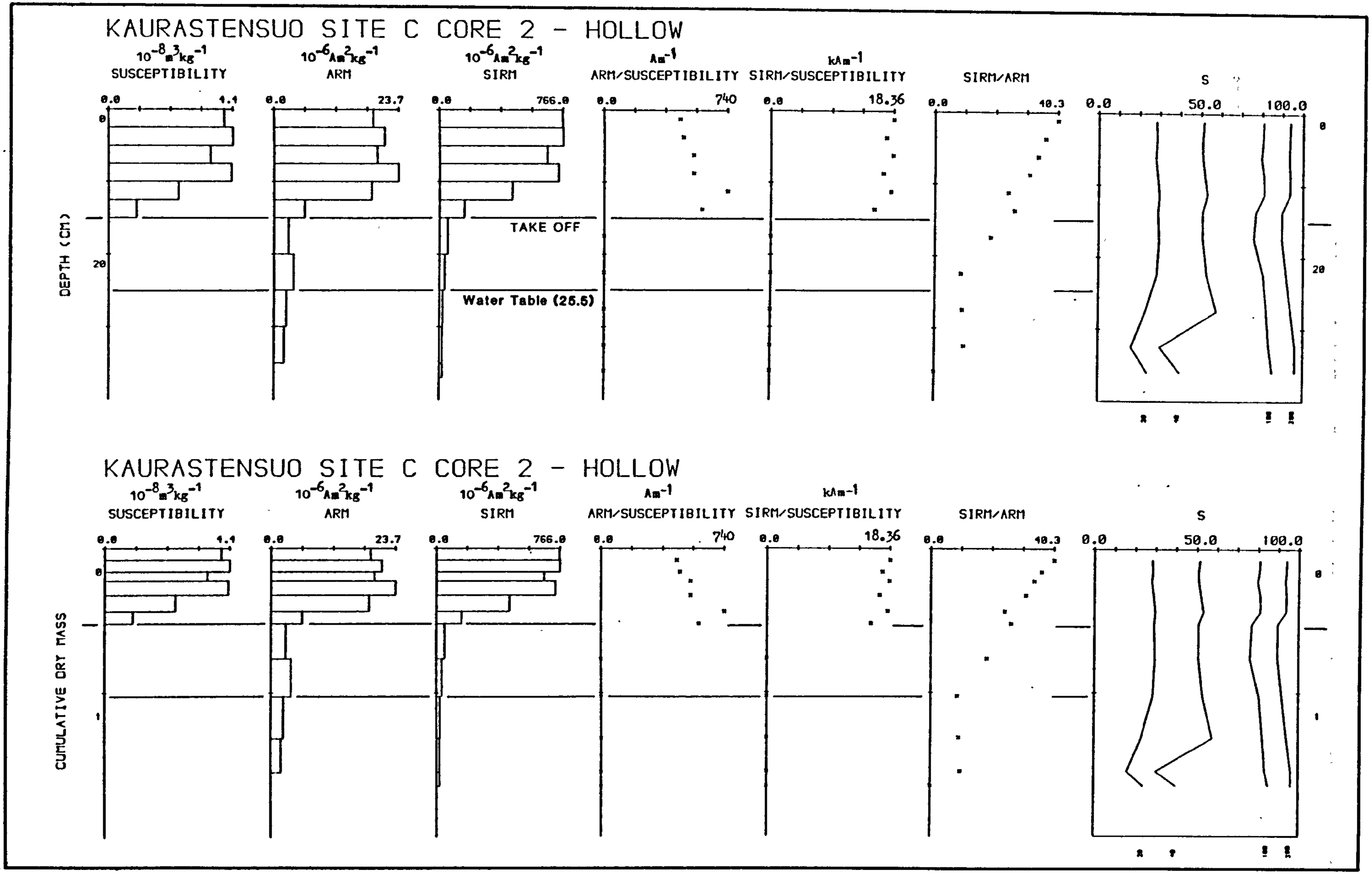


**Figure 2.7** Magnetic measurements of hollow core C2, site C (Cii), Kaurastensuo

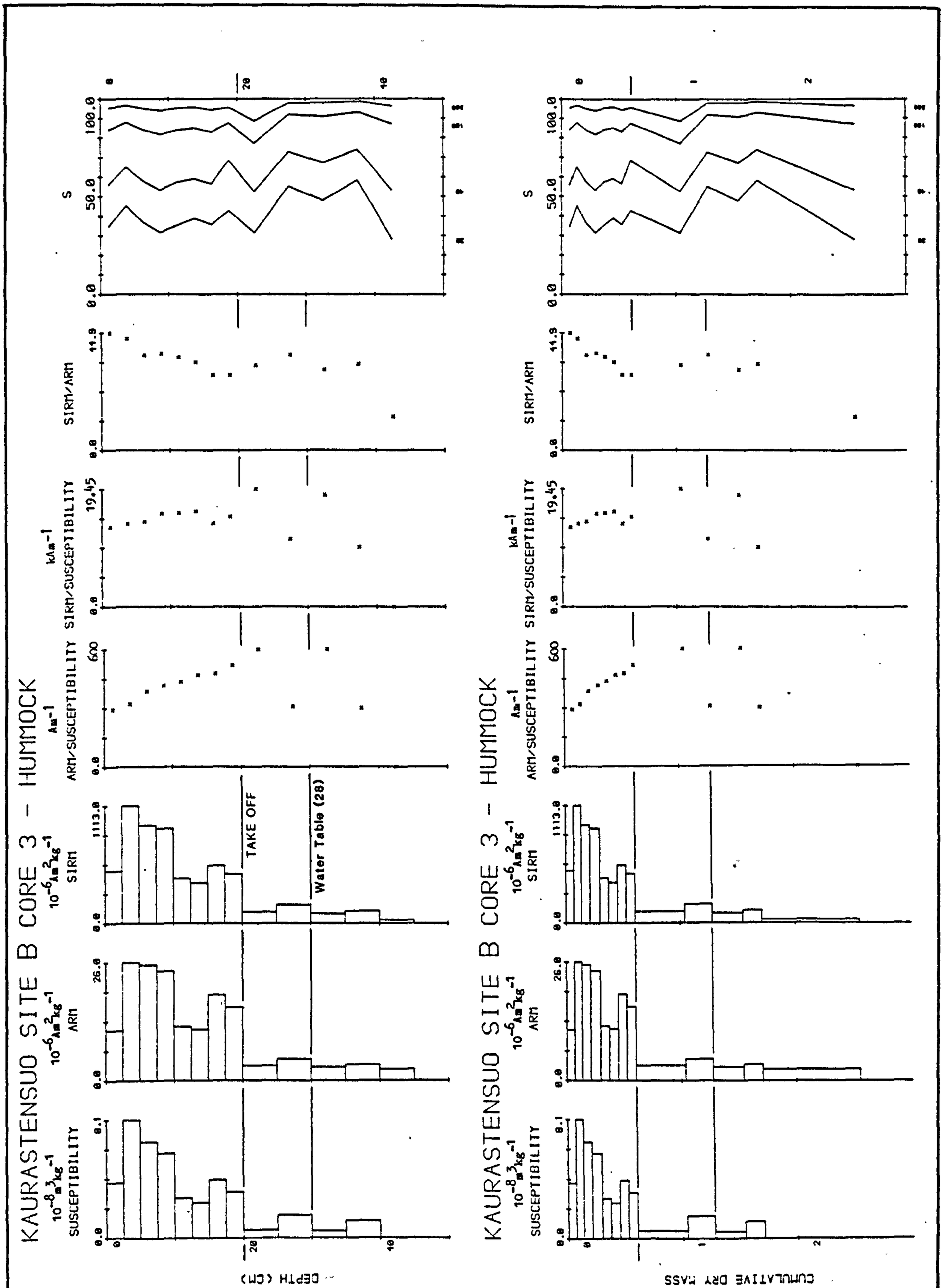


**Figure 2.8** Magnetic measurements of hummock core C3, site B (Bi), Kaurastensuo

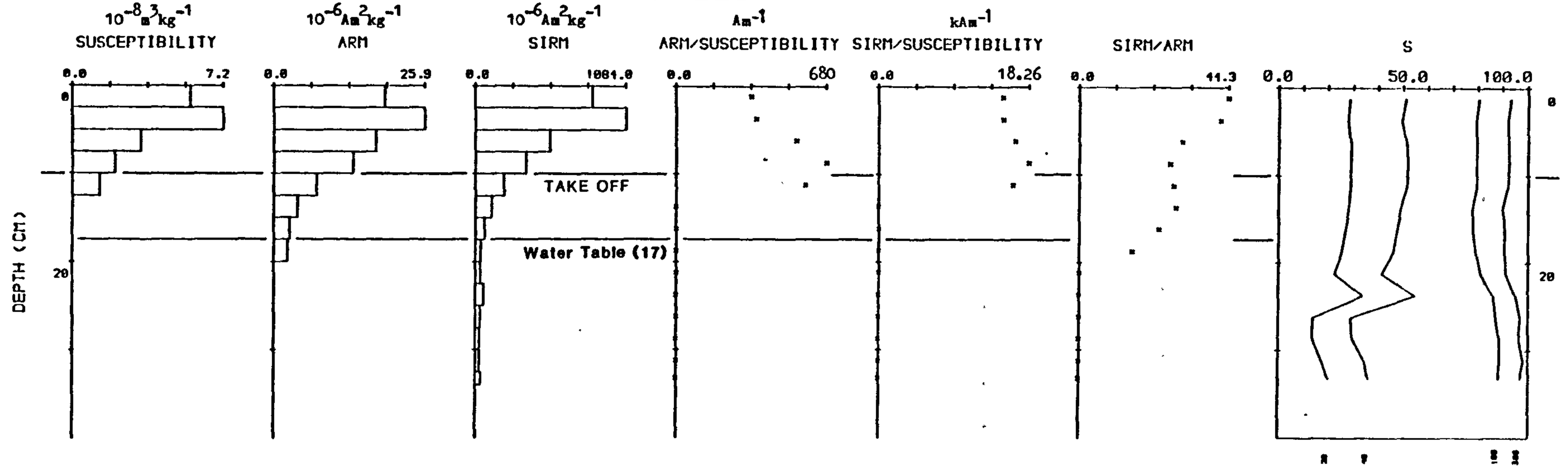


**Figure 2.9** Magnetic measurements of hollow core C4, site B (Bii), Kaurastensuo

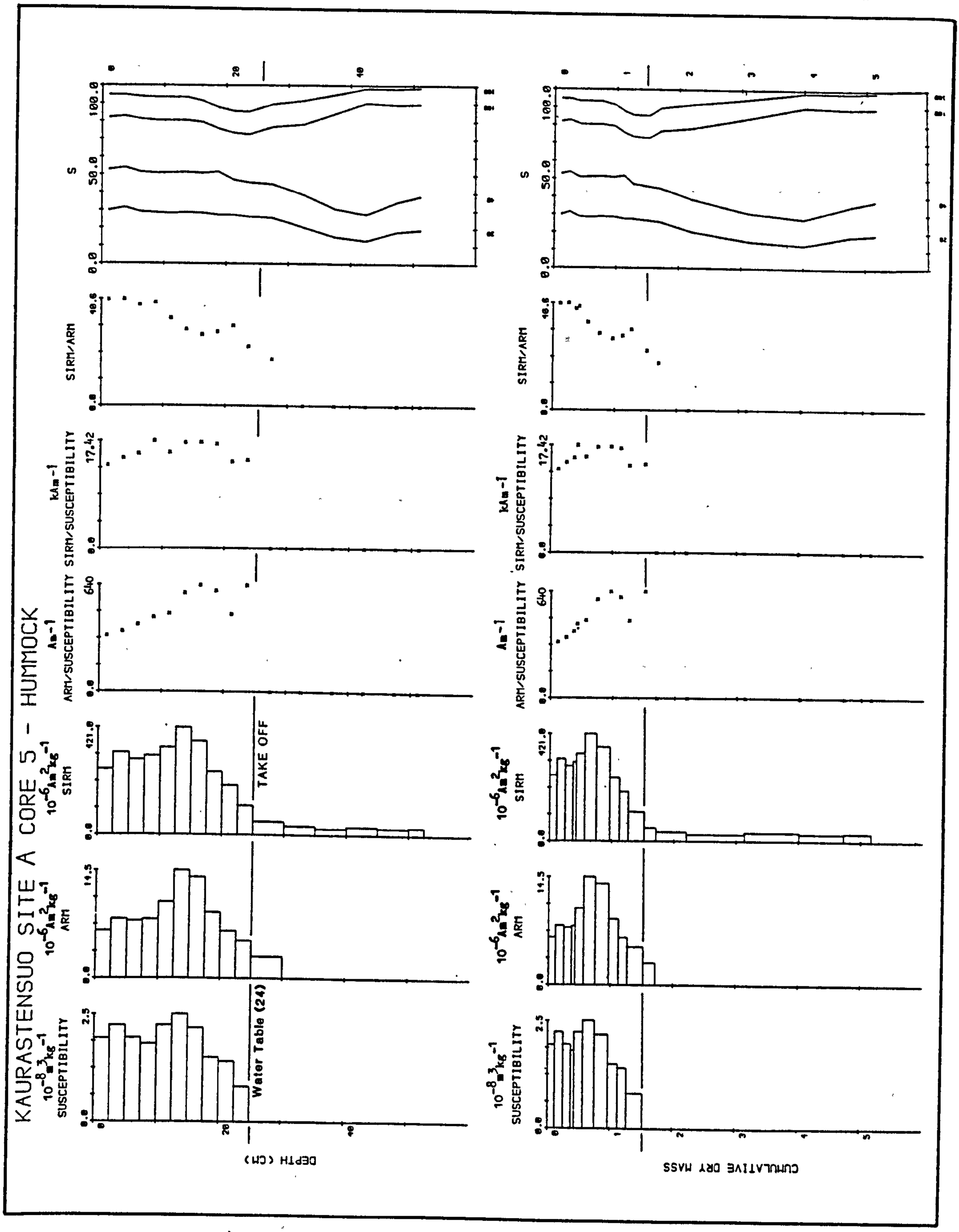


**Figure 2.10** Magnetic measurements of hummock core C5, site A (Ai), Kaurastensuo

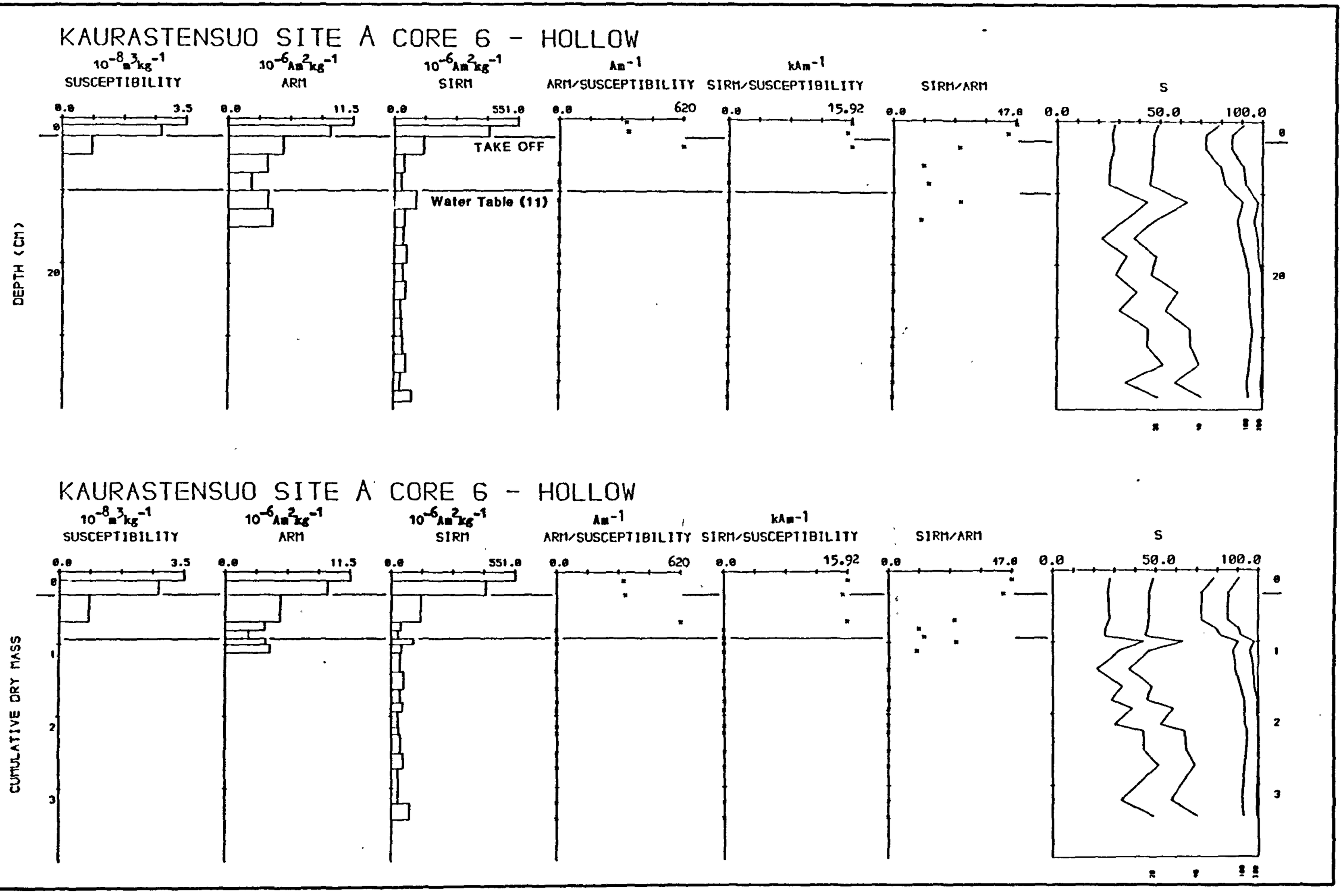


**Figure 2.11** Magnetic measurements of hollow core C6, site A (Aii), Kaurastensuo

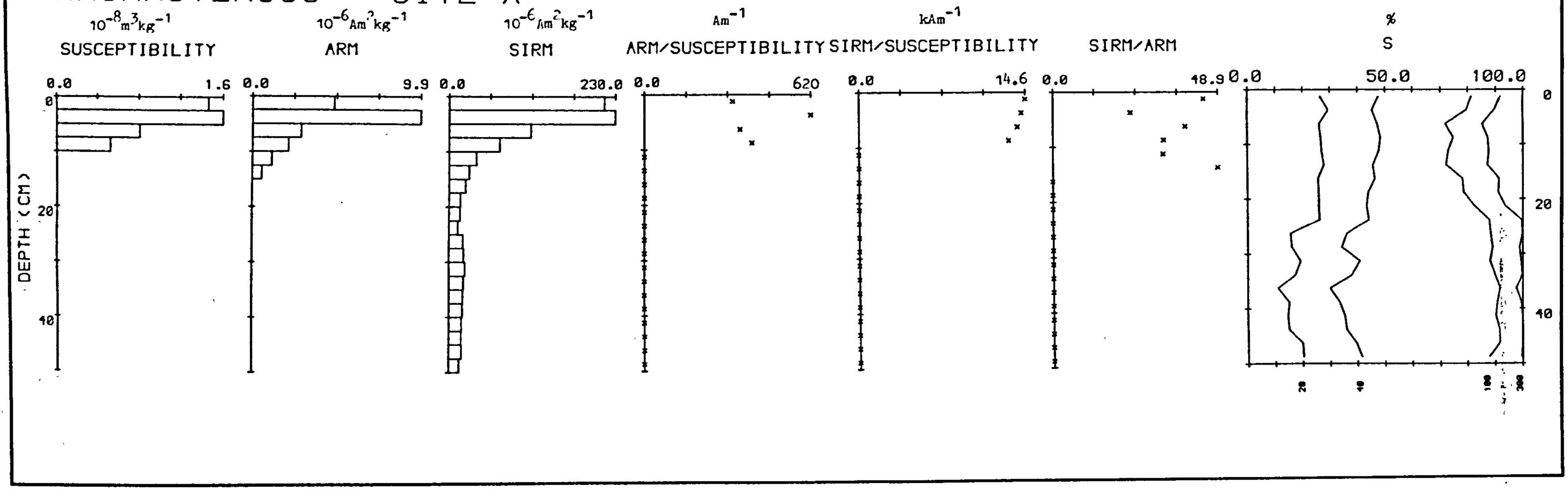


**Figure 2.12** Magnetic measurements of KAX (top 50cm), Kaurastensuo

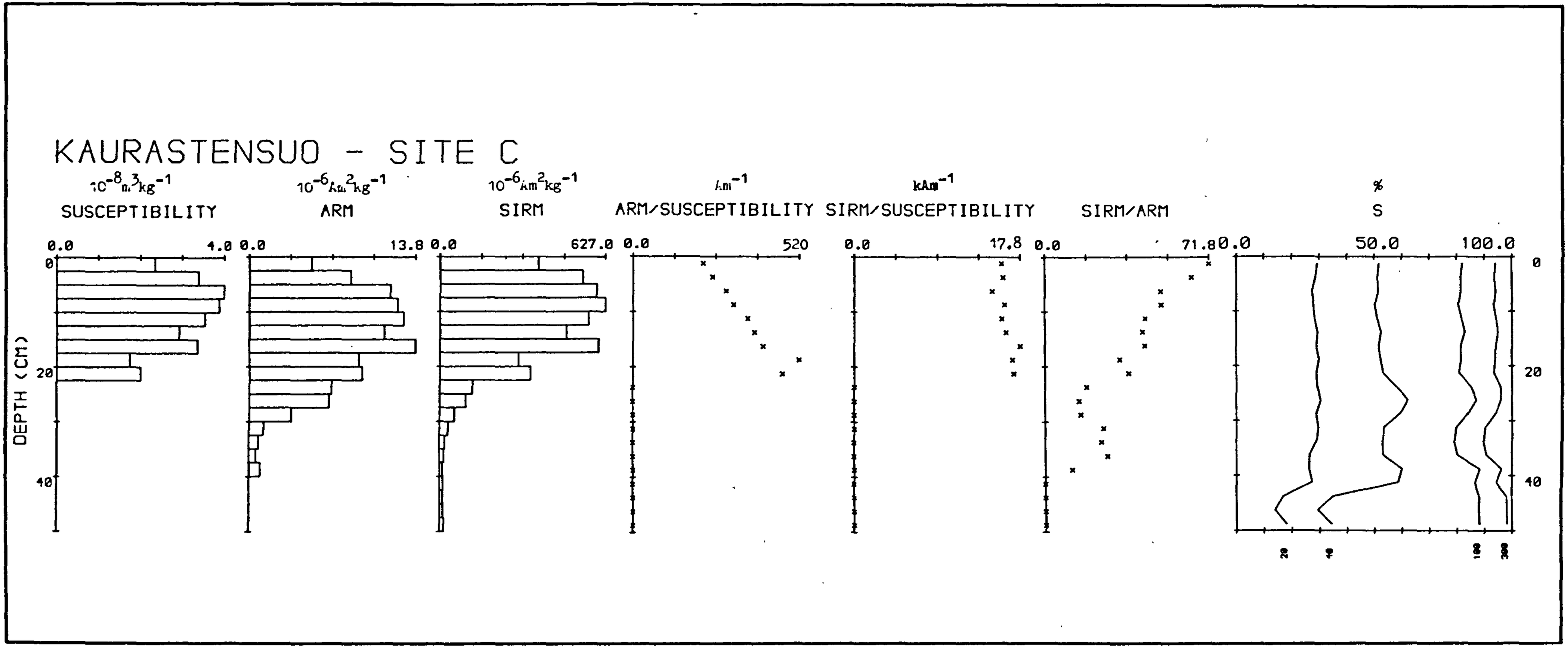


**Figure 2.13** Magnetic measurements of KAC (top 50cm), Kaurastensuo

lower than peak SIRM values above take-off.

SIRM/ARM values increase from the take-off point to the surface corresponding with a decrease in ARM/X (figs 2.6-2.13). The relationship between these ratios and qualitative changes in mineralogy and grain size are discussed in section 2.8.

The backfield ratios displayed in figs. 2.6-2.13 have been selected to display the maximum variation in demagnetisation remanence. There are three identifiable features within the ratios, evident in the majority or all of the cores. The coercivity of remanence curves for samples displaying these features are presented in fig. 2.14. The relative depths are given in Table 2.5 and a brief description of each is given below.

1. HH1

Present in the higher backfield ratios ($IRM_{-100mT}$/SIRM and $IRM_{-300mT}$/SIRM), this feature is represented by a shift toward lower percentage values, implying a resistance to demagnetisation, termed 'hardness' for convenience. The position of HH1 relative to the other two features , take-off and the water table varies from core to core although it is located closest to the surface in all cores. HH1 is not restricted to a single-slice increment, usually extending over 2-3 increments (5-7.5cm). The coercivity of remanence curves from the different samples and different cores vary little in relation to each other (fig. 2.14a) . The mineral assemblages exhibit $(B_0)_{CR}$ values of between 40-45mT, which compare with <100mT for samples containing (canted) antiferromagnetic assemblages. An antiferromagnetic component is present within samples dislaying this hardness feature, reflected by the resistance to demagnetisation in the first instance, and the inability of the sample to fully reverse saturate at high backfields ($IRM_{-850mT}$/SIRM) in the second.

**Table 2.5** Magnetic Features of Cores from Kaurastensuo
The table summarises the take-off depths within the SIRM profiles, including the depth of maximum SIRM values. The depths of three features taken from the reverse field ratios are also given: HH1 is a 'hard' feature in the high reverse fields, SS1 a 'soft' feature in the low reverse fields and LH2 a 'hard' feature within the low reverse fields.

| Core | Take-Off (cm) | Peak (cm) | HH1 (cm) | SS1 (cm) | LH2 (cm) |
|---|---|---|---|---|---|
| C1, Hum. | 17.5-20 | 7.5-10 | 30-35 | 35-40 | 45+(?) |
| C2, Hol. | 12.5-15 | 2.5-5 | 12.5-20 | 25-30 | 30-35 |
| C3, Hum. | 17.5-20 | 2.5-5 | 20-25 | 25-30/ 35-40 | 40-45+(?) |
| C4, Hol. | 7.5-10 | 2.5-5 | 12.5-22.5 | 22.5-25 | 25-30 |
| C5, Hum. | 22.5-25 | 2.5-5 | 20-22.5 | - | 35-45 |
| C6, Hol. | 2.5-5 | 0-1 | 1-5 | 10-12.5 | 15-17.5 |
| KAX, Hum. | 10-12.5 | 2.5-5 | 5-17.5 | 30-32.5 | 45-47.5 |
| KAC, Hum. | 22.5-25 | 7.5-10 | 30-37.5 | 37.5-40 | 42.5-50 |

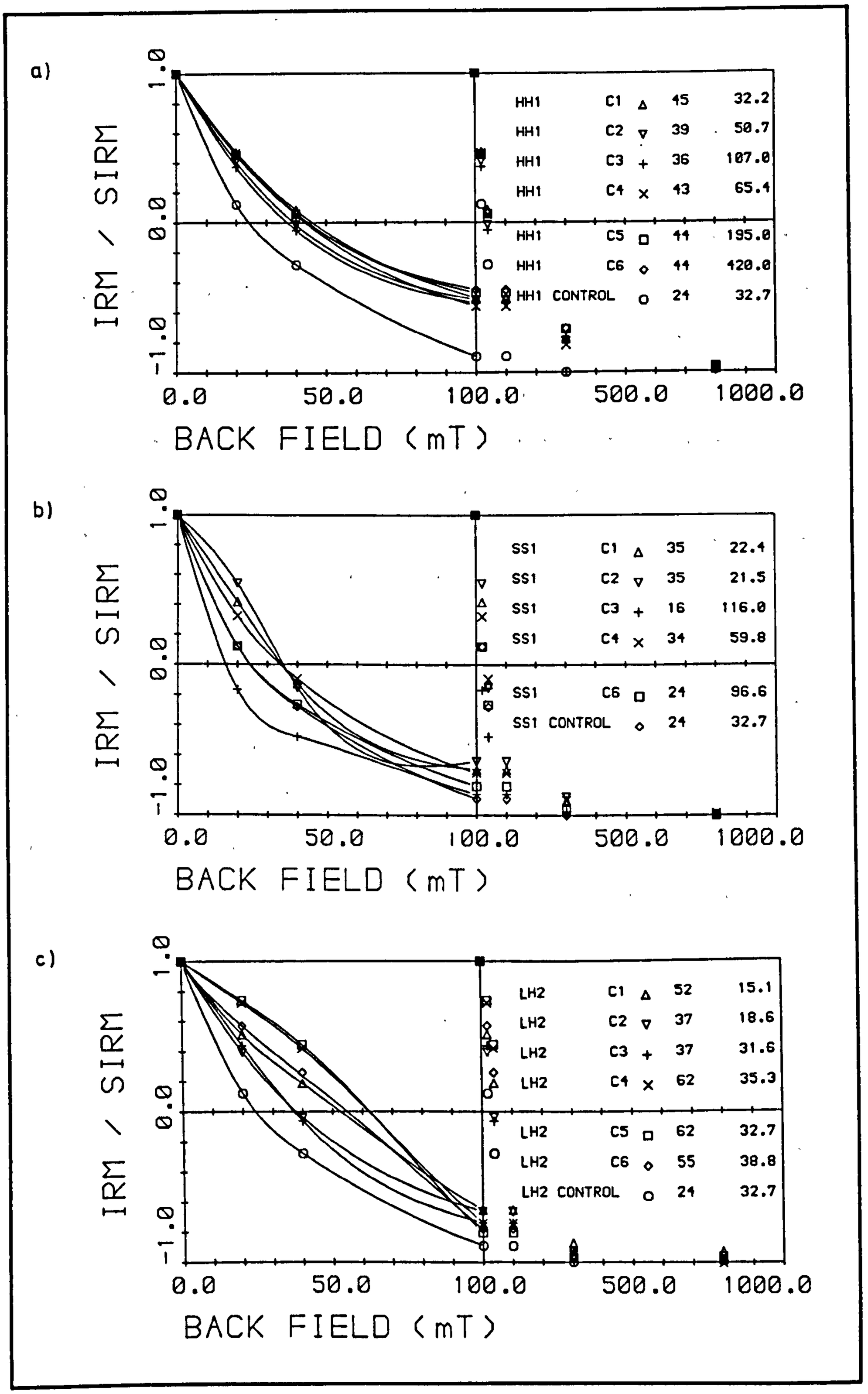


**Figure 2.14** Coercivity of remanence curves (linear plots) (cores C1-C6) of the backfield ratio features:
a) HH1, hardness feature in the higher backfield ratios, $IRM_{-100mT}/SIRM$ and $IRM_{-300mT}/SIRM$
b) SS1, soft feature in the lower backfield ratios, $IRM_{-20mT}/SIRM$ and $IRM_{-40mT}/SIRM$
c) LH2, hardness feature in the lower backfield ratios, $IRM_{-20mT}/SIRM$ and $IRM_{-40mT}/SIRM$

2. LH2

A second hardness feature present in the lower backfield ratios ($IRM_{-20mT}$/SIRM and $IRM_{-40mT}$/SIRM). LH2 appears much closer to the base of the profiles, being less evident than HH1 (eg. C1 and C3). This feature is marked by a divergence between the $IRM_{-40mT}$/SIRM and $IRM_{-100mT}$/SIRM ratios. The coercivity of remanence curves of samples displaying this feature show a greater variation in shape than those of HH1 (fig. 2.14b). This is evident in the wide range of the $(B_0)_{CR}$ values, 37-62mT. Values in the upper part of this range come from the hummock cores and those from the lower, from hollows.

3. SS1

This is denoted by a single sample 'spike', which is evident in all the cores, with the exception of C5. SS1 is present only in the lower backfields ($IRM_{-20mT}$/SIRM and $IRM_{-40mT}$/SIRM) and is represented by a marked increase in the percentage values of the respective ratios, implying the relative ease with which the samples acquire a demagnetisation remanence, termed 'softness' for convenience. It appears at an intermediate depth between the two hardness features and is strongly reflected in the concave shape of the coercivity of remanence curves in fig. 2.14c. The $(B_0)_{CR}$ values range between 16mT and 35mT.

The coercivity of remanence curves throughout individual cores may be divided into two groups. The first are the pre-take-off samples, which display no regular or uniform shape in curves or similar $(B_0)_{CR}$ values. The second are the post-take-off samples which display a strong similarity between samples within each core and also in post-take-off samples from one core to another. There is no discernable difference between hummock and hollow cores for these samples. The coercivity of remanence curves for KAC are presented in fig. 2.15 as an example of the similarity of this post-

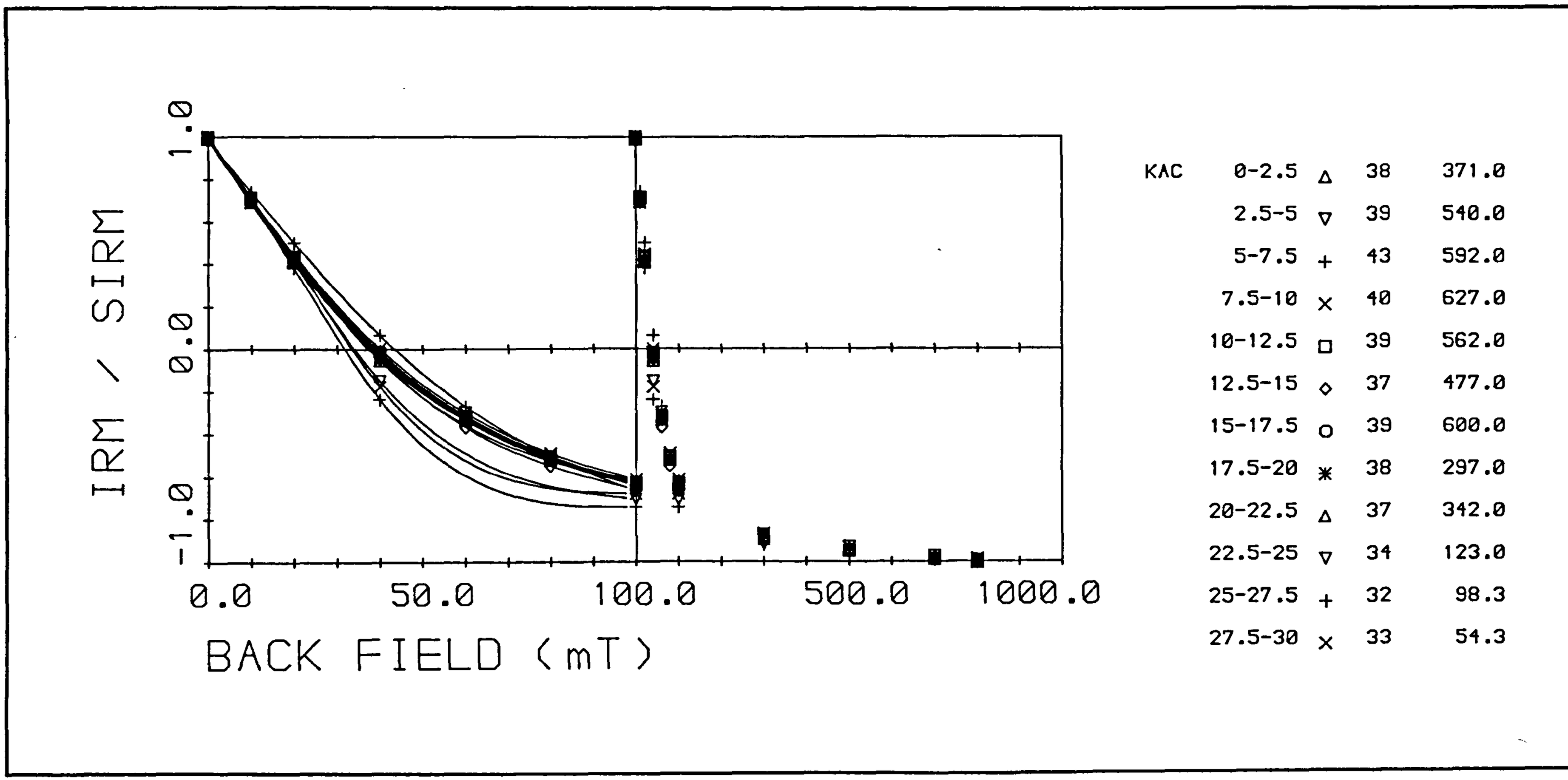


**Figure 2.15** Coercivity of remanence curves (linear plot) for KAC (0-30cm), Kaurastensuo

take-off group. The $(B_0)_{CR}$ values for samples within this group are typically between 38-40mT for all post-take-off samples in all cores at Kaurastensuo. The curve shapes for the pre-take-off samples range on either side of the post-take-off 'envelope'.

2.3.3 Age Relationships and the Magnetic Record

Slice volume SIRM ($SIRM_{VS}$) and Cumulative Deposition ($D_C$) are presented for cores C1-C6 in Table 2.6. Cumulative deposition represents a cumulative total of $SIRM_{VS}$ above a designated point, in this case, the take-off. $SIRM_{VS}$ is calculated as:

$$SIRM_{VS} = \frac{SIRM \times Ws}{Vs} \times Depth \qquad [2.2]$$

where: $SIRM = 10^{-6}Am^2kg^{-1}$

$Ws$ = Slice weight (g)

$Vs$ = Slice volume ($cm^3$)

Cumulative deposition is the sum of equation [2.2] for each slice above take-off:

$$D_C = \sum SIRM_{VS} \qquad [2.3]$$

Cumulative deposition is highest at site A toward the west side of the bog, decreasing through site B at the bog centre, to the lowest values at site C on the east side of the bog.

Using the data presented in Table 2.4, a minimum and maximum age for each slice may be determined, corresponding to the upper and lower limits of that slice respectively. The annual influx rates, are expressed as Mean Annual Deposition Rates ($10^{-6}Am^2yr^{-1}$). The mean deposition rate above take-off may be calculated by dividing $D_C$ by the

**Table 2.6** Volume SIRM ($SIRM_{VS}$), Cumulative Deposition ($D_c$) and SIRM Deposition ($SIRM_{DR}$) above Take-Off at Kaurastensuo

| C1, Hummock | | | C2, Hollow | | | KAC, Hummock | | | C3, Hummock | | |
|---|---|---|---|---|---|---|---|---|---|---|---|
| Depth (cm) | $SIRM_{VS}$ $10^{-6}Am^2$ | $SIRM_{DR}$ $10^{-6}Am^2yr^{-1}$ | Depth (cm) | $SIRM_{VS}$ $10^{-6}Am^2$ | $SIRM_{DR}$ $10^{-6}Am^2yr^{-1}$ | Depth (cm) | $SIRM_{VS}$ $10^{-6}Am^2$ | $SIRM_{DR}$ $10^{-6}Am^2yr^{-1}$ | Depth (cm) | $SIRM_{VS}$ $10^{-6}Am^2$ | $SIRM_{DR}$ $10^{-6}Am^2yr^{-1}$ |
| 0-3 | 32.9 | 3.3 | 0-2.5 | 43.5 | 5.4 | 0-2.5 | 13.3 | 4.4 | 0-2.5 | 24.4 | 4.07 |
| 3-5 | 12.5 | 2.78 | 2.5-5 | 43.4 | 5.6 | 2.5-5 | 24.7 | 4.94 | 2.5-5 | 53.2 | 10.6 |
| 7.5-10* | 38.7 | 7.04 | 5-7.5 | 30.5 | 6.1 | 5-7.5 | 23.0 | 6.4 | 5-7.5 | 48.5 | 6.93 |
| 10-12.5 | 35.0 | 7.4 | 7.5-10 | 51.1 | 4.6 | 7.5-10 | 29.0 | 5.4 | 7.5-10 | 53.8 | 6.0 |
| 12.5-15 | 29.1 | 5.82 | 10-12.5 | 36.4 | 2.38 | 10-12.5 | 25.3 | 5.1 | 10-12.5 | 23.6 | 3.37 |
| 15-17.5 | 33.2 | 5.53 | 12.5-15 | 9.1 | 1.01 | 12.5-15 | 20.8 | 5.2 | 12.5-15 | 21.0 | 3.0 |
| 17.5-20 | 38.1 | 4.76 | | | | 15-17.5 | 35.1 | 4.4 | 15-17.5 | 28.5 | 4.07 |
| | | | | | | 17.5-20 | 12.7 | 2.5 | 17.5-20 | 26.1 | 3.73 |
| | | | | | | 20-22.5 | 19.0 | 2.7 | | | |
| | | | | | | 22.5-25 | 10.7 | 0.56 | | | |
| $D_c$ $10^{-6}Am^2$ | 220 | | | 214 | | | 214 | | | 279 | |

| C4, Hollow | | | KAX, Hummock | | | C5, Hummock | | | C6, Hollow | | |
|---|---|---|---|---|---|---|---|---|---|---|---|
| Depth (cm) | $SIRM_{VS}$ $10^{-6}Am^2$ | $SIRM_{DR}$ $10^{-6}Am^2yr^{-1}$ | Depth (cm) | $SIRM_{VS}$ $10^{-6}Am^2$ | $SIRM_{DR}$ $10^{-6}Am^2yr^{-1}$ | Depth (cm) | $SIRM_{VS}$ $10^{-6}Am^2$ | $SIRM_{DR}$ $10^{-6}Am^2yr^{-1}$ | Depth (cm) | $SIRM_{VS}$ $10^{-6}Am^2$ | $SIRM_{DR}$** $10^{-6}Am^2yr^{-1}$ |
| 0-2.5 | 66.9 | 4.46 | 0-2.5 | 10.1 | 1.84 | 0-.25 | 21.4 | 1.26 | 0-1 | 7.5 | - |
| 2.5-5 | 253[1] | 2.71 | 2.5-5 | 10.0 | 2.22 | 2.5-5 | 30.2 | 1.37 | 1-2.5 | 21.3 | - |
| 5-7.5 | 55.6 | 2.06 | 5-7.5 | 5.2 | 1.04 | 5-7.5 | 25.2 | 1.4 | 2.5-5 | 34.3 | - |
| 7.5-10 | 29.0 | 1.93 | 7.5-10 | 3.0 | 0.6 | 7.5-10 | 11.7 | 3.9 | | | |
| | | | 10-12.5 | 2.0 | 0.29 | 10-12.5 | 34.2 | 1.37 | | | |
| | | | | | | 12.5-15 | 54.9 | 1.3 | | | |
| | | | | | | 15-17.5 | 56.7 | 0.93 | | | |
| | | | | | | 17.5-20 | 27.2 | 0.91 | | | |
| | | | | | | 20-22.5 | 19.2 | 0.8 | | | |
| | | | | | | 22.5-25 | 21.0 | 0.24 | | | |
| $D_c$ $10^{-6}Am^2$ | 405 | | | 30.3 | | | 302 | | | 63.1 | |

* 5-7.5cm is missing, therefore an average of 3-5cm and 7.5-10cm was used for $D_c$
** $SIRM_{DR}$ is not available for C6 (site A) as the chronological control is not reliable
1 Value is probably a spurious result based on anomalously high bulk density for this depth

number of years above take-off and multiplying by a factor of 10 to convert from $cm^2$ to $m^2$. Similarly this may be done for each slice:

$$SIRM_{DR} = \frac{SIRM_{VS}}{a} \times 10 \qquad [2.4]$$

where $SIRM_{DR}$ = Mean Annual Deposition Rate

$SIRM_{VS}$ = Slice volume SIRM

a = Number of years represented by the slice

The $SIRM_{DR}$ for each slice in cores C1-C6 is given in Table 2.6.

The age at take-off is calculated for cores C1-C4, KAX and KAC and these are presented along with the estimated magnetite deposition rates for each slice above take-off, in Table 2.7. The influence of hepatics and other non-Sphagnum plants in the surface layers of C5 and C6 at site A (Table 2.2) precluded the reliable estimation of age curves, and hence estimates of deposition above take-off. Calculation of 'magnetite' deposition rates are based on the method used by Oldfield et al. (1981). It is assumed that the SIRM of magnetite is 5 $Am^2kg^{-1}$. From the range of grain diameters observed in magnetic extracts Oldfield et al. (op cit) concluded that the calculations would yield a close approximation of the magnetite concentrations, although estimates will be low for samples with a modal magnetite grain size larger than 6μm, and vice versa. These results are compared and discussed with particular reference to Karpansuo (Oldfield et al., op. cit.) in section 2.9.

### 2.3.4 Ash Residue and Magnetic Concentration Relationships

The ash content of cores C1-C6 (fig. 2.2) varies between a minimum at the base of the core, eg. 0.7% in C3, and a maximum at or near the surface, eg. 3.11% in C4. These values are close to the range of 1-4.2% reported by Vuorela (1983) for remote Finnish sites. The inorganic content

**Table 2.7** Estimated Magnetite Deposition above Take-Off at Kaurastensuo.
The lower depth of each slice has been calculated as a given age using the growth rate equation [2.1]. The cumulative influx above the oldest date in each core is also given. Data for cores C5 and C6 (site A) are omitted as the species composition of the cores does not meet the requirements of the equation.
M = $10^{-6}$kg.m$^{-2}$ atmospheric 'magnetite'

| C1, Hummock | | C2, Hollow | | C3, Hummock | |
|---|---|---|---|---|---|
| Date | 'M' | Date | 'M' | Date | 'M' |
| 1978 | 0.66 | 1979 | 1.08 | 1980 | 0.814 |
| 1971 | 0.556 | 1971 | 1.12 | 1978 | 2.12 |
| 1961 | 1.41 | 1964 | 1.22 | 1968 | 1.386 |
| 1956 | 1.48 | 1957 | 0.92 | 1961 | 1.2 |
| 1950 | 1.16 | 1943 | 0.476 | 1952 | 0.674 |
| 1942 | 1.11 | 1930 | 0.202 | 1946 | 0.6 |
| 1932 | 0.952 | | | 1938 | 0.814 |
| | | | | 1932 | 0.746 |
| Cumulative influx $10^{-6}Am^2$ | 54.1 | | 37.6 | | 49.6 |

| C4, Hollow | | Kax, Hummock | | KAC, Hummock | |
|---|---|---|---|---|---|
| Date | 'M' | Date | 'M' | Date | 'M' |
| 1975 | 0.892 | 1978 | 0.368 | 1981 | 0.88 |
| 1957 | 0.542 | 1967 | 0.444 | 1977 | 0.988 |
| 1932 | 0.412 | 1957 | 0.208 | 1973 | 1.28 |
| 1925 | 0.386 | 1947 | 0.12 | 1968 | 1.08 |
| | | 1936 | 0.058 | 1963 | 1.02 |
| | | | | 1959 | 1.04 |
| | | | | 1953 | 0.88 |
| | | | | 1946 | 0.5 |
| | | | | 1940 | 0.54 |
| | | | | 1928 | 0.112 |
| Cumulative influx $10^{-6}Am^2$ | 29.9 | | 10.6 | | 38.9 |

Background Deposition (pre-1931) = $0.081 \pm 0.061$ $10^{-6}$kg.m$^{-2}$yr$^{-1}$

of all the cores increases towards the surface in all the cores from background values of ca.1% to surface or near surface peaks. The correlation (r) and causal relationship ($r^2$ and $r^2_{DF}$) have been determined for the ash residue and SIRM values in all the cores. These have been arranged on a comparative basis for hummocks and hollows, different sites and individual cores. The samples sets have been divided further into subsets of samples above take-off in each core. The results of these statistical relationships are presented in Table 2.8 and discussed in section 2.7. The relationship between ash residues and SIRM for KAX and KAC along with the regression equation for each relationship (fig. 2.16), are also discussed in section 2.7.

## 2.4 Deposition and the Magnetic Record

### 2.4.1 Summary of Depositional Theory

The following sub-section provides a brief summary of the depositional processes which are known to occur over ombrotrophic peat bogs. Variations in surface vegetation are fundamental in any appraisal of depositional processes operating across the bog surface. Clough (1975) observes that the method of particulate retention is probably via an ion exchange process which is retained even on dead moss, as at site A (C5). Lycopodium spores (32µm) were shown to be deposited almost wholly on the windward side of mosses. At Kaurastensuo the dominant wind direction is westerly during the short summer period.

Higher deposition values have been ascribed to the greater hairiness of the moss structure by Clough (op. cit.), which reduce the bounce-off of the larger particles especially at higher wind speeds. At Kaurastensuo, the windspeed factor is assumed to be negligible given its limited importance to particles >20µm (Chamberlain, 1966; Clough, op. cit.). Inorganic ash

**Table 2.8** Correlation of Ash, SIRM and X at Kaurastensuo. Pearson's product moment correlation for different locations, cores and hummock-hollow microtopography, where: n= number of cases, r= coefficient, $r^2$= coefficient of determination and $r^2_{DF}$= coefficient of determination adjusted for the degrees of freedom.

| VARIABLE | Y = ASH, X = SIRM All Samples | | | Y = ASH, X = SIRM Above Take-Off | | | | Y = ASH,X = SIRM Below Take-Off | | Y = ASH,X = X, SIRM | | | Y = ASH,X = SIRM All Samples | | |
|---|---|---|---|---|---|---|---|---|---|---|---|---|---|---|---|
| | n | r | $r^2$ | n | r | $r^2$ | $r^2_{DF}$ | n | r | n | $r^2$ | $r^2_{DF}$ | n | r | $r^2$ |
| All 8 Cores | 83 | 0.54** | 29 | 53 | 0.29** | 8 | - | 30 | 0.125 | - | - | - | 58 | 0.35** | 12 |
| All Hummocks (5) | 55 | 0.42** | 18 | 40 | 0.06 | 0 | 0 | 15 | 0.052 | 44 | 3 | 0 | 44 | 0.15 | 2 |
| All Hollows (3) | 28 | 0.75** | 56 | 13 | 0.70** | 49 | 45 | 15 | 0.265 | 14 | 60 | 52 | 14 | 0.75** | 56 |
| Site A (C5, C6) | 18 | 0.23 | 5 | 13 | 0.11 | 1 | 0 | 5 | -0.030 | 13 | 38 | 26 | 13 | 0.22 | 5 |
| Site B (KAX, C3, C4) | 27 | 0.49** | 24 | 17 | 0.21 | 4 | 0 | 10 | 0.273 | 21 | 17 | 7 | 21 | 0.34 | 12 |
| Site C (KAC, C1, C2) | 38 | 0.78** | 61 | 23 | 0.63** | 40 | 37 | 15 | -0.372 | 24 | 40 | 34 | 24 | 0.61** | 37 |
| Cores C1-C6 | 63 | 0.64** | 41 | 38 | 0.43** | 18 | 16 | - | - | - | - | - | 45 | 0.51** | 26 |
| KAX & KAC | 20 | 0.29 | 8 | 15 | -0.14 | 2 | 0 | - | - | - | - | - | 13 | -0.35 | 12 |
| KAC (hummock) | 14 | 0.81** | 66 | 10 | 0.46 | 21 | 11 | - | - | - | - | - | 9 | 0.14 | 2 |
| KAX (hummock) | 6 | 0.97** | 94 | 5 | 0.97** | 94 | 91 | - | - | - | - | - | 4 | 0.95* | 90 |
| C1 (hummock) | 13 | 0.79** | 62 | 7 | 0.31 | 10 | 0 | - | - | - | - | - | 9 | 0.72* | 52 |
| C2 (hollow) | 11 | 0.92** | 85 | 6 | 0.89* | 79 | 74 | - | - | - | - | - | 6 | 0.86* | 74 |
| C3 (hummock) | 13 | 0.62* | 38 | 8 | 0.30 | 9 | 0 | - | - | - | - | - | 12 | 0.53 | 28 |
| C4 (hollow) | 8 | 0.94** | 88 | 4 | 0.93 | 86 | 79 | - | - | - | - | - | 5 | 0.92* | 85 |
| C5 (hummock) | 11 | -0.13 | 2 | 10 | -0.37 | 14 | 3 | - | - | - | - | - | 10 | -0.20 | 4 |
| C6 (hollow) | 7 | 0.45 | 20 | 3 | 0.40 | 16 | 0 | - | - | - | - | - | 3 | 0.44 | 19 |

* Significant at the 0.05 level

** Significant at the 0.01 level

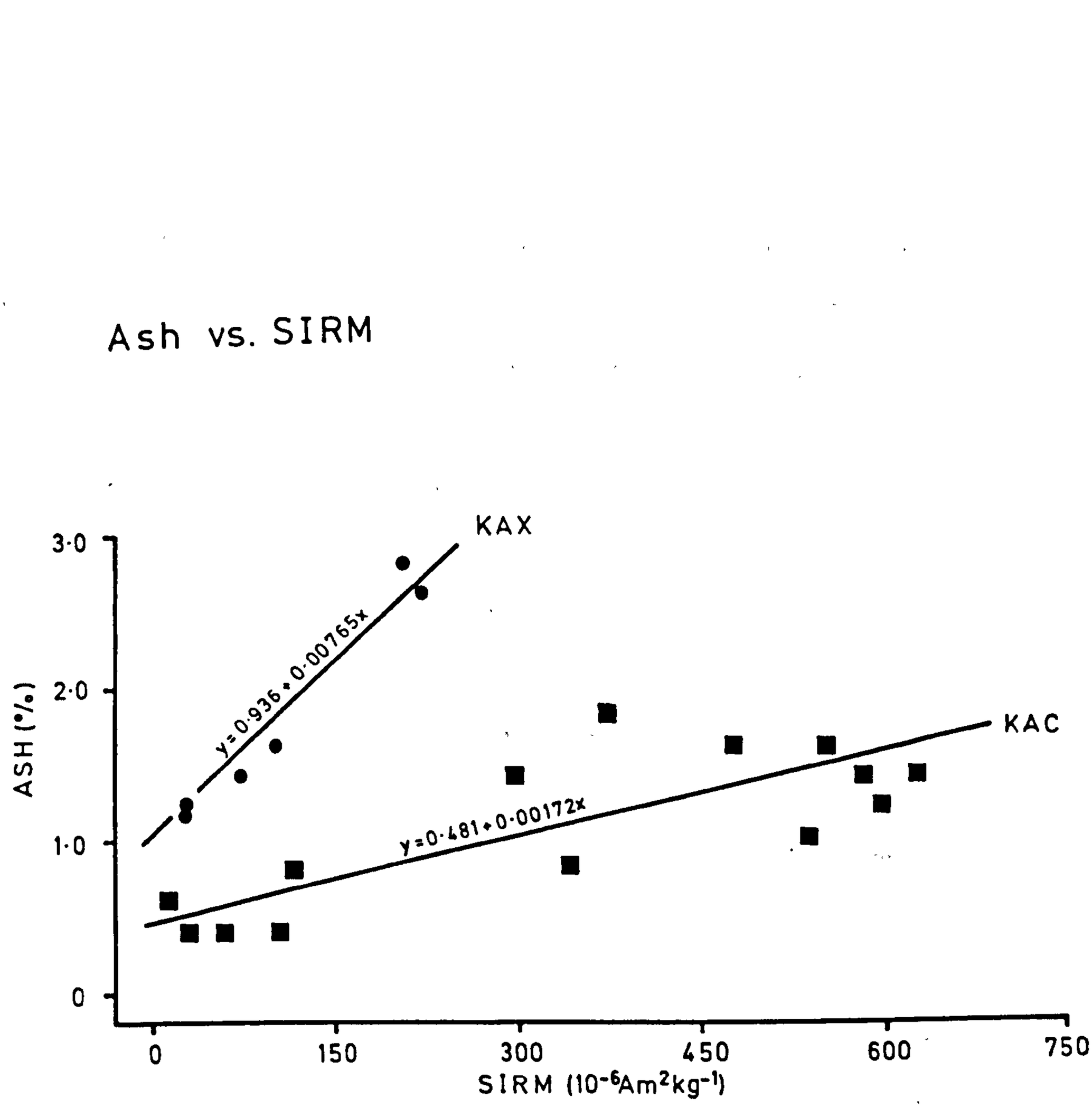


**Figure 2.16** Relationship between ash content and magnetic concentrations. Relationship between ash content and SIRM for KAX (Pearson's r= 0.97) and KAC (Pearson's r= 0.81). The correlation coefficient for KAX and KAC combined is r= 0.29.

analysis and SEM data on magnetic extracts have shown the dominant size range to be within 1-10µm.

The actual process of atmospheric deposition on to vegetated surfaces is a function of the interactions between the transfer process (how particulates arrive at the surface); atmospheric conditions (windspeed, tolerance, humidity and temperature); particulate geometry (size, shape and surface structure); and the sink (surface geometry, vegetation type and plant moisture). Once in contact with the vegetation surface, other processes occur due to interactions caused by particle geometry and surface vegetation. These include bounce-off, blow-off, reinsertion and resuspension (Davis, 1973). Particulate deposition may occur either as **dry** or **wet** deposition. In the case of **wet** deposition, particle scavenging by impaction for particles >5µm (Hales, 1983) and diffusion for micron and sub-micron size ranges (Prupacher & Klett, 1978) can lead to a flushing of particles from the atmosphere onto the bog surface. With **dry** deposition the same processes of diffusion and impaction help particles penetrate the viscous sub-layer a few millimetres above the vegetation surface (Fowler, 1984). Sedimentation from the atmosphere, under the influence of gravity accounts for a small fraction of aerosols (Whitby, 1978) and is valid only for the largest particles.

The concepts of **trapping efficiency** (Cp) and **deposition velocity** (Vg), proposed by Gregory (1961) and Chamberlain (1953) respectively, are important when considering the particle filtering effect of vegetation surfaces. A definition of Cp is given by:

$$Cp = N/(x_v A) \qquad [2.5]$$

where N = Number of particles caught

x = Concentration of particles (per $m^2$ multiplied by the duration of exposure in seconds)

A = Area of obstacle ($m^2$)

v = Windspeed ($ms^{-1}$)

The deposition velocity is more a function of the surface of the sink, in this case the bog surface, and whether it is wet or dry. Deposition velocity (Vg) is defined as:

$$Vg = Nx/A \qquad [2.6]$$

therefore the trapping efficiency (Cp) in equation [2.5] may be redefined:

$$Cp = Vg/v \qquad [2.7]$$

Changes in surface vegetation across the bog, and therefore in surface resistance to deposition affect the controlling 'resistance' to particle deposition (Sehmel, 1971). Therefore, with changes in species composition one would expect a variation in deposition according to the ability of a particular vegetation type to trap particles, for example, the amount of cover provided by vascular plants on hummocks or hollows. The varying roughness factor of differing vegetation types, termed [Zo] by Sehmel (op. cit.) also disturbs the ordered laminar flow directly above the deposition surface. This subsequently affects deposition velocities (Vg) and hence total concentrations of particles deposited.

2.4.2 Deposition at Kaurastensuo

Cumulative deposition is higher in the respective hummocks and hollows towards the west side of the bog (site A) than on the east side (site

C). The microtopographical aspects of hummocks and hollows are discussed in section 2.5 (Table 2.6). If this trend is real, given the limited number of sampling locations, then plausibly it may be explained by the prevailing wind direction (westerly), taking account of the considerations in deposition made in sub-section 2.4.1. From the pattern of deposition at Kaurastensuo, it would appear that any trend in selective deposition across the bog is a function of location, wind direction and vegetation type notwithstanding any variations in particle size geometry.

The basis for calculating cumulative deposition ($D_c$) is provided in Doyle et al. (1976) and Oldfield et al. (1978, 1979a, 1981). They concluded that the dominant sources of magnetic atmospheric particulates are of anthropogenic origin and that an increase in anthropogenic emissions has resulted in the often sharp inflexions noted within the upper peat layers in British and Finnish sites. The increase in influx of these minerals has been by up to three orders of magnitude since the first widespread use of fossil fuel for industrial and domestic purposes (Oldfield et al., 1978). Cumulative deposition values for recent peat of a constant surface area are therefore interpreted as being proportional to the rate of atmospheric input of anthropogenically derived magnetic particulates. The cumulative deposition for site C is similar for all three cores (Table 2.6). Site B displays greater variation between the cores, for example, the cumulative deposition above take-off at KAX is almost 6 times less than that of the other hummock core (C3) at the same site. This is due mainly to the low initial SIRM concentrations coupled with a relatively shallow take-off point in KAX. The core KAX also displays some of the highest growth rates, which has the effect of increasing the length of the magnetic record under normal conditions (cf. section 2.5). With the exception of KAX, the cumulative deposition patterns suggest a slightly higher deposition rate in

the hummocks than in the hollows. This conclusion is also drawn by Oldfield et al. (1979a) on a much larger scale, with over an order of magnitude difference between the hummocks and the hollows, for sites located near industrialised areas of South Lancashire, England.

The deposition rates for the whole bog are low in comparison with bogs from other parts of Finland (Oldfield et al., 1981). These comparisons will be discussed in more detail in section 2.8.

## 2.5 Effects of Growth Rates and Vegetation on the Magnetic Record

The surface vegetation pattern on ombrotrophic mire crowns forms a small scale mosaic that gives rise to spatial variations within the microtopography (Oldfield et al., 1979). Hummock and hollow complexes characteristic of NorthWest Eurpoean bogs are an example of such variations. Small-scale relief patterns of up to 1m amplitude are common within an area of $10m^2$ (Table 2.2). The relief may be emphasised by the form of vegetation growing in the different habitats, such as Sphagnum pools and hollows, or tussocky sedges (eg. E. vaginatum) crowning hummocks. There are also differences within the habitats of species from one moss family, for example, Sphagnum spp. and their responses to changes in pH. There is a progression from S. cuspidatum which prefers wet, less acid habitats (pools and hollows) through to S. papillosum, S. fuscum and S. acutifolum which prefer drier more acidic habitats (Clymo, 1963). The cores from Kaurastensuo are predominantly composed of S. fuscum, a hummock-forming species. This mosaic of vegetation creates variations in the surface roughness which affects the ability of the respective surfaces to trap particulates, and complicates the pattern of spatial variations in deposition densities. A further consideration is the variation in relative contributions from particulates trapped from dry eddy

diffusion or from wet fall-out (sub-section 2.4.1).

The problem of differing rates of entrapment is partially resolved by the use of cores consisting mainly of the species S. fuscum, similar to that used in the growth rate equation [2.1] (Table 2.2). Only core C6 contained no S. fuscum within the surface layers, hence its omission from subsequent considerations. Having 'standardised' the species composition of the cores as far as possible, the variation in habitat will produce differing growth rates which will affect the magnetic record in that particular core. This effect may be seen in the different depths of the take-off point noted within the cores (figs. 2.6-2.13).

Clymo (1970) noted that the term 'growth' is ill-defined, though an element of irreversible increase is usually involved. Not all the methods used in estimating growth can always be related to production terms. Since there is no clear division between live plant, dead plant and peat, the terms 'standing crop' and 'biomass' have no useful meaning when applied to peat. The term 'growth' is used here within the context of net vertical height increase as defined by the equation [2.1].

At Kaurastensuo the hummocks exhibit faster growth rates than their respective hollows. This conclusion is the same for average core growth rates and more precisely, for slice increment growth rates and surface samples. If the take-off point within the SIRM profiles is interpreted as a synchronous horizon (sections 2.8 and 2.9), then the effect on the magnetic record is to extend the profile over greater depths in the hummocks (Table 2.5). The exception at Kaurastensuo is KAX which exhibits high surface growth rates ($5.2 \pm 0.5 mm.yr^{-1}$) and a shallow take-off point (10-12.5cm). There are also differing growth rates within a core, evident from Table 2.3. The effects of these differing growth rates are noticeable when the magnetic profiles are plotted against cumulative dry mass in figs. 2.6-2.11

(C1-C6). Only in KAC and KAX are the growth rates consistent from one slice increment to the next throughout the core. The uniformity of the bar widths downprofile is analogous to consistent growth rates. For example, the top 20cm (in 2.5cm slices) of C3 (fig. 2.8) indicates the consistency of growth rates within that particular section of the core. Conversely the variation in bar widths displayed in core C5 (fig. 2.10) is a reflection of the variation within the growth rates for the top 25cm of that core. This within-profile variation is also evident in the varying curve shapes noted in fig. 2.3. Consistent growth rates are represented by a straight line response, the gradient of which is a function of the growth rate (eg. KAX, KAC).

Maximum growth rates are exhibited within the top 10-15cm (with the exception of C6) which is similar to the decrease in values from the surface downwards noted by Pakarinen & Tolonen (1977) in the top 10cm of profiles from two southern Finnish bogs, Kuhmoinen and Karpansuo.This apparent decrease in growth rates has been linked with the humification process and autocompaction (Aaby & Tauber, 1975) although evidence from KAX and KAC (Table 2.2) indicates that humification remains between H1 and H2 for the top 60cm of both cores.

There is a reasonable degree of similarity between the growth rate data presented by Tolonen (1985, pers. comm.) and the surface samples from cores C1-C5. The range of 4.01 - 1.32mm.yr$^{-1}$ for C1-C5 compares with the value of 2.44mm.yr$^{-1}$ obtained by Tolonen. However, if only the hummocks are used then the range is slightly higher, 4.01 - 2.49mm.yr$^{-1}$. These rates display the variation noted by Pakarinen & Tolonen (op. cit.) of growth rates with differing location on the bog surface, even from adjacent hummocks (eg. KAX and C3).

Higher surface bulk density values in the hollows are a result of the

slower growth rates (Clymo, 1965). This results in a greater accumulation of dry mass per unit area of a given depth below the surface, a feature noted by Aaby & Tauber (1974) and Tolonen (1977). The extremely small growth rates at the surface of C6 are interpreted as a result of the colonisation by hepatics and lichens on dead Sphagna. There is a possibilty that the tightly packed capitula of the Sphagna affect the surface bulk density values and hence the vertical height increase of that slice (Clymo, 1983). However, this effect is assumed to be minimal, given the thickness of the surface slice (2.5cm or more with the exception of C6, cf. Table 2.1), compared with the thickness of the capitula (ca. 0.5cm).

## 2.6 Water Table Movements in Relation to the Magnetic Record

There are two possible ways in which the water table may influence the magnetic record within the ombrotrophic peat bog. First, there is the physical displacement of particles within the peat column by fluctuating levels within the water table. This is dependent upon the compactness of the peat layers, which in turn is influenced by the growth rates and accumulation of organic matter. It is assumed that cores with faster growth rates and lower accumulation will be more susceptible to this form of influence, for example, cores from rapidly growing hummocks such as KAC and KAX (Table 2.3). The second possible influence is the chemical change and dissolution of magnetic particles below the water table as a result of interaction with chelating agents bound within the acid solution in the peat.

An extensive monitoring programme by the Department of Botany, University of Helsinki, at Kaurastensuo has provided water table data for Kaurastensuo (fig. 2.17). This shows cumulative frequency curves for hummock and hollow observation wells at Kaurastensuo. It is believed that

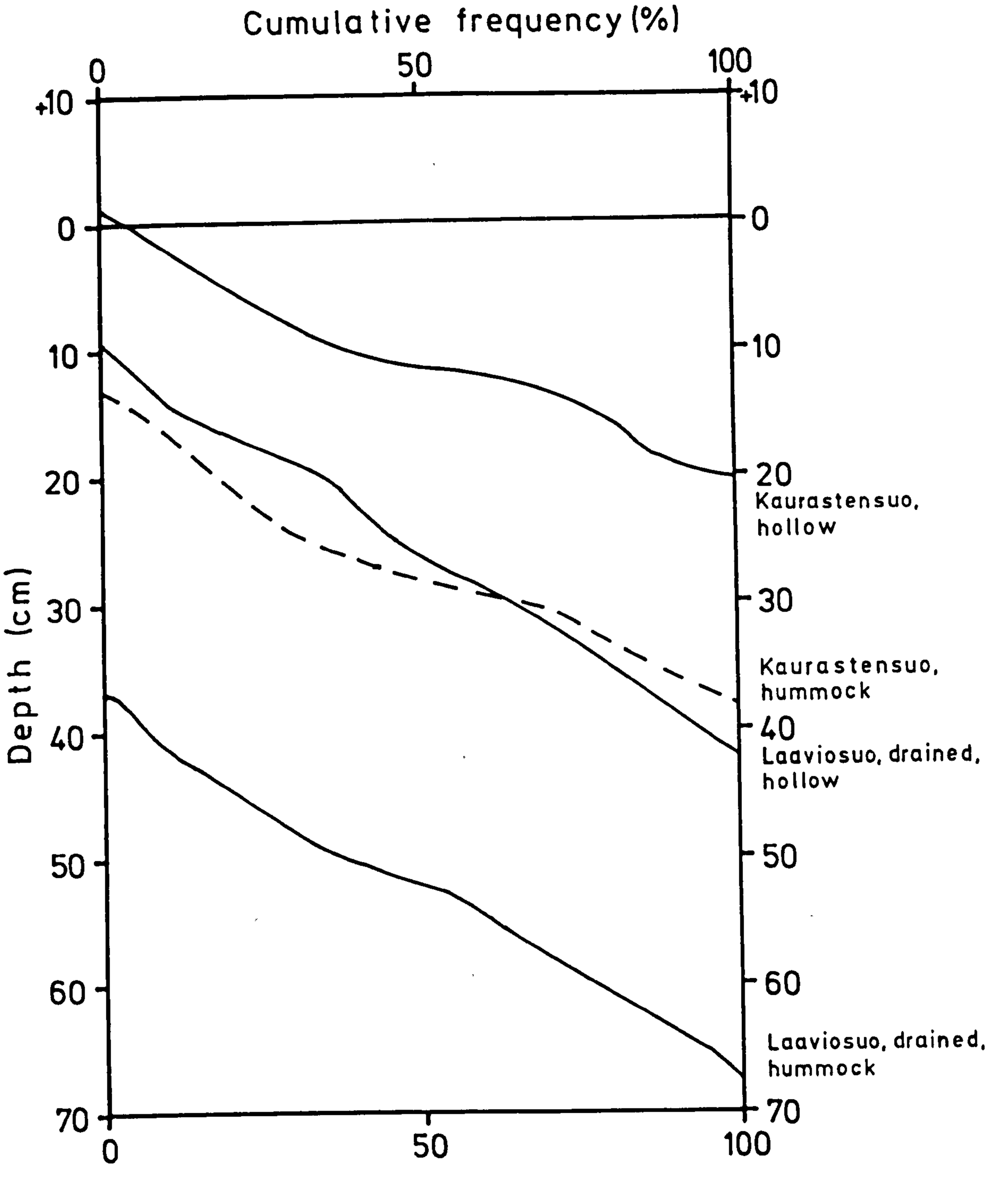


**Figure 2.17** Water table fluctuations at Kaurastensuo and Laaviosuo, 1983. The cumulative frequency curves represent the proportion of measurements showing a water table at, or above, a given level in hummocks and hollows.

the water table at Kaurastensuo behaves synchronously over different parts of the bog depending on topography (Reinikainen et al., 1984). Therefore, the data are extrapolated across to provide seasonal minimum and maximum depths of the water table at the 8 core sites (Table 2.9). The water table fluctuations are based on measurements taken at the time of sampling in August, 1983. These are also presented in Table 2.9. The bog exhibits a wide range of water table movements throughout the year. Rapid fluctuations occur in late April -early May as a result of the spring melt, increasing the total input of water or 'meteoric recharge' (Ingram, 1983). Further fluctuations occur around late July -early August when storage in the acrotelm is at its lowest due to minimal summer meteoric recharge and maximum evapotranspiration rates. In winter, the precipitation is stored as snow on the surface of the bog in sub-zero temperatures. The data in fig. 2.17 and Table 2.9 indicates that at some stages during the year the bog surface becomes saturated, with all but the tallest hummocks being submerged.

Such rapid fluctuations may promote movement of particles within loosely compacted Sphagnum cores. Therefore, if any major displacement of particles were occurring it would be reflected in the proximity of significant features of the magnetic profiles (notably the take-off point and maximum concentration values) to the water table. For example, with low water tables there is a possibility that particles could be displaced downwards as the plant structure shrinks. This would lead to a loss of moisture, so increasing the interstitial pore space. There is no evidence of this occurring to any noticeable degree in the cores. For example, the core KAX (fig. 2.12) has the lowest surface bulk density values, indicating a low degree of compactness. The magnetic profiles from KAX (fig. 2.12) exhibit surface peaks in spite of this. The effect on the magnetic record is assumed

**Table 2.9** Water Table Data for Kaurastensuo

| Core | Depth on 22-8-83 (cm) | Estimated Minima (April) (cm) | Estimated Maxima (July/August) (cm) |
|---|---|---|---|
| C1, Hum. | 35 | 18 | 42.5 |
| C2, Hol. | 24 | 7 | 28.5 |
| C3, Hum. | 28 | 11 | 35.5 |
| C4, Hol. | 17 | 2 | 23.5 |
| C5, Hum. | 25.5 | 8.5 | 33 |
| C6, Hol. | 11 | ca.4 | 17.5 |
| KAX, Hum. | 32.5 | 15.5 | 40 |
| KAC, Hum. | 30.5 | 13.5 | 38 |

to be negligible although further evidence is needed before any positive statement can be made. There is also no evidence from the magnetic profiles to indicate any synchroneity between take-off points or peak values and the level of the water table (figs. 2.6-2.13). The variations in depth are adequately explained by growth rates within the Sphagnum (section 2.5). The increase in ash residue values also appears to have little relationship with the location of the water table at the time of sampling (fig. 2.2).

Eisenreich & Urban (1984, pers. comm.) have attributed the fact that SIRM profiles in North American peats decline sharply within the zone of water table fluctuation do so as a result of dissolution. The difference in magnitude between concentrations in hummocks and hollows is also attributed to the dissolution of magnetite within the hollows. The evidence from Kaurastensuo suggests that the first point is not applicable here, as the water table fluctuations also take in the peak values recorded in the surface samples and extend well below the point of inflection into the low 'background' values. The backfield ratios presented in figs. 2.6-2.13 show no qualitative shifts that might reasonably be linked to the wide range of water table fluctuations as opposed to the smaller range of post-take-off samples which is immediately evident. The backfield features outlined in sub-section 2.3.2 show no apparent relationship between their location within the core and the proximity of the water table (figs. 2.6-2.13). With regard to the second point, at Kaurastensuo the total deposition (Table 2.6) and concentrations (Table 2.10) noted within hummock and hollow cores do not differ markedly. The use of this as evidence of dissolution is therefore considered inappropriate at Kaurastensuo and the effects of any dissolution occurring are considered to be negligible given the evidence available (cf. Chapter 3, section 3.11).

The assumptions made above take no account of redox reactions and gradients within the acrotelm. Data are not available for sites used in this thesis, therefore the possible effects upon the magnetic record and its subsequent interpretation cannot be estimated. The influence of redox gradients on the $Fe^{3+}$-$Fe^{2+}$ oxidation-reduction system and the availability of iron for chemical transformation is examined in Chapter 3, sub-section 3.9.1.

## 2.7 Interpretation of the Ash Residue and Magnetic Mineral Concentrations

The data presented in Table 2.8 indicate that there are variations from site to site in statistical associations between the ash residues (fig. 2.2) and SIRM values (figs. 2.6-2.13). The highest correlation coefficients (Pearson's product moment) are found towards the east side of the bog (site C) and they decline westwards through site B to the lowest at site A. This observation is limited by the small number of locations used on the bog surface, and the site-specific anomalies noted within core C6 (Table 2.2). Vascular plants and bog mosses produce different ash residue values (Clymo, 1983; Vuorela, 1983) which will therefore affect the correlations with SIRM. This may also be an important factor in accounting for the low correlations noted at site A, given the species composition of the cores (Table 2.2). Both KAC and KAX show a strong linear relationship between ash content and SIRM ($r= 0.81$ and $r= 0.97$ respectively, both significant at the 0.01 level). However the correlation for the two cores combined is only $r= 0.29$ which is insignificant at the 0.05 level (fig. 2.16). This suggests that, unlike the statistical relationship between X and SIRM (fig. 1.3), the relationship between magnetic mineral concentrations and ash residues may vary with location on the bog surface. Again this conclusion is based on the limited number of sites available, which must be borne in mind with

all further conclusions.

The statistical correlation between SIRM and ash residues differs for each sample set between the total set and the post-take-off subset (Table 2.8). In all cores, those samples above take-off display consistently lower correlations than for all cases in each respective core (Table 2.8). The pre-take-off sample subset (n= 30 compared with n= 53 for post-take-off samples) displays even less correlation, ie. no statistical relationship between the inorganic deposition, as represented by the ash residues, and SIRM within hummocks and hollows and from site to site. These data appear to confirm the division between pre-take-off and post-take-off deposition based on the different statistical correlations of the two subsets. The statistically significant correlations for all variables above take-off therefore suggest a strong link between the rise in total inorganic deposition to the bog as a whole, and the increasing concentrations of mineral magnetic particulates. The fluctuations in inorganic deposition within the pre-take-off samples is not as obviously linked with fluctuations within the pre-take-off SIRM concentrations (r= 0.125).

There also appear to be microtopographical variations controlling the relationship between inorganic deposition and mineral magnetic particles. The higher correlation noted within the hollows (r= 0.75 compared with r= 0.42 for hummocks) might suggest that the magnetic record of deposition as a function of total inorganic deposition, is more consistent between hollow cores than between the hummock cores on the bog. However, both correlations are significant at the 0.01 level given the degrees of freedom for each respective sample set. The same tentative conclusion may also be made regarding site-to-site variations, with site C being the most consistent (r= 0.78 significant at the 0.01 level) decreasing through site B (r= 0.49 significant at the 0.01-0.05 level) to site A (r= 0.23 insignificant at

the 0.05 level).

Stepwise regression data presented in Table 2.8 appear to confirm the supposition that the increase in inorganic deposition is strongly linked with the increase in mineral magnetic particulate deposition in hollows, as exemplified by SIRM and X ($r^2$= 60%).

## 2.8 Interpretation of the Magnetic Record

The results summarised in sub-section 2.3.2 appear to confirm the initial premise of mineralogical contrasts between the two sub-groups, pre-take-off and post-take-off, within each core. For ease of reference, the range of results for parameters and interparametric ratios are further summarised in Table 2.10 detailing the relative consistency of the post-take-off samples compared with pre-take-off, or 'background' samples, both in terms of measurability and qualitative variation (eg. SIRM/X ratios). The contrast between values given for hummocks and hollows in Table 2.10 supports the conclusion made in section 2.7 that the depositional record in the hollows is more consistently reproducible than that in the hummocks.

The trends noted within the interparametric ratios of the post-take-off samples ie. increasing SIRM/ARM values toward the surface, coupled with a decrease in ARM/X , are similar to those used by Hunt et al. (1984) as a basis for particulate source differentiation and identification. These have pointed toward heavy metal-magnetic linkages within urban dusts and aerosols comprising power station, industrial sources and vehicular emissions. This anthropogenically derived sub-group is evident in all cores sampled, and is exemplified by the coercivity of remanence curves for KAC, presented in fig. 2.14. Variation in the convexity of the background sample curve is possibly attributable to the varying proportion of

**Table 2.10** Summary of Magnetic Data
Summarising the range of values for pre- and post-take-off samples within hummock and hollow cores at Kaurastensuo

| | SIRM $10^{-6}Am^2Kg^{-1}$ | ARM $10^{-6}Am^2kg^{-1}$ | X $10^{-8}m^3kg^{-1}$ | ARM/X $Am^{-1}$ | SIRM/X $Am^{-1}$ | SIRM/ARM | $(B_0)_{CR}$ mT |
|---|---|---|---|---|---|---|---|
| **Hollow Pre-Take-Off** | 18-65.4 | <3.77 | Diamagnetic | - | - | 8.7-28.7 | 41-62 (35) |
| **Hollow Post-Take-Off** | 115-1084 | 4-26.0 | 0.8-7.17 | 335-741 | 13.5-18.3 | 26.4-44.3 | 36-40 |
| **Hummock Pre-Take-Off** | 11.3-107 | <6.83 | Diamagnetic <1.55 | 297-1019 | 9.83-19.5 | 10.9-36.6 | 16-56 |
| **Hummock Post-Take-Off** | 111-1113 | 2.87-26.0 | 0.53-8.1 | 219-618 | 12.7-18.9 | 25.6-71.8 | 23-48 |

antiferromagnetic minerals present within the sample relative to the magnetically dominant, but much smaller ferrimagnetic component. The similarity in the mineralogical characterisation illustrated by the narrow envelope of remanence curves suggests a common particulate source, or set of sources. The $(B_0)_{CR}$ values for the post-take-off samples within the hollows are 36-40mT. The dominant mineralogy contributing to the mineral magnetic behaviour of the anthropogenically derived sub-group is consistent with an impure multidomain ferrimagnetic component. The intermediate $(B_0)_{CR}$ values and continued resistance to fully reverse saturate imply the presence of a finer grained component, or even shape related changes, from a dominantly multidomain grain assemblage toward a higher proportion of the finer grains, tending toward single domain dimensions, within this sub-group. These mineralogical interpretations are confounded to an extent by the increasing concentrations of particulates within samples close to the surface, which might have the effect of altering the proportions of fine grained material within the sample. The inability of some of the samples within this sub-group to fully reverse saturate, even at higher backfields, also demonstrates the presence of the antiferromagnetic component. This inability to fully demagnetise at high backfields ($IRM_{-850mT}$/SIRM) has also been noticed in truly haematitic soils from North America (Maher, 1984).

The increase in SIRM/ARM ratios toward the surface corresponds with the increase in SIRM and $SIRM_{VS}$ (Table 2.6) reflecting the increase in deposition of the anthropogenically derived particulates within the bog. This increase is not limited by microtropographical variations. Oldfield et al. (1985) have also noted this relationship between SIRM/ARM ratios and anthropogenic deposition in a variety of samples from diverse locations and sediment environments.

## 2.9 Quantification of Influx Rates to the Bog Surface

The calculations based on the growth rate equation [2.1] (Tables 2.6 and 2.7) are by their nature extremely tentative (sub-section 2.3.3). Variations in some of the $SIRM_{vs}$ values are a result of abnormally high bulk density values (cf. core C4, 2.5-5cm, Table 2.6) which in turn will affect the $D_c$ values above take-off. The calculations also imply a strong linear relationship between age of the peat and depth within a core, which appears to be stronger in hummock profiles with fast growth rates, such as KAX and KAC (fig. 2.4). This relationship is confounded by four factors. First, the compression of peat by weight of the overlying material. Second, there are changes in the composition of surface vegetation which will affect the rate of breakdown (Clymo, 1965). Third, there are changes in the decomposition rate with aeration and location of the water table (Burgeff, 1961; Clymo, op. cit.). Fourth, there are changes in growth rates of the same vegetation type from year to year (Damman, 1978). These factors have been noted and are taken into account when discussing the influx rates to the Kaurastensuo bog surface (see below).

The age at take-off is taken to be around 52 years BP (1983) or ca. 1931, from the results in Table 2.7. The consistency between the hummock and hollow cores from site B to site C is very good, given the limitations of the equation. If the data in Table 2.7 are compared with that of Oldfield et al. (1981) from southern Finnish and British sites (Table 2.11), a number of observations may be made about trends in total deposition of mineral magnetic particulates to remote sites.

The age at take-off for Kaurastensuo (ca.1931) corresponds closely to the dates from Harpar Lilltrask, Karpansuo, Munasuo and Kunonniemensuo (inset, fig. 2.1) of ca. 1935. This date coincides with the beginning of marked increases in influx rates per unit area from slowly increasing

**Table 1] Estimated magnetite and measured total iron deposition at sites of ombrotrophic peat growth in Finland and Britain. The Table summarizes (A) annual deposition rates for atmospheric magnetite and total iron deposition rates for the years 1850, 1900, 1935 and 1973 at each site; (B) the total cumulative post-1850 and post-1950 deposition of atmospheric magnetite and total iron at each site, and for comparison: (C) total post-industrial deposition of atmospheric magnetite at British sites using the sampling methods described in Oldfield et al (9) and the estimation procedure outlined in the text.**

| Annual influx and accumulation rates | Harpar Lillträsk | | | Karpansuo | | | | Munasuo | | | | | |
|---|---|---|---|---|---|---|---|---|---|---|---|---|---|
| | | | | Profile III | | | [mean of 4] | Profile I | | | Profile II | | |
| M | M | Fe | $Fe/_M$ | M | Fe | $Fe/_M$ | M | M | Fe | $Fe/_M$ | M | Fe | $Fe/_M$ |
| A 1973 | 314 | 567 | 1.8 | 31 | 88 | 2.8 | 24 | 31 | 125 | 4.0 | 64 | 213 | 3.3 |
| B 1935 | 16 | 122 | 7.6 | 7.5 | 74 | 9.9 | 5 | 6.6 | 65 | 9.8 | 2.7 | 40 | 14.8 |
| C 1900 | – | – | – | 0.7 | 67 | 95.7 | 0.4 | – | – | – | – | – | – |
| D 1850 | – | – | – | 0.3 | 49 | 163 | 0.2 | – | – | – | – | – | – |
| $A/_B$ | 20 | 4.6 | 0.2 | 4.2 | 1.2 | 0.28 | 4.7 | 4.7 | 1.9 | 0.40 | 24 | 5.3 | 0.22 |
| $A/_D$ | – | – | – | 113 | 1.8 | 0.02 | 101 | – | – | – | – | – | – |
| Cumulative influx | M | Fe | $Fe/_M$ | M | Fe | $Fe/_M$ | [mean of 4] | M | Fe | $Fe/_M$ | M | Fe | $Fe/_M$ |
| Post 1950* | 6051 | 10 227 | 1.7 | 980 | 1767 | 1.8 | 710 | 630 | 3252 | 5.2 | – | – | – |
| Post 1850* | – | – | – | 1230 | 8107 | 6.6 | 1030 | – | – | – | – | – | – |

| Kunoniemmensuo | | | | | | | | | British Sites | | | | | | |
|---|---|---|---|---|---|---|---|---|---|---|---|---|---|---|---|
| [mean of 2] | | | Profile 7 | | | Profile 9 | | | [mean of 2] | | | Northwest Scotland | Northwest England (Head of Morecambe Bay) | | | | Industrial Southern Yorkshire near Sheffield |
| M | Fe | $Fe/_M$ | M | Fe | $Fe/_M$ | M | Fe | $Fe/_M$ | M | Fe | $Fe/_M$ | Achnahaird [4] | L Broom [2] | Duddon Valley [4] | Leven/ Rusland Valley [5] | Lyth Valley [2] | Ringinglow Bog [6] |
| 47 | 169 | 3.6 | 22 | 119 | 5.4 | 40 | 213 | 5.3 | 31 | 166 | 5.4 | | | | | | |
| 4.6 | 53 | 11.5 | 7.6 | 38 | 5.0 | 6.6 | 40 | 6.1 | 7.1 | 39 | 5.5 | | | | | | |
| – | – | – | 2.3 | 18 | 7.8 | 1.9 | 44 | 23 2 | 2.1 | 31 | 14.8 | | | | | | |
| – | – | – | 0.4 | – | – | 0.3 | 23 | 76.7 | 0.3 | – | – | | | | | | |
| 10 | 3.2 | 0.31 | 2.9 | 3.1 | 1.1 | 6 | 5.3 | 0.87 | 4.5 | 4.3 | 1 | | | | | | |
| – | – | – | 55 | – | – | 133 | 9.3 | 0.07 | 94 | – | – | | | | | | |
| M | Fe | $Fe/_M$ | M | Fe | $Fe/_M$ | M | Fe | $Fe/_M$ | M | Fe | $Fe/_M$ | M | M | M | M | M | M |
| – | – | – | 380 | 1849 | 4.9 | – | – | – | – | – | – | 280 | 700 | 2600 | 390 | 830 | 12 400 |
| – | – | – | 730† | 4053 | 5.6 | – | – | – | – | – | – | | | | | | |

M = $10^{-6}$kg $m^{-2}$ atmospheric "magnetite" (see text)
Fe = $10^{-6}$kg $m^{-2}$ total iron
*Surface values extrapolated to end of 1977
† 1876 value extrapolated back to 1850. Figures in square brackets refer to numbers of profiles used.

**Table 2.11** Estimated Magnetite and Iron Deposition in Finland and Britain (source: Oldfield et al, 1979)

background levels, dated to around 1860 (Oldfield et al., op. cit.).

The influx rates at Kaurastensuo are substantially lower than those of the other Finnish sites (Table 2.11). Background levels of influx are however, similar, varying between 0.057 and 0.197 $10^{-6}kg.m^2yr^{-1}$ of magnetite for Oldfield et al. (op. cit.) and 0.081 $\pm$ 0.061 $10^{-6}kg.m^2yr^{-1}$ for this study (Table 2.7). Although the calibration of the respective sets of measuring equipment has not been taken into consideration, this suggests that it cannot be assumed to be responsible for the difference in post-take-off influx rates between the two sets of data.

The trend in influx rates appears to show a decrease at the surface from a sub-surface peak (Table 2.7). It is inferred from this that deposition at Kaurastensuo reached a peak around the beginning of the 1970's, and has been declining ever since, up to 1983. The peak around 1970-1975 corresponds with the surface peak noted by Oldfield et al. (op. cit.) suggesting that the trends noted within the influx rates may have been occurring on a regional scale.

The maximum influx rates at Kaurastensuo are typically between 1 and 2 orders of magnitude lower than the sites used by Oldfield et al. (op cit), which displayed values ranging between 424 $10^{-6}kg.m^2yr^{-1}$ for Harpar Lilltrask, 7.8km northwest of the steel works at Koverhar, southern Finland and 22 $10^{-6}kg.m^2yr^{-1}$ for Kunonniemensuo, a remote site in East Finland. The estimated post-1850 influx of magnetite at Karpansuo and Kunonniemensuo are 3.7 and 2.6 times higher respectively than the lowest estimate obtained from remote sites in Britain (eg. Archnahaird, northwest Scotland). The highest estimate for Kaurastensuo when extrapolated back to 1850, using background rates (Table 2.7) is 60.7 $10^{-6}kg.m^2yr^{-1}$. This being 4.6 times lower than Archnahaird (Table 2.11) and 16 times lower than the estimated value at Karpansuo (980

$10^{-6}kg.m^2yr^{-1}$).

## 2.10 Conclusions

The magnetic record at Kaurastensuo appears to demonstrate an acceptable level of reproducibility both spatially and temporally. Variations in the consistency of the magnetic record are adequately explained by variations in species composition, habitat, growth rates and microtopography (sections 2.4 and 2.5). Within the limitations of this study the magnetic record for surface cores at Kaurastensuo appears unaffected by seasonal adjustments in the water table level (section 2.6).

Within the spatial and microtopographical frames of reference, the growth rates towards the east side of the bog are generally higher for hummocks than hollows. This observation is however, limited to the small number of sites available.

Evidence from ash residues and SIRM correlations suggests that the hollows retain a more consistent record spatially than perhaps their hummock counterparts. Regression analysis suggests that the increase in inorganic deposition is linked strongly with the increase in magnetic particulate deposition above the take-off point (section 2.7).

The age at take-off is estimated to be about 52 years BP (1983) or around 1931. This corresponds closely to the date proposed by Oldfield et al. (op. cit.) of ca.1935 as the beginning of a period of marked increase in influx rates at Finnish sites, culminating in peak influx rates around 1975. The evidence for Kaurastensuo follows this conclusion and also suggests that since 1975, deposition has decreased slightly. The cumulative influx rates at Kaurastensuo are much lower than expected, given the data in Oldfield et al. (op. cit.) for other remote southern Finnish sites. Evidence from Kaurastensuo follows the conclusions of Oldfield et al. (op. cit.)

which point to a gradual increase in magnetic particulate deposition, from low background values to higher 'post-industrialisation' values. It is not always possible to depict an arbitrary take-off point during this gradual rise (cf. Chapter 4). The evidence from Kaurastensuo, however, would suggest that the take-off points depicted are, in most cores, fairly reasonable estimates.

Having adequately established the reproducibility of the magnetic record, it is appropriate to examine the persistence of the record over time periods longer than ca.50 years. The persistence of the magnetic particulates within acid environments is examined in Chapter 3, along with interactions and relations between peat chemistry and the environment over time.

# 3. Stratigraphy and Magnetostratigraphy

## 3.1 Introduction

A brief description of five long profiles from four bogs; Kaurastensuo (KAC and KAX), Laaviosuo (LaavX), Varrassuo (VAX) and Haukilampi, is given. The results of geochemical and magnetic analyses from these cores are then interpreted with regard to the development of the bog profile over time, spanning the initial minerotrophic phase and subsequent ombrotrophic phase.

The rationale for choosing the bogs within this area (fig. 3.1), between Tampere (61°30'N 23°45'E) and Lahti (61°0'N 25°40'E) reflects the fact that southwest Finland contains the most complete biostratigraphical record in Finland, hence its designation as a 'type area' (Donner, 1971). The area is also located near the nickpoints of Salpausselkä I and Salpausselkä II, at the top of the parallel SW-NE trending limbs.

Pollen analytical data from Varrassuo are published by Donner (1951, 1966, 1967 and 1971), Donner et al. (1978) and Tolonen (1966). Carbon-14 ($C^{14}$) dating of Varrassuo is given in Alhonen et al. (1977), Donner et al. (op cit) and Tolonen (1978, unpubl. data). Further work at Varrassuo has included the measurement of peat and energy yields by Tolonen (1982) and Tolonen et al. (1982b), as well as moss increment dating of surface (0-50cm) cores (Tolonen, 1979, unpubl. data).

Published work from the bog Laaviosuo includes the measurement of Sphagnum fuscum growth rates (ca.10mm.yr$^{-1}$) in hummocks (Lindholm, 1981), and the ecological variation of mire site types, with specific reference to neighbouring Heininsuo (Reinikainen et al., 1984). Tolonen (1984) has also interpreted the changes in ash content of the ombrotrophic peat layers at Laaviosuo. $C^{14}$ dates for Laaviosuo are also available (Tolonen, 1979; unpubl. data).

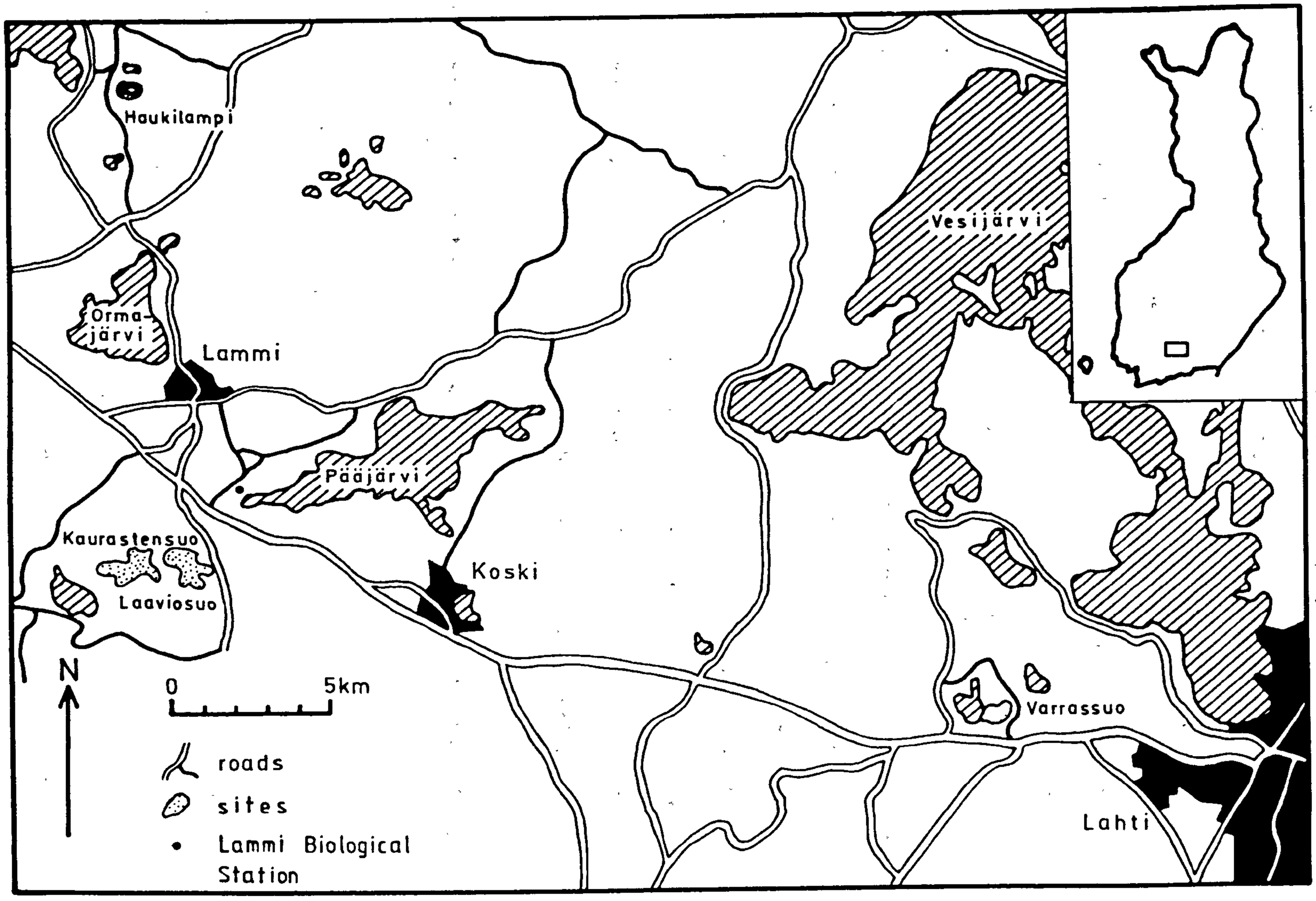


**Figure 3.1** General location of mire sites in southern Finland

Published work on Kaurastensuo includes detailed stratigraphic analyses (Niiranen, 1973), long term accumulation rates (Tolonen, 1979), peat and energy yields (Tolonen et al., 1982a; 1982b), and $C^{14}$ dating (Tolonen, 1979; unpubl. data). The location of core KAX corresponds to site AVIII (Niiranen, op. cit.), as well as the location of stratigraphic and $C^{14}$ boreholes sampled by Tolonen (see above). At Laaviosuo and Varrassuo[1] the coreholes both correspond closely with the location of the boreholes sampled by Tolonen (1979, unpubl. data) for $C^{14}$ determinations.

The 1978 bog surface has been marked at the sites on Kaurastensuo, Laaviosuo and Varrassuo as a $C^{14}$ reference surface to which subsequent coreholes at that location on the bog may be calibrated for $C^{14}$ dates. The 1983 surface (this study) was 25cm, 7cm and 14cm below the reference surface at Kaurastensuo, Laaviosuo and Varrassuo respectively. In the absence of further, more recent age determinations these $C^{14}$ dates (Appendix 4) are tentatively applied to the stages in stratigraphic development of the long profiles from adjacent sites, presented here.

## 3.2 Summary of Post-Glacial Vegetation History and Flandrian Pollen Assemblage Zones

### 3.2.1 Introduction

A brief summary of the biostratigraphical record from southwest Finland is given below as a context for the stratigraphic description of the profiles and subsequent geochemical and magnetic interpretations. The following section draws heavily on the work of Donner (1951, 1965, 1966 and 1971), Tolonen (1966), Sauramo (1949, 1958) and indirectly, Jessen (1935). There is no 'type site' described in Finland in which the pollen assemblage zones could be used as Flandrian chronozones, hence the

---

1. Site-X at Varrassuo is also adjacent to the site described in Donner et al. (op. cit.) and referred also to, as site-X.

designation of southwest Finland as a 'type area' (Donner, 1971). As a basis for sub-division into zones, the regional assemblage zones are used and correlated with each other by means of available $C^{14}$ dates (Donner, op cit).

It was on the basis of pollen diagrams from southwest Finland that Sauramo (1949) introduced into Finland the zonation used by Firbas (1949) in Central Europe, a modification of the zonation introduced earlier by Jessen (op. cit.) in Denmark.

3.2.2 Pollen Assemblage Zones

Starting with the oldest Flandrian assemblage zone, the following division into four zones is based on Sauramo (op. cit.) and acknowledged in subsequent work (see above).

**1. IV Pre-Boreal**

Characterised by a marked decline in non-tree pollen (NAP) and a rise in tree pollen (AP), reflecting the change in vegetation from open tundra to closed forest. This zone exhibits a prominent Betula maximum with values often rising to 80-90%. Regarding forest history, the shorelines YI, YII, YIII and YIV (Donner, 1966), belonging to the Finniglacial Yoldia Sea, fall within the older part of the pre-Boreal Betula maximum.

**2. V Boreal**

The transition from zone IV to V is marked by a strong increase in Pinus representation, usually to about 60-70%. This zone is often broken down into three parts: Va, Vb and Vc (eg. Donner, 1951). The lowest sub-zone, Va, and the highest, Vc, are dominated by Pinus, whilst the intermediate sub-zone, Vb, displays a rise in Betula.

**3. VI, VII and VIII Atlantic and Sub-Boreal**

The zones lie between the steep rise in the Alnus curve and the rise in the Picea curve, marking the beginning of the Sub-Atlantic Time.

Delimitation of the three zones cannot be based on changes in the values for Betula and Pinus, since their curves have a different course in different diagrams. Betula, however, is dominant in most of them. The zones mentioned correspond to the different stages of the Litorina Sea in the evolution of the Baltic Sea (Donner, op. cit.).

**4. IX Sub-Atlantic**

This is the first zone in which Picea displays a strong rise, generally to ca.20-30% though sometimes exceeding 50%. At the lower limit of this zone the curves for Tilia and Quercus usually end and Corylus and Ulmus either disappear, or show a marked decrease becoming discontinuously represented.

The Pre-Boreal zone IV is preceded by three Pre-Flandrian zones which Jessen (op. cit.) called the Older Dryas (I), Allerød (II) and Younger Dryas (III). During the general improvement after the last glaciation in northern Europe, the Allerød indicates a transient optimum in temperatures, followed by a cold period, the Younger Dryas. The late glacial and early post-glacial pollen stratigraphy in Scania, South Finland and East Finland is summarised in Table 3.1 (after Donner, 1966).

## 3.3 Methods

### 3.3.1 Coring Methods

The top 50-60cm of the long profiles were extracted from hummocks as a single core by means of a partial vacuum, 12cm diameter stainless steel corer. The compression of the peat extracted by this method was less than 4cm in all cases. The remainder of the profiles were extracted from alternating, adjacent coreholes in 50cm sections, using a 5cm radius (2.5cm radius in the case of KAC) 'Russian' type peat sampler (cf. Tolonen, 1968; Oldfield, 1982). The unsuitability of the corer for sampling woody rich peat

**Table 3.1** Comparison of the Late-Glacial and Early Post-Glacial Pollen Stratigraphy in Scania, Varrassuo Bog, Southern Finland, and Eastern Finland with the Retreat Stages of the Ice and the Stages in the Development of the Baltic Sea. (after Donner, 1966)

| Scania | | | Finland | | | |
|---|---|---|---|---|---|---|
| Pollen Stratigraphy | | | Stages of ice retreat as dated with varve chronology | Stages of the Baltic Sea | Pollen Stratigraphy as dated with $^{14}C$ determinations | |
| | | | | | Varrassuo Bog (and the two oldest $^{14}C$ dates in S. Finland) | Eastern Finland |
| Post-Glacial | Atlantic | VI ca.6000 B.C. | | | VI ca.5800 B.C. | |
| | Boreal | VII ca.6500 B.C. | | Ancylus Lake<br>Echineis Sea | V ca.6800 B.C. | V ca.6500 B.C. |
| | | VIII | | | IV oldest organic sediment ca.7000 B.C. | IV |
| | | ca.7600 B.C. | | Yoldia Sea | Vävarsbacka ca.7600 B.C. | oldest organic sediment ca.7500 B.C. |
| | Pre-Boreal | IX ca.8000 B.C. | Salpausselkä III ca.8200-8300 B.C. | | Kihniö ca.7900 B.C. | |
| Late-Glacial | Younger Dryas | X | Salpausselkä II<br>Salpausselkä I | Baltic Ice Lake | | |
| | Alleröd | XI | | | | |

layers (Tolonen, op. cit.) was evident at Varrassuo and Haukilampi, where the profiles were terminated at 450cm and 238cm respectively. Basal samples from Varrassuo, spanning the peat-mineral soil interface were provided by Dr. K. Tolonen.

In order to avoid the possibility of metallic contamination, resulting from samples with such a high proportion of surface area-to-sample volume (cf. KAC, sub-section 3.4.3), the exterior of each sample slice was removed as soon after coring as possible. This procedure had the disadvantage of precluding bulk density measurements (eg. at Varrassuo; KAC and Laaviosuo, below 320cm) unless replicate cores were taken.

### 3.3.2 Chemical Analyses

Chemical analysis of the peat profiles is based on five elements: iron (Fe), lead (Pb), copper (Cu), zinc (Zn) and nickel (Ni). Total concentrations in $\mu g.g^{-1}$ were determined from air dried (40°C) peat samples digested in nitric acid, using atomic absorption flame spectroscopy (Varian AA-1275 series). Two replicates of each sample were used throughout, and element concentrations were automatically calibrated to nitric acid blanks during calculations of replicate means (Appendix 3).

### 3.3.3 Magnetic Measurements

Samples were taken from 2.5cm and 5cm slices for magnetic analyses. X, SIRM, and backfield ratios (cf. Chapter 1) were measured for all samples. ARM measurements were carried out on selected samples. Where the signal-to-noise ratio of a sample approached unity, primarily in the mid-sections of the cores, the ARM measurements were not plotted. This reduced any errors in the calculation and subsequent interpretation of the interparametric ratios using ARM. The relevant interparametric ratios for the long profiles are plotted where available. In addition, slice volume SIRM ($SIRM_{VS}$) data has also been calculated for the surface samples

(above 50cm), and in the case of KAX, for the whole core.

## 3.4 Kaurastensuo

### 3.4.1 Introduction

Two long profiles, KAC and KAX, were obtained from Kaurastensuo (61°02'N 24°59'E). Site descriptions are presented in detail in Chapter 2, section 2.2. KAC (0-600cm) is from site C in figure 2.1 (Chapter 2) and KAX (0-485cm) from site B (fig. 2.1). The general location of Kaurastensuo and its proximity to the other three bogs is shown in figure 3.1.

A stratigraphic description of KAC and its preliminary magnetic measurements are presented in sub-sections 3.4.2 and 3.4.3 respectively. These are followed by a stratigraphic description of KAX (sub-section 3.4.4) and subsequent geochemical and magnetic results from KAX (sub-sections 3.4.5 and 3.4.6 respectively). A site specific interpretation and discussion of the results is then presented in sub-section 3.4.7.

### 3.4.2 Stratigraphic Description of KAC

Preliminary coring at Kaurastensuo, site C resulted in the 600cm long core, KAC (fig. 3.2). The peat core overlies limnic sediments (600-580cm) corresponding to the ancient lake sediments noted by Niiranen (op. cit.). These sediments are overlain by telmatic peats (580-548cm) upon which the bog proper rests. The telmatic peats may be differentiated from the limnic sediments below and the minerotrophic peat, above, by their intermediate mineral content values (ca.30%), compared with >80% for the limnic sediments, and <15% for the basal peats.

The basal peat comprises mainly Phragmites overlain by minerogenic Carex-Sphagnum peats. The minerotrophic phase within the bog development is represented by the peats spanning 548-ca.300cm. The boundary at ca.300cm marks the transition between the end of the

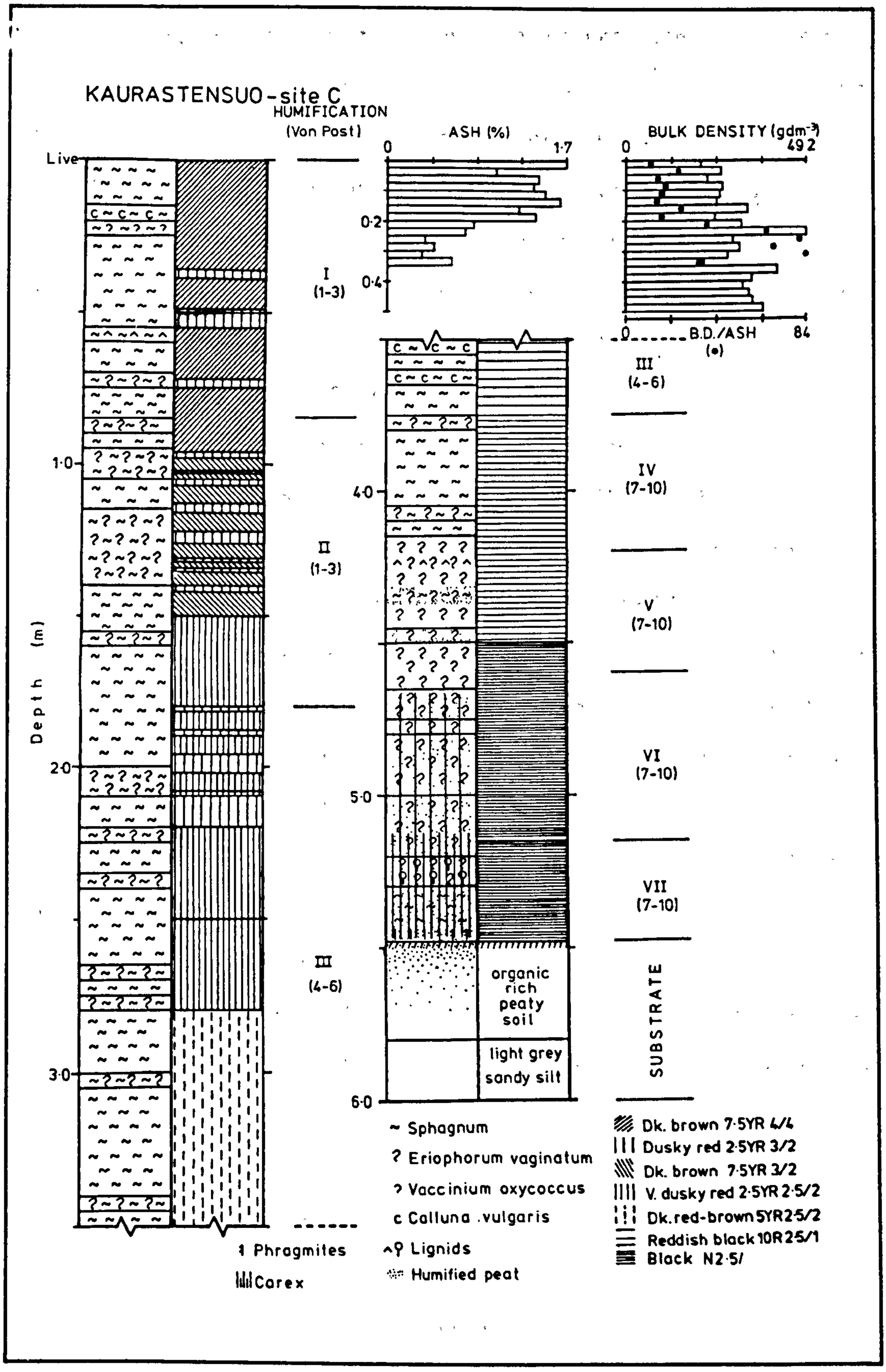


**Figure 3.2** Stratigraphy of KAC, site C, Kaurastensuo

minerotrophic, and start of the ombrotrophic peat phases. Above this boundary the peat strata comprises mainly Sphagnum spp., with the top 100cm consisting of the remains of loosely compacted S. fuscum.

The top of KAC culminates in a tall hummock, comprising S. fuscum, Polytrichum strictum, Empetrum nigrum, Calluna vulgaris, and Vaccinium oxycoccus in varying proportions. The hummock vegetation at the surface is characterised by low bulk density values, ca.20-30 $gdm^{-3}$.

### 3.4.3 Preliminary Magnetic Results from KAC

Preliminary magnetic measurements of KAC are presented in figure 3.3. The concentration parameters (SIRM, X and ARM) may be divided into three sections within the core. The bottom section is characterised by relatively high values for all three parameters between 600-580cm. Above 580cm the concentration parameters decrease in values although there is a peak in all three at approximately 548cm, around the peat-mineral soil interface. The limnic sediments display ARM/X values of ca.100$Am^{-1}$ and a linear decrease in SIRM/ARM values from 600-580cm (36-18). These contrast with the overlying telmatic peats which display a range of ARM/X values (150-350$Am^{-1}$) and relatively constant SIRM/ARM values (ca.9). The peat-mineral soil interface displays an increase in ARM/X to 400$Am^{-1}$ from 150$Am^{-1}$. The backfield ratios for the samples within this section reflect the differences noted in the parametric and interparametric profiles.

The mid-section comprises the majority of the core. This includes the end of the minerotrophic phase (460-ca.300cm) and the majority of the ombrotrophic phase, to about 40cm below the surface. This section consists of peat strata displaying low, or unmeasurable SIRM and ARM values. The majority of the samples within this section (300-40cm) were characterised by negative X values, indicative of the diamagnetic properties of the

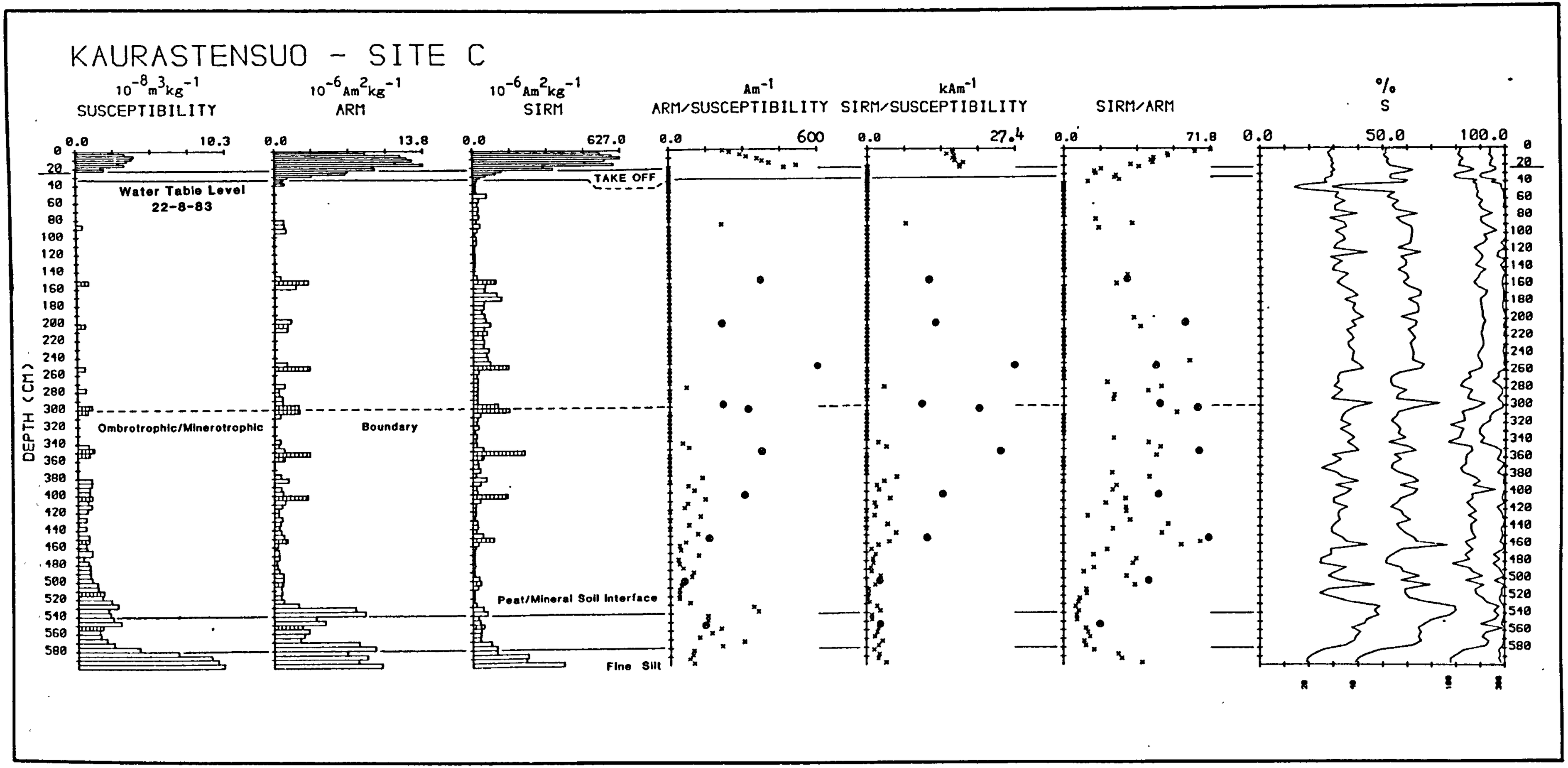


**Figure 3.3** Magnetic measurements for KAC, site-X, Kaurastensuo. 'Contaminated' samples in hatched shading (see text for explanation).

sample peaks in ARM and SIRM concentrations. These are at approximately regular intervals up through the profile and are associated with a wide range of ARM/X (150-600$Am^{-1}$), SIRM/X (9-27.4$kAm^{-1}$) and SIRM/ARM values (30-72) values. The peaks in the concentration dependant parameters correspond with the presence of 'soft' spikes within the backfield ratios.

The topmost section of the core, from 40cm to the surface is characterised by increasing values of X, ARM and SIRM. The increase in values occurs simultaneously for SIRM and ARM at 22.5-25cm below the surface, whilst for X it is reflected by the presence of measurable, positive values above 20-22.5cm, which increase toward the surface. The concentration parameters peak between 17.5-7.5cm below the surface. The ARM/X curve for the top section displays a near linear decrease from 25cm to the surface (525-200$Am^{-1}$), whilst for the same samples SIRM/ARM values increase toward the surface (18-72). SIRM/X values from the samples above 25cm are relatively constant, at about 16$kAm^{-1}$.

3.4.4 Stratigraphic description of KAX

The stratigraphy of KAX is presented in figure 3.4 along with water content, pH (0-350cm), ash residues (0-20cm) and bulk density. The column on the left of the diagram, bounded by the stratigraphy and the colour coding is subdivided according to microscopic plant analyses by Niiranen (op. cit.) from pre-existing work at the same site. The depths in this column have been corrected to the 1983 surface, the stratigraphy of the two cores were matched by the well defined ombrotrophic-minerotrophic boundary (O/M) at 300cm. The cores matched within 20cm at the surface and within 18cm at the base of the minerotrophic phase.

The base of the core (485-462cm) is composed of the same telmatic peat material noted in KAC (section 3.4.2). The water content and bulk

## KAURASTENSUO Site X

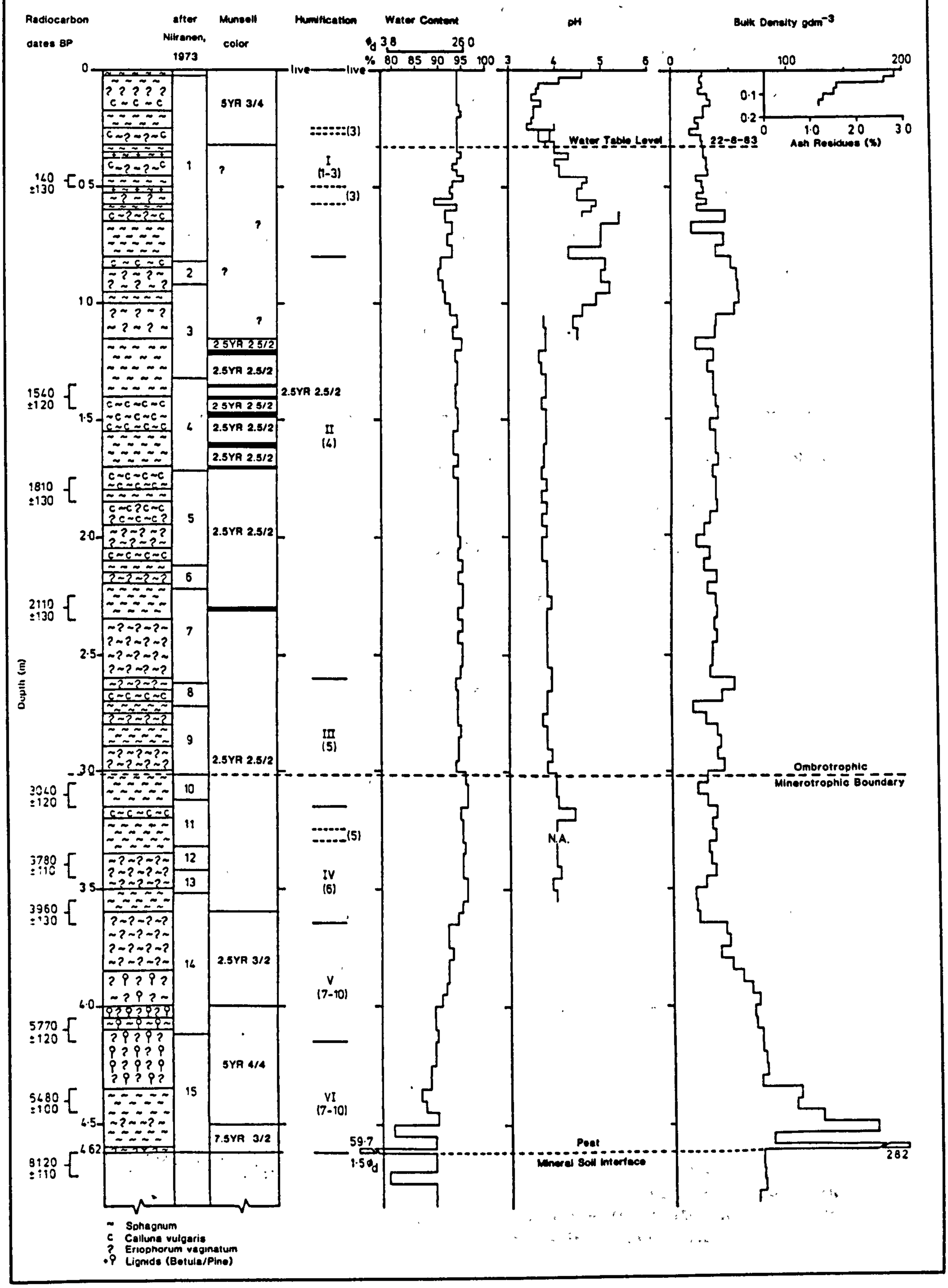


Figure 3.4 Stratigraphy of KAX, site-X, Kaurastensuo. $C^{14}$ dates from Appendix 4.

density values of these samples reflects their homogeneous nature regarding their sedimentation over time. The basal peats directly above the telmatic peats consist of Phragmites, Eriophorum and possibly some comminuted Sphagnum remains. The bulk density of this layer (462-460cm) is almost twice as high (282 $gdm^{-3}$) as values directly above, and ca.9 times higher than values from the ombrotrophic phase. Bulk density values decrease through the minerotrophic phase to 370cm (60$gdm^{-3}$) which corresponds with an increase in water content from 59.7% at the base (462cm) to 95% at 350cm.

The stratigraphy shows a higher frequency of Sphagnum remains between 300cm and the surface. Between 235-125cm, seven highly humified bands were visible before oxidation of the outer core material, these consisted largely of decomposed Sphagnum remains. From 125cm to the water table[1] at 32.5cm the water content, bulk density values and most noticeably pH values all display marked fluctuations, in contrast to samples above and below. The pH values display a sideways shift from pH 3.6 to pH 4.5 at 120cm, and from pH 5.4 to pH 4.5 at 60cm. The peat becomes more acidic towards the surface, with lowest pH values (pH <3.7) between 25-5cm. From 5cm to the surface values increase.

3.4.5 Geochemical Results from KAX

Profiles of total iron, nickel, copper, lead and zinc concentrations are presented on a dry weight basis for KAX in figure 3.5. The water chemistry of samples above 355cm are presented in figure 3.6 for the same elements and, additionally manganese (Mn).

Iron, copper and less conspicuously, the nickel profile display similar

---

1. The water table can, when near the surface, fluctuate by up to 10cm within a few days (Chapman, 1965). The idea of a water table, as such, isdubious (Clymo, 1984), although for consistency the water level at the time of sampling is referred to as the 'water table' throughout.

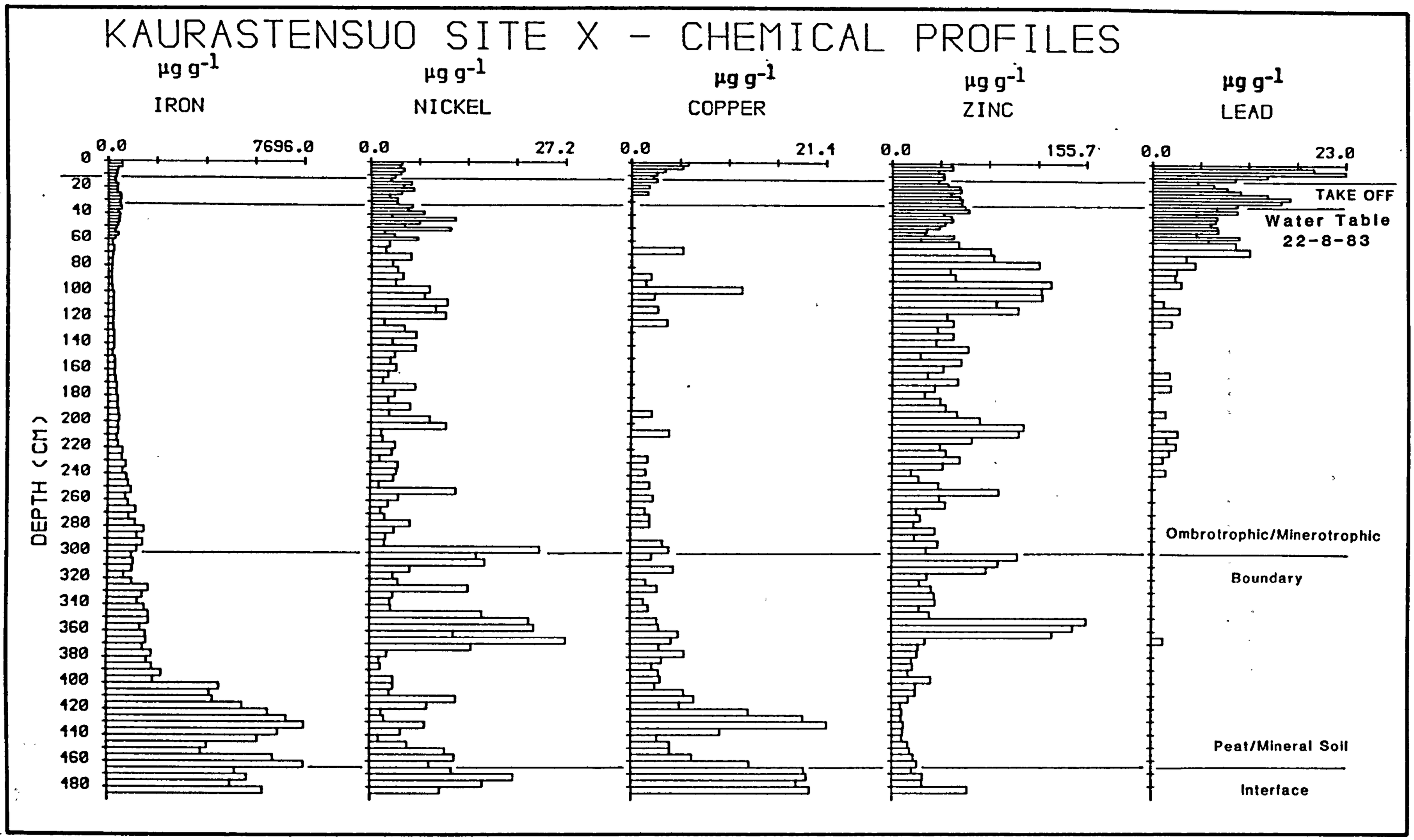


Figure 3.5 Geochemical profiles for KAX, site-X, Kaurastensuo

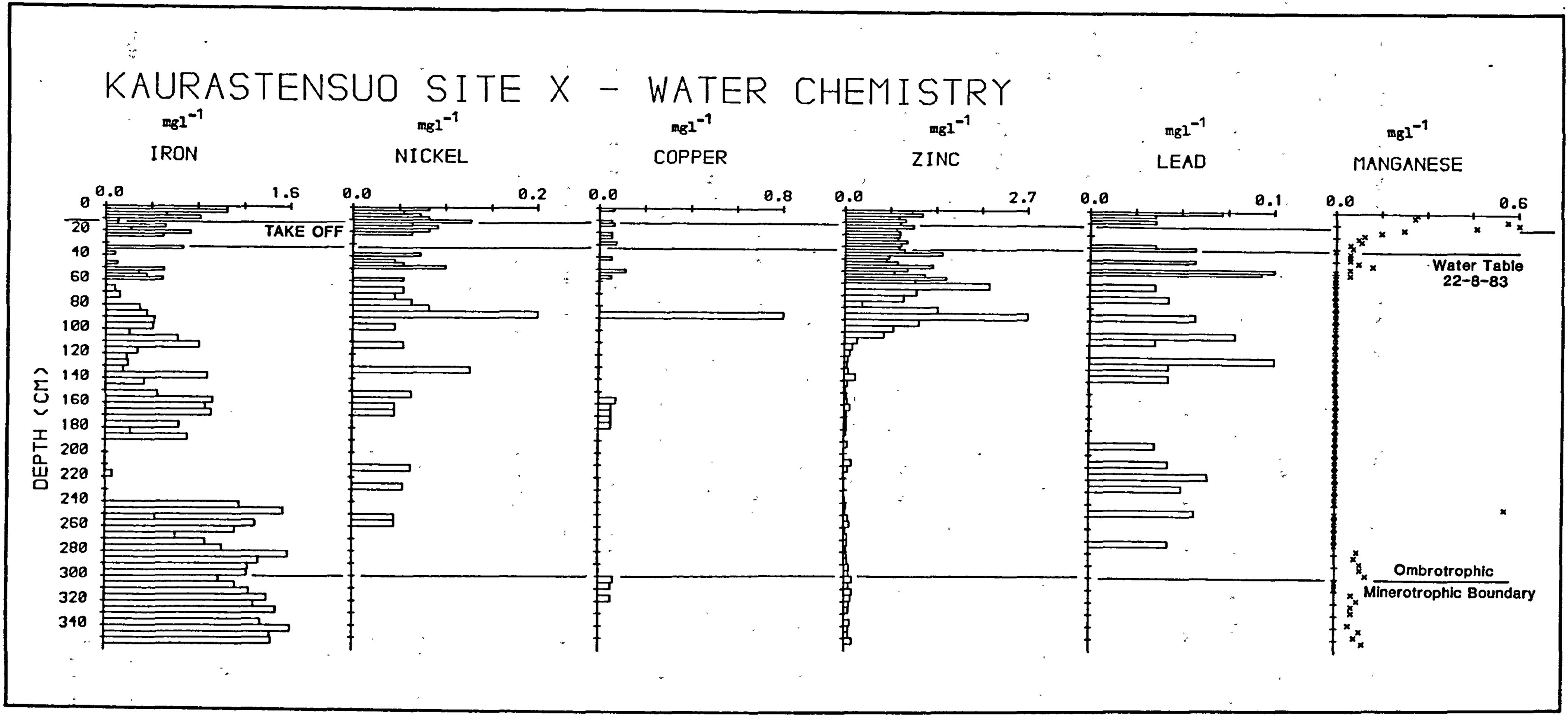


**Figure 3.6** Peat water chemistry for KAX (0-355cm), site-X, Kaurastensuo,

general trends throughout the profiles. These comprise a large peak in concentrations at, or near the peat-mineral soil interface, followed by decreasing concentrations upwards, through the minerotrophic phase. Concentrations decrease within the ombrotrophic phase to minimal, or undetectable values before increasing again near the surface, culminating in a small surface peak. Superimposed on this general pattern are more specific features, for example the low peaks in iron, nickel, zinc and lead at about 30-35cm, corresponding with the level of the water table at the time of sampling.

All the elements are present within the mineral soil underlying the peat, with the exception of lead which is undetectable in all but the upper ombrotrophic peat layers. Iron and copper exhibit twin peaks, of similar magnitude (within each profile) at the base (462cm) and at 430cm, 7696$\mu g.g^{-1}$ for iron and 21.4 $\mu g.g^{-1}$ for copper. Iron concentrations decrease by an order of magnitude from the lower minerotrophic peats (7696$\mu g.g^{-1}$) through to the ombrotrophic peats around 220cm (ca. 400$\mu g.g^{-1}$). However, there is a small increase just above 300cm corresponding with the start of the ombrotrophic phase, noted also in the nickel, zinc and less conspicuously, copper profiles.

The zinc profile displays a number of sharply defined peaks throughout its length. The increase in concentrations associated with each of the six peaks is limited to less than three samples either side of the maximum value (generally more than twice the 'background' concentrations).

The lead concentrations within the ombrotrophic phase display low or undetectable values between 240cm and 125cm (<3$\mu g.g^{-1}$) before increasing markedly towards the surface. There are three discernible peaks within the increased lead concentrations, at 75cm (11.6$\mu g.g^{-1}$), 27.5-25cm

(16.4µg.g$^{-1}$) and a sub-surface peak at 7.5-5cm (23µg.g$^{-1}$).

Within the water chemistry profiles (fig. 3.6) only zinc and manganese display any obvious pattern. Zinc concentrations remain low between 355-115cm (ca.0.07mgl$^{-1}$) rising sharply above , to a peak at 90-85cm (2.7mgl$^{-1}$) and consistently above 0.7mgl$^{-1}$ up to the surface. The manganese profile exhibits detectable concentrations within the zone of the upper minerotrophic and lower ombrotrophic phases (355-275cm). Above 274cm manganese concentrations are undetectable until 50cm below the surface. From 25cm upwards concentrations increase from 0.8mgl$^{-1}$ to a sub-surface peak at 10-17.5cm (0.65 mgl$^{-1}$).

3.4.6 Magnetic Measurements of KAX

Like KAC, the magnetic profiles of KAX (figure 3.7) may be divided into three sections: bottom samples (485-385cm), the mid-section (385-15cm) and the surface samples (15cm upwards). The basal samples may be further sub-divided into the telmatic peats, basal peats and minerotrophic peats.

The telmatic samples are characterised by low SIRM/X values (1.99-2.38 Am$^{-1}$) due to relatively high X values and low SIRM values. ARM/X and SIRM/ARM ratios are correspondingly low. The backfield ratios (with the exception of IRM$_{-300mT}$/SIRM) are noticeably 'softer' in comparison to those for the overlying samples. The basal peats (462-455cm) at the peat-mineral soil interface display low X, high SIRM and very high ARM values in comparison with the underlying samples. The peak ARM values (11.2-14.3 10$^{-6}$Am$^2$kg$^{-1}$), produce the highest ARM/X ratios in the core, 348-634 Am$^{-1}$. Between 455cm and 385cm X, ARM and SIRM decrease.

The mid-section consists of the upper minerotrophic phase and the majority of the ombrotrophic phase (355-15cm). This is characterised by very low SIRM values (4-30 10$^{-6}$Am$^2$kg$^{-1}$), unmeasurable ARM values and

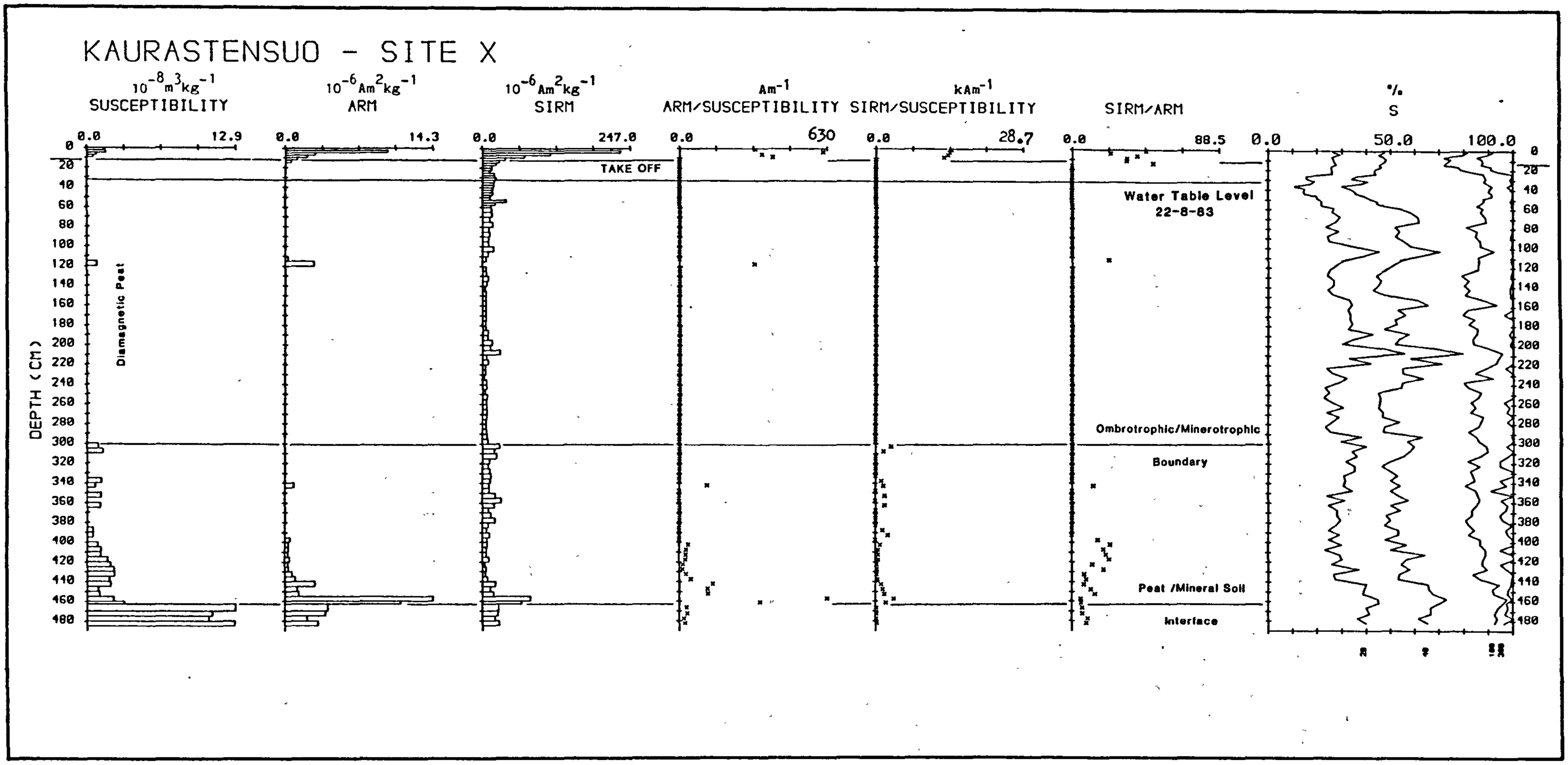


**Figure 3.7** Magnetic measurements for KAX, site-X, Kaurastensuo

diamagnetic X values (-0.32 to -0.46 $10^{-8}m^3kg^{-1}$).

The surface samples from 15cm upwards are characterised initially by measurable ARM values which increase in a linear manner along with SIRM and X values, the latter from 10cm onwards. There is a sub-surface peak for all three parameters at 5-2.5cm. The increase in magnetic mineral concentrations between 15-12.5cm coincides with a stepwise shift in the higher backfield ratios ($IRM_{-100mT}$/SIRM and $IRM_{-300mT}$/SIRM) towards a 'harder' remanence. This stepwise shift is directly above a similar shift in the lower backfield ratios ($IRM_{-20mT}$/SIRM and $IRM_{-40mT}$/SIRM) between 50-35cm.

Volume SIRM ($SIRM_{VS}$) measurements for the whole core presented in figure 3.8 display the variation between the three basic groups markedly. Values decline rapidly from 462cm to 440cm. Above 440cm the minerotrophic samples display similar, very low values. At the beginning of the ombrotrophic phase the values rise slightly between 300-20cm. Above 20cm values increase smoothly to a surface peak.

3.4.7 Discussion

The series of peaks running through the magnetic profiles of KAC at regular 50cm intervals, is probably due to magnetic contamination. This is likely to be the result of the down-carrying of surface material during sampling (section 3.3.1). The peak values represented in the X, ARM and SIRM profiles of these samples are accompanied by large variations in the interparametric ratios and 'soft' spikes in the backfield ratios (fig. 3.3). The regular spacing of the contaminated samples suggested a link with the ends of the 'Russian' corer which contain the pivot housing (cf. Tolonen, 1968; Oldfield, 1982). The use of the small radius (2.5cm) corer appears to have increased the likelihood of contamination due to the large surface area:volume ratio. The subsequent use of a larger (5cm radius) corer and

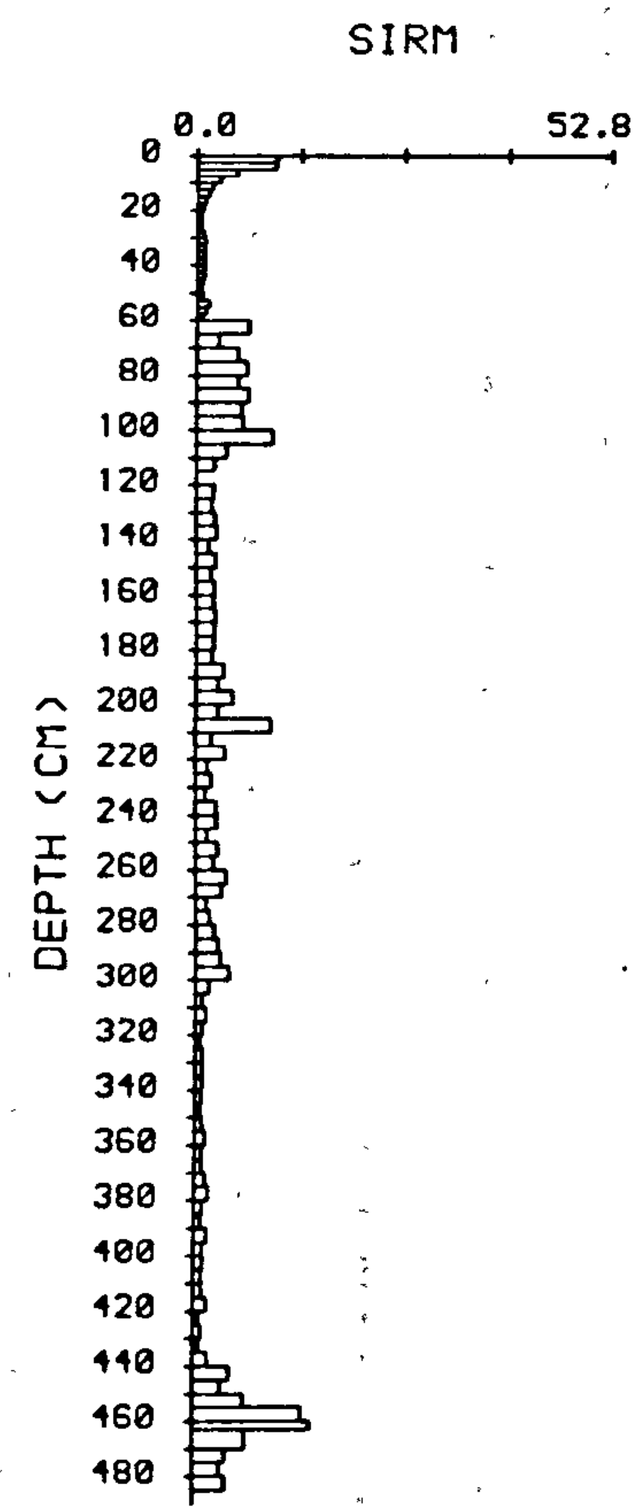


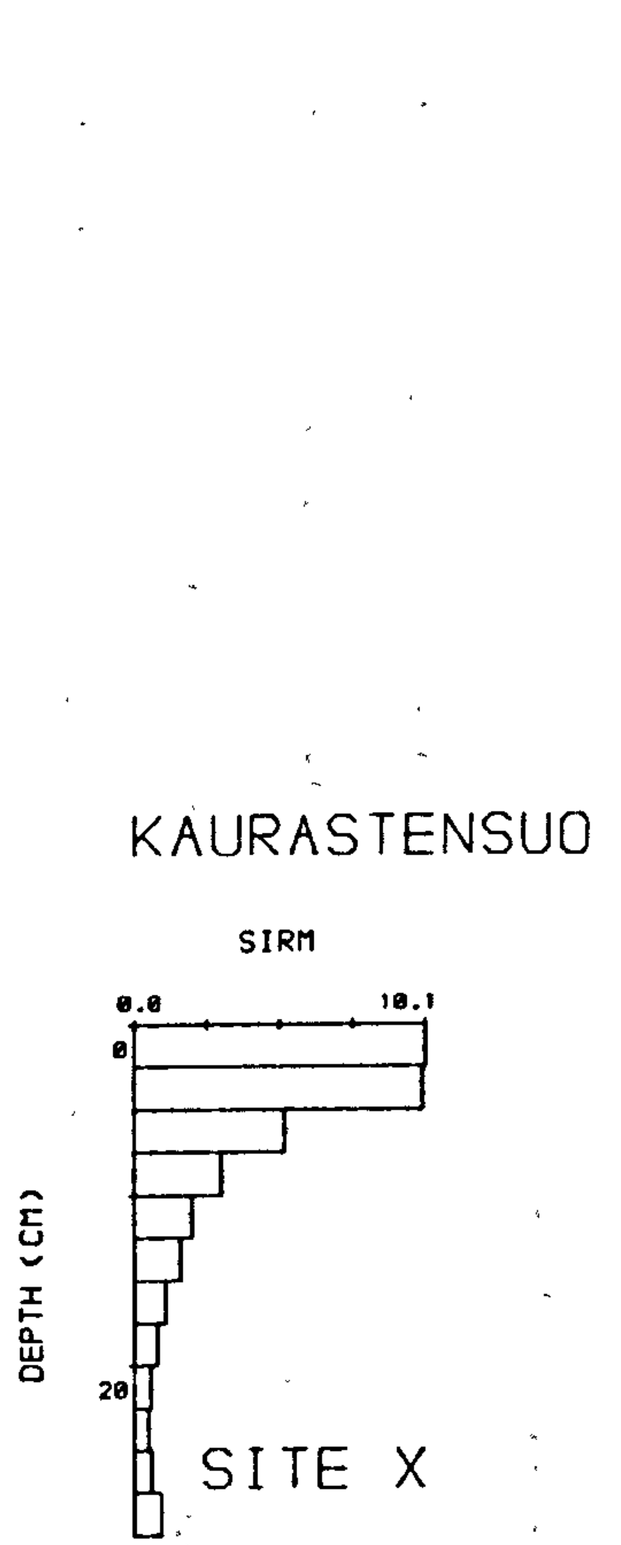






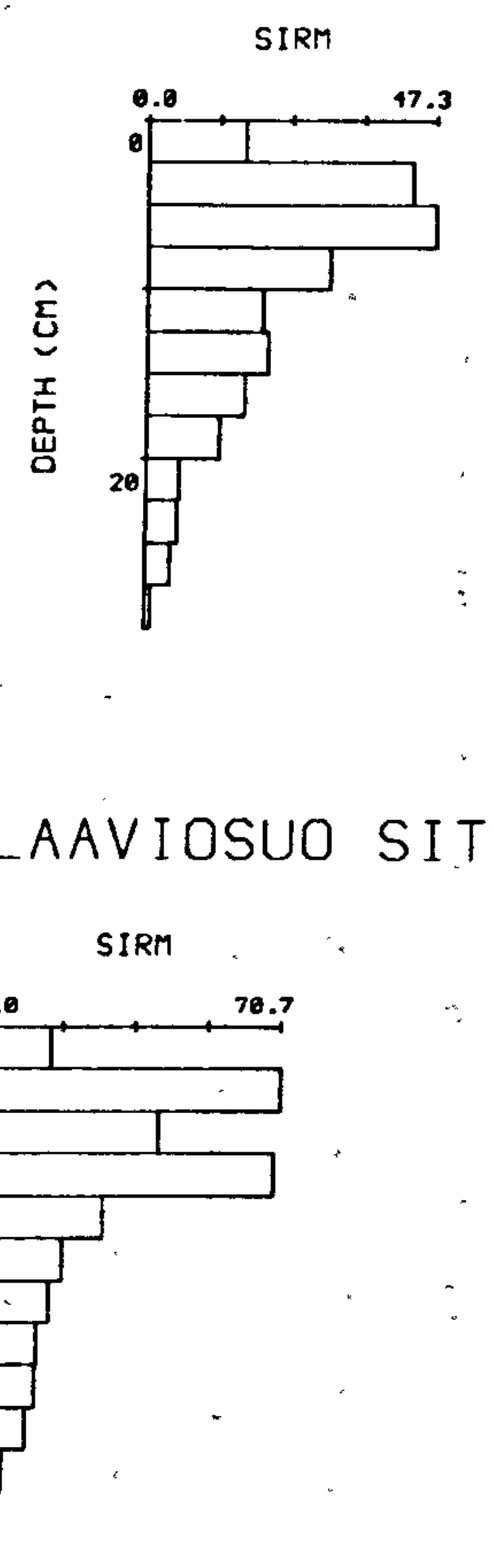





**Figure 3.8** Slice volume SIRM ($SIRM_{VS}$) for Kaurastensuo (KAC, KAX), Laaviosuo, Varrassuo and Haukilampi. Units in $10^{-6}$ Amperes per metre squared.

the rapid removal of the external peat layers appears to have reduced the risk of magnetic contamination of the end-samples (fig. 3.7). However, the nickel and zinc profiles (fig. 3.5) suggest that the regular peaks noted, are linked with the residual, magnetically undetectable contamination. All subsequent coring was accomplished with the larger corer. Recent work on lake sediments from Peckforton Mere, Cheshire has confirmed this source of contamination with the small corer (G. Yates, unpubl. data). The evidence for contamination of some samples within KAC and the large surface area:volume ratio of samples was a contributory factor in not choosing to measure any chemical concentrations from KAC.

An observation on the stratigraphy of KAC (fig. 3.2) and KAX (fig. 3.4) follows Clymo (1965) in suggesting that any reconstruction of past vegetation surfaces from the remains found in peat is tenuous. Clymo (op cit) noted that some bog species will be growing in positions which ultimately lead to preferential preservation eg. vascular plants. A further observation is that the mass of roots and shoot bases of Eriophorum become over-represented in the profiles compared with Sphagnum spp., especially where relatively long time periods have elapsed before the Sphagnum has passed below the sulphide level (Clymo, op. cit.). This observation explains the increased presence of Eriophorum with depth in KAC and KAX even though the surface that gave rise to the peat contained a large proportion of Sphagnum.

The bulk density and water content profiles of KAX are in good agreement with pre-existing data from site-X, Kaurastensuo (Tolonen, 1981; unpubl. data) displaying high bulk density values and low water content at the base of the peat, gradually decreasing and increasing, respectively, up through the minerotrophic phase. The range of pH values for KAX (pH 3.5-5.4) is slightly larger than that given by Reinikainen et

al. (1984) for sites within the same area (pH 4.0-5.4). However, the values are close to the range of pH 2.9-5.2 (mean pH 4.0) reported by Urvas et al. (1979) for Sphagnum peats in Finland. The strong acidity of the profile at the surface, a tall hummock, is probably related to time of sampling ie. late summer, when the surface peat is dry relative to other times of the year. Clymo (1984) noted that the lowest pH values were observed in hummocks during drier periods, and that larger, tall hummocks (eg. KAX) tended to be more acidic than lower, smaller hummocks.

The ash residues in peat, corresponding to fluctuations in particulate deposition within ombrotrophic peat (Vuorela, 1983; Tolonen, 1984) show a statistically significant correlation, with SIRM above take-off, r= 0.97, at the 0.01 level. The significance of the correlation regarding magnetic particulates has been interpreted in sub-section 2.4.4, Chapter 2.

The high concentrations of iron, copper and nickel at the base of the peat profile follow a similar pattern described in Clymo (1983) for aluminium, quartz and manganese. The large basal peaks are directly attributable to the chemical composition of the underlying mineral soil. The transition from high concentrations at the base to the lower values in the mid-section is most likely a function of the change from a eutrophic, mineral soil water-dependent fen peat, to an oligotrophic, precipitation-dependent bog peat. The surface peak in manganese, being removed from the water table and effects of long term translocation, dissolution and mobility, would therefore appear to be most closely analogous to the true depositional record (cf. sub-section 3.11.2). This overall interpretation of the chemical profiles takes account of translocation at the base of the core (Sillanpää, 1972; Clymo, 1983) as well as the relocating activities of live plants and animals at the surface (Clymo, op. cit.).

## 3.5 Laaviosuo

### 3.5.1 Introduction

Laaviosuo bog (61°02'N 25°02'E) is located less than 1km to the east of Kaurastensuo and ca.3km south of Lammi Biological Station in Koski Hl commune, Lammi (fig. 3.1). The mire succession of the region (ombrotrophic raised bogs) is typical of the transitional zone between the concentric bogs of the Finnish coast and the eccentric bogs of the inland lakes (fig 3.9a). Along with Kaurastensuo, Varrassuo and Haukilampi, Laaviosuo lies within the present southern Boreal vegetation zone. The average growing season (threshold value +5°C) lasts 163 days from approximately April 29th to October 9th according to Reinikainen et al. (1984). Meteorological data for the area, including Kaurastensuo, are presented in Table 3.2.

The bog has undergone considerable drainage at some stage since 1945 (fig. 3.9a). The net result has been a lowering of the water table, which within the profile was located at 42.5cm, with an estimated maximum depth of 62.5cm (cf. Table 3.6).

### 3.5.2 Stratigraphy of LaavX

The peat stratigraphy of the core LaavX is presented in fig. 3.10. Although the core spans 538cm of peat, the peat-mineral soil interface is not evident at the base. The minerotrophic peat evident in the core (538-320cm) consists primarily of Eriophorum and highly decomposed Sphagnum remains. Within the ombrotrophic phase, from 320cm upwards, there are several highly humified bands at 315cm, 230cm, 180cm, 100cm and 50cm below the surface. The stratigraphy also records the presence of two woody layers within the peat at 150-130cm and 80cm.

Bulk density (0-320cm) and ash residue (0-40cm) profiles are presented in fig. 3.11. The bulk density values are generally low, varying

**Table 3.2** Meteorological Data for Lammi Parish, S. Finland. Data from Lammi Biological Station, 125m.a.s.l., mean values from 1961-1970. (Source: Ruuhijärvi, 1974)

| | |
|---|---|
| Mean Annual Temperature | +3.1°C |
| Period with mean Temperature below 0°C | 181 days |
| Mean annual Precipitation | 600mm |
| Evapotranspiration | 450mm |
| Duration of Snow Cover | 137 days |
| Period of Snow Cover | early December-late April |

a.

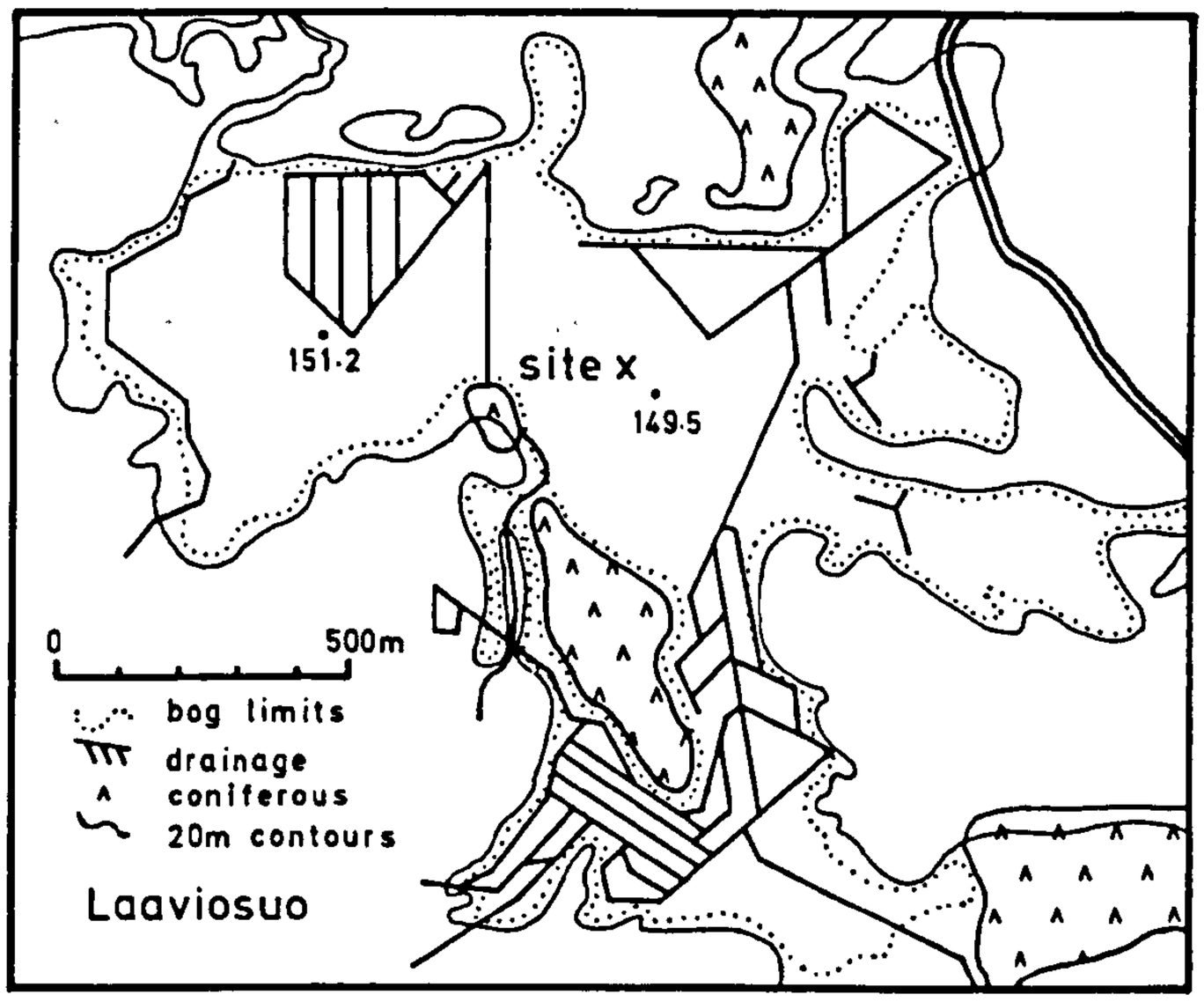


b.

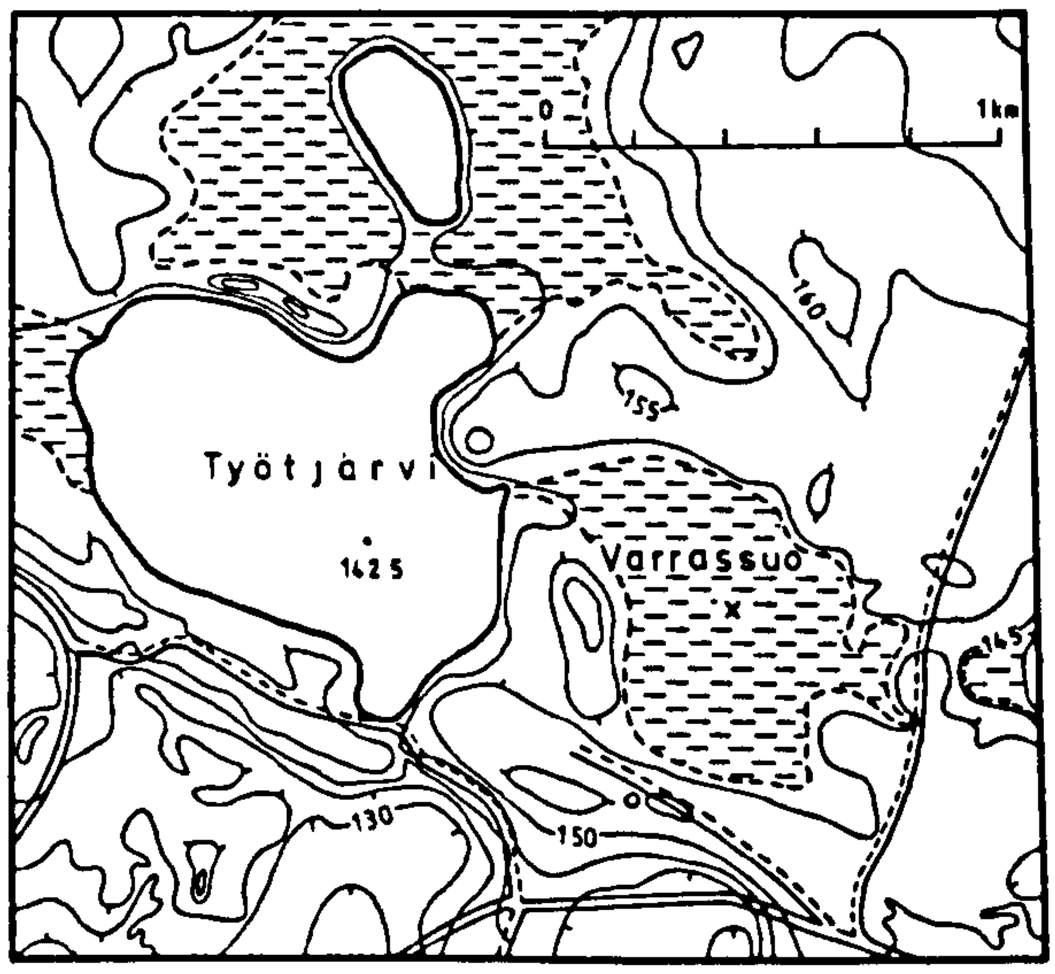


C.

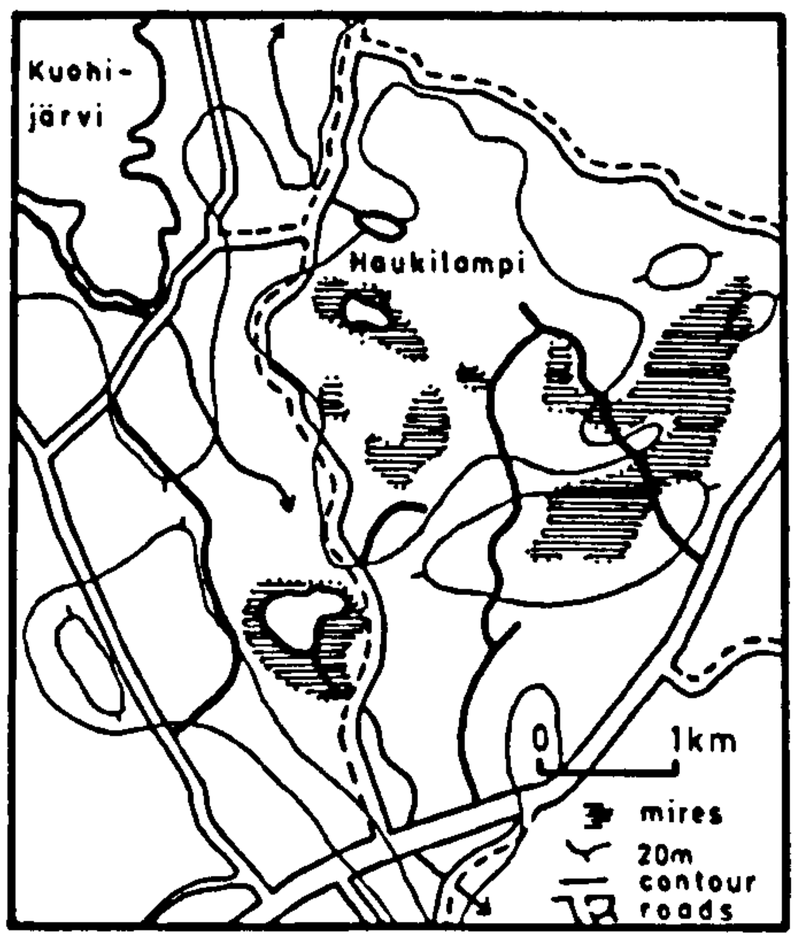


**Figure 3.9** Site location of a) Laaviosuo b) Varrassuo and c) Haukilampi. c.f. fig. 3.1 for general location in southern Finland.

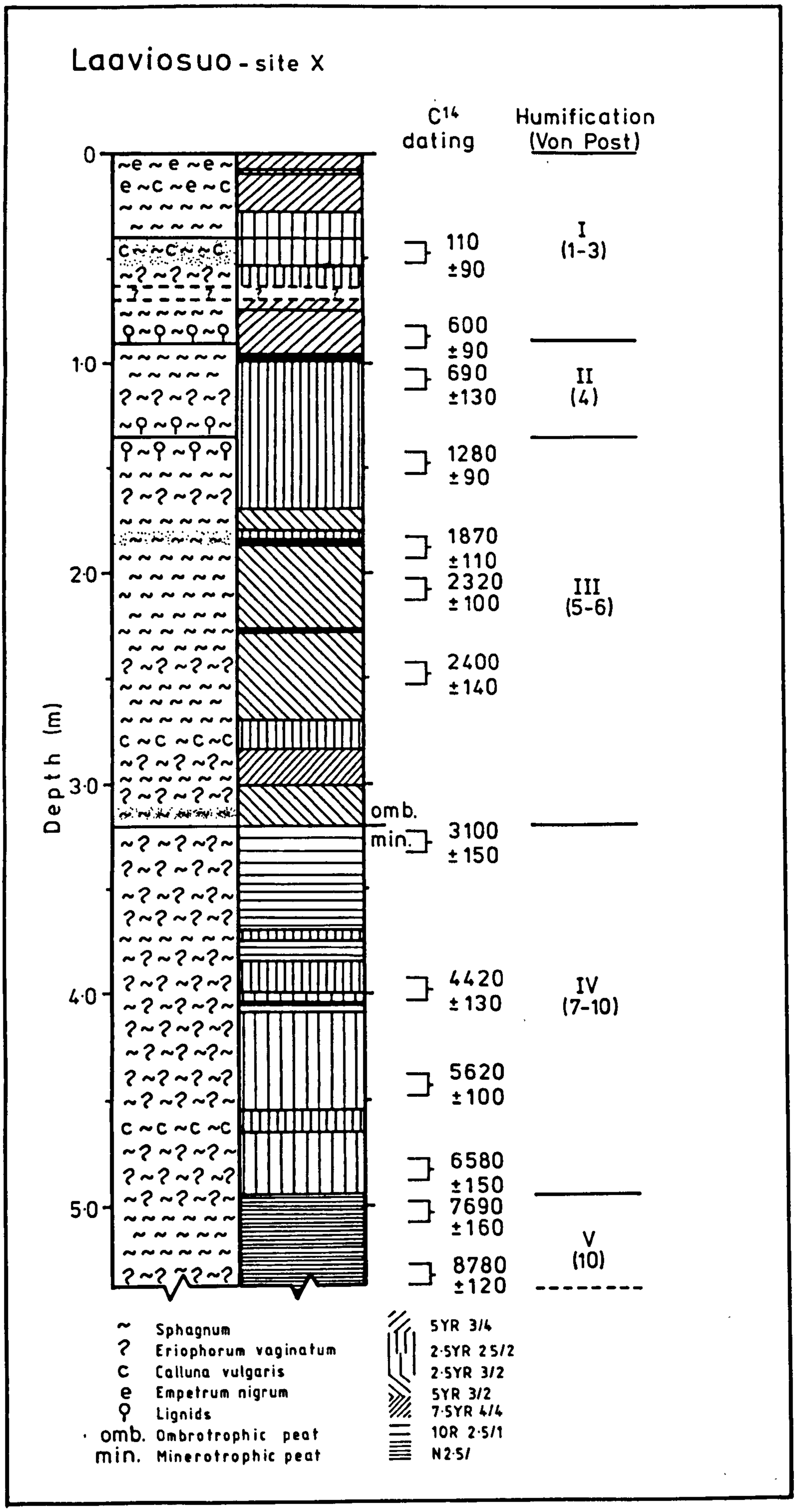


**Figure 3.10** Stratigraphy of site-X, Laaviosuo. $C^{14}$ dates from Appendix 4.

between 64.2gdm$^{-3}$ at 320cm and 23.4gdm$^{-3}$ towards the surface. The ash residues display a sub-surface peak between 15-17.5cm (2.76%) and a smaller surface peak of 2.07%.

### 3.5.3 Geochemical Results from LaavX

Geochemical profiles are presented in fig. 3.11. Although the profile terminates above the peat-mineral soil interface, the three stages in the chemical profiles from Kaurastensuo are evident. The lower section, from 538-320cm corresponds with the minerotrophic phase of the bog. Within the section iron concentrations decrease from 2000µg.g$^{-1}$ at 538cm to 400µg.g$^{-1}$ at the end of the minerotrophic phase (320cm). The lower section extends upwards to only 440cm for nickel, copper and less conspicuously, lead, all characterised by low but measurable concentrations.

The mid-section, like that at Kaurastensuo, comprises the majority of the profile and is characterised by low, often undetectable (cf. Appendix 3) concentrations. For nickel, copper and lead, this section extends between 440-50cm, whilst for iron it extends throughout the majority of the ombrotrophic phase (320-50cm). The top section includes a peak in iron, zinc and lead around the level of the water table (42.5cm). Iron, copper, zinc and lead also exhibit sub-surface peaks at 7.5-10cm, 2.5-5cm (copper and zinc) and 5-10cm respectively.

### 3.5.4 Magnetic Measurements

The magnetic profiles presented in fig. 3.12 display a similar basic pattern to the profiles for Kaurastensuo. The basal samples from 538-500cm are represented by low, but measurable ARM, SIRM and occasionally X values. The SIRM/X and SIRM/ARM ratios for samples within this small section are low, where measurable (<4 kAm$^{-1}$ and 12 respectively). The basal samples also exhibit the ability to acquire and

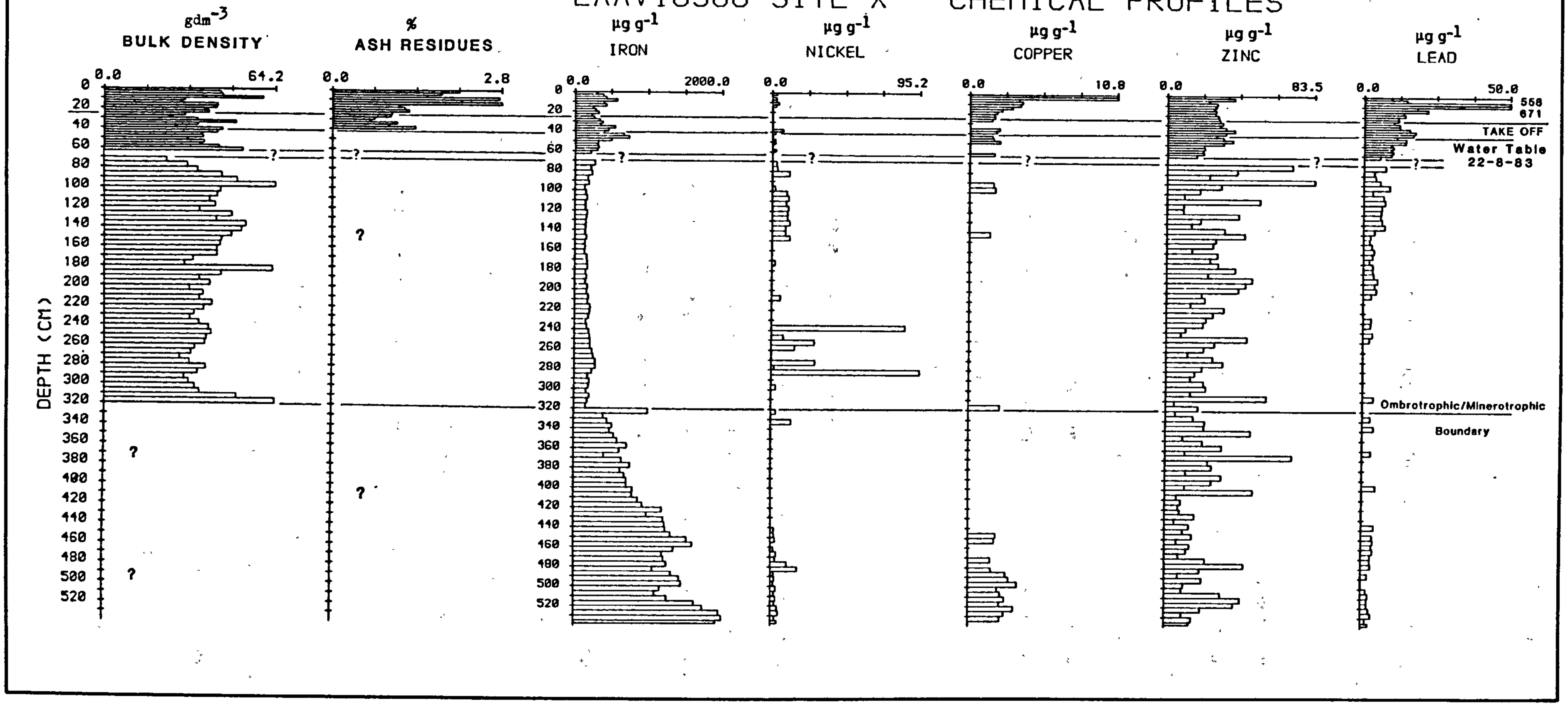


**Figure 3.11** Bulk density, ash residues and geochemical profiles for site-X, Laaviosuo

retain a larger remanence within the backfields displayed in fig. 3.12. The majority of the core (500-30cm) exhibits low SIRM, unmeasurable ARM and diamagnetic X.

Above 30cm, ARM and SIRM values gradually rise to a sub-surface peak (16 and 910 $10^{-6}Am^2kg^{-1}$ respectively), at 5-7.5cm below the surface. The rise in X starts at 25-22.5cm, also reaching a sub-surface peak at 5-2.5cm (5.7 $10^{-8}m^3kg^{-1}$). ARM/X values decrease in a linear fashion to a minimum at 7.5-5cm with a corresponding linear increase in SIRM/ARM to a maxima at 7.5-5cm. Above 5cm there is shift in the backfield ratios towards a softer reverse field remanence, increasing ARM/X values and a decrease in SIRM/ARM.

3.5.5 Discussion

Laaviosuo and to a lesser extent, Kaurastensuo, have experienced artificial drainage in recent times. The result at Laaviosuo has been a permanent lowering of the water table, 42.5cm at the time of sampling. The general effect on peat growth is an acceleration of the normal pathways of hydroseral change (Tallis, 1983). Similarly, artificiallyinduced changes in the water level of a lake, as at Tyotjärvi (sub-section 3.6.1), may affect the marginal wetland communities solely by advancing or retarding the hydroseral pathway. Following drainage, the peat mass may shrink in volume and develop a semi-impermeable surface skin, restricting water uptake and modifying the autogenic responses of the peat mass to changes in the water supply.

The iron profile discriminates quite effectively between the end of the minerotrophic phase and consequently the influences of the minerogenic waters, and the start of the ombrotrophic phase. Concentrations vary significantly between the two phases, being approximately two times higher at the end of the minerotrophic phase than

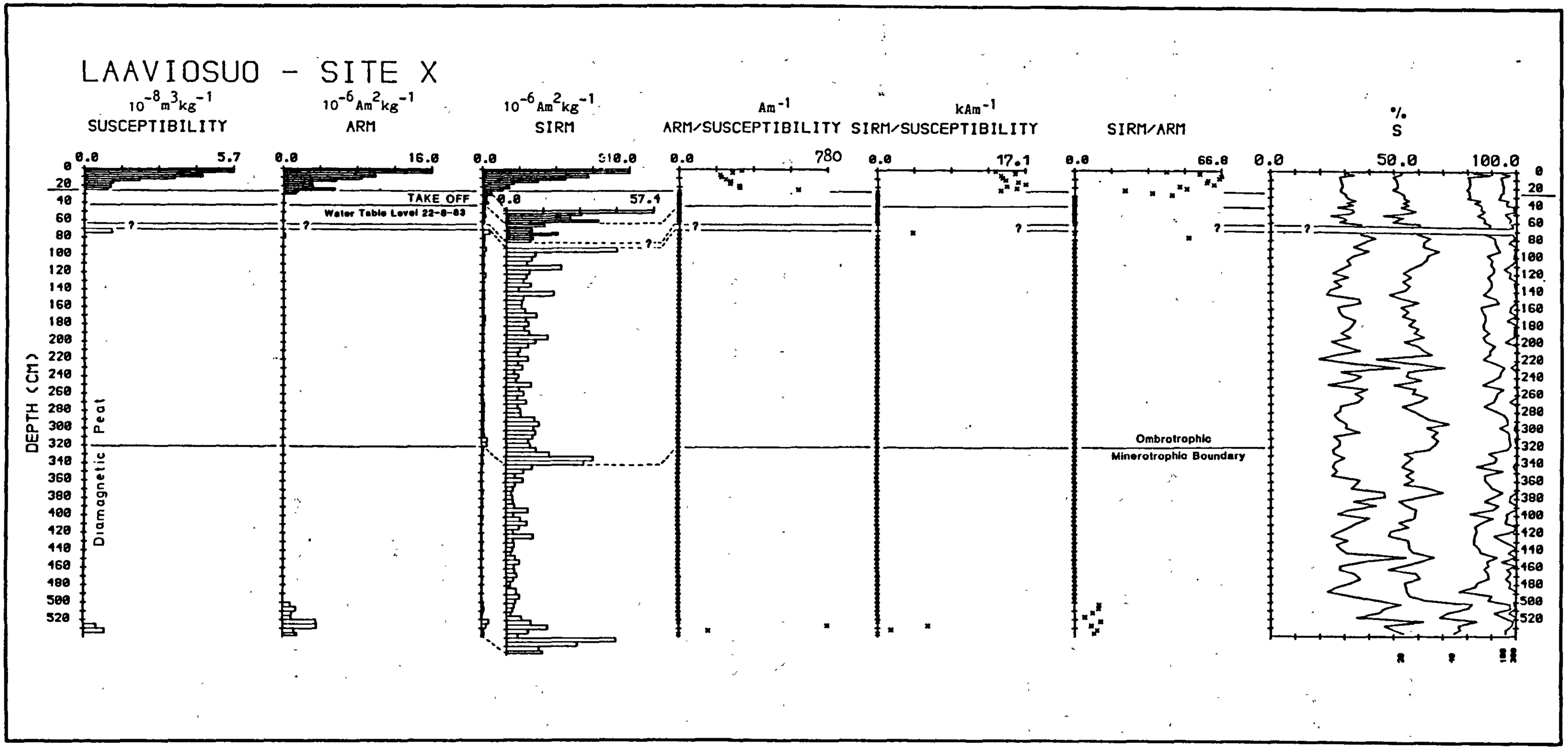


**Figure 3.12** Magnetic measurements for site-X, Laaviosuo. The inset within the SIRM profile is an expanded scale for samples below 30cm.

at the beginning of the ombrotrophic phase. The former is also marked by a single sample peak in iron concentrations.

The presence of lead concentrations within the minerotrophic phase may suggest concentrations of lead in the underlying mineral soil, probably in the form of oxides, as at Varrassuo (section 3.6.3). The high lead concentrations within the surface samples (0-50cm) are attributed to the increasing atmospheric deposition of lead associated with anthropogenic emissions. This conclusion follows previous work undertaken by, for example, Pakarinen & Tolonen (1976, 1977) and Rühling & Tyler (1970, 1971, 1973, 1984).

## 3.6 **Varrassuo**

### 3.6.1. Introduction

Varrassuo (60°59'N 25°29'E) is located in Hollola commune, ca.10km west of Lahti (fig. 3.1). It lies within the transition between the concentric, 'Kermi' bogs of coastal Finland and the eccentric, raised bogs of inner Finland (Eurola, 1962). An outline of the bog limits and its location with regard to Lake Tyotjärvi is shown in fig. 3.9b.

The central plateau of the bog (ca. 50ha) is covered with dwarf Pinus species, 1-3m high. The prevailing forest type in the area surrounded by the bog is dry pine forests of the Vaccinium type, along with Alnus, Picea and Betula spp. (Tolonen, 1966). As at the other three sites, S. fuscum communities dominate the vegetation of the hummocks with Vaccinium and Eriophorum spp. present. Between the hummocks there is a covering of Eriophorum vaginatum and some S. angustifolium (= S. parvifolium). The moss hollows are dominated by E. vaginatum, S. balticum and S. tenellum communities.

The centre of the bog has become drier in recent times, probably as

partial result of drainage, though this has now been abandoned and the ditches are largely overgrown, where present, in the southeast part of the bog (Tolonen, op. cit.). A more plausible explanation is the drainage of nearby Tyotjärvi (fig. 3.9b), noted by Donner (1951). The present lake level is 142.8m.a.s.l. compared with 147m.a.s.l. for the surface of Varrassuo.

### 3.6.2 Stratigraphy of VAX

The stratigraphy of VAX along with Flandrian chronozones and pollen rational limits are presented in fig. 3.13. The pollen rational limits and Flandrian chronozones are derived from the study by Donner (1966) using core samples from site-X. The data are correlated to the present core by reference to the ombrotrophic-minerotrophic boundary. Underlying the profile, at an undetermined depth between 400cm and 500cm below the surface, are fine sands of terrestric origin. The composition of the profile up to 245cm is predominantly Eriophorum with some decomposed Sphagnum remains. Directly above the terrestric sands is a woody layer.

The location of the ombrotrophic-minerotrophic boundary is less distinct than at either Kaurastensuo or Laaviosuo, where the transition is abrupt. Tolonen (1966) noted the boundary at 305cm-335cm-380cm on a SE-NW axis, using detailed peat and rhizopod analyses. Donner et al. (1978) place the boundary somewhere between 350-300cm. In fig. 3.13, using the above data corrected to the radiocarbon reference surface the boundary is probably somewhere around 310cm (cf. sub-section 3.11.3).

Between 320-200cm there is a series of very well humified bands of peat. The two uppermost bands contain noticeable amounts of charcoal. At 114cm the light/dark boundary or 'Grenzhorizont' (RYIII; after Weber, 1908) is evident, marked by an abrupt transition from humified, almost black Sphagnum-Eriophorum peat (below 114cm) to virtually unhumified, purely Sphagnum peat above 114cm.

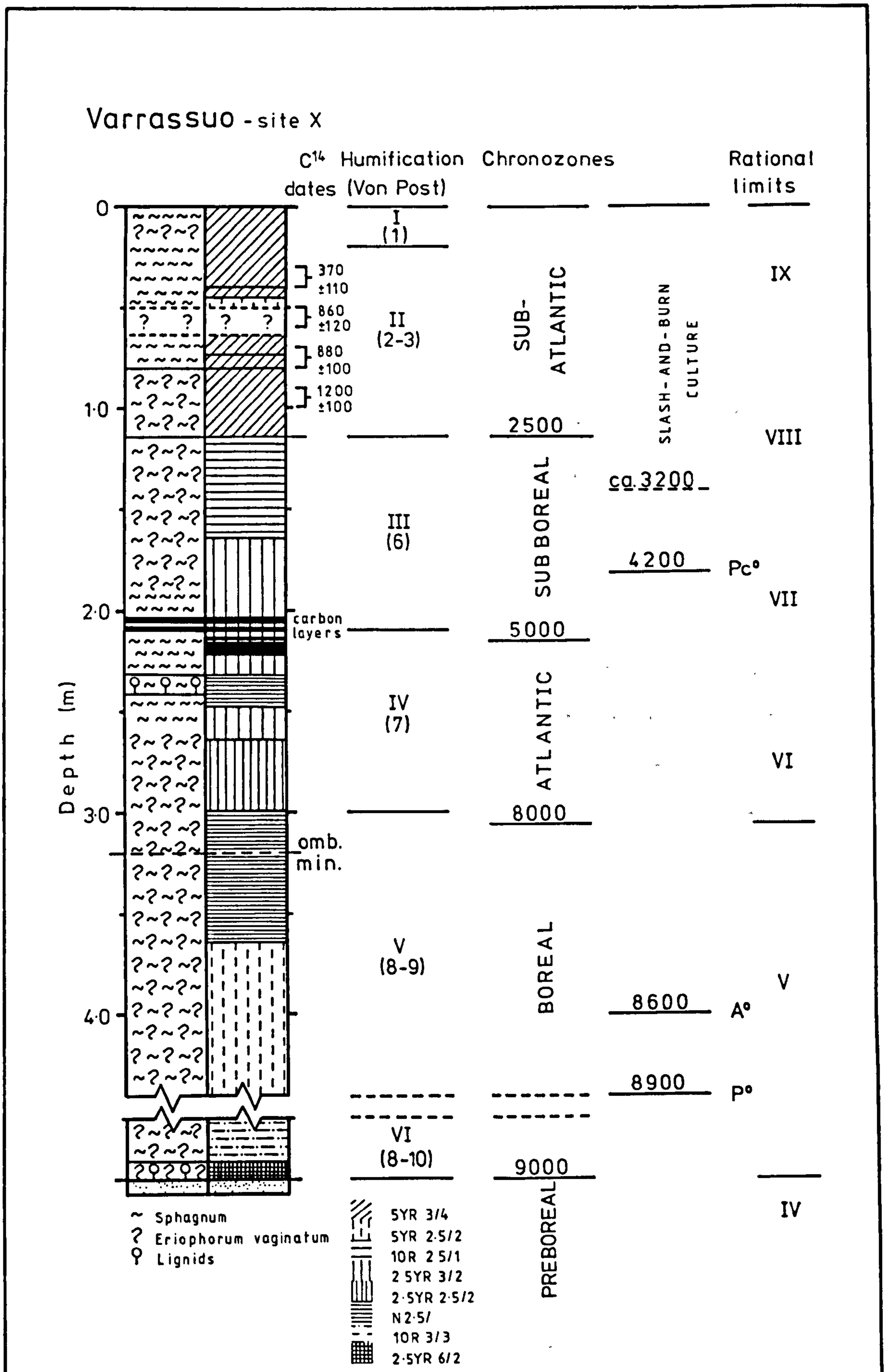


**Figure 3.13** Stratigraphy of site-X, Varrassuo. $C^{14}$ dates from Appendix 4, Flandrian chronozones and pollen rational limits from Donner (1966). See text for explanation.

Bulk density data (fig. 3.14), available for the top 50cm, display a decrease in values from 55.7-70.4gdm$^{-3}$ for samples below 40cm, to 27.8-50.4gdm$^{-3}$ above 40cm. The results of selective ashing throughout the profile are given in fig. 3.14. These were based on observations on the inorganic residue after nitric acid digestion (Appendix 3) for chemical analyses. The results of the ashing reveal marked variations in ash residues throughout the profile, ranging from 4.7% (159-154cm) to 0.63% (174-169cm). The ash residue of the underlying sediment was 88.1% for the contact sample (0-4cm).

3.6.3 Geochemical Profiles from VAX

The fine sands underlying Varrassuo exhibit high concentrations of all five elements, relative to the peat samples directly above (fig. 3.14). The most notable difference is in the iron profile where the underlying mineral is approximately eight times higher than the overlying peats. The mineral soil has a lead concentration of 4.7$\mu g.g^{-1}$ whilst the peat samples directly above it have unmeasurable amounts of lead.

If the profile is split into three parts, as with the previous sites, then the basal section extends from 414cm to about 300cm, marked by decreasing iron concentrations as peat accumulation increases. A notable feature of this basal section at Varrassuo is the increase in zinc concentrations between 410-369cm. Between 410cm and 399cm concentrations increase from 121$\mu g.g^{-1}$ to 288$\mu g.g^{-1}$. Between 399-369cm they increase by an order of magnitude to 1576-5161$\mu g.g^{-1}$.

The mid-section is similar to previous sites, with low but measurable iron concentrations and often unmeasurable nickel and copper concentrations between 300-50cm. The lead profile exhibits almost wholly undetectable concentrations within the basal and mid-sections.

The top 50cm of the profile is characterised by small peaks in iron,

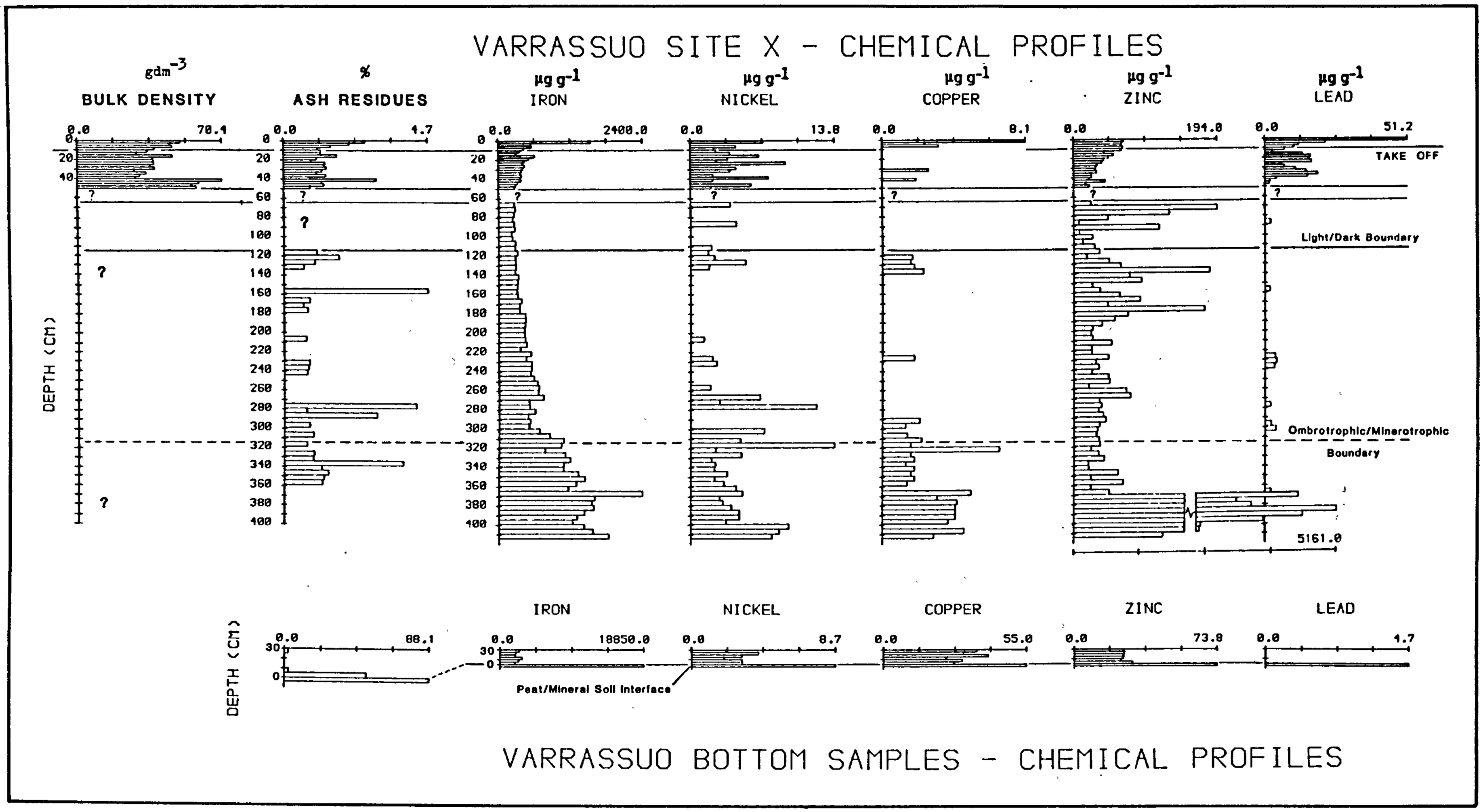


**Figure 3.14** Bulk density, ash residues and geochemical profiles for site-X, Varrassuo

lead and less conspicuously, nickel between 17.5-15cm. The surface sample also exhibits a two-fold increase in concentrations of iron, nickel, copper and lead.

### 3.6.4 Magnetic Measurements

The underlying mineral soil displays a significantly different set of magnetic characteristics to the basal peats (fig. 3.15). On relative terms these include an eight-fold decrease in X, lower SIRM and SIRM/ARM, and an increase in ARM/X and SIRM/X from the sediment to the peat. The backfield ratios show a harder reverse field remanence in all ratios compared with peat samples above it. The limit of detectable ARM values and positive X values extends upwards to 380cm characterised by low SIRM/X and SIRM/ARM ratios. The mid-section, from 380-15cm is similar to previous sites, low SIRM values, unmeasurable ARM and diamagnetic X ($-0.3 - -0.59\ 10^{-8}m^3kg^{-1}$).

The top samples (15cm to the surface) are characterised by increasing X, ARM, SIRM and SIRM/ARM, and decreasing ARM/X towards the surface. The surface sample exhibits peaks in X, ARM and SIRM, being more than four times as high as the preceding sample for X and SIRM, and over twice as high for ARM. The reverse field remanence for the surface sample (0-2.5cm) is markedly softer than for the preceeding sample, especially for $IRM_{-100mT}$/SIRM and $IRM_{-300mT}$/SIRM.

### 3.6.5 Discussion

The two charcoal layers between 210-200cm correspond to the layers noted by Tolonen (1966) occurring in the western part of the bog, extending about 500m in from the bog margin toward the centre. Tolonen concluded that, given the synchroneity of the upper layer neither the marginal scarp nor the convexity of the bog had developed at the time of the ancient fire, around the end of the Atlantic Time (ca. 8000BP). This hypothesis is

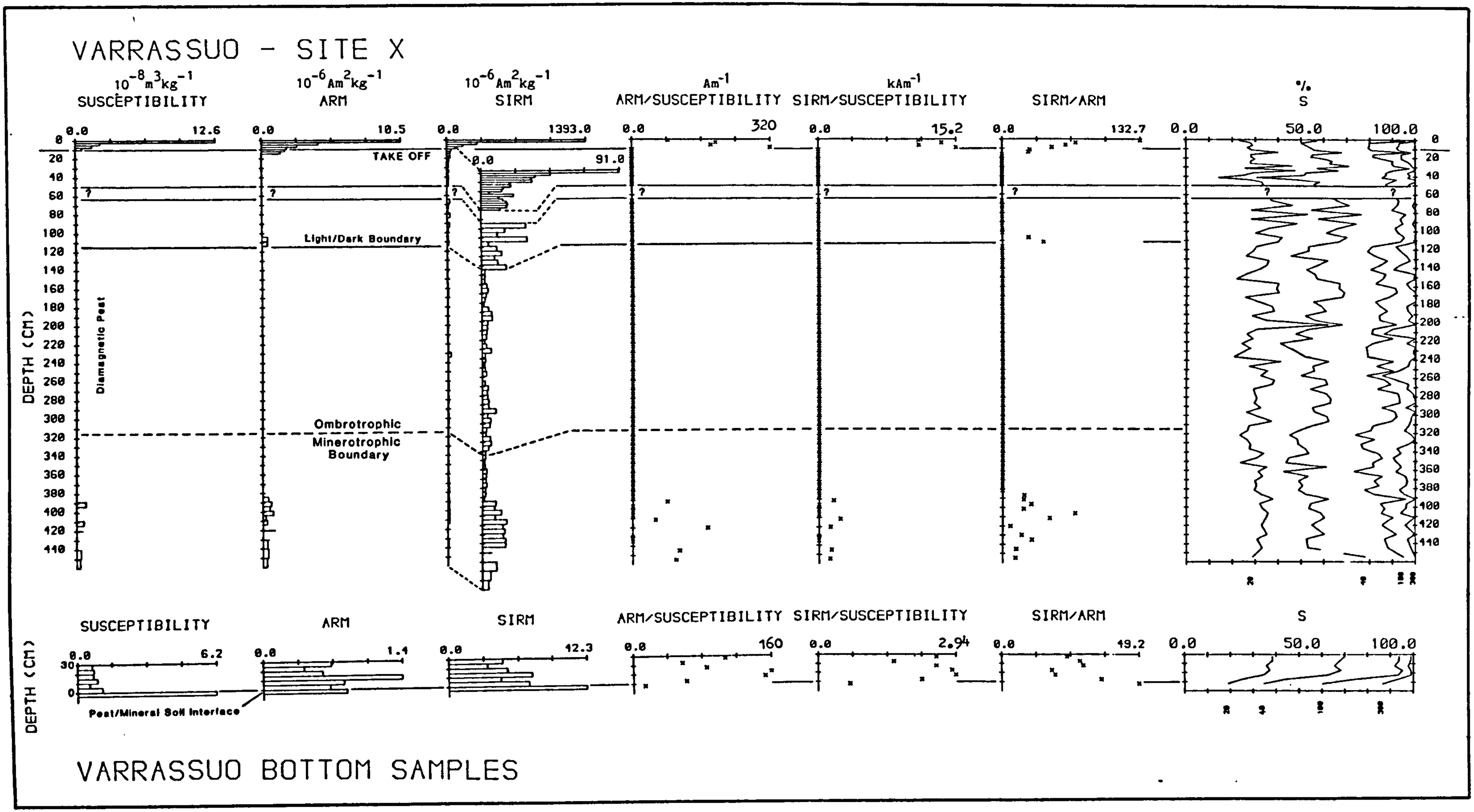


**Figure 3.15** Magnetic measurements for site-X, Varrassuo. The inset within the SIRM profile is an expanded scale for samples below 7.5cm.

supported by an observation made by Tallis (1983) that burning seldom affects the mire uniformly, presumably because of local variations in the wetness of the surface peat layers.

Natural or Man-induced fires provide extreme environmental conditions of high temperature and anaerobia associated with the natural formation of magnetite. The combustion of organic compounds within the surface layers causes both great temperatures (up to 700°C) and the production of a reducing atmosphere. Under these conditions, non-ferrimagnetic oxides present are likely to be reduced to magnetite. However, in ombrotrophic peat layers, receiving nutrition and particulate supply from the atmosphere, the concentration of non-ferrimagnetic oxides available for reduction is very low. Hence, there is no apparent enhancement of magnetic minerals. There is however, a suggestion of some change occuring within the backfield ratios. Between 205-200cm there is a marked shift towards a soft reverse field remanence associated with ferrimagnetic minerals.

The location of the light/dark boundary or 'Grenzhorizont' (RYIII) at 114cm is usually associated with a major change in climate from the sub-Boreal to the sub-Atlantic (Gore, 1983). Using chronozones provided by Donner (1966) this change occurred somewhere around 2500BP.

Although the position of the water table at Varrassuo is not known for core VAX, it may be inferred from the iron, lead and nickel profiles (fig. 3.14). These elements show peak concentrations around the level of the water table at the other three sites. The sub-surface peaks in iron, lead and nickel at Varrassuo suggest that the level was probably around 15-17.5cm below the surface at the time of sampling.

The distinctive surface peak in magnetic and chemical concentrations is interpreted as a direct result of output from a recently built factory and

stack on the southeast margin of the bog, occupying the site between the bog margin and the road junction (fig. 3.9b). The construction of the factory was probably completed sometime between 1974 and 1978. The older date is the lower limit, based on moss increment counting (cf. Chapter 4), of the topmost sample (0-2.5cm), which appears to be the only sample affected by such a marked increase in magnetic and chemical concentrations. The upper date is based on the existence of the factory in the 1978 aerial photograph 75162:31(213312) presented in Donner et al. (1978).

The proximity of the point source at Varrassuo appears to be reflected in the fact that all the indicators of increasing anthropogenic deposition (increased X, ARM, SIRM and SIRM/ARM) display such a marked increase from 5-2.5cm to the surface sample. This may be further interpreted as the local, site-specific magnetic characteristics superimposed on the lower 'regional' characteristics displayed from 10-2.5cm at Varrassuo, and above the take-off points at other sites (cf. Kaurastensuo, Laaviosuo and Haukilampi,above).

## 3.7 Haukilampi

### 3.7.1 Introduction

Haukilampi (61°08'N 24°58'E) is situated about 8km north of Lammi (fig. 3.1). In contrast with the other sites, the peat bog at Haukilampi encompasses a small lake (fig. 3.9c). The present lake level is approximately 100-105cm below the surface of the bog. S. fuscum and Empetrum nigrum dominate the hummock communities, with occasionally S. rubellum. E. vaginatum and S. balticum -found ... in the moss hollows. The bog surface has a covering of dwarfed Pinus spp. ca.3m high.

The long profile terminates in a log rich layer at 238cm. However,

probing indicated that the depth of the peat mass at the coring site was over 500cm. The core site was located some 50m from the north side of the lake margin.

### 3.7.2 Stratigraphy of Haukilampi

The peat stratigraphy, humification and water content profiles from Haukilampi are presented in fig. 3.16. Bulk density values and ash residues (0-30cm) are presented in fig. 3.17. The peat stratigraphy profile contains numerous woody layers, notably between 238-200cm, 80-70cm and 40cm. There is also evidence of a burnt horizon at 82-75cm corresponding with a decrease in bulk density values and water content immediately above, and an apparent change in humification values (cf. section 3.7.5).

The ash residue values, above the water table (32.5cm) show a marked rise to a surface maximum of 2.8%. This increase reciprocates with a decrease in bulk density values towards the surface.

### 3.7.3 Geochemical Profiles from Haukilampi

The truncated chemical profiles presented in fig. 3.17 display only the upper portion of a theoretically complete profile from the peat-mineral soil interface to the surface. Therefore, the section from 238-50cm represents only a part of the mid-section, as described at previous sites. This section is characterised by decreasing iron concentrations from 238cm upwards, low but detectable nickel and zinc concentrations and predominantly undetectable copper and lead concentrations.

Lead concentrations begin to increase from 70cm upwards to a peak at 32.5cm which corresponds with a similar peak in iron concentrations, around the level of the water table. Iron, lead and nickel display sub-surface peaks between 10-5cm whilst copper and zinc display surface peaks. Copper concentrations increase markedly from 17.5cm to the surface.

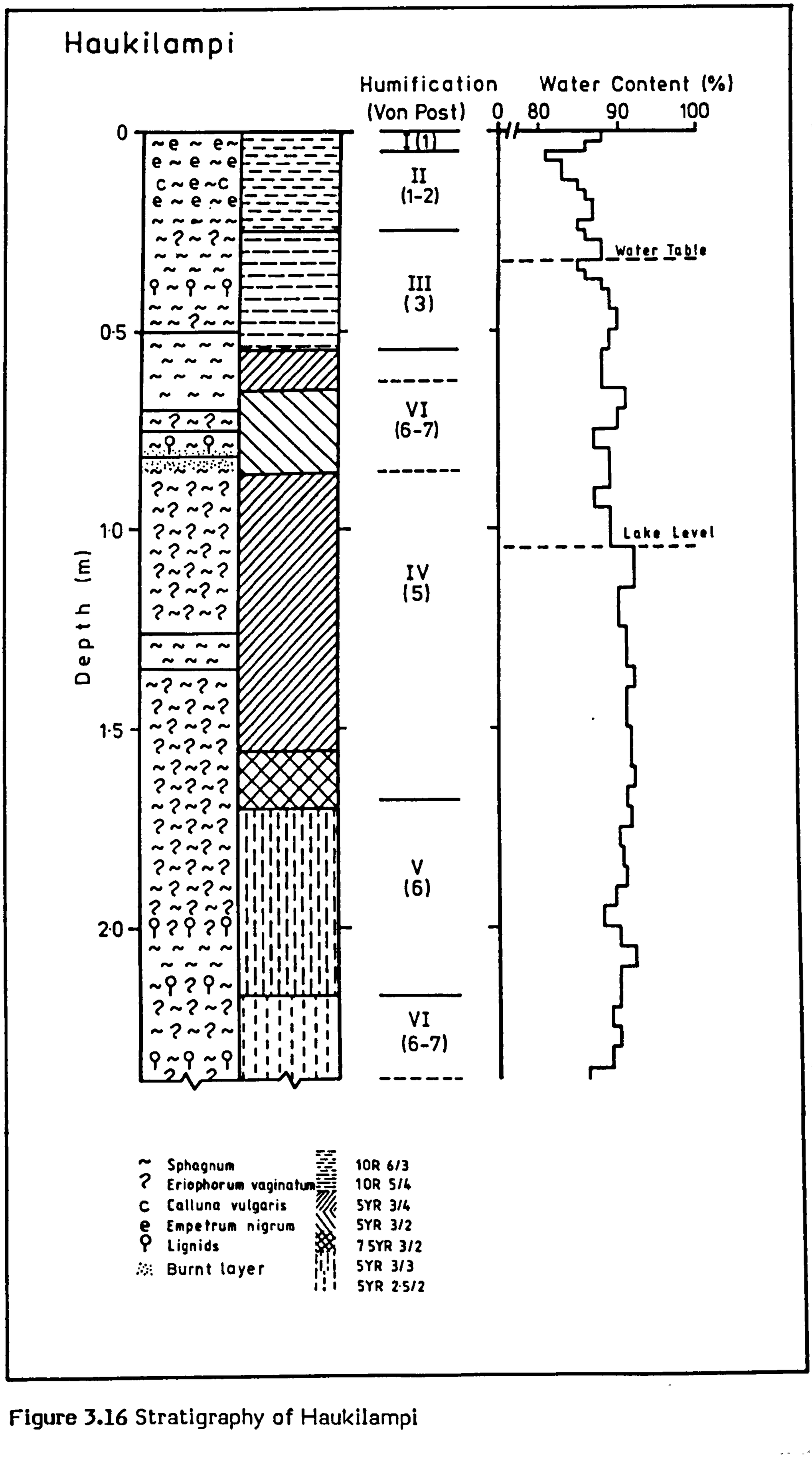


**Figure 3.16** Stratigraphy of Haukilampi

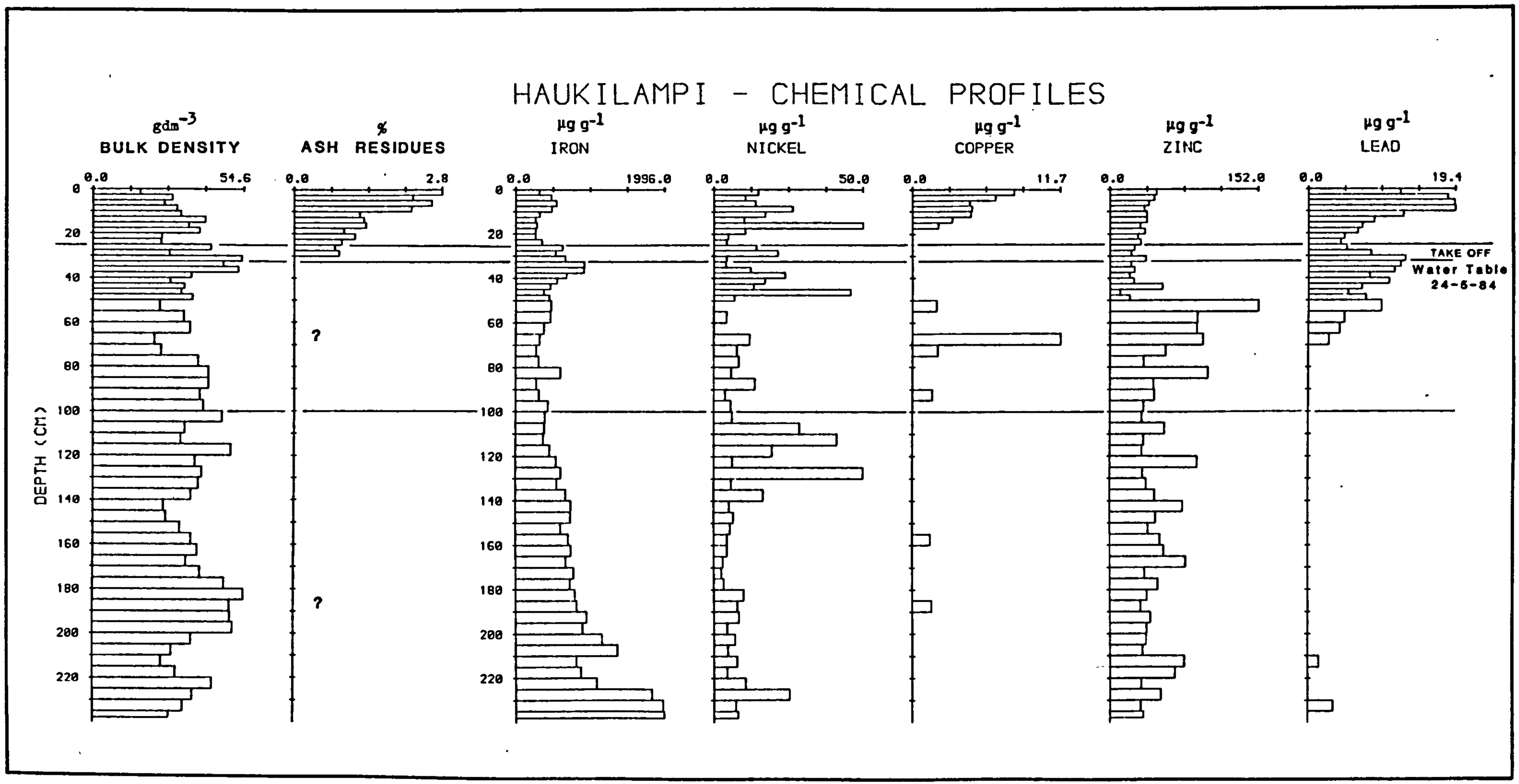


**Figure 3.17** Bulk density, ash residues and geochemical profiles for Haukilampi peat core

3.7.4 Magnetic Measurements

Similar to the chemical profiles, the magnetic measurements indicate that the base of the core lies somewhere within the mid-section of a complete magnetic profile. From 238-30cm the core displays low SIRM values, with unmeasurable ARM values and diamagnetic X values ($\chi$= -0.33 $10^{-8}m^{-3}kg^{-1}$). Within the backfield ratios for samples in this section there are a number of single sample, 'soft' spikes, notably in the lower backfield ratios, $IRM_{-20mT}$/SIRM and $IRM_{-40mT}$/SIRM. These spikes appear at 220-215cm and 125-120cm. Between 40-30cm, directly beneath the level of the water table there is also a prominent 'hard' feature within all the backfield remanences, but notably within the upper backfields, $IRM_{-100mT}$/SIRM and $IRM_{-300mT}$/SIRM.

The surface section of the magnetic profiles, as at previous sites is characterised by increasing X (17.5cm upwards), ARM (20cm upwards), SIRM (25cm upwards) and SIRM/ARM. ARM, SIRM and $SIRM_{VS}$ (fig. 3.8) peak below the surface at 7.5-5cm, whilst X, ARM/X and SIRM/ARM peak above at 5-2.5cm.

3.7.5 Discussion

The apparent effect of the burnt horizon on humification, water content and bulk density is consistent with observations made by Tallis (op cit) given in sub-section 3.6.5. As well as forming a semi-permeable skin, thus altering the seepage and water retention characteristics, the resulting surface deposits of ash also give rise to temporarily increased nutrient levels, particularly phosphate. Consequently, after a severe burning there may be an initial recolonising stage dominated by nitrophilous species, resulting in changes to the bulk density of layers post-dating the fire (cf. fig. 3.17).

The 'soft' spikes noted within the backfield ratios correspond with

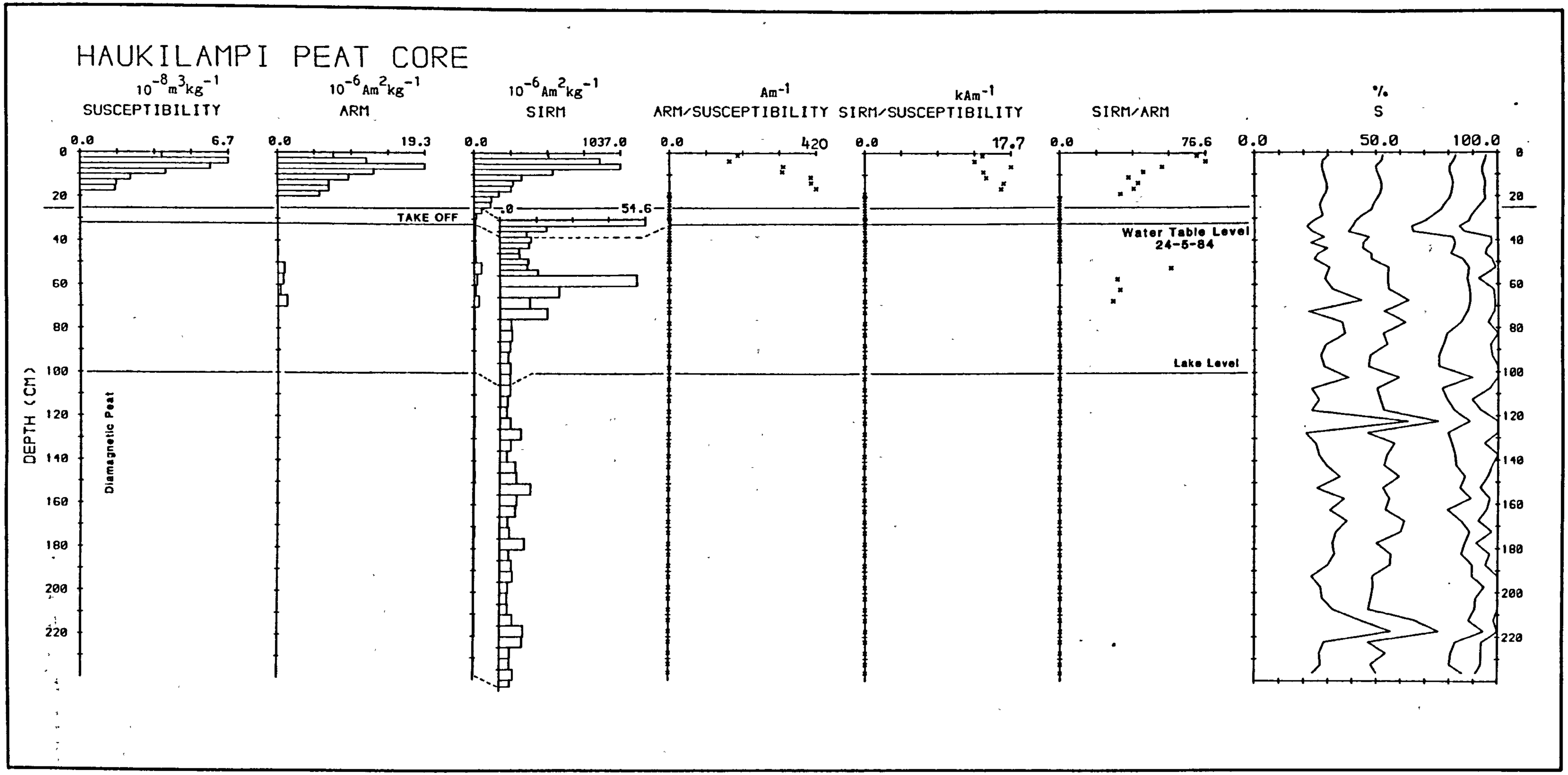


**Figure 3.18** Magnetic measurements for Haukilampi peat core. The inset within the SIRM profile is an expanded scale for samples below 25cm.

small peaks in the SIRM profile. These peaks also correspond with predominantly single sample peaks in the zinc profile (fig. 3.17). Further corresponding SIRM and zinc peaks are also evident at 175-170cm, 150-145cm and 70-50cm. Given the problems of contamination noted within earlier profiles (sub-section 3.4.7) the correspondence between the magnetic and chemical profiles in these samples implies that they may also be attributable to coring contamination.

The difference in depth of the sub-surface peaks within the magnetic profiles is probably a result of small shifts in grain size, type or shape, as well as a quantitative change within the surface samples. These qualitative shifts, as noted by stepwise shifts in interparametric ratios (eg. ARM/X and SIRM/ARM) appear to augment the dominant magnetic characteristics of the surface samples, as seen at Varrassuo (sub-section 3.6.5).

## 3.8 Interpretation of Bog Development in Southern Finland

Two of the four peat bogs sampled have basal limnic deposits (Kaurastensuo and Haukilampi), Varrassuo has post-glacial fine sands whilst the underlying deposits of Laaviosuo are not known. Tolonen (1967) noted only five profiles from thirtyfive sites within southeast Finland containing basal limnic deposits. In the majority of cases minerotrophic wetland communities developed above post-glacial sands as at Varrassuo (Tolonen, 1966).

In the early stages of development most wetland habitats are affected by laterally flowing groundwaters which may be either relatively rapid (soligenous vegetation) or low flow movements of water (topogenous vegetation). Soligenous vegetation types trap appreciable quantities of silt around the base of reed-swamp plants as well as considerable deposition of the accumulating plant remains. Water flow initially directed over the

majority of the high density surface gradually becomes canalised with a progression towards localised ombrotrophic conditions (Tallis, op. cit.). Rapid accumulation of low density peat occurs under low initial flow conditions, directing the flow of groundwater around its mass, forming a raised reservoir with its own 'perched' water table. Pre-existing stratigraphical investigations (Niiranen, 1973) suggest that at Kaurastensuo the former, relatively rapid flow conditions prevailed.

The oldest dates at Varrassuo, Laaviosuo and Kaurastensuo are ca.9000yrs BP (Donner et al., op. cit.), 8780±120yrs BP and 8120±110yrs BP respectively. These dates correspond with the transition from the Pre-Boreal to Boreal Times, zones IV and V respectively (sub-section 3.2.2) marking the beginning of peat formation in the area.

At Varrassuo, the initially rapid peat accumulation rates of the Carex-Equisetum-Bryales peat and overlying Sphagnum-Carex peat decrease toward the end of the Boreal time, largely as a result of peat growth (Donner et al., op. cit.). The transition from Boreal to Atlantic Times, corresponding with the end of zone V around 8000yrs BP is marked by the lowest rates in accumulation, with possibly a standstill in peat growth. Above this, the accumulation of peat within the ombrotrophic phase reflects changes in humidity, dependent on precipitation and temperature, throughout the Atlantic, sub-Boreal and sub-Atlantic chronozones.

In contrast with Varrassuo, the minerotrophic phase at Kaurastensuo and Laaviosuo appears to have lasted much longer. The $C^{14}$ date for 315-305cm at Kaurastensuo, at the very end of the minerotrophic phase is 3040±120yrs BP. The corresponding date for Laaviosuo, also at the end of the minerotrophic phase is 3100±150yrs BP (327-322cm). The dates from Kaurastensuo and Laaviosuo are in good agreement with each other but are

some 5000 years younger than the corresponding transition at Varrassuo. The difference is most plausibly explained by the development of the respective bogs, initially under different conditions. At Varrassuo, the bog developed above the groundwater level and associated mineral soil water influences. At Kaurastensuo and presumably Laaviosuo, the influence of minerogenic waters persisted as a result of development above aquatic sediments. The constraints of topography (cf. figs. 2.1 and 3.9a) may also have contributed to the persistence of the minerotrophic environment.

Previous studies (eg. Eurola, 1962; Tolonen, 1966) have tended to associate the dark banding noted within the ombrotrophic stratigraphy peat (eg. figs. 3.4, 3.10 and 3.13) with cyclical growth within the bog. Any inference based on a single boring at each bog (eg. this study), rather than examination of exposed peat faces (eg. Barber, 1978) is tenuous. This is supported by subsequent re-examinations of the bogs in the same general area resulting in different interpretations (eg. Tolonen, 1971).

## 3.9 Geochemical Relationships and Peat Bog Development

### 3.9.1 Oxidation-Reduction Process

The relationships between water table fluctuations, redox potential and chemical transformations are important in the interpretation of biogeochemical profiles. At some stage in the accumulation of the peat, the organic remains come into contact with the redox boundary, usually as the peat is passing through the acrotelm into the catotelm (Clymo,1984). A brief summary of these relationships is given below.

Submergence of peat through fluctuations in the water table cuts off the oxygen supply causing reducing conditions, as defined by Eh values below that at which dissolved oxygen becomes undetectable (Ponnamperuma, 1972). The requirements for reduction are the absence of

oxygen, presence of decomposable organic matter and anaerobic bacterial activity. The rate, course and degree of reduction are influenced by the nature and content of electron acceptors participating in the oxidation-reduction reaction. Sikora & Keeney (1983) and Clymo (1983) note, however, that microbial activity in peat is low, potentially limiting the redox reactions.

On submergence the aerobic organisms within the peat use up the available oxygen until they become quiescent or die. On a seasonal scale this stage usually occurs after a rise in temperatures in late spring (Clymo, op. cit.). Facultative and obligate anaerobes (Table 3.3) then proliferate using the carbon compounds as a substrate and the oxidised peat components and dissimilation products of organic matter as electron acceptors in respiration. The switch from aerobic to anaerobic respiration occurs at very low oxygen concentrations of $3x10^{-6}M$ initiating the reduction process (Ponnamperuma, op. cit.).

The intensity of the oxidation-reduction reaction is measured by redox potential (Eh) which is normally positive and high in strongly oxidising systems or negative and low in strongly reducing systems (Table 3.3). All chemical reactions within the peat strata involving the exchange of electrons will be influenced by the redox potential (Eh). For example, the seasonal cycle of sulphide production through the reduction of $SO_4^{2-}$ - $S^{2-}$ (Urquhart & Gore, 1973; Clymo, op. cit.).

Urquhart & Gore (op. cit.) in a systematic study of the Eh of 4 acid peat profiles (pH= 2.7-3.17) in northern England over a one year period, found that Eh decreased with depth; ie. the environment became more reducing. The greatest quantity of sulphate reducing bacteria (Desulfovibrio) was detected within the 10-20cm horizon. Clymo (1965) noted that the rate of breakdown within this horizon was intermediate

**Table 3.3** Possible Systems Operating in Flooded Environments as Related to the Redox Potential
(after Sikora & Keeney, 1983)

| System | Redox Potential Range (mV)* | Micro-organisms Involved |
|---|---|---|
| Oxygen disappearance | +500 to +350 | aerobes |
| Nitrate disappearance | +350 to +100 | facultative anaerobes |
| $Mn^{2+}$ formation | <+400 | facultative anaerobes |
| $Fe^{2+}$ formation | <+400 | facultative anaerobes |
| Sulphide formation | 0 to -150 | |
| hydrogen, methane formation | below -150 | obligate anaerobes |

* corrected to pH 7 ($Eh_7 = Eh-0.59\ [pH-7]V$)

**Table 3.4** Correlation of SIRM, Iron and Lead in Surface Samples from Southern Finland. Using Pearson's product moment, r, where n = the number of cases.

| Site | n | SIRM v. Fe | SIRM v. Pb | Fe v. Pb |
|---|---|---|---|---|
| Kaurastensuo KAX (0-12.5cm) | 5 | 0.990** | 0.588 | 0.479 |
| Laaviosuo LaavX (0-20cm) | 8 | 0.707* | 0.425 | 0.758* |
| Varrassuo VAX (0-10cm) | 4 | 0.994** | 0.991** | 0.971* |
| Haukilampi | 8 | 0.873** | 0.907** | 0.871** |

* Significant at the 0.05 level

** Significant at the 0.01 level

between the high surface rates and the relatively slower rates of greater depths. The effect of temperature on Eh values also becomes more significant with depth, presumably because of the lessening of oxygen diffusion effects on the redox potential (Clymo, op. cit.).

Redox potential reported by Wilde et al. (1950) and Haavisto (1974) confirm that a waterlogged peat profile is generally anaerobic. Thus, denitrification (Table 3.3) can readily occur, although nitrate is often scarce in acid peats (Sikora & Keeney, op. cit.). Iron and manganese become reduced and mobilised, $S^{2-}$ ions can form and ferrous sulphide (see below) may be precipitated. Under anaerobic conditions the reduction of iron occurs at a lower redox potential than, for example, the reduction of nitrate. Therefore, because of the greater amounts of iron usually occurring in submerged soils than nitrates, the resulting Eh is probably governed most by the $Fe^{3+}$ - $Fe^{2+}$ oxidation-reduction system (Takai & Kamura, 1966). There are, however, numerous errors noted with regard to measurement of Eh (Ponnamperuma, op. cit.; Gore, 1983; Clymo, op. cit.) rendering retrospective analysis inappropriate. Intrinsic errors include pH effects, absence of a true equilibrium, liquid junction potential errors, heterogeneity of the medium and the discrepancy of potentials measured in submerged soils and those of their medium (Ponnamperuma, op. cit.). Extrinsic errors include those of sampling methods and extraction of the interstitial solutions without altering their composition, where applicable.

### 3.9.2 Chemical Profiles and Transformations in Peat

The most important chemical change that takes place when a soil is submerged is the reduction of iron and the accompanying increase in solubility (Ponnamperuma, op. cit.). This has several major consequences within the peat profile: a) the concentration of water soluble iron increases; b) pH increases; c) cations are displaced from exchange sites; d)

the solubility of phosphorus and silica increases, new minerals are formed; and e) the dynamics of $Fe^{2+}$ and $Mn^{2+}$ affect the concentrations of other cations. The direct effect in organic matter is that iron concentrations build up, as high as 600ppm within 1-3 weeks. Mobilisation of iron from stable compounds, including the crystalline lattices of minerals such as siderite ($FeCO_3$) and vivianite [$Fe_3(PO_4)_2.8H_2O$] formed within the peat (Ponnamperuma, op. cit.), occurs through metabolic / microbial activity in organic soils. The latter is associated with the high concentrations of ligands, humic and fulvic acids found in peat bogs (Clymo, 1983). The effect of this increase in mobilisation of iron is the increase in concentrations around the water table corresponding to the top of the catotelm. The corresponding water soluble manganese ($Mn^{2+}$) profile displays this pattern (cf. fig. 3.6). The concentration of mobilised iron ($Fe^{2+}$) is presumably responsible for the iron concentration peaks around the water table noted in KAX, LaavX, VAX and Haukilampi (figs. 3.5, 3.11, 3.14 and 3.17 respectively). The paucity of concentrations noted in the ombrotrophic peat below the water table may be partly explained by the diffusion upwards of the $Fe^{2+}$ to the oxygenated soil-water interface (water table) on reduction from $Fe^{3+}$.

The contrast in peat bog development at Kaurastensuo and Varrassuo is evident from the chemical profiles, notably iron. Decreasing concentrations upwards from the peat-mineral soil interface at Kaurastensuo is seen as a result of the decreasing influence of the minerogenic waters through increasing peat accumulation. At Varrassuo there is a sharp contrast in element concentrations of the mineral soil and basal peats (fig. 3.14).

The environmental conditions prevailing in the initial stages of peat development at Kaurastensuo; ie. telmatic, with fluctuating redoxcline and

alternating aerobic and anaerobic conditions may also have been conducive to the precipitation of Fe-minerals (fig. 3.19). The precipitation of pyrite under such conditions is noted by Ponnamperuma (op. cit.), Berner (1970, 1984) and Sikora & Keeney (op. cit.).

Although the forms of copper and zinc, among others, are probably not involved in redox reactions, their mobility may be affected by some of the consequences of submergence below the water level. The reduction of hydrous oxides of Fe(III) and Mn(IV) and the production of organic complexing agents should increase the solubility of copper and zinc. This is evident from KAX, LaavX and Haukilampi (figs. 3.6, 3.10 and 3.11 respectively). The net result of submergence is to increase the availability of copper and depress that of zinc (Ponnamperuma, op. cit.) as evident by the paucity of copper in the mid profiles compared with zinc (figs. 3.5, 3.11, 3.14, 3.17). The mobilisation of iron and zinc is noted by Damman (1978) at Tranerods Mosse and Store Mosse in Sweden and Malmmyran in Norway. Translocation of zinc above the water level was low or negligible, but below the permanent water level it is almost completely removed. This feature is also noticeable within the soluble zinc ($ZnSO_4$ or $ZnSO_3$) profile at Kaurastensuo (fig. 3.6). During periods of high water level the zinc in the zone of water table fluctuations can be reduced to insoluble ZnS. This becomes mobile when oxidised to soluble $ZnSO_4$ or $ZnSO_3$ at lower water levels resulting in higher concentrations around the water level.

The presence of lead within the profile is seen as a function of recent atmospheric deposition (allocthonous) rather than any authigenic response to autogenic processes. It is discussed in detail with regard to links with anthropogenic deposition in sub-section 3.9.4. The general pattern of the profiles (figs. 3.5, 3.11, 3.14 and 3.14) follow a trend noted by Damman (op. cit.) suggesting that lead is not removed from aerated hummock peat. As a

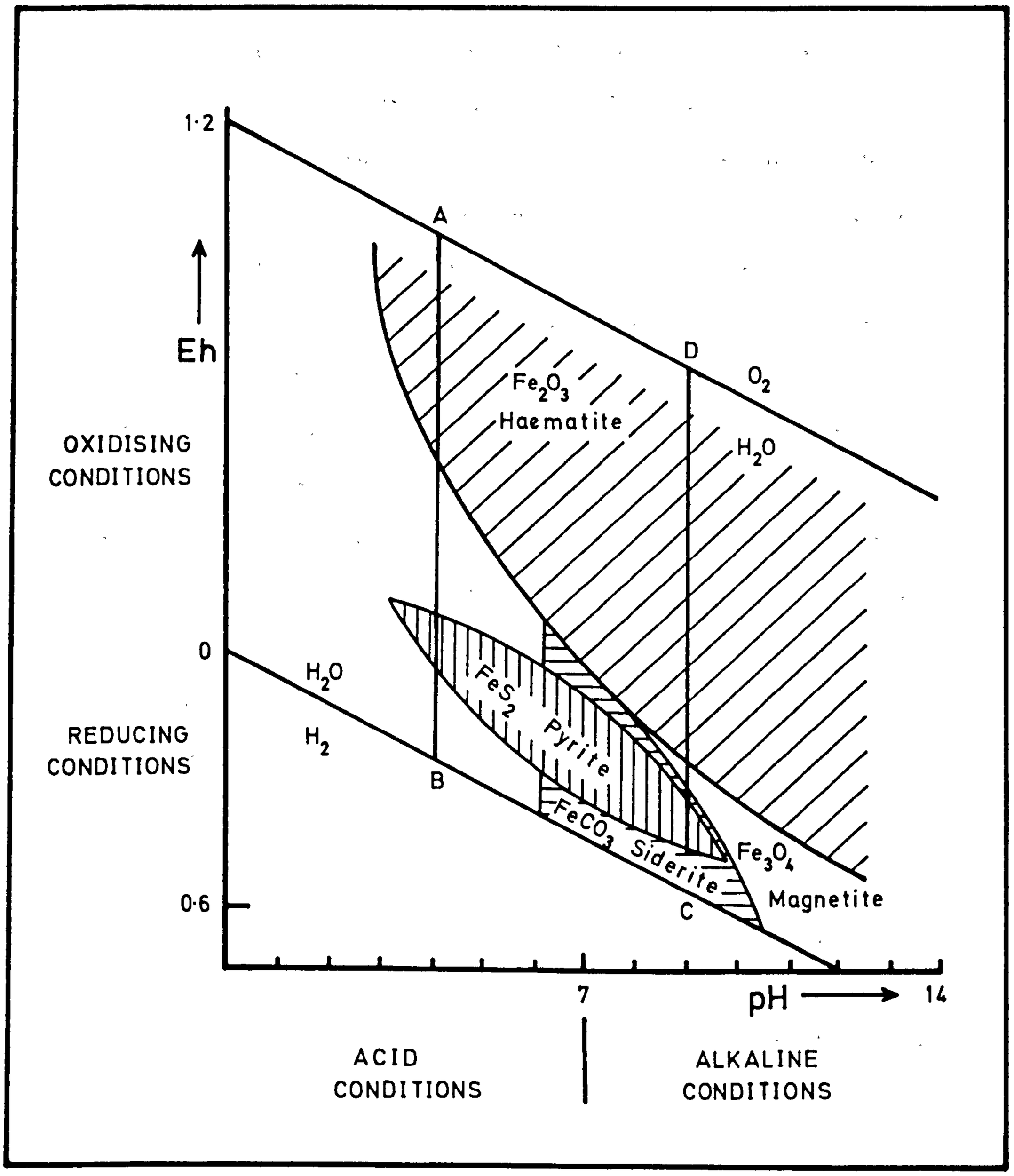


**Figure 3.19** Conditions for precipitation of different iron minerals (Redrawn from Walton, 1977)

result of its solubility lead accumulates in the zone of water table fluctuations, being removed, where present, almost completely from the anaerobic peat. Lead probably occurs as insoluble PbS within the peat, during periods of reducing conditions. The PbS is then oxidised to slightly soluble $PbSO_4$ during periods of oxidising conditions, for example dry periods when the water table is low. This would explain how lead is almost completely removed before entering the permanently anaerobic zone, and its concentration around the zone of water table fluctuations.

In general, the long profiles correspond to the patterns outlined by Clymo (1983) and Sillanpää (1972) regarding the distribution of elements throughout deep profiles. The distinction between high concentrations within the zone of mineral soil influence (minerotrophic) and the low concentrations of the ombrotrophic phase are also noted by Mornsjo (1968). The increasing concentrations towards the base (cf. fig. 3.5) are consistent with the development of the bog under telmatic conditions, whilst the much lower concentrations within the basal peats noted at Varrassuo (fig. 3.8) is consistent with development under terrestrial or semi-terrestrial conditions, remote from minerogenic water influence (Tolonen, 1966).

Finally, a common feature of the deep profiles is the randomly located single sample peaks, for example within the copper profile at Laaviosuo (fig. 3.11). These appear to be independent of any regularly spaced peaks associated with coring contamination (sub-section 3.3.1). Clymo (1983) has also noted these occasional anomalous concentrations. At Varrassuo (fig. 3.14) between 410-370cm the zinc profile displays anomalously high values. These are difficult to interpret as the concentrations are an order of magnitude greater than any samples 'contaminated' by the corer. There are two possible explanations: the first involving some form of chemical contamination within the laboratory

analysis, the second involving some form of chemical sink for zinc. The use of chemical profiles for prospecting of minerals and ore, underlying peat bogs is noted by Salmi (1955).

Superimposed on the chemical profiles associated with bog development is the increase in deposition of anthropogenic pollution in recent times. These trends are discussed with regard to the magnetic measurements in sub-section 3.9.4, and with regard to spatial variations in Chapter 4, section 4.6.

## 3.10 Magnetostratigraphy and Bog Development

The underlying sediments at Kaurastensuo (limnic and telmatic) and Varrassuo (post-glacial sands) are clearly characterised within the demagnetisation parameters (Figs. 3.3, 3.7 and 3.15). When these are plotted as coercivity of remanence curves (fig. 3.20), the discriminating nature of the curve shape and $(B_0)_{CR}$ is evident (Oldfield et al., 1978b). These differentiate between the limnic sediments, $(B_0)_{CR}$ 41-52mT; and the overlying telmatic deposits, $(B_0)_{CR}$ 25-30mT, at Kaurastensuo; and the post-glacial sands, $(B_0)_{CR}$ 68mT, at Varrassuo.

The increase in ARM/X at KAX (32-634 $Am^{-1}$) and KAC (154-361 $Am^{-1}$) at the very base of the peat profile, is possibly an indication of the precipitation of Fe-minerals. The increase, restricted to <10cm is too high to represent solely a loss of paramagnetic minerals, or even an artefact of the difficulty in assessing the diamagnetic factor within the peat. The increase is interpreted as a shift toward finer grain sizes (Maher, 1984). At both sites the increase in ARM/X corresponds with shifts in the backfield ratios, toward a softer remanence, typical of ferrimagnetic mineral types. The restriction of these features to within 10cm of the interface at each site is probably a function of the limited environmental conditions required

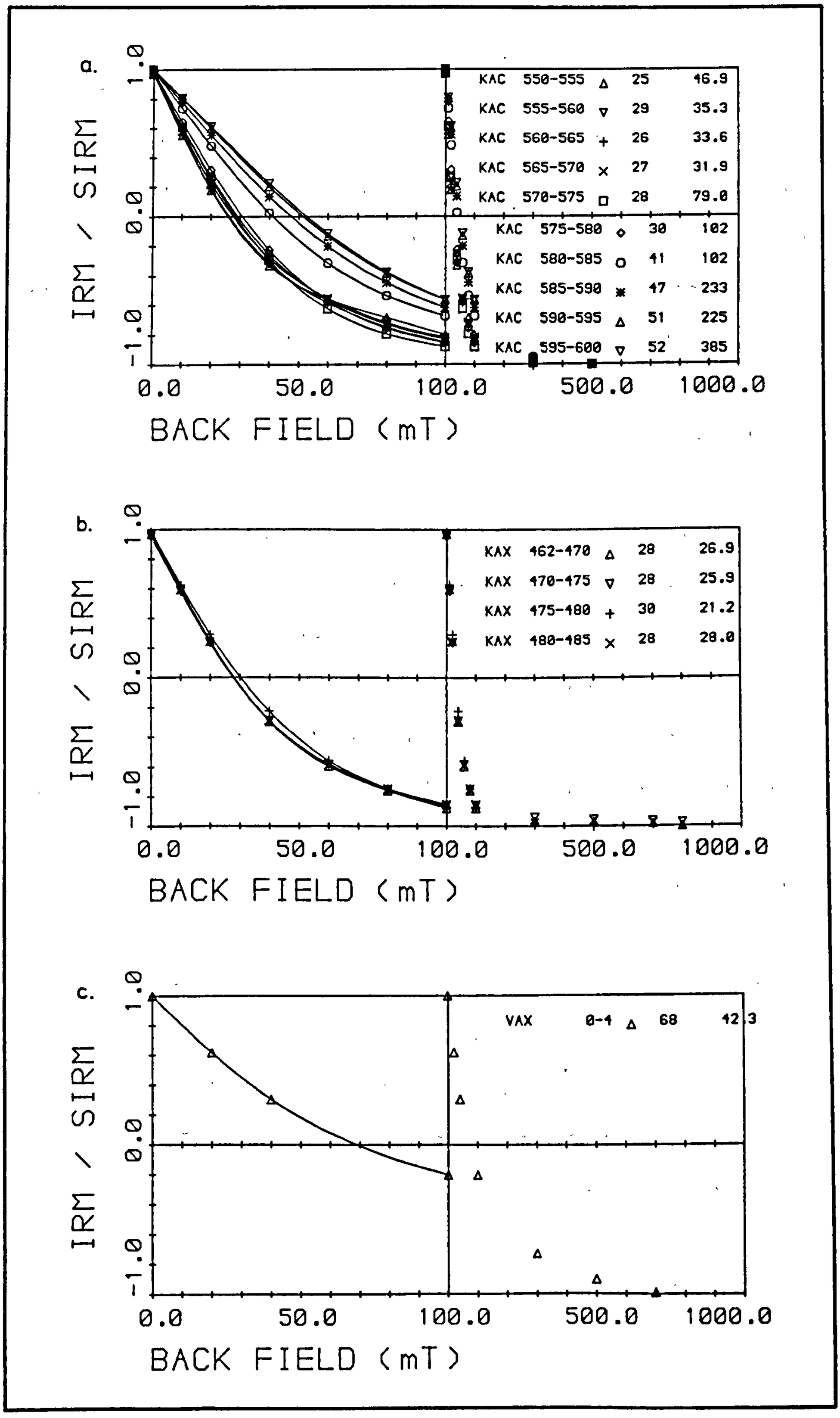


**Figure 3.20** Coercivity of remanence curves (linear plots) for Kaurastensuo and Varrassuo:
a) KAC; telmatic peats $(BO)_{CR}$= 25-30mT; limnic sediments $(BO)_{CR}$= 41-52mT
b) KAX; telmatic peats $(BO)_{CR}$= 28-30mT
c) Varrassuo; terrestric sediments $(BO)_{CR}$= 68mT

for mineral precipitation (fig. 3.19).

The decrease in chemical concentrations above the peat-mineral soil interface has already been noted as a reflection of the decreasing influence of the minerogenic waters and underlying sediments (sub-section 3.9.2). The same explanation may also be applied to decreasing mineral magnetic concentrations, notably the point above which the diamagnetic properties of the peat are evident. The contrast between the limited influence of the post-glacial sands at Varrassuo and the telmatic deposits at Kaurastensuo is again obvious.

At the surface, the increase in X, ARM and SIRM values, marked by the take-off point, corresponds with changes within the mineralogy of samples above and below that point. Above take-off the trend toward a course, multidomain mineral assemblage is inferred from decreasing ARM/X, increasing SIRM/ARM and a shift toward a soft demagnetisation response. This pattern is similar for all the peat bogs, and the apparent similarity of the anthropogenic component between sites appears to correspond closely with the pattern found within cores from the same bog (Chapter 2).

Where SIRM and X are proportional, the SIRM may be interpreted as reflecting concentrations of the ferrimagnetic minerals present. The SIRM/X ratios confirm that this is the case for post-take-off samples at all the sites (13.3-17.8 $kAm^{-1}$). Apart from corroborating the anthropogenic deposition within the surface layers (see above), the spatial variation in concentrations of ferrimagnetic mineral deposition are evident from site to site. These variations are discussed in more detail in Chapter 4, section 4.6.

## 3.11 Biogeochemical and Magnetic Mineral Relationships

### 3.11.1 Post-Take-Off samples

The increase in mineral magnetic concentrations above the take-off point, associated with increasing particulate deposition, corresponds with an increase in iron, copper, lead and less conspicuously nickel at the majority of sites. Regional studies of iron and lead deposition in Scandinavia have linked increasing element concentrations with increased anthropogenic deposition (eg. Pakarinen & Tolonen, 1977; Pakarinen, 1981; Rühling & Tyler, 1984). Table 3.4 demonstrates the statistical relationship between iron, lead and SIRM at the four sites. A strong statistical association between iron and SIRM is present at all sites. The lack of any significant statistical correlation between lead and SIRM at Laaviosuo is probably due to the anomalously high lead concentrations (558-671$\mu g.g^{-1}$) between 2.5-7.5cm (fig. 3.11).

### 3.11.2 Movement of Matter Through the Acrotelm

The survival of any record of deposition within a peat bog over long periods of time has yet to be fully evaluated. The relationship between the soluble fractions of iron, lead, zinc and copper around the level of the water has already been noted (sub-section 3.9.2), however, the effect of these two factors (mobility and water table movements) on the magnetic record, if any, is less obvious. The evidence from the chemical and magnetic records suggests that there is no statistically significant relationship between SIRM and iron for samples spanning the present water table level, and the estimated permanent water table level at any of the sites (Table 3.5). The lack of any correspondence between the two variables around the water table level is in marked contrast to the relationship between the magnetic and chemical profiles above the take-off point (sub-section 3.11.1). It may be inferred from this that the iron fraction

**Table 3.5** Correlation Coefficients for SIRM and Heavy Metals Around the Level of the Water Table. Using Pearson's product moment, r, where n = the number of cases.

| Site | Water Table Depth (cm) | Correlation Range (cm) | n | SIRM v. Fe | SIRM v. Pb | SIRM v. Zn | Fe v. Pb | Fe v. Zn | Pb v. Zn |
|---|---|---|---|---|---|---|---|---|---|
| Kaurastensuo KAX | 32.5 | 25-45 | 8 | 0.239 | 0.398 | 0.546 | 0.563 | 0.903** | 0.491 |
| Laaviosuo LaavX | 42.5 | 37.5-52.5 | 6 | 0.081 | 0.841* | 0.413 | 0.475 | 0.836* | 0.585 |
| Varrassuo VAX | 15-17.5 | 12.5-32.5 | 8 | 0.260 | 0.037 | 0.853** | 0.547 | 0.646 | 0.425 |
| Haukilampi | 32.5 | 25-42.5 | 7 | -0.218 | -0.763* | -0.011 | 0.482 | -0.077 | 0.427 |

* Significant at 0.05 level

** Significant at 0.01 level

**Table 3.6** Depth of Water Table (late summer) and Magnetic Take-Off

| **Site** | **Take-Off** (cm) | **Estimated Maxima** (cm) Late July/Early August |
|---|---|---|
| Kaurastensuo<br>KAX | 10-12.5 | 40 |
| KAC | 22.5-25 | 38 |
| Laaviosuo<br>LaavX | 22.5-25 | 67.5* |
| Varrassuo<br>VAX | 7.5-10 | 17.5-25** |
| Haukilampi | 22.5-25 | 32.5 |

* Partially drained bog, cf. fig. 2.15

** Inferred from Fe and Pb profiles, cf. fig. 3.14

contributing to the saturation remanence above take-off is not the same as the soluble fraction concentrating around the water table level.

### 3.11.3 SIRM/Fe Ratios

The ability of the SIRM/X ratios to distinguish the importance of superparamagnetic and paramagnetic effects in samples with very low magnetite concentrations has been noted in previous studies (eg. Bloemendal, 1982; Thompson & Oldfield, in press). In the absence of positive X values from the mid-sections, where magnetic particulate concentrations are very low, the use of an SIRM/Fe ratio may give some indication of the relative importance of paramagnetic minerals, based on the following considerations.

Where X and SIRM are proportional, the SIRM may be interpreted as a reflection of increasing crystalline, ferrimagnetic mineral concentrations. This is the case for all the post take-off samples at each site, where the SIRM/X is between 13.3-17.8 $kAm^{-1}$. When the X and SIRM values diverge, the X parameter reflects diamagnetic and paramagnetic behaviour within the samples. This is evident in low SIRM/X ratios, which in paramagnetic minerals including some iron and manganese minerals, is a function of their inability to carry a remanence at room temperature. Failure to exhibit spontaneous magnetisation arises because their crystal structures are not conducive to positive exchange interactions, holding the iron and manganese ions apart at inappropriate distances or crystal geometries (Thompson & Oldfield, op. cit.). The X of these minerals depends on the number of free electrons available, that is, directly on the number of iron and manganese ions per gram of material.

Precipitated Fe-minerals (sub-section 3.9.1), eg. siderite and pyrite, exhibit ferrimagnetic and canted antiferromagnetic behaviour respectively. The relative X values for siderite and pyrite are ca.100 $10^{-8}m^3kg^{-1}$ and

ca.10 $10^{-8}m^3kg^{-1}$ respectively.

Substituting the concentrations of iron in place of the concentrations of magnetic minerals (X), it appears possible to infer the presence of paramagnetic iron where SIRM values and iron concentrations diverge. This is represented in the SIRM/Fe ratio by low values. The relationships between X and iron, and SIRM and iron are plotted in fig. 3.21. In both cases the samples cluster into three distinct groups dependent upon their location within the core, and hence to an extent, the mineral assemblage. When X and iron are plotted (fig. 3.21a), the coarse multidomain, post-take-off samples plot out in the lower left hand part of the diagram. Samples from the base of the peat profiles, with low SIRM/X (where measurable), plot out in the top right hand on the diagram. For SIRM and iron (fig. 3.21b) the groupings are reversed, being top left and bottom right respectively.

SIRM/Fe curves for Kaurastensuo (KAX), Laaviosuo, Varrassuo and Haukilampi are plotted in fig. 3.22. If the mineralogy of the crystalline component remains uniform within a suite of samples (section 3.10) for example, the basal peat samples, then the lower the SIRM/Fe ratio the more significant the contribution of paramagnetic iron to the mineral assemblage. This is most noticeable in the mid-sections of profiles during the latter stages of the minerotrophic phase. Variations noted within the ombrotrophic peat layers contrast with the relatively smooth curve of the majority of the minerotrophic phase. An example of this is Varrassuo, where there is little variation in the curve up to 115cm below the surface. This depth corresponds approximately to the beginning of slash-and-burn culture within the area, from about 3200yrs BP onwards (Donner et al., 1978). The fluctuations in SIRM/Fe above 115cm possibly represent a shift in inputs to the bog surface as a result of field erosion by wind, connected

a. Susceptibility vs. Total Iron

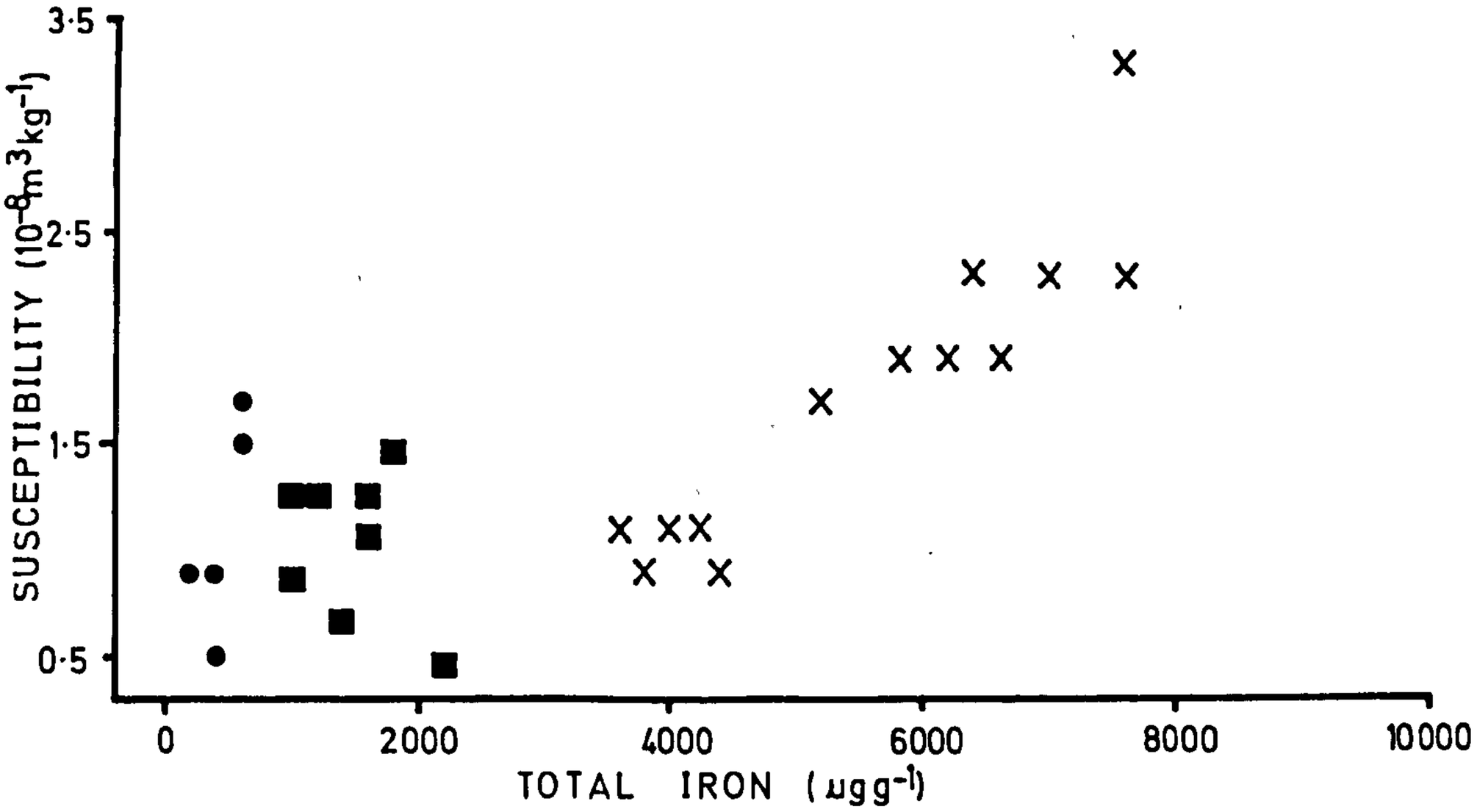


b. SIRM vs. Total Iron

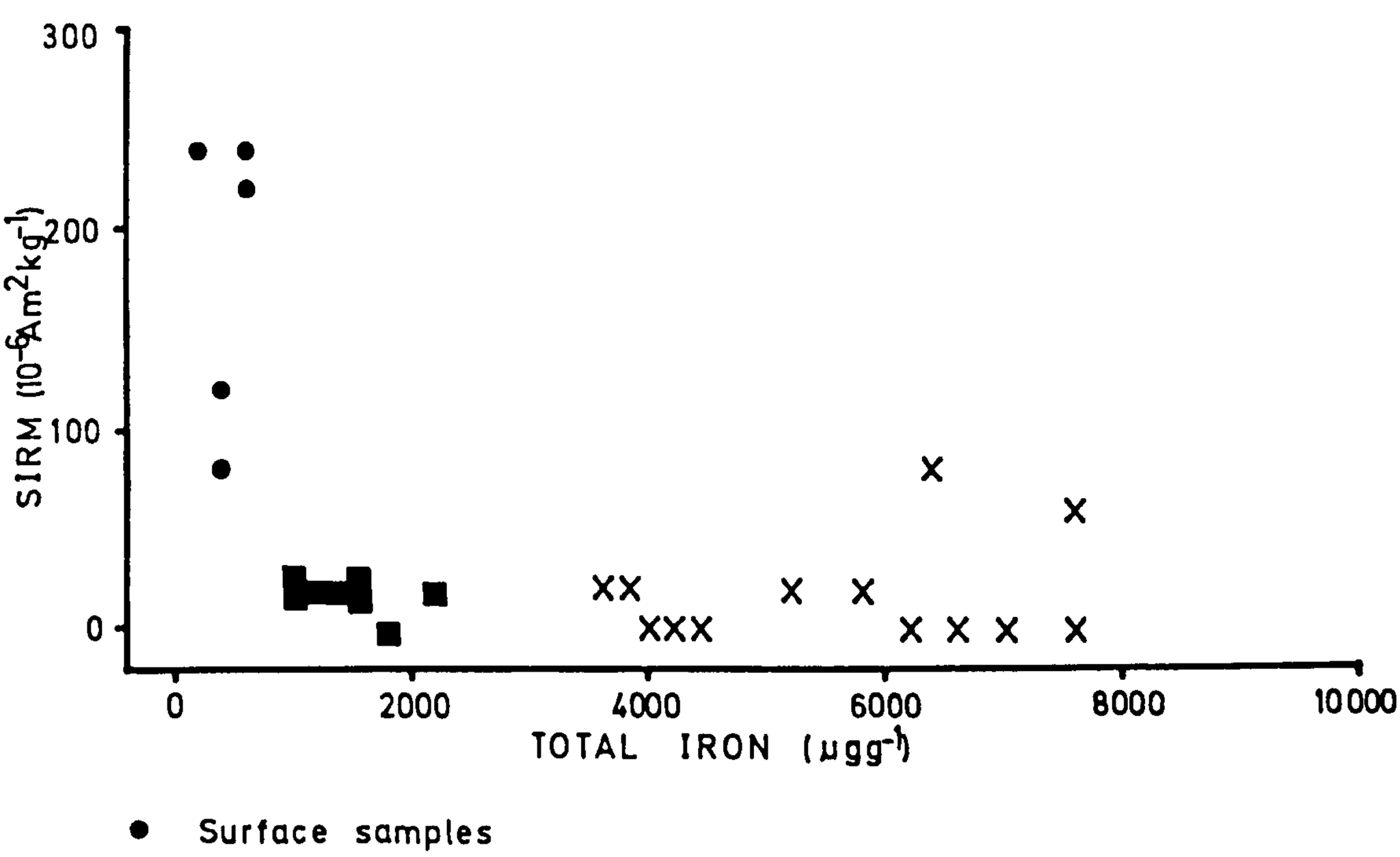


● Surface samples
■ Minerotrophic samples
X Mineral soil influenced samples

**Figure 3.21** Relationship between X, SIRM and total Iron (Fe) for selected samples (see text):
a) X and Fe
b) SIRM and Fe

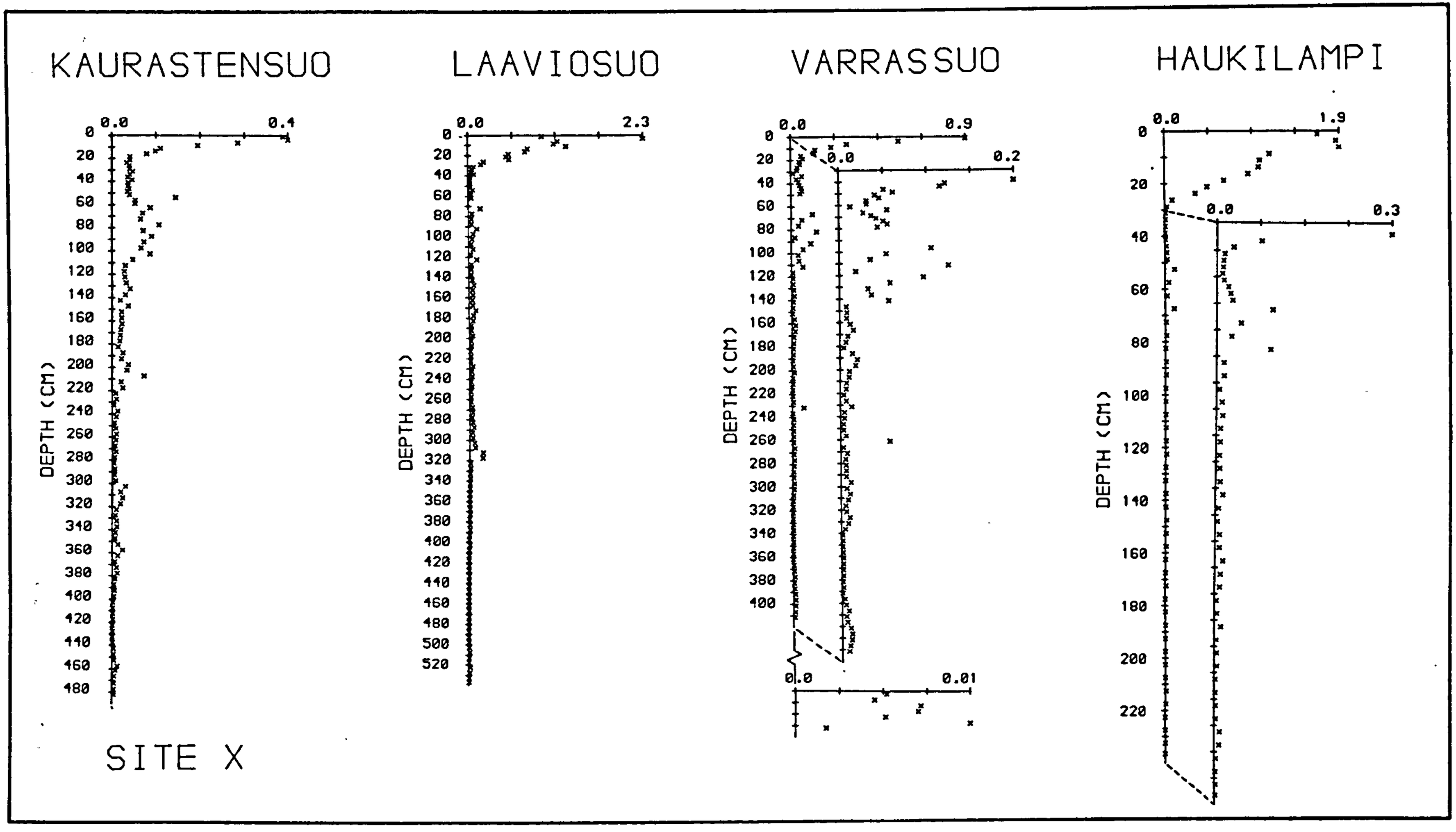


**Figure 3.22** SIRM/Fe profiles for Kaurastensuo, Laaviosuo, Varrassuo and Haukilampi

with the increased human activity within the area, noted by Tolonen (1984).

There is good agreement between changes in the SIRM/Fe ratio and the location of the ombrotrophic-minerotrophic boundary. This is clear at Kaurastensuo (300cm) and at Laaviosuo (320cm) corresponding with the stratigraphic indicators. A distinction may also be made at Varrassuo (310cm) which corresponds with earlier stratigraphic estimates (sub-section 3.6.1).

## 3.12 Conclusions

The interpretation of stratigraphy from Kaurastensuo, Laaviosuo, Varrassuo and Haukilampi follows the observations made by Clymo (1965). The increased proportions of E. vaginatum down-profile relate to the preferential preservation of fibrous material and vascular plants within acid environments. Their over-representation in the lower peat layers is, therefore, related to the proportion of vascular plants present within the surface vegetation at the time of formation. This point is important when considering any reconstruction of past surface vegetation, especially when there is a strong Sphagnum presence.

The chemical and magnetic profiles may reasonably be divided into three sections. The lower, basal section comprises the underlying mineral and basal peats. The upper limit of this section is based largely on the upper limit of the zone of minerogenic water influence. Only KAX, KAC and Varrassuo have a complete record of the basal section, although at Varrassuo there is a hiatus at 414cm. The base of Laaviosuo terminates somewhere within this section though above the peat-mineral soil interface. The mid-section comprises the upper minerotrophic peats and the beginning of the ombrotrophic peats. The base of Haukilampi profile terminates somewhere within this section. Finally, the upper section

extends from a maximum of 30-40cm below the surface, to the top of the core. The length of this section varies from site to site. The main conclusions relating to each section are given below.

3.12.1 The Basal Section

The differences between underlying sediments and the mineral soil at Kaurastensuo and Varrassuo respectively, may be distinguished by the magnetic characteristics of each. Contrasts are evident in the $(B_0)_{CR}$ values which range between 41-52mT for the limnic sediments (KAC); 25-30mT for the overlying telmatic deposits (KAC, KAX); and 68mT for the glacial sands underlying Varrassuo. The post-glacial sands exhibit an antiferromagnetic response to reverse field remanence within all the backfields measured.

The contrast in underlying sediments extends to their influences on the basal (minerotrophic) peats. At Kaurastensuo, where the bog developed above a small lake, the influence of the minerogenic waters extends upwards for about 60cm, reflected primarily by the gradually diminishing chemical concentrations (eg. iron). The result is that the minerotrophic phase appears to have persisted much longer, ie. until about 3000yrs BP, compared to the majority of other sites in southern Finland where the transition corresponded with the change from Boreal to Atlantic Times (ca.8000yrs BP). An example of the latter is the bog, Varrassuo, where the influence of minerogenic waters was limited by its development above terrestrial sands. This is illustrated by the abrupt changes in chemical concentrations at the base of Varrassuo compared with the gradual decrease in concentrations at Kaurastensuo.

Fluctuating redox conditions during the transition of the bog from swamp fen to Carex-Equisetum-Bryales peat has been shown to be favourable to the precipitation of Fe-minerals under limited environmental

conditions. The increase in ARM and ARM/X at peat-mineral soil interface (KAC, KAX) is linked with increasing concentrations of fine grained and ultra fine-grained magnetic minerals. These minerals are either a product of Fe-precipitation or of a limited episode of fine grained detrital input.

The contribution of paramagnetic iron to total iron concentrations, as interpreted from the SIRM/Fe ratio is very high within the basal section. The ratio picks out the upper limits of the minerogenic soil water influence at Kaurastensuo and Varrassuo, as well as the boundary between the underlying mineral soils and the basal peats at both sites. In both cases, at each site, the ratio is markedly lower below the transition than above it.

3.12.2 The Mid-Section

Characterised by generally low or unmeasurable chemical and magnetic concentrations, the mid-section spans the majority of the peat strata within all the cores. At the upper end, the permanent and present water table levels are marked by increases in iron, lead, zinc and nickel concentrations, associated with the soluble fractions of those elements. There is no statistically significant relationship between total element concentrations and SIRM, for samples located around the water table and displaying increased element concentrations. It may be inferred, therefore, that the minerals contributing to SIRM are not those which are most readily dissolved or chelated and translocated to the level of the water table.

Fluctuating SIRM/Fe ratios above 155cm at Varrassuo and within this mid-section, are tentatively linked with shifts in the mineral inputs to the bog surface, associated with the beginnings of human agricultural activity in the area. This coincides with the beginning of slash-and-burn practices ca.3200yrs BP noted by Donner et al. (1978). Similar fluctuations in the SIRM/Fe ratio at Kaurastensuo are noted, where there are two inflection

points: the first at 220cm (2110±130yrs BP), and the second at 110cm (<1500yrs BP).

3.12.3 The Upper Section

Extending from just above the water table to the surface, this section corresponds approximately with the acrotelm (Ingram, 1978). The upper section encompasses the magnetic take-off point, between 7.5-20cm above the water table within the five cores (Table 3.6). The relationship between SIRM and iron, indicative of recent atmospheric deposition is statistically significant at all sites, above the take-off point and remote from the water table. This contrasts sharply with the lack of correspondence between the two variables at the water table. The correlation above take-off is interpreted as a direct influence of recent anthropogenic particulate deposition (cf. Chapter 4). An example of this is evident at Varrassuo, in the surface sample, where increased concentrations of mineral magnetic particulates, iron, copper, lead and nickel are associated with the output from the recently constructed factory, in close proximity to the bog.

# 4. Regional Deposition of Magnetic Particulates and Heavy Metals

## 4.1 Introduction

Ombrotrophic bryophytes have been used extensively since the late 1960's in assessing regional and temporal variability of atmospheric heavy metal deposition in Scandinavia (eg. Rühling & Tyler, 1968, 1971, 1973; Tyler, 1971; Gelting & Ponten, 1971; Pakarinen & Tolonen, 1976). The tissue of bryophytes possesses no epiderm layer or cuticle and they have a higher cation exchange capacity, usually 0.9-1.5meq.$g^{-1}$ for Sphagnum (Puustjärvi, 1955), along with the ability to chelate heavy metal ions, the latter property being dependent on the properties of the metal ion. More recent studies have attempted to estimate atmospheric deposition rates with the aid of Sphagnum in the UK (Clymo, 1978), Scandinavia (Damman, 1978; Pakarinen, 1978) and Denmark (Aaby & Jacobsen, 1979). Estimates of magnetic particulate deposition into peat are few, due mainly to the lack of reasonable chronologies for the dating of recent peat accumulation. An example of one such estimate is Oldfield et al. (1981) who used S. fuscum dated by the moss increment method, from four sites in southern Finland (see below).

This chapter attempts to use the rationale outlined above to compare the depositional flux in three sites from southern Finland compared with five sites in northern Finland and one in northern Norway. The post-1900 deposition record of magnetic particulates is estimated from sites with an available chronology, in most cases based on the moss increment dating method. The mean annual flux of SIRM, iron, manganese, lead, copper, zinc and nickel is also estimated for the topmost samples in an attempt to identify any regional differences in deposition over Finland that may exist.

### 4.1.1 Metal Retaining Capacity of Bryophytes

Bryophytes can accumulate metals by both ion exchange and

particulate trapping. The lack of a cuticle in Sphagnum mosses means that like ectohydric mosses they absorb minerals and water over the entire surface of the plant. Work by Clymo (1963) and Rühling & Tyler (1970) on Sphagnum mosses and Hylocomium splendens, respectively, demonstrated how $H^+$ ions were exchanged for dissolved cations from the plant's habitat at the plant apex. The cation uptake by extracellular ion exchange in Hylocomium splendens for metals was in the order:

$$Cu, Pb > Ni > Co > Zn, Mn$$

whether the cations were supplied singularly or as mixtures (Rühling & Tyler, op. cit.). This sequence contrasts slightly with the earlier work of Hasler (1943) and Mellor & Maley (1947, 1948) who suggested the average sequence of:

$$Pb > Cu > Ni > Zn > Fe > Mn$$

For the ion exchange process it may be concluded that the passive retention of metal ions supplied in precipitation should almost be complete for copper, lead and nickel whereas the retention of zinc should be less than complete unless an active uptake by the moss tissues occurs in the field (Rühling & Tyler, 1973).

Work by Taylor & Witherspoon (1972) noted that densely packed cushion-forming and carpet-forming mosses entrapped particulates with up to 90% efficiency. This efficiency appears to be retained even in dead Sphagnum (Richardson et al., 1980) and the use of Sphagnum moss bags as entrappers of atmospheric particulate pollution is well documented (eg. Goodman & Taylor , 1971).

## 4.2 Methods

### 4.2.1 Site Locations

Nine sites throughout Finland were available with some form of.

recent chronology. The three sites in southern Finland, Kaurastensuo (61°21'N 24°59'E), Laaviosuo (61°02'N 25°02'E) and Varrassuo (60°59'N 25°29'E) are the same sites described in Chapter 3. Kaurastensuo and Laaviosuo are dated by means of the growth rate equations (sub-sections 2.2.4 and 4.3.7 respectively), Varrassuo is dated by the moss increment dating method outlined in sub-section 4.2.2. The sites in northern Finland comprise Liikanen (66°22'N 29°03'E), Jänkivuopajanaapa (67°23'N 26°42'E), Pousujärvi (68°20'N 23°37'E), Ahmajänkä (69°05'N 27°10'E) and Utsjoki (69°50'N 27°12'E). A further site, Norja (69°23'N 24°12'E), is located in northern Norway. A general location map of the sites is presented in fig. 4.1.

The five sites from northern Finland and the one site from northern Norway were sampled by Dr. K. Tolonen in 1979. Chemical determinations of iron, manganese, copper, lead and zinc on a dry weight basis and moss increment dating were also carried out by Dr. K. Tolonen. The use of the core material for subsequent magnetic measurements and the use of chemical data for this chapter is acknowledged.

4.2.2 Moss Increment Dating Method

The method has been used frequently in Finland from 1977 onwards (eg. Pakarinen & Tolonen, 1977b; Tolonen, 1977). The technique has evolved from the ability to recognise annual increments in Finnish mosses with a low degree of humification, notably within Sphagnum mosses (notably S. fuscum), Polytrichum strictum, Aulacomnium palustre and Dicranum undulatum. The annual increments are recognised primarily from a combination of their branching pattern (Malmer, 1962), cyclic pigmentation (Bellamy & Rieley, 1967), innate time markers (Clymo, 1970) and changes in growth direction (Pakarinen & Tolonen, op. cit.).

Malmer (op. cit.) divided S. papillosum samples into segments,

designated by uniform appearance and separated from adjacent segments by branches closer together than in other parts. The uppermost segment was noted to be green whilst the lower segments were more or less brown. He suggested a periodicity in the growth of these segments, with alternating increase in length and weight of the top segment, although he refrained from referring to this as an annual cycle. The branching pattern noted usually, but not always, occurred just at the border between two segments. Hagerup & Petersson (1960) noted that in S. fimbriatum the stem of the top bud extends only slightly in spring but that the branches grow vigorously. In the autumn the stem beneath the bud extends its length. As the branches are more densely arranged beneath the boundaries between parts of different age, Hagerup & Petersson (op. cit.) suggested that it may be possible to calculate the production of dry matter per unit area in that way. According to Overbeck & Happach (1956) the growth in length of Sphagna in mires occurs in two periods yearly: in the spring, and in autumn. This periodicity, however, is a function of external conditions such as temperature, water level and moisture content.

In a few cases the cyclic change is of pigment density, for example, in S. rubellum in some habitats. The red pigment, related to the anthocyanins, is an aglycone, production of which is increased at low temperatures. The pigment is difficult to separate from the cell walls and often remains conspicuous after other pigments have disappeared (Clymo, op. cit.). Bellamy & Rieley (op. cit.) calculated the net annual production of S. fuscum at a site in northern England using this method of cyclic pigmentation.

Clymo (op. cit.) also noted the possibility of using innate markers for estimating time. Cyclic fluctuations may sometimes be found in the length of Sphagnum branches and in their spatial density. Tamm (1953) used

similar cyclic fluctuations to measure the growth of the moss Hylocomium splendens. The main disadvantages of these innate time markers appeared to be that in the English climate at least, the cyclic changes in the growth pattern are often not sufficiently marked for it to be possible to make a clear separation of the segments. There must also be a subjective element in deciding where a cycle ends. However, Tamm (op. cit.) estimated that the error was 1-2% of the segment weight in Hylocomium splendens. It is also possible that some further growth may occur on a particular segment in the second or subsequent years. However, Clymo (op. cit.) noted that this is unlikely to be of any importance.

The changes in growth direction noted by Pakarinen & Tolonen (op. cit.) are a product of high latitude mire sites, with extreme annual temperature ranges. The changes in growth direction are interpreted as a direct result of the pressure from the seasonal overlying snow cover (Tolonen, op. cit.).

In order to estimate the age of the moss, between 15-20 stems are taken from the peat section and their actual lengths measured after straightening. From these stems the annual increments which include one year of growth, may be identified and their lengths measured. Microscopic observations allow the changes in pigmentation to be identified for very short increments. The average number of years of a certain peat is calculated by dividing the mean stem length by the mean increment length.

The use of P. strictum in addition to the Sphagnum provides a reference marker for the increments (cf. Longton, 1972). A combination of these innate markers has enabled Sphagnum hummocks to be dated to between 50 to 200 years BP with reasonable accuracy dependent on the stem lengths and degree of humification with increasing depth. The moss

increment dates used in this chapter were determined by Dr. K. Tolonen.

4.2.3 Calculation of Heavy Metal Deposition

Annual accumulation rates of the heavy metals used in this chapter are calculated using the following formula:

$$F = \frac{C \times D_b \times d}{1000 \times a} \qquad [4.1]$$

where: F = Annual accumulation rate of metals ($\mu g.cm^{-2}yr^{-1}$)

C = Concentration in $\mu g.g^{-1}$

$D_b$ = Slice bulk density ($g.dm^{-3}$)

d = Depth increment of the slice (cm)

a = Time interval in years

The conversion from $\mu g.cm^{-2}yr^{-1}$ to $mg.m^{-2}yr^{-1}$ is a factor of 10 increase. The results of the calculations using the above formula are presented and discussed in sub-section 4.6.3.

## 4.3 Site Locations and Results

### 4.3.1 Liikanen

Liikanen (66°22'N 29°03'E) is the furthest south of the northern Finnish sites used (fig. 4.1). The bog is situated to the north of Kuusamo (population ca.4500) in Kuusamo commune, Oulun Lääni province, in the north east close to the Soviet border. The bog lies within the zone of main aapa mires (Eurola & Ruuhijärvi, 1961).

The 48cm long core represents about 150 moss increment years (before 1979). Bulk density values and ash residues are presented along with the profiles of five chemical elements: iron, manganese, copper, zinc and lead in fig. 4.2. Magnetic measurements comprising X, SIRM, interparametric and backfield ratios are also presented in fig. 4.2.

U Utsjoki
N Norja
P Pousujärvi
A Ahmajänkä
J Jänkivuopajanaapa
L Liikanen
Av Ahvenjärvenvuoma

KAX Kaurastensuo
LaavX Laaviosuo
VAX Varrassuo

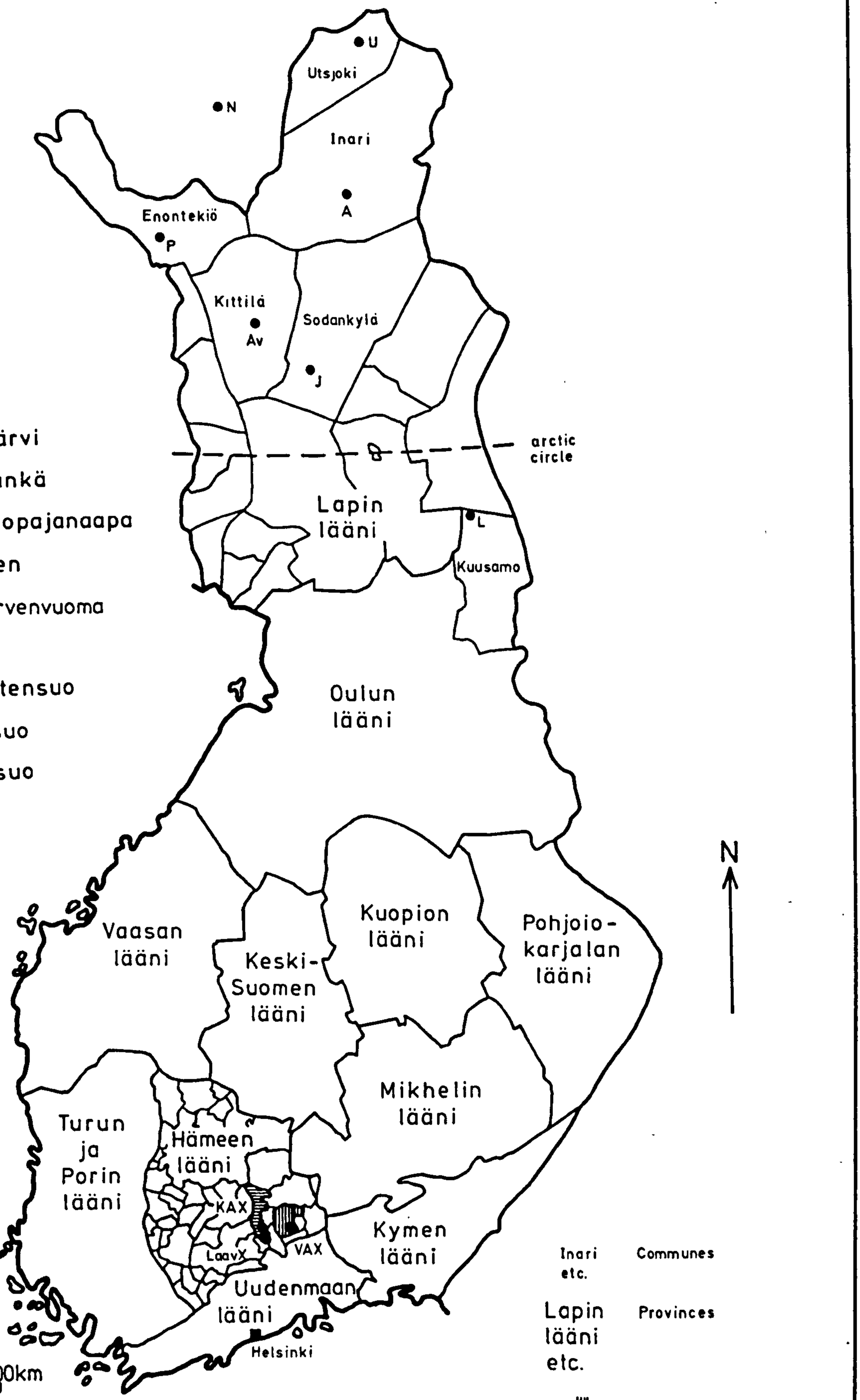


**Figure 4.1** Location of sites

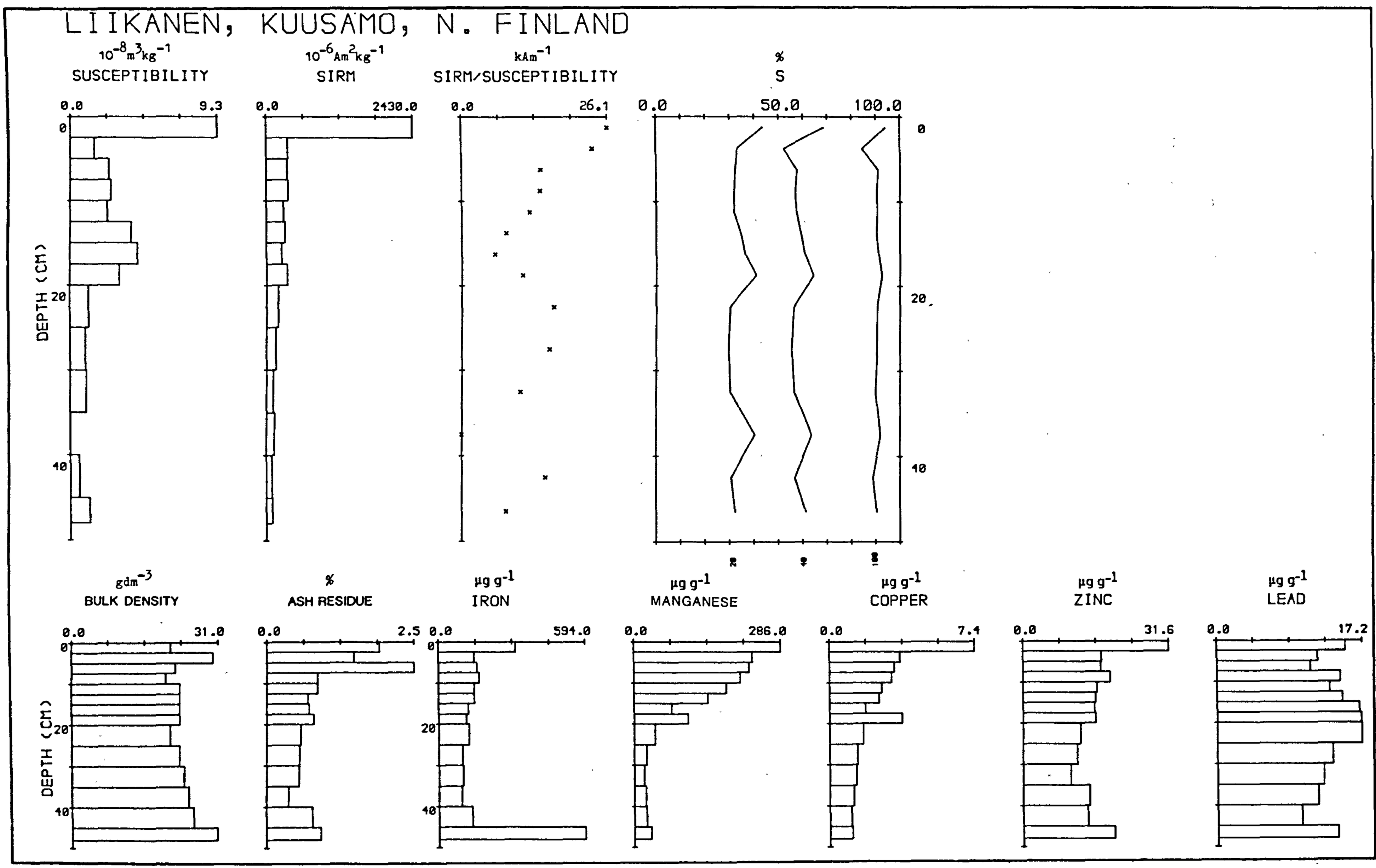


**Figure 4.2** Magnetic measurements and chemistry for Liikanen, northern Finland

The magnetic profiles display a gradual increase up through the core (SIRM) culminating in a marked increase in the surface sample, 0-2.5cm (X and SIRM). Manganese and copper display increasing concentrations from 20cm upwards to a peak value at the surface. Iron, zinc and to a lesser extent, lead, all display a similar peak value within the surface sample. The moss increment date for the base of this slice is 3.6 years before 1979 (2.5cm), equivalent to 7mm.yr$^{-1}$ growth of Sphagnum.

Using the moss increment dates the mean annual flux of SIRM and Fe has been calculated and the results plotted against time in fig. 4.12. The SIRM profile displays a peak in the surface sample, over 6 times greater than the preceeding slice.

The flux rates are used to calculate cumulative influx since 1973 (corresponding approximately to the surface sample for most sites), 1945 and 1900. The cumulative influx at Liikanen is presented in Table 4.1 for iron, manganese, copper, lead, zinc and SIRM. The estimates are compared with pre-existing data from four southern Finnish sites (Oldfield et al., 1981; El-Daoushy & Tolonen, 1982) over similar time periods.

4.3.2 Jänkivuopajanaapa

Jänkivuopajanaapa (67°23'N 26°42'E) lies just south of the town of Sodankylä (population ca.4000), to the northwest of Liikanen in the Sodankylä commune in Lapin Lääni province. Like Liikanen, it is situated within the zone of main aapa mires, according to Eurola & Ruuhijärvi (op. cit.).

Two cores are available from Jänkivuopajanaapa: JC (0-57cm) and JD (0-50cm). The growth rates in each core are comparable over 50cm, 146 years and 154 years before 1979 respectively. Bulk density and ash residues are available for JD along with iron, manganese, copper and zinc profiles (fig. 4.4). The manganese, copper and zinc profiles all display increasing

**Table 4.1** Cumulative Influx Rates of SIRM ($10^{-6}Am^2$) and Heavy Metals ($mg.m^2$) for Some Finnish Peat Bogs. All dates are up to 1979 except for Kaurastensuo, Laaviosuo and Varrassuo which are up to 1983. A mean value has been taken for sites where more than one dated core is available.

| Site | Post-1973 (0-2.5cm) | | | | | | | Post-1945 | | | | | | | Post-1900 | | | | | | |
|---|---|---|---|---|---|---|---|---|---|---|---|---|---|---|---|---|---|---|---|---|---|
| | SIRM | Fe | Mn | Pb | Ni | Cu | Zn | SIRM | Fe | Mn | Pb | Ni | Cu | Zn | SIRM | Fe | Mn | Pb | Ni | Cu | Zn |
| Kaurastensuo, KAX | 24.3 | 25.9 | - | 0.84 | 0.21 | 0.30 | 2.25 | 123 | 68.6 | - | 2.76 | 0.61 | 0.73 | 6.12 | 188 | 151 | - | 5.0 | 1.66 | 1.61 | 17.3 |
| Laaviosuo, LaavX | 14.8 | 15.1 | - | 0.48 | 0.15 | 0.31 | 1.80 | 85.5 | 45.5 | - | 1.62 | 0.15 | 1.15 | 4.78 | 195 | 140 | - | - | 0.64 | 1.83 | 9.6 |
| Varrassuo, VAX | 124 | 138 | - | 4.56 | 0.62 | 0.72 | 6.10 | 168 | 257 | - | 8.10 | 1.13 | 1.17 | 21.2 | 179 | 406 | - | 11.9 | 2.41 | 1.17 | 37.6 |
| Liikanen | 90.2 | 11.5 | 10.6 | 0.56 | - | 0.28 | 1.16 | 184 | 51.9 | 59.4 | 4.68 | - | 1.15 | 5.96 | 375 | 185 | 93.6 | 22.7 | - | 3.03 | 22.0 |
| Jänkivuopajanaapa | 27.5 | 6.7 | 29.8 | - | - | 0.30 | 2.10 | 141 | 68.2 | 90.2 | - | - | 1.76 | 12.8 | 210 | 196 | 130 | - | - | 3.62 | 32.2 |
| Pousujärvi | 13.5 | 9.9 | 3.93 | 0.31 | - | 0.20 | 1.02 | 37.7 | 39.6 | 7.2 | 1.20 | - | 0.81 | 4.1 | 73.5 | 171 | 10.5 | 3.5 | - | 2.80 | 12.4 |
| Ahmajänkä | 6.2 | 6.7 | 22.4 | - | - | 0.15 | 0.90 | 69.9 | 61.3 | 108 | - | - | 9.60 | 7.4 | 146 | 137 | 159 | - | - | 10.30 | 15.2 |
| Norja | 15.1 | 24.7 | 12.2 | 0.30 | - | - | 1.20 | 24.6 | 71.4 | 27.0 | 1.14 | - | - | 4.21 | 71.1 | - | 45.0 | 6.76 | - | - | 19.6 |
| Utsjoki | 7.6 | 5.8 | 2.68 | 0.72 | - | 0.18 | 0.66 | 34.4 | 35.7 | 4.76 | 2.70 | - | 0.91 | 2.40 | 57.5 | 35.7 | 8.71 | 4.80 | - | 1.69 | 5.3 |
| | | | | | | | | Post-1950 | | | | | | | Post-1850 | | | | | | |
| [1]Harpar Lilltrask | 94.2 | 170 | - | - | - | - | - | 1210 | 2045 | - | - | - | - | - | - | - | - | - | - | - | - |
| [1]Karpansuo* | 7.2 | 26.4 | - | - | - | - | - | 142 | 353 | - | - | - | - | - | 206 | 697 | 79.0 | 22.0 | - | 5.0 | 70.0 |
| [1]Munasuo | 14.1 | 50.7 | - | - | - | - | - | 126 | 650 | - | - | - | - | - | - | - | - | - | - | - | - |
| [1]Kunnoniemensuo* | 9.3 | 49.8 | - | - | - | - | - | 76.0 | 370 | - | - | - | - | - | 146 | 731 | 335 | 22.0 | - | 4.0 | 65.0 |

1. Cumulative influx of SIRM and Fe from Oldfield et al (1981)

* Cumulative influx of heavy metals from El-Daoushy & Tolonen (1982)

values towards the peak surface value, with an inflection point at 10cm below the surface. This pattern is most marked in the manganese profile. The iron profile displays its greatest concentrations at the base of the core (45-50cm) similar to the Liikanen profile.

Magnetic measurements are presented in fig. 4.3 for JC and fig. 4.4 for JD. The magnetic measurements include X, SIRM, SIRM/X and backfield ratios for both cores and additionally ARM, ARM/X and SIRM/ARM for JC (fig. 4.3).

The ARM and SIRM values increase gradually up through the core, JC, to a surface peak. The X measurements are positive above 20cm, again increasing to a surface maximum. ARM/X and SIRM/X display decreasing values from 20cm up to the surface.

In addition to the top 50cm in core JD, there are the magnetic measurements of a further six non-contiguous samples between 50cm and 110cm (fig. 4.4). Above 50cm the SIRM profile displays the same gradual increase towards a surface maximum. X values show a marked increase from below 5cm to the surface. The mean annual flux of SIRM to both cores has been calculated and an average obtained for the site. This is presented in fig. 4.12. The cumulative influx of each of the heavy metals in core JD are presented in Table 4.1 along with an average of the cumulative SIRM from cores JC and JD.

### 4.3.3 Pousujärvi

Pousujärvi (68°20'N 23°37'E), in the far northwest of Finland (fig. 4.1) lies to the east of the town of Enontekio (population ca.500), in Enontekiö commune, Lapin Lääni province. The bog is situated on the boundary between the northern aapa mires to the south, and the palsa mires to the north according to Eurola & Ruuhijärvi (op. cit.).

Three cores are available from this site. Core PA is 33cm long with

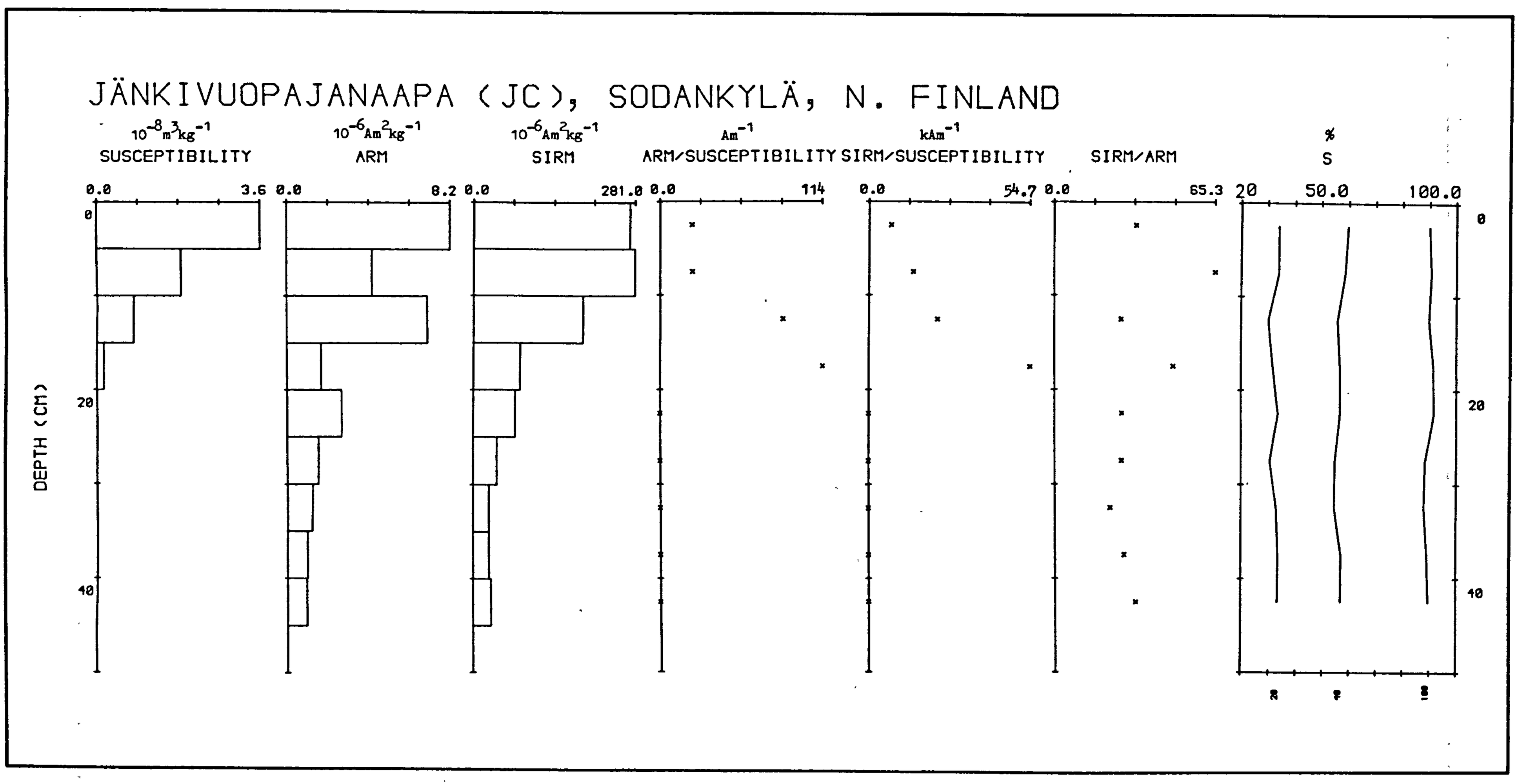


**Figure 4.3** Magnetic measurements for Jänkivuopajanaapa (JC), northern Finland

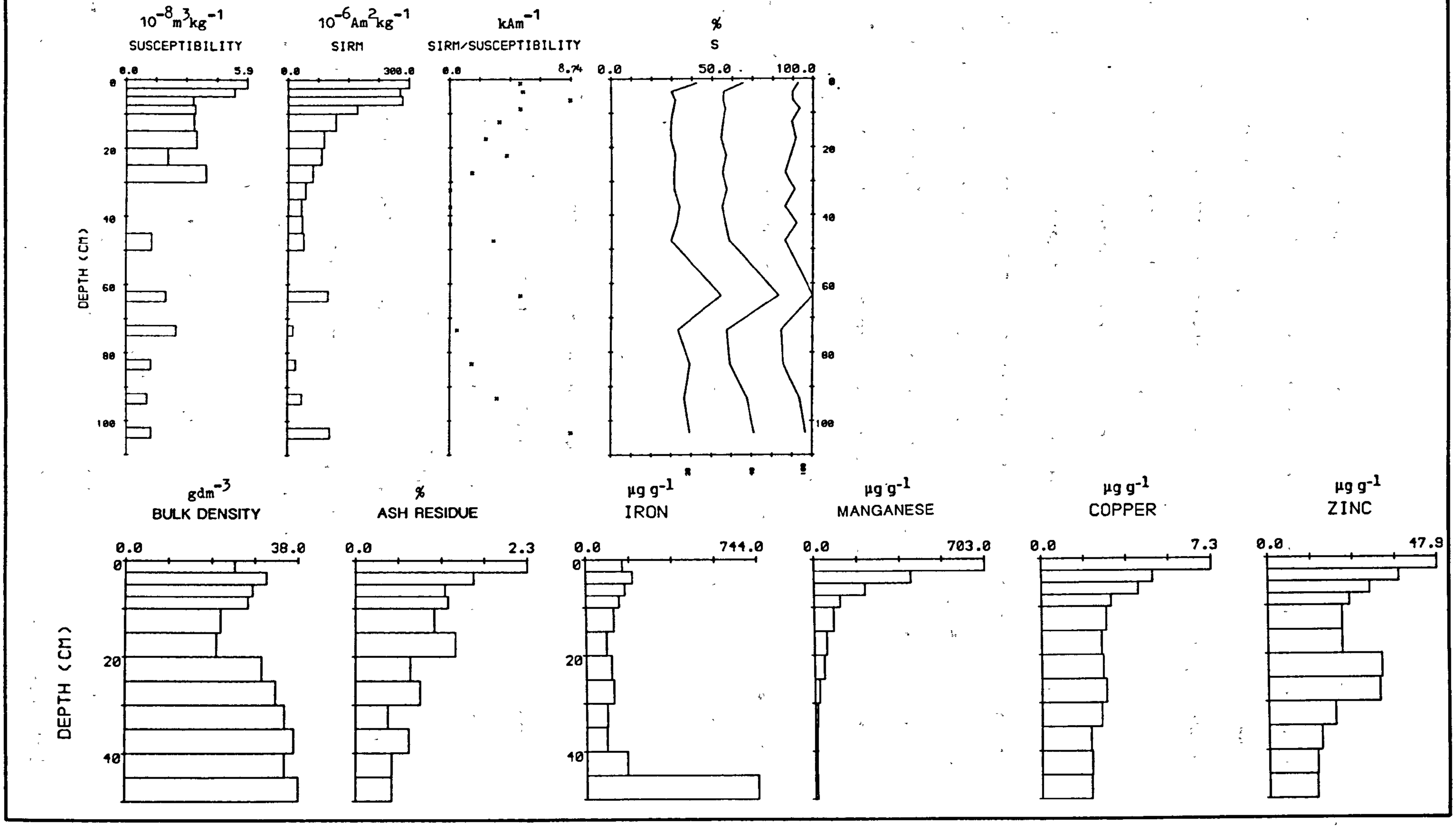


**Figure 4.4** Magnetic measurements and chemistry for Jänkivuopajanaapa (JD), northern Finland

complete magnetic measurement and element profiles (fig. 4.5). Core PB, 34cm long, has complete magnetic measurement and the five element profiles, presented in fig. 4.6. The final core, PC, is 15cm long and has only the magnetic measurements available. These comprise X, SIRM, SIRM/X and backfield ratios presented in fig. 4.7.

The chemical profiles from PA and PB display very similar patterns between the two cores, for all the elements. The manganese profiles display the same exponential increase towards a surface maximum as at other sites, although the concentrations in PA at the surface are 1.7 times greater than in PB. There is very little variation between concentrations at comparable depths within the remaining element profiles. The iron profiles display a similar pattern of increasing concentrations with depth, more markedly than at previous sites, being approximately 8 times greater than surface concentrations within each core. Copper concentrations display the same type of pattern as iron although basal concentrations are approximately 2 times greater than at the surface.

The SIRM profiles for the three cores are similar to those of previous sites with generally increasing values towards a surface sample peak. There is no clearly distinguishable take-off point within any of the cores. Maximum surface concentrations are similar, with a mean value of $243 \pm 13.6\ 10^{-6} Am^2 kg^{-1}$. Susceptibility and ARM measurements, where applicable, show considerably greater variance between the cores, at relative depths. For example, the mean X value for the surface samples is $4.31 \pm 3.2\ 10^{-8} m^3 kg^{-1}$.

The mean annual fluxes of SIRM in the cores have been averaged and are presented for the site in fig. 4.12. This shows increasing influx rates from 15cm ($0.33\ 10^{-6} Am^2 yr^{-1}$) up to a surface peak of $1.44\ 10^{-6} Am^2 yr^{-1}$.

An average of the cumulative influx to the three cores is presented

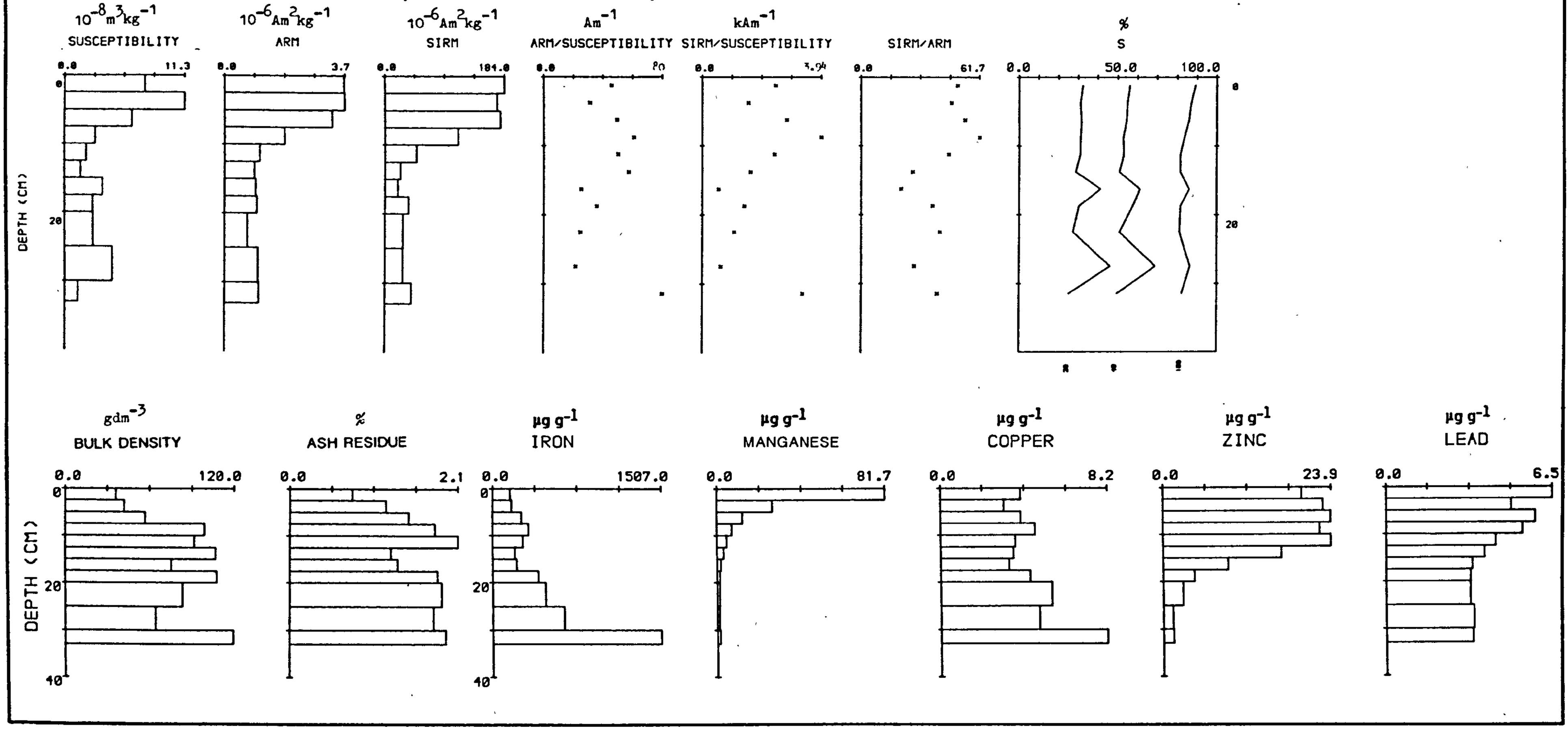


**Figure 4.5** Magnetic measurements and chemistry for Pousujärvi (PA), northern Finland

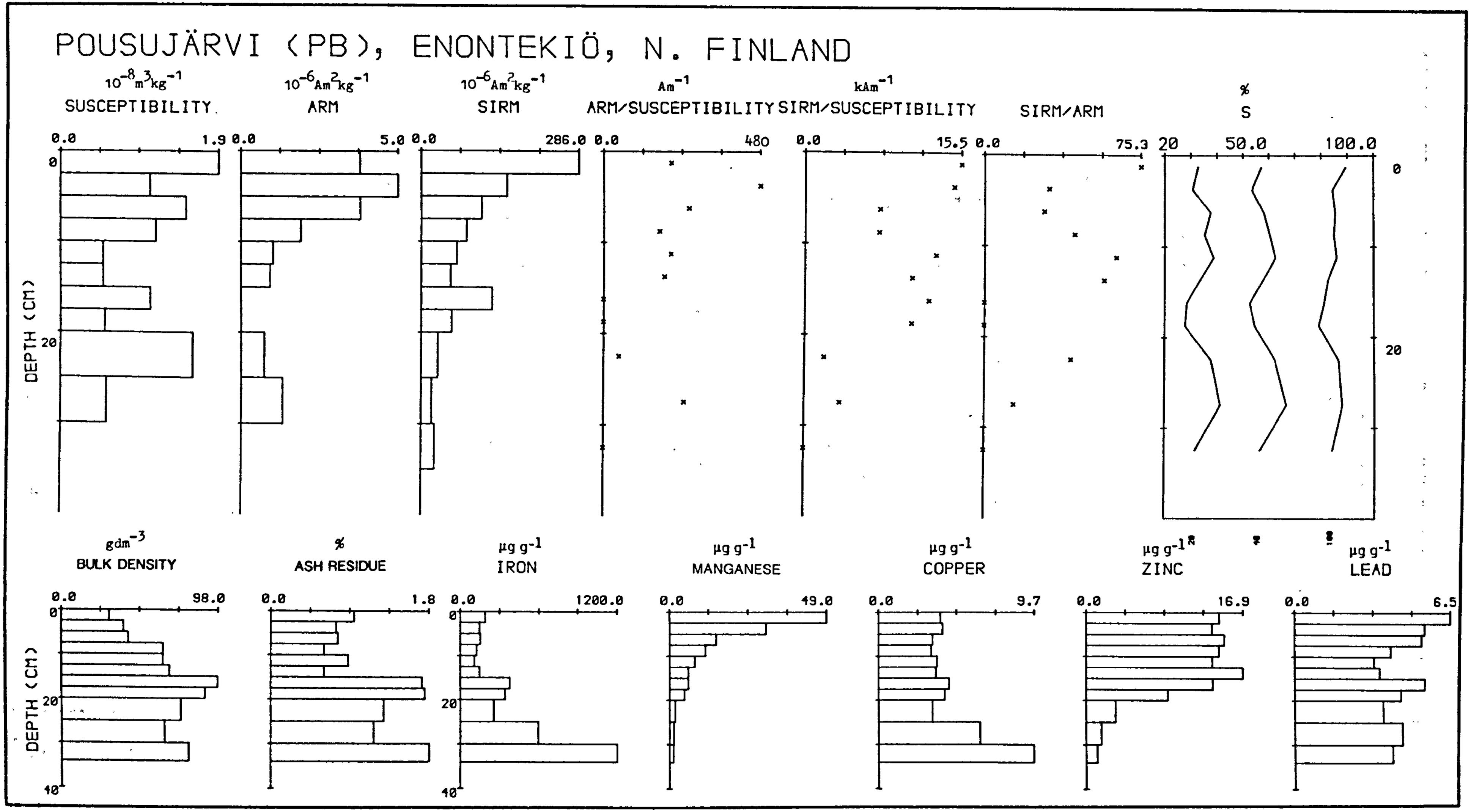


**Figure 4.6** Magnetic measurements and chemistry for Pousujärvi (PB), northern Finland

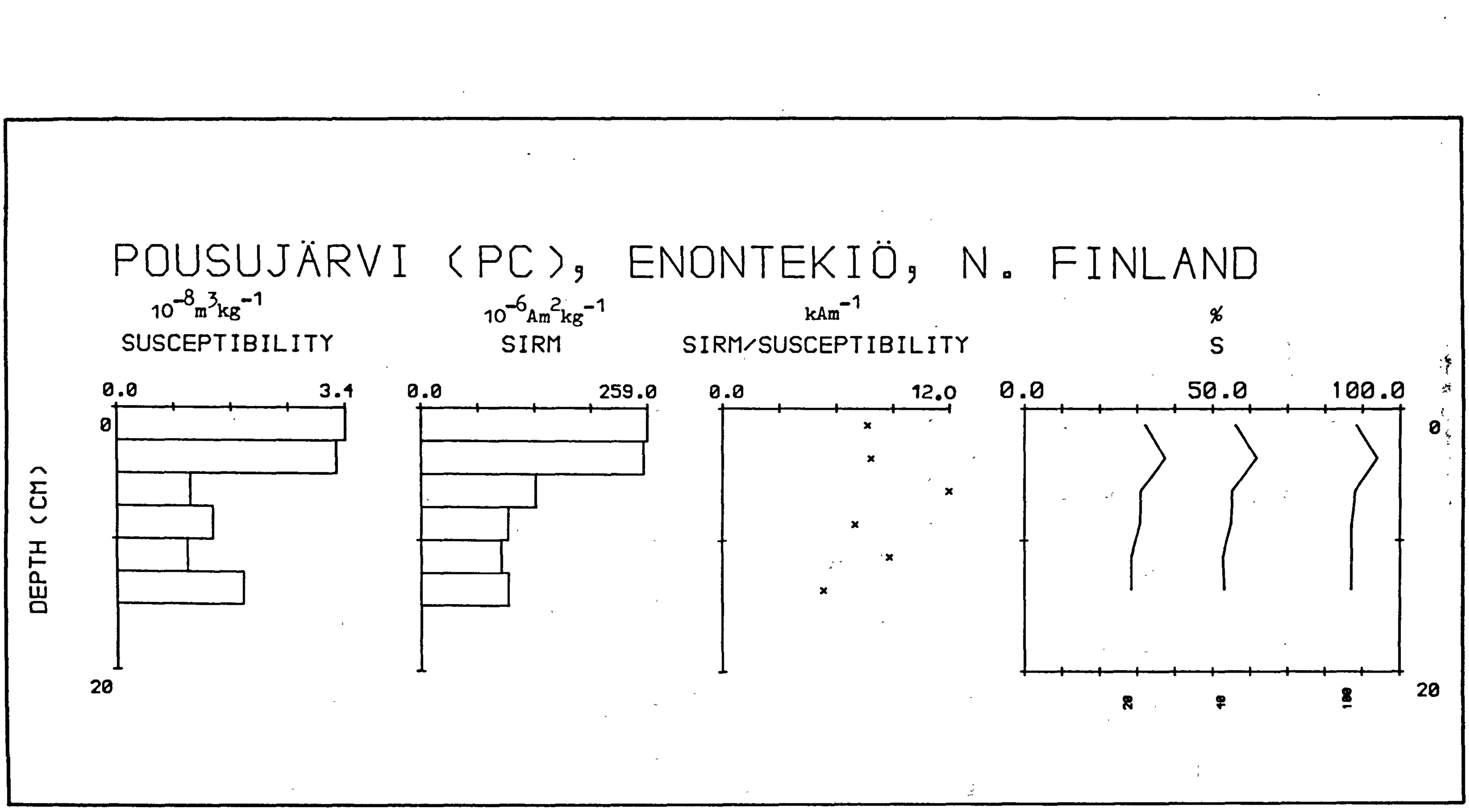


**Figure 4.7** Magnetic measurements for Pousujärvi (PC), northern Finland

for the site in Table 4.1 for comparison with the other sites over the three time intervals. An interpretation of Table 4.1 is given in section 4.4.

4.3.4 Ahmajänkä

Ahmajänkä (69°05'N 27°10'E) lies 15km to the north of Inari (population ca.200) on the south east shore of Inarijärvi, the largest lake in the region (fig. 4.1). Like Pousujärvi, the bog lies on the boundary between the northern aapa mire zone to the south and the palsa mire zone to the north, according to Eurola & Ruuhijärvi (op. cit.).

The 90cm long core available from this site has been moss increment dated throughout its length, the base of which is dated at 1247 moss increment years before 1979. The cumulative age for the top 45cm is more reliably estimated to be 156 years before 1979, due to the lesser influence of humification and compaction in the upper layers of the peat strata. The concentrations of iron, manganese, copper and zinc throughout the profile are presented in fig. 4.8. Iron concentrations in the lower half of the profile, below 45cm, are between 1 and 2 orders of magnitude higher than concentrations above 45cm. The manganese profile displays the same exponential increase toward the surface from 45cm upwards. Copper and zinc both increase from about 15-20cm up to a surface maximum. There is also a marked increase in zinc concentrations above 55cm, coinciding with a decrease in bulk density values over the same depth range (fig. 4.8).

Magnetic measurements presented in fig. 4.8 include X, SIRM, SIRM/X and the backfield ratios. The base of the SIRM profile is marked by a small peak decreasing upwards in the following 10cm (85-75cm). There is a gradual, approximately linear increase in values from 55cm up to 12.5cm (182 $10^{-6}Am^2kg^{-1}$). SIRM values then rise very slightly to a surface peak of 194 $10^{-6}Am^2kg^{-1}$. The X values exhibit a marked variation with increasing concentrations from 55cm to a peak of 13.2 $10^{-8}m^3kg^{-1}$ at 20-

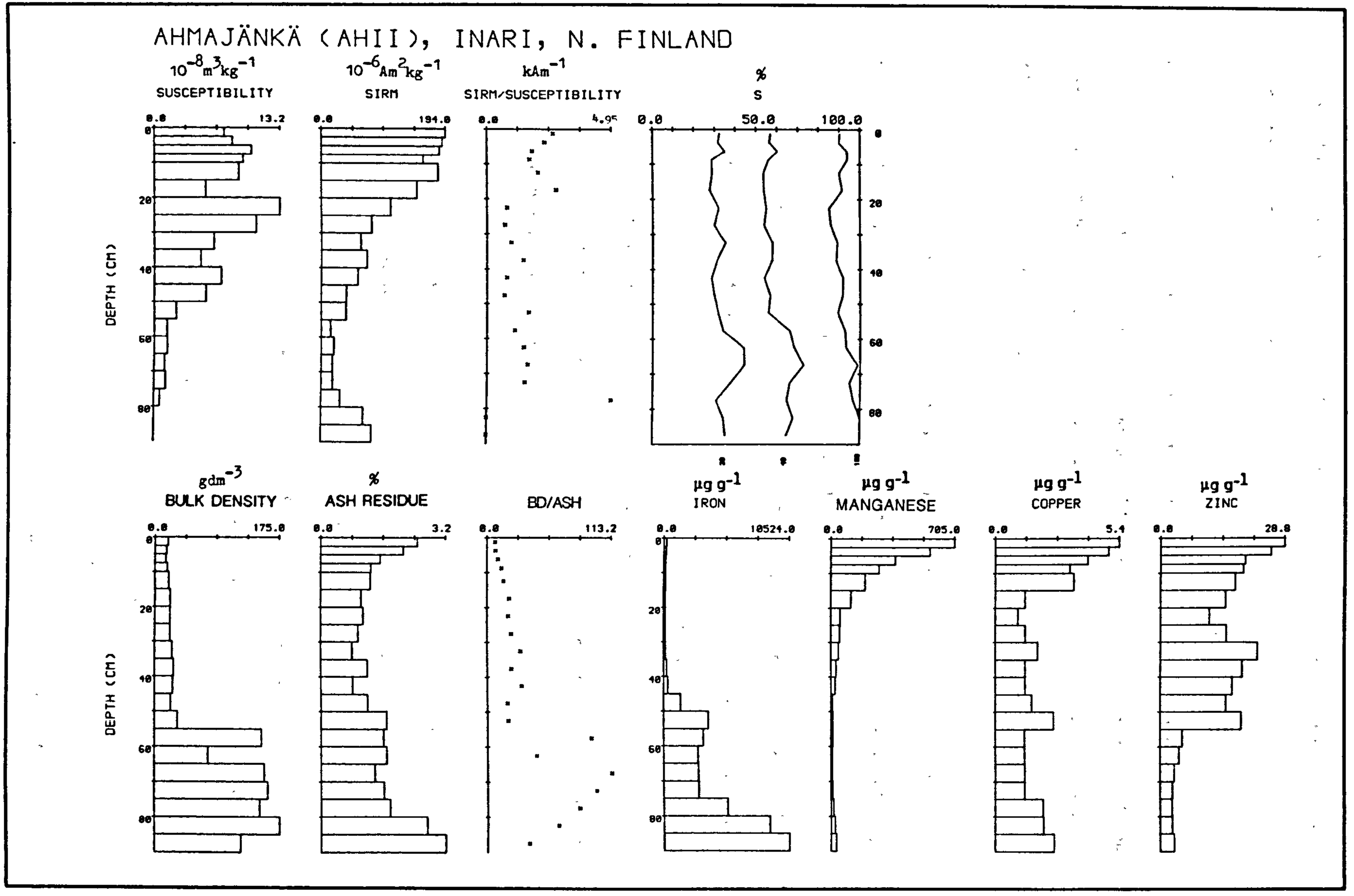


**Figure 4.8** Magnetic measurements and chemistry for Ahmajänkä, northern Finland

25cm below the surface. From 7.5cm to the surface of the core there is a decrease in X concentrations.

The mean annual flux of SIRM is plotted against time in fig. 4.12, with the SIRM profile displaying a surface peak. The cumulative estimates of heavy metal and SIRM deposition post-1900, post-1945 and post-1973 are presented in Table 4.1, for comparison with the other sites and additional data from Oldfield et al. (op. cit.).

4.3.5 Norja

Norja (69°23'N 24°12'E) is the second most northerly site in the data set, and is the only site located in Norway (fig. 4.1). The bog lies within the zone of palsa mires according to Eurola & Ruuhijärvi (op. cit.). Two cores, ND and NE are available from this site. Core ND is 20cm long, equivalent to 150 moss increment years before 1979. The deepest reliably dated point within the core is 15cm, corresponding to 75 years before 1979. Core NE is 30cm long, the maximum depth again being tentatively dated at about 500 moss increment years before 1979. The oldest reliable date is 130 years before 1979, corresponding to a depth of 20cm.

The chemical and magnetic profiles for core ND are presented in fig. 4.9. The elements determined are iron, manganese, lead and zinc. The complete range of magnetic measurements are available, and additionally, bulk density and ash residue values are available. These are also presented in fig. 4.9. Despite the shallow depth of the core, the base of the iron profile shows a marked increase in concentrations, being over an order of magnitude greater than the samples above it. The manganese profile displays the same trend as at all the other sites, with an exponential increase up to a surface maximum. The magnetic concentration dependent parameters (X, ARM and SIRM) all show a marked rise in values from those below 5cm to a surface maximum. The chemical and magnetic profiles for

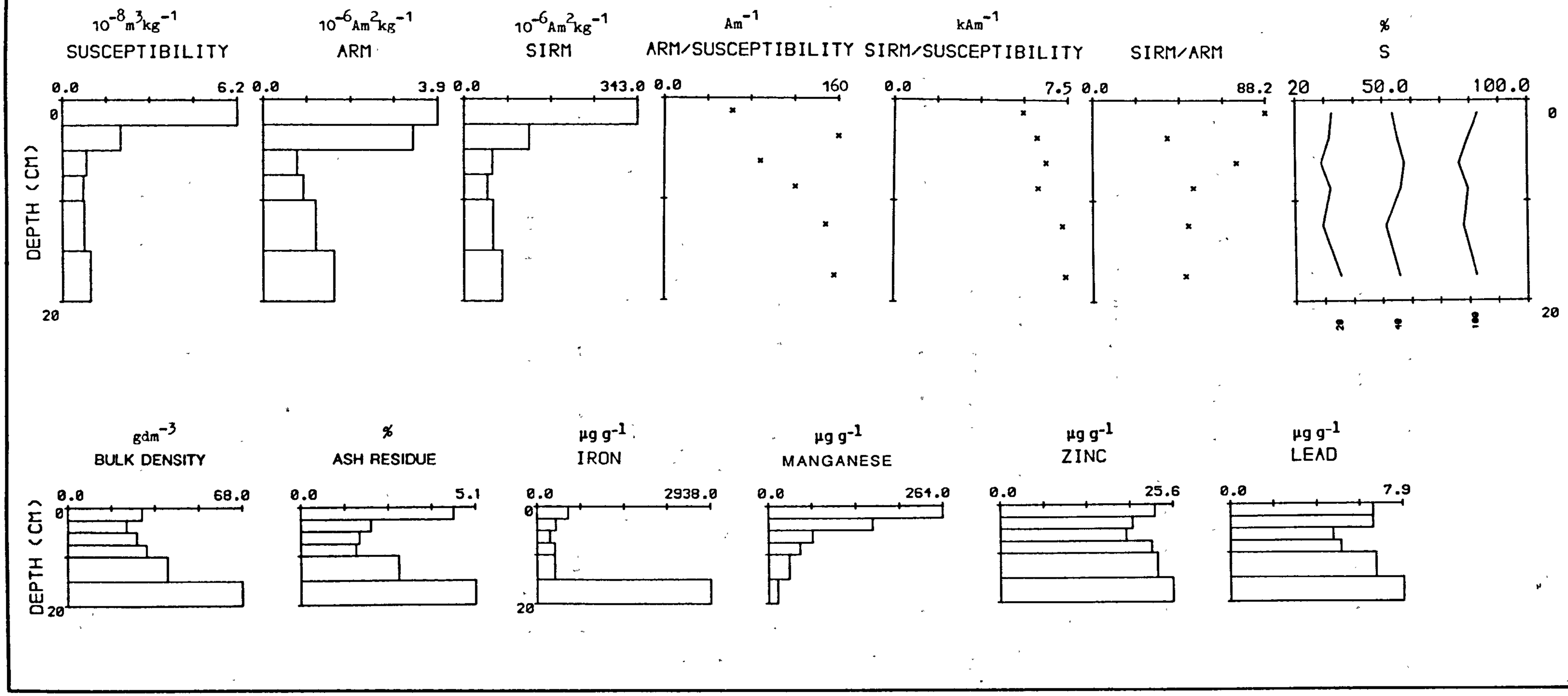


**Figure 4.9** Magnetic measurements and chemistry for Norja (ND), northern Norway

NE are presented in fig. 4.10. Like ND, the elements determined are iron, manganese, lead and zinc. A complete range of magnetic measurements are also available for this core, these being presented in fig. 4.10 along with bulk density and ash residue values.

The iron profile of core NE displays a similar pattern to that of ND, though extended over a slightly greater depth. The remaining elements all display similar patterns to their respective profiles in core ND, with the exception of zinc where there is a gradual, though distinct rise in concentrations from the base of the core to a surface maximum. There is also a similarity within the ARM and SIRM profiles of the two cores, displaying an increase from 5cm up to the surface. The X profile of NE, however, displays a sub-surface peak of 10.2-10.8 $10^{-8}m^3kg^{-1}$ between 2.5-7.5cm below the surface.

The mean annual flux of SIRM from the two cores have been averaged for the site as a whole, and plotted against time in fig. 4.12. Both cores show a surface sample maximum with the mean annual flux being comparable between both cores, 2.2-1.79 $10^{-6}Am^2yr^{-1}$.

The cumulative influx estimates post-1900, post-1945 and post-1973 are tabulated in Table 4.1 as an average for the site as a whole, for iron, manganese, lead, zinc and SIRM.

4.3.6 Utsjoki

The last, and most northerly site from the northern Scandinavian sites is Utsjoki (69°50'N 27°12'E), just south of the town of Utsjoki (population between 200-500) on the northern-most Finno-Norwegian border (fig. 4.1). Like Norja it is situated within the zone of palsa mires, the northern-most zone according to Eurola & Ruuhijärvi (op. cit.).

The maximum age of the 34cm long core is estimated to be about 445 moss increment years before 1979. The oldest reliable date is 82 years

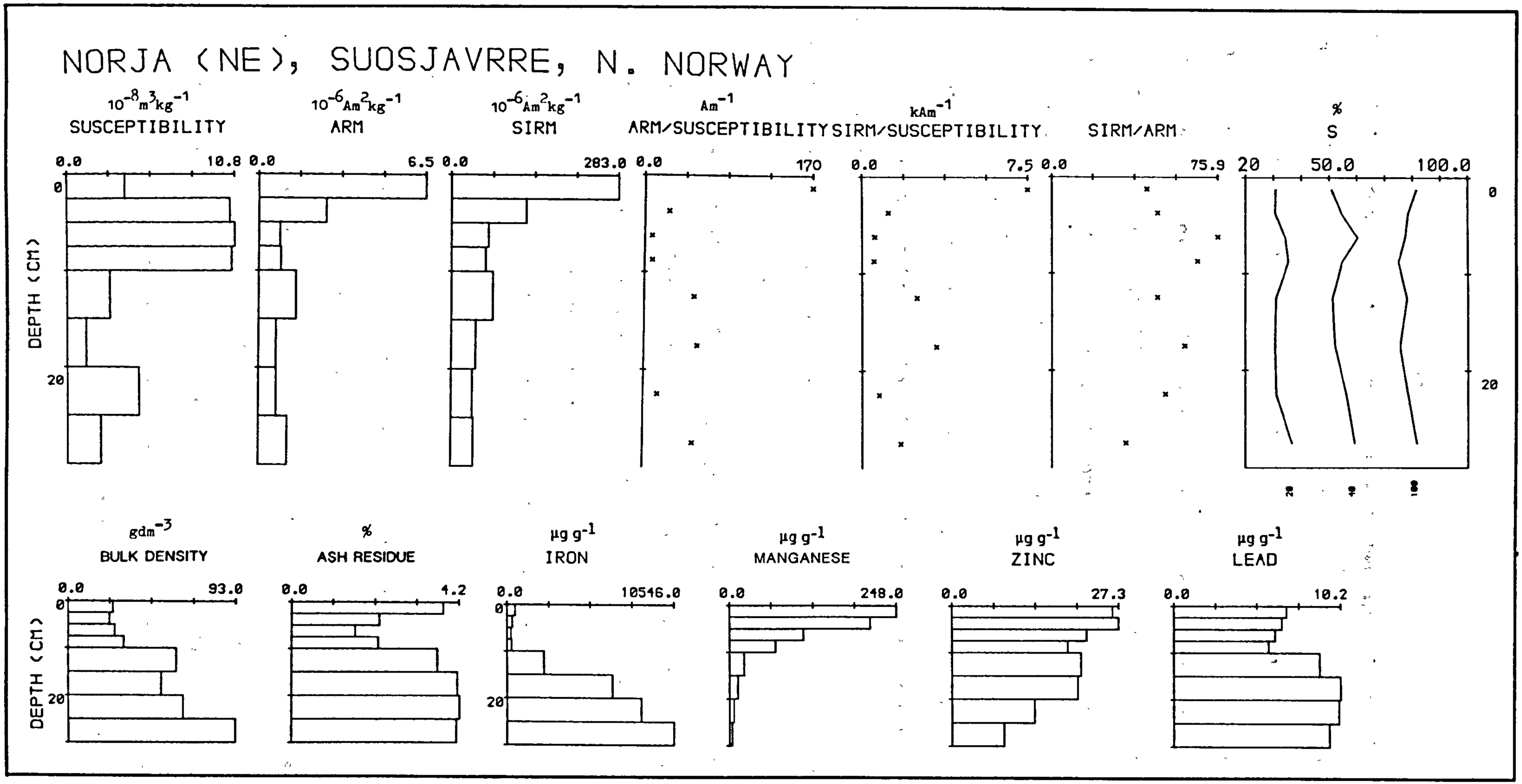


**Figure 4.10** Magnetic measurements and chemsitry for Norja (NE), northern Norway

before 1979, corresponding to 17.5cm. The peat chemistry of Utsjoki is presented in fig. 4.11 with profiles for iron, manganese, lead, copper and zinc. The iron concentrations decrease almost exponentially above 17.5cm, from 3250-3823$\mu g.g^{-1}$ (34-17.5cm) to less than 100$\mu g.g^{-1}$ (0-5cm). Superimposed on the exponential increase up through the manganese profile is a marked peak (19.65$\mu g.g^{-1}$) between 12.5-20cm, a feature not noted within any of the previous manganese profiles. Zinc concentrations increase from the base of the core to 7.3$\mu g.g^{-1}$ at 20cm, fluctuating between 7.3-11.6$\mu g.g^{-1}$ up to the surface.

The magnetic profiles presented in fig. 4.11 comprise X, SIRM SIRM/X and the backfield ratios. The SIRM profile displays an increase in values from 20cm up to a sub-surface peak at 5-7.5cm (152 $10^{-6}Am^2kg^{-1}$). This sub-surface peak is also unique to the SIRM profile for Utsjoki compared with the other northern sites.

The mean annual flux of SIRM is again plotted against time and presented in fig. 4.12. The SIRM profile culminates in a maximum mean annual flux for the surface sample of 1.3 $10^{-6}Am^2yr^{-1}$, in contrast to the SIRM profile in fig. 4.11, as noted, with a peak at 5-7.5cm.

The cumulative deposition over the three time intervals is presented for comparison in Table 4.1.

4.3.7 Additional Sites

In order to assess any geographic variation in the cumulative deposition, three cores from three southern Finnish sites are also used (Table 4.1). Comparable data are available from the previously used sites; Kaurastensuo (KAX), site-X (Chapters 2 and 3); Laaviosuo (LaavX), site-X (Chapter 3); and Varrassuo (VAX), site-X (Chapter 3). The dating method used for Kaurastensuo and Laaviosuo is the growth rate equation based on bulk density. The equation [2.1] given in sub-section 2.3.1 of Chapter 2

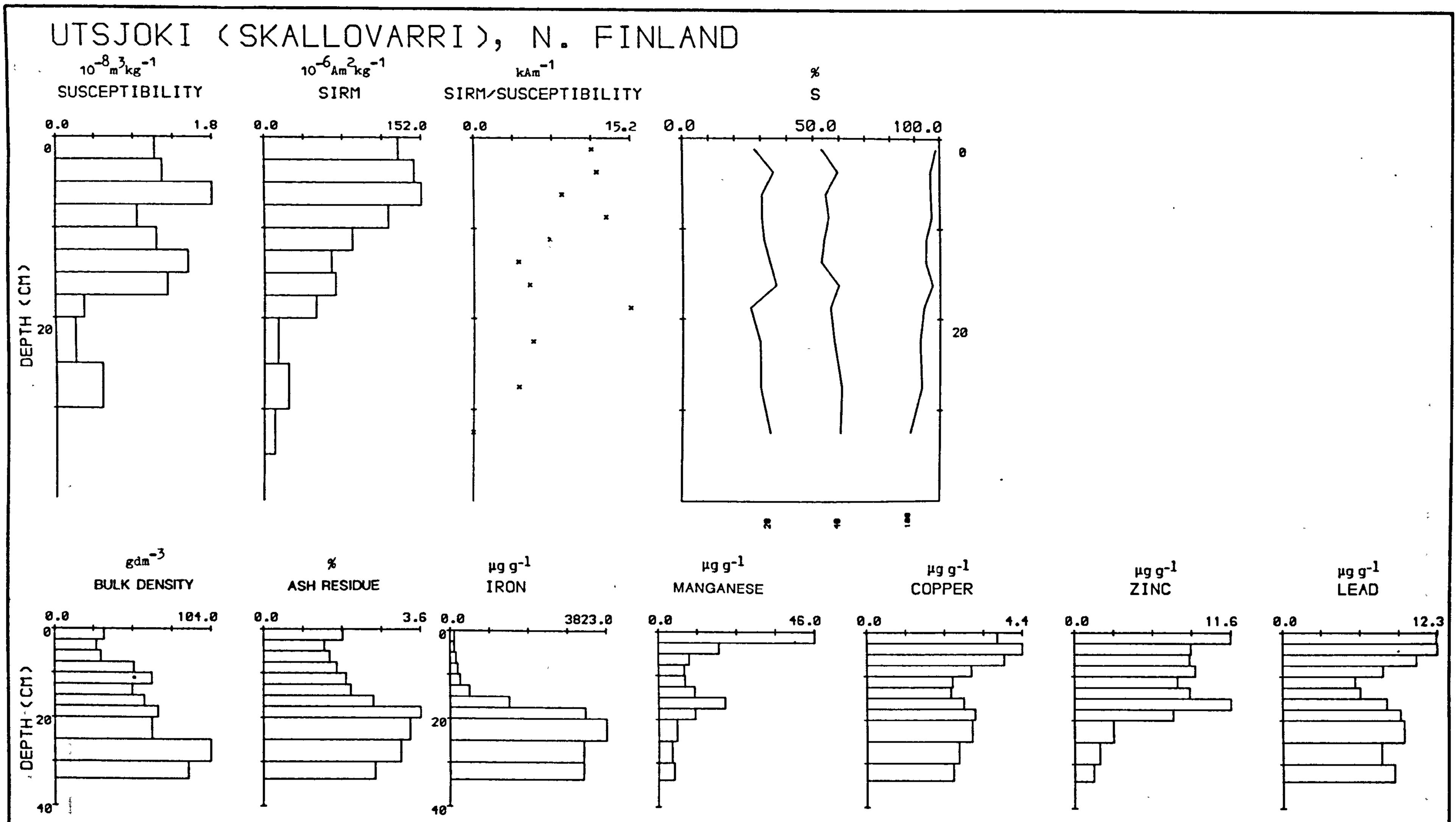


**Figure 4.11** Magnetic measurements and chemistry for Utsjoki, northern Finland

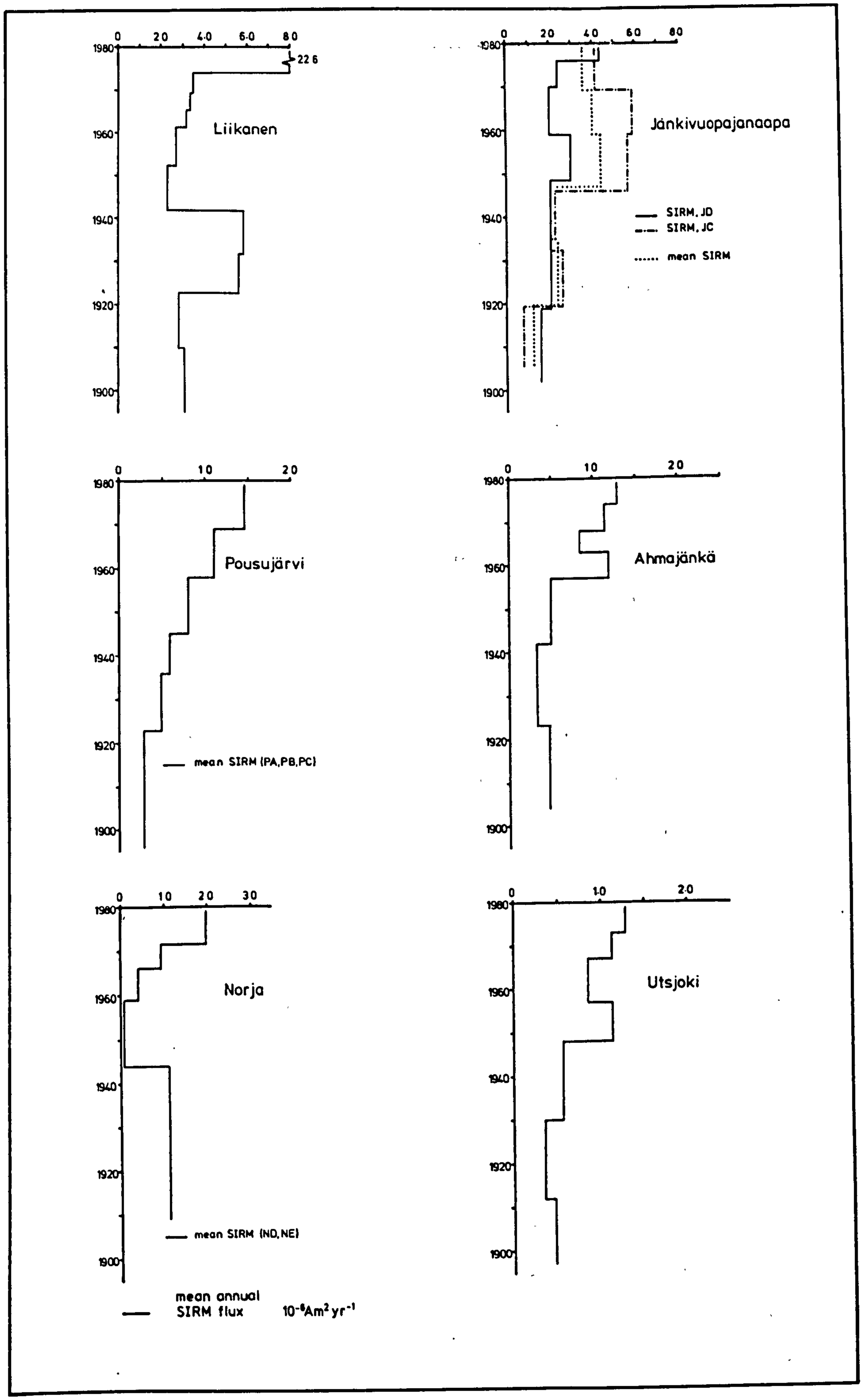


**Figure 4.12** Changes in SIRM deposition over time for the northern Scandinavian sites

provides the chronology for the surface of KAX. A similar equation, [4.2], is available for Laaviosuo bog. Like equation [2.1] it is statistically significant (r= 0.938) at the 0.01 level of significance and is derived from a separate core taken by Tolonen (pers. comm., 1985) at site-X. Equation [4.2] is:

$$\ln.y = 8.971 - 2.28\ \ln.x \qquad n= 10 \quad [4.2]$$

where ln = natural logarithm

x = bulk density ($g.dm^{-3}$)

y = growth rate, r ($mm.yr^{-1}$)

The core, VAX, from Varrassuo is dated by means of the moss increment dating method, giving depths of 1.9cm, 10.2cm and 20.5cm for the years 1973, 1945 and 1900 respectively.

Further data from Harpar Lilltrask, Karpansuo, Munasuo and Kunonniemensuo, in southern Finland are also available. The four sites are taken from Oldfield et al. (op. cit.) and El-Daoushy & Tolonen (1982). These additional data are presented in Table 4.1.

## 4.4 High Latitude Scandinavian Sites

### 4.4.1 Interpretation of the Chemical Profiles

The iron concentrations display similar trends through the profiles, both within, and between sites. The main feature of the iron profiles is the distinction between samples with very high iron concentrations, near the base of the profiles, and those with lower concentrations, towards the surface. At Ahmajänkä and Norja (NE), the decrease is 2 orders of magnitude. This pattern corresponds with that noted in southern Finnish profiles from long cores (Chapter 3). The increased iron concentrations between 10-50cm below the surface are probably linked with the influence of the water table. The evidence from sites available

suggests that the zone of water table fluctuation is closer to the surface in the more northerly sites. For example, the inflection point in the iron concentrations is only 10cm below the surface at Norja, in northern Norway, in contrast to the deeper inflection point (ca.50cm) noted at Jänkivuopajanaapa, one of the southernmost sites. Another possible hypothesis which might explain the order of magnitude increase in concentrations is the influence of localised permafrost conditions. The increase in concentrations may be related to the penetration of soligenous waters into formerly ombrotrophic peat, possibly as a result of the influence of permafrost. The absence of any water table data for these sites leaves any interpretation open to speculation.

The manganese profiles with their distinctive exponential curve, decreasing from a surface maximum, are typical of the vertical distributions of manganese noted within hummocks (Pakarinen, 1978; Pakarinen et al., 1983). The vertical distribution of this element is controlled by the redox potential of the peat. Under anaerobic conditions, manganese is reduced from a tetravalent to a divalent state, that is, from insoluble $MnO_2$ to a mobile cation. Pakarinen (op. cit.) noted that S. fuscum actively takes up manganese in the live layer. The manganese is apparently depleted from the peat layers by recycling or leaching, especially under prevailing wet conditions, for example, in hollows. It may be possible, therefore, to gain a crude indication of the local habitat conditions from observations of the total manganese concentrations. Local site conditions were probably wettest at Utsjoki and Pousujärvi, where manganese concentrations are lowest. Conversely, the conditions at Jänkivuopajanaapa (JD) and Ahmajänkä were probably the driest. A further contributory factor to the pattern is the increasing concentration gradient from coastal, or near coastal sites (eg. Utsjoki) to inland sites (eg.

Jänkivuopajanaapa), noted by Hvatum et al. (1983). The explanation given is that there appears to be an inverse relationship between manganese and annual precipitation. Hvatum et al. (op. cit.) suggest that manganese is loosely bound within the peat and available for exchange with ions in the precipitation such as $Mg^{2+}$, of marine origin.

The lead and zinc profiles, where available, display similar trends. This is in agreement with Damman (op. cit.) and Pakarinen (op. cit.). Damman (op. cit.) concluded that translocation of these elements above the water table was negligible. Copper, zinc and lead all display surface peaks, although the surface peak for lead is contrary to the results of Pakarinen & Tolonen (1977a), which indicated sub-surface peaks of lead in S. fuscum profiles from hummocks in Finnish peat bogs. At Pousujärvi the copper profiles from PA and PB both display increased concentrations at the base of the cores. The similarity between the iron and copper profiles could imply sulphide formation, since at all other sites available there is no direct relationship evident between the copper profiles and the inferred zone of water table fluctuation. Alternatively, as there is no evidence available of any significant copper deposits in the area, the increased copper concentrations might imply the location of an element sink, or localised, site-specific source of copper underlying the bog (cf. Yliruokanen, 1976).

Table 4.2 presents the enrichment ratios of the elements from the various sites in north and south Finland. The ratio has been calculated from the mean accumulation rates ($mg.m^{-2}yr^{-1}$) of the surface sample (0-2.5cm) and the slice representing the year 1900. The accuracy of the ratio is subject to site-specific features, for example at Varrassuo, where there are pronounced increases in element concentrations within the surface sample, related to the output from the nearby industrial source (Chapter 3,

**Table 4.2** Enrichment Ratios for Finnish Peats. Derived from the ratio of deposition ($mg.m^{-2}yr^{-1}$) at 0-2.5cm:A.D.1900.

| Site | Fe | Mn | Pb | Cu | Zn | Ni |
|---|---|---|---|---|---|---|
| Liikanen | 5.8 | 21.9 | 2.2 | 10.8 | 3.8 | - |
| Jänkivuopajanaapa, JD | 5.7 | 158 | - | 11.2 | 6.5 | - |
| Pousujärvi, PA | 0.56 | 16.5 | 1.5 | 1.07 | 0.82 | - |
| PB | 2.3 | 14.6 | 3.2 | 1.9 | 1.5 | - |
| Ahmajänkä | 2.6 | 19.8 | - | 6.0 | 3.9 | - |
| Norja, ND | 0.26 | 13.5 | 0.93 | - | 1.5 | - |
| NE | 1.1 | 15.5 | 1.8 | - | 1.9 | - |
| Kaurastensuo, KAX | 1.1 | - | 1.8 | 3.5 | 0.81 | 0.9 |
| Laaviosuo, LaavX | 0.69 | - | 0.43 | 1.8 | 1.3 | 1.2 |
| Varrassuo, VAX | | | | | | |
| 0-2.5cm:A.D.1900 | 8.0 | - | 7.5 | - | 3.8 | 6.1 |
| 2.5-5cm:A.D.1900 | 2.5 | - | 2.8 | - | 2.8 | - |
| Mean of N. Scandinavia | 2.3 | 32.9 | 2.0 | 5.5 | 2.7 | - |
| Mean of S. Finland* | 1.4 | - | 1.7 | 2.7 | 1.6 | 1.1 |
| Mean of All Sites* | 1.85 | 32.9 | 1.85 | 4.1 | 2.15 | 1.1 |
| N. Scandinavian Rank | Mn > Cu > Zn > Fe > Pb | | | | | |
| S. Finland Rank | Cu > Pb > Zn > Fe > Ni | | | | | |
| Mean of All Sites Rank | Mn > Cu > Zn > Fe, Pb > Ni | | | | | |
| Pakarinen et al (1983) | Mn > Zn, Cu, Pb > Fe | | | | | |

* Excluding Varrassuo (0-2.5cm)

sub-section 3.11.1). The average values from the northern Finnish sites produce the following rank of the elements:

Mn > Cu > Zn > Fe > Pb

The ranking for the southern Finnish sites is of the order:

Cu > Pb > Zn > Fe > Ni

whilst the average for all sites produces the ranking:

Mn > Cu > Zn > Fe, Pb > Ni

These ranks are in contrast with the order determined by Pakarinen et al. (1983) in a similar study:

Mn > Zn, Cu, Pb > Fe

Manganese, as noted, appears to be depleted to a large extent in the Sphagnum peat by recycling or leaching. Conversely, iron appears to be stored at greater depths. In all elements the ratio is lower in the average of northern Finnish sites compared with southern Finnish sites. The significance of this in terms of regional variations is discussed in section 4.6.

### 4.4.2 Interpretation of the Magnetic Profiles

The interpretation of the magnetic measurements is deliberately brief, concentrating on three points. First, the concept of a take-off point; second, the similarity of cores from the same site location; and third, the similarity of different sites from within the same region.

Although a reasonably well defined take-off point is detectable in the bogs from southern Finland (Chapter 3), and the age at take-off within cores from the same bog is reasonably consistent (Chapter 2), the sites from northern Scandinavia display noticeably different profiles. The SIRM profiles for most sites increase gradually toward surface or sub-surface peaks, without any obvious inflection point that might be interpreted as a take-off point. At Norja (ND, NE) and Liikanen there are distinctive

increases in SIRM, although these are limited to the surface sample. Below the surface peaks from these sites, the SIRM values increase in the same gradual, approximately linear manner as at other sites. The remoteness of these sites from any major sources of industrial activity is one possible explanation for this particular trend, given the obvious influences of point sources, for example, at Harpar Lilltrask (Oldfield et al., 1981) and at Varrassuo (Chapter 3, sub-section 3.6.5). The availability of a moss increment dated chronology has allowed the use of a specified time period, post-1900, to be used, rather than infer the presence of any take-off points. This approach is similar to that used by Oldfield et al. (op. cit.).

The reproducibility of the magnetic measurements in separate cores from the same site appears to be equally as valid as in southern Finland. The atmospheric deposition record at Pousujärvi (PA, PB, PC), Jänkivuopajanaapa (JC, JD) and Norja (ND, NE) shows a reasonable consistency between cores from the same site, for all the concentration dependent parameters and the interparametric ratios. Maximum SIRM values are similar between cores at the same site though there is a variance in X concentrations and hence, SIRM/X, notably at Jänkivuopajanaapa. Any further comparison would be unreliable, as there are no data concerning the prevailing conditions at each core site and the proximity of one core to another on the same bog.

The similarity of the general trend in SIRM profile shape is evident between sites, culminating in a surface peak at every site, with the exception of Utsjoki. The trend of a surface maximum is also evident when the mean annual flux rates are calculated. The variation in magnitude, temporally and spatially, is examined in sections 4.5 and 4.6 respectively.

## 4.5 Post-1900 Deposition

The post-1900 cumulative SIRM influxes given in Table 4.1, show a range of values between 375 (units as defined in in Table 4.1) at Liikanen and 57.5 at Utsjoki. This range includes the cumulative rates for Kaurastensuo, Laaviosuo and Varrassuo in southern Finland. Additional data (Table 4.3) are available from three sites: Ringinglow Bog, in an area of extensive urbanisation and industrial development on the southern edge of Sheffield, England (Jones, 1985); Rotmell Moss, between Pitlochry and Blairgowrie in Central East Scotland (Jones, op. cit.); and Harpar Lilltrask, 7.8km north of the steelworks at Koverhar on the southern Finnish coast Oldfield et al., op. cit.). The total cumulative depostion of SIRM post-1900 are 1.31 and 8.4 times lower at Liikanen and Utsjoki respectively than the mean estimate from the 'remote' Scottish site, Rotmell Moss. The respective values for Liikanen and Utsjoki are 3.2 and 21 times lower compared with the post-1950 deposition at Harpar Lilltrask in southern Finland (cf. fig. 4.13). Finally, compared with the post-industrial deposition at Ringinglow Bog, corresponding to approximately the same time scale (Table 4.3), the values for Liikanen and Utsjoki are 11.6 and 76 times lower respectively. Given the relationship between iron and SIRM in surface samples containing particulates of anthropogenic origin (Chapter 3, sub-section 3.11.1; Chapter 5, sub-section 5.4.6), a similar comparison may be made for the post-1900 cumulative iron. Where the increased basal concentrations of iron are evident in cores above the projected date of 1900, the core is ignored in subsequent discussion. The range of iron values for the north Scandinavian sites is between 196mg per square metre (Jänkivuopajanaapa) and 35.7mg per square metre (Utsjoki). Compared with the post-1900 iron deposition at Harpar Lilltrask (Table 4.1), these sites display values 10.4 times and 57 times lower respectively.

Table 4.3 Additional Cumulative SIRM Data. The units are in Ax$10^{-6}$ per square metre.

| Site | Cumulative SIRM | Remarks |
|---|---|---|
| Harpar Lilltrask, S. Finland* | 1210 | Post-1950 |
| Rotmell Moss, E. Scotland** | | |
| RM2 | 586.4 | |
| RM4 | 377.6 | |
| $\bar{x}$ | 482 | Post-'take-off' |
| Ringinglow Bog, S. Yorkshire** | | |
| RB5 | 6335 | |
| RB6 | 2380 | |
| $\bar{x}$ | 4357 | Post-'take-off' c.1900-1920[1] |

* Oldfield et al (1981)

** Jones, unpubl. thesis (1985)

1. $^{210}Pb$ dates from Ringinglow place the major increase at about 1945-50 but this is still to be cross-checked with a pollen-derived basal date (Jones, pers. comm.).

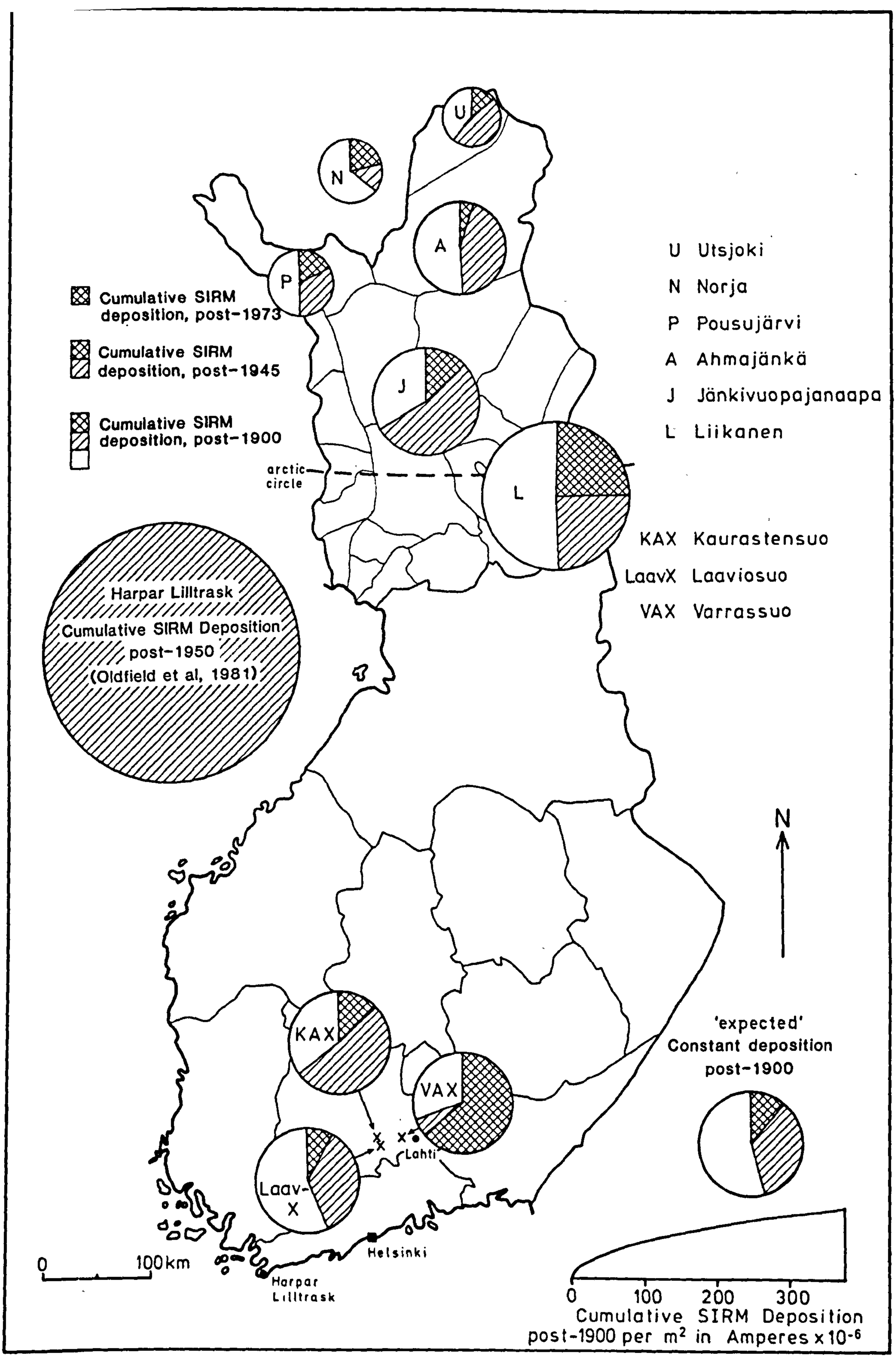


**Figure 4.13** Spatial and temporal variation in SIRM deposition over Finland. Including Norja, northern Norway.

The mean annual SIRM flux rates for the years 1900, 1945 and 1979 (Table 4.4) give an indication of the changes in particulate flux contributing to SIRM, over time. If the ratios A/B (mean annual flux for 1979/mean annual flux for 1945) and A/C (mean annual flux for 1979/mean annual flux for 1900) given in Table 4.4 are considered, then some indication is given of the order of change. The higher the ratio, the greater the order of change. For example, at Varrassuo the A/B ratio for VAX (50) represents the the highest ratio value calculated. This has been produced by a disproportionately large mean annual flux for 1979 at the site, linked with increased anthropogenic deposition (Oldfield et al., op. cit.). However, in the case of Norja, ND (12.9), the higher ratio is the result of a disproportionately low mean annual flux for 1945 (Table 4.4). In all cores, with the exception of Liikanen and Norja (ND, NE), the 1945 flux is greater than the 1900 flux. Without exception, the 1979 flux is greater than the 1945 flux.

In recent years attempts have been made in Finland to estimate deposition of heavy metals on a unit area and time basis (Table 4.1), with specific reference to ombrotrophic peat bogs (eg. Pakarinen & Tolonen, 1977b, 1980; Pakarinen, 1977, 1981; Pakarinen et al., 1981, 1983). Related investigations on metal distribution and deposition rates in bogs have also been conducted elsewhere in northern and western Europe (eg. Clymo, 1978; Damman, 1978; Aaby & Jacobsen, 1979). Pakarinen et al. (1983) also used an enrichment ratio of surface:deep peat (anaerobic) in order to assess, indirectly, the amount of recycling, mobility and leaching of elements. The age of the anaerobic peat varied between 400-2700yrs BP and yielded the elemental ranking given in sub-section 4.4.1. A similar ranking (sub-section 4.4.1) derived from the enrichment ratios given in Table 4.2 is in good agreement with this. The main difference in the

**Table 4.4** Mean Annual Flux ($10^{-6}Am^2yr^{-1}$) for c.1979, 1945 and 1900 in Northern Scandinavian Sites.

| Site | 1979 A | 1945 B | 1900 C | A/B | A/C |
|---|---|---|---|---|---|
| Liikanen | 22.6 | 2.31 | 3.1 | 9.8 | 7.3 |
| Jänkivuopajanaapa, JC | 4.15 | 2.23 | 0.99 | 1.9 | 4.19 |
| JD | 4.23 | 2.16 | 1.77 | 1.96 | 2.4 |
| Pousujärvi, PA | 1.4 | 1.0 | 0.26 | 1.4 | 5.4 |
| PB | 1.81 | 0.62 | 0.19 | 2.9 | 9.5 |
| Ahmajänkä | 1.24 | 1.02 | 0.63 | 1.21 | 1.97 |
| Norja, ND | 2.2 | 0.17 | 0.44 | 12.9 | 4.0 |
| NE | 1.79 | 0.21 | 0.55 | 8.5 | 3.25 |
| Utsjoki | 1.3 | 0.57 | 0.47 | 2.3 | 2.8 |
| Kauarstensuo, KAX | 3.25 | 0.18 | 0.15 | 18.1 | 21.7 |
| Laaviosuo, LaavX | 2.1 | 2.3 | 1.6 | 1.1 | 1.31 |
| Varrassuo, VAX | 15.5 | 0.31 | 0.14 | 50 | 111 |

calculation of the ratios is that those in Table 4.2 are based on peat of a similar, known age (ca. A.D.1900). The conclusions based on the use of enrichment ratios is that due to preferential removal of elements such as manganese, zinc and lead, and the storage of other elements such as iron, precludes any detailed use of accumulation rates for these elements in all but the surface sample. There are also problems encountered when using only the surface sample slice, these are discussed in sub-section 4.6.2 and section 4.7.

The differential mobility of mineral elements, in unknown proportions, is therefore an additional factor to be taken into consideration when interpreting the chronological development of atmospheric elemental fall-out in ombrotrophic bog profiles (cf. Pakarinen & Tolonen, 1977a). This appears to be a prime consideration in weakly to moderately decomposed Sphagnum peats (cf. Pakarinen et al., op. cit.). To minimise these problems as far as possible, the regional variations in chemical concentrations and SIRM (section 4.6), are therefore given for the surface sample only, predominantly 0-2.5cm, unless otherwise stated.

## 4.6 Regional Variation in Deposition

### 4.6.1 Introduction

The rationale for using bryophytes as indicators of the fallout of heavy metals in Scandinavia, is based mainly upon the early work of Rühling & Tyler (eg. 1968, 1970, 1971, 1973). Initial studies were carried out on Pleurozium schreberi and Hypnum cupressiforme to measure regional and historical trends in the deposition of lead over southern Scandinavia (Rühling & Tyler, 1968). Subsequent studies identified the capacity of the moss Hylocomium splendens for uptake and accumulation of heavy metal ions (Rühling & Tyler, 1970). The use of S. fuscum (Rühling

& Tyler, 1973) was based on the studies of Puustjärvi (1954) and Clymo (1963), as noted in section 4.1. Pakarinen (1981a) noted that with regard to lead, zinc, iron and copper the variation between Sphagnum species growing in similar microhabitats in the same site appears to be fairly small compared with the regional variation between bogs.

In this section the results are interpreted initially on a concentration/dry weight basis (sub-section 4.6.2), similar to the earlier studies and subsequently on a depositional basis (sub-section 4.6.3). The interpretation in these respective sub-sections is limited to the chemical determinations for the surface sample (0-2.5cm, unless otherwise stated). The final sub-section gives a brief overview of chemical and magnetic (SIRM) deposition, for all sites available in Finland. This sub-section also takes account of both the spatial and temporal variations, where applicable, within the data set.

### 4.6.2 Regional Variation on a Dry Weight Basis

The regional variations in element concentrations are given in Table 4.5 for the six sites in northern Finland and three sites in southern Finland. In addition to the sites from northern Finland is Ahvenjärvenvuoma (67°37'N 25°16'E). The elements iron, lead, copper, zinc and nickel are compared with three published sources: Rühling & Tyler (1973), Pakarinen & Tolonen (1976) and Pakarinen (1981a). The data are tentatively compared bearing four main considerations in mind. The first consideration is the relative age of the data sets. All the published sources are surface samples collected between 1 and 2 years before publication. The samples used in this chapter were collected in the summer of 1979 (Tolonen, 1980; pers. comm.), therefore the pre-existing published results relate to vegetation surfaces, 7, 4 and 2 years before 1979 respectively. Given the 2.5cm thickness of each slice interval, with a mean age of 7.1±5.3 years before

1979 (for 2.5cm depth) it is assumed that this slicing interval encompasses the three previous vegetation surfaces, allowing a basic comparison to be made. A second consideration relates to the species composition of the relative samples. Rühling & Tyler (1970) used Hylocomium splendens which was considered to have an almost completely passive retention of copper, lead and nickel ions. The retention of zinc is estimated to be incomplete unless active uptake by the moss tissues occurs in the field (Rühling & Tyler, op. cit.). The studies by Pakarinen & Tolonen (op. cit.) and Pakarinen (op. cit.) involved the use of the moss S. fuscum, the same moss being the predominant species in the surface layers of the cores used in this chapter. Thirdly, related to the species type, is a further consideration of microhabitat and the time of year of the sampling, the latter being important through differing productivity of species and differing deposition rates seasonally. The samples of Hylocomium splendens came from moss carpets in woodland areas, Calluna heaths and alpine heaths (Rühling & Tyler, 1973). The S. fuscum samples used by Pakarinen & Tolonen (op. cit.) and Pakarinen (op. cit.) and Tolonen (sub-section 4.2.1) were from low or intermediate moss hummocks. The majority of the S. fuscum samples were collected in late summer. The Hylocomium splendens samples were also collected during the summer months. The samples were all digested by similar nitric acid preparations on a dry weight basis. Further discussion about the effect of digestion methods are discussed in sub-section 4.6.3.

The fourth consideration is the size of the relative data sets. The data set used within this chapter is neither large enough or evenly distributed enough to provide an adequate, independent assessment of regional heavy metal concentrations over Finland. This is exemplified by the small number of sites available from southern Finland (four), and their limited geographical distribution. The mean values of such a small number of sites

becomes much more easily influenced by site specific factors, for example, at Varrassuo.

There are three main points to note within the data from Table 4.5. The first is that the mean concentrations for the northern Finnish sites are within the published limits for all the elements. The second point is that the mean concentrations of the four southern Finnish sites are much more variable compared with the published results. The mean iron and zinc concentrations are substantially lower than the published equivalents, for iron these are 675$\mu g.g^{-1}$ and ca.1000$\mu g.g^{-1}$ respectively, whilst for zinc the values are 49.5$\mu g.g^{-1}$ and >60$\mu g.g^{-1}$ respectively. Lead and copper correspond approximately with the published limits, whilst mean nickel concentrations from the southern Finnish sites are actually higher than the published limits. The third observation is the apparent difference in retained element concentrations between the mosses Hylocomium splendens and S. fuscum. The element values given for the former (Table 4.5) are consistently higher than those of the latter in each of the north, central and southern regions. There are two possible explanations for this, the first being a temporal variation, and the second a physiological variation. It may well be that the difference in concentrations is reflecting a temporal variation in deposition; ie. a decrease in deposition from the early 1970's through to the end of the decade. Rühling & Tyler (1984) have noted such a decrease over this period in southern Sweden, and infer that it has probably occurred in other parts of Europe as well. A second possible explanation is that the two different moss types have different retention capacities resulting in variations within element concentrations. This is partly controlled by the limiting pH conditions of the microhabitat which corresponds with the cation exchange capacity of the moss (Clymo, 1963). No data are available on the northern Finnish sites relating to the

**Table 4.5** Regional Distribution of Elements in Surface Samples (0-2.5cm) from Scandinavia

| Site/Location | Fe | Pb | Cu | Zn | Ni | Source |
|---|---|---|---|---|---|---|
| | | | $\mu g.g^{-1}$ dry weight | | | |
| Liikanen | 310 | 15.2 | 7.4 | 31.6 | - | |
| Jänkivuopajanaapa | 159 (179) | - | 7.3 (3.1) | 11.5 (22.1) | - | (Pakarinen, 1978) |
| Ahvenjärvenvuoma | 314 | 5.4 | 4.3 | 26.6 | - | |
| Pousujärvi | 156 | 6.5 | 4.2 | 19.0 | - | |
| Ahmajänkä | 211 (113) | - | 5.4 (3.1) | 28.9 (19.6) | | (Pakarinen, 1978) |
| Norja, N. Norway | 517 | 6.75 | - | 24.6 | - | |
| Utsjoki | 100 | 12.3 | 3.7 | 11.5 | - | |
| x̄ | 252 | 9.23 | 5.4 | 22.0 | - | |
| Kaurastensuo, KAX | 541 | 17.6 | 6.3 | 47.1 | 4.4 | |
| Laaviosuo, LaavX | 294 | 9.4 | 6.0 | 35.0 | 3.0 | |
| Varrassuo, VAX | 1550 | 51.0 | 8.1 | 68.6 | 7.0 | |
| Haukilampi | 314 | 12.1 | 8.1 | 47.3 | 14.8 | |
| x̄ | 675 | 22.5 | 7.1 | 49.5 | 7.3 | |
| | | | ppm dry weight | | | |
| N. Finland | | <10 | | | 2-4* | Rühling & Tyler, 1973 |
| C. Finland | <500 | 10-20 | <6.0 | 40-60 | ca.4** | |
| S. Finland | ca.1000 | ca.40 | ca.8 | >60 | 4.0 | |
| N. Finland | 236 | <10 | 4.7 | 32.6 | 1.3 | Pakarinen & Tolonen, 1976 (Tolonen, 1974) |
| C. Finland | 224 | x̄=7.3 | 5.5 | 35.3 | 1.2 | |
| S. Finland | - | (16-40.5) | | | | |
| N. Finland | - | <10 | - | - | - | Pakarinen, 1981a |
| C. Finland | - | 10-20 | - | - | - | |
| S. Finland | - | 20-30 | - | - | - | |

* Norja, Pousujärvi, Jänkivuopajanaapa and Liikanen)
** Utsjoki, Ahmajänkä and Ahvenjärvenvuoma

prevailing microhabitat conditions at the coring sites.

Manganese has been omitted from Table 4.5 because of its weak retentive capacity as demonstrated by Rühling & Tyler (1970) and noted by Pakarinen & Tolonen (op. cit.). The rapid translocation of the element has also been demonstrated in the peat profiles described in section 4.3.

The published sources on regional heavy metal variations in Finland all agree that iron, lead and zinc all display strong regional gradients, with the highest values in the south decreasing northwards. The limited site data available for this chapter show substantially higher mean concentrations of all the elements for southern Finnish sites compared with the northern Finnish sites.

4.6.3 Regional Variation in Mean Annual Flux

Table 4.6 comprises the mean annual flux of SIRM and the heavy metals for surface samples from both the northern and southern Finnish sites used previously. This includes the site, Ahvenjärvenvuoma used in sub-section 4.6.2.

Any evidence of a north-south gradient is masked by the limited size of the sample set, and also site specific anomalies, for example at Liikanen. It would therefore seem more appropriate to compare the means of the different values obtained from the northern Finnish sites with those from the southern Finnish sites (Table 4.6). Two sets of mean values are given for the southern Finnish sites, one set including the site Varrassuo and the other excluding it. This is done on the premise that the high SIRM and heavy metal fluxes in the surface sample are due to site-specific factors (Chapter 3). The limited number of sites available in southern Finland has a pronounced effect on the mean of the southern region as a whole, which must be taken into consideration when comparing the sets of mean values. A comparison between the means of the northern Finnish

**Table 4.6** Regional Variation in Mean Annual Flux. The flux rates have been calculated from the surface sample, 0-2.5cm.

| Site | SIRM | Fe | Mn | Pb | Cu | Zn | Ni |
|---|---|---|---|---|---|---|---|
| | $10^{-6}Am^2yr^{-1}$ | | | $mg.m^{-2}yr^{-1}$ | | | |
| Utsjoki | 1.3 | 13.7 | 6.3 | 1.7 | 0.5 | 1.6 | - |
| Norja, N. Norway | 2.0 | 46.5 | 23.0 | 0.61 | - | 2.2 | - |
| Ahmajänkä | 1.24 | 19.0 | 63.5 | - | 0.48 | 2.6 | - |
| Pousujärvi | 1.58 | 20.0 | 5.2 | 0.53 | 0.32 | 1.38 | - |
| Ahvenjärvenvuoma | - | 48.9 | 48.1 | 0.85 | 0.66 | 4.1 | - |
| Jänkivuopajanaapa | 4.19 | 31.7 | 141 | - | 1.5 | 9.6 | - |
| Liikanen | 22.6 | 45.3 | 41.7 | 2.2 | 1.1 | 4.6 | - |
| x̄ | 2.1* | 32.2 | 47.0 | 1.18 | 0.76 | 3.7 | - |
| Kaurastensuo, KAX | 3.25 | 66.5 | - | 2.2 | 0.77 | 5.8 | 0.54 |
| Laaviosuo, LaavX | 2.1 | 30.5 | - | 0.97 | 0.61 | 3.6 | 0.31 |
| Varrassuo, VAX | 15.5 | 247 | - | 8.2 | 1.3 | 10.9 | 1.1 |
| x̄ | 6.95 | 115 | - | 3.8 | 0.89 | 6.8 | 0.65 |
| x̄** | 2.7 | 48.5 | - | 1.6 | 0.69 | 4.7 | 0.43 |

* Excluding Liikanen

** Excluding Varrassuo

sites and that of KAX and LaavX shows that for SIRM, iron, lead and zinc the values are higher in the south. For copper the mean value for the south is 0.69mg.m$^{-2}$yr$^{-1}$, compared with 0.76mg.m$^{-2}$yr$^{-1}$ for the north. The former observations concur with the results of Pakarinen (1981a) who noted a strong north-south gradient for iron, lead and zinc but a less distinct pattern for copper.

Compared with the published rates of influx (Pakarinen, 1978; Pakarinen et al., 1983) the values given in Table 4.6 are consistently lower. For example, the lead consumption rate given in Pakarinen (op. cit.) for southern Finnish sites is 4.6mg.m$^{-2}$yr$^{-1}$ compared with 1.6mg.m$^{-2}$yr$^{-1}$ given in Table 4.6. The corresponding estimate from Pakarinen et al. (op. cit.) is 5.7mg.m$^{-2}$yr$^{-1}$. There are several possible explanations for this slight discrepancy in the flux rates. The first relates to differences in the initial concentrations of elements within the different studies. The average concentration for surface hummock samples from southern Finland in published material was 23.9$\pm$2.9µg.g$^{-1}$ (Pakarinen op. cit.), compared with 13.5µg.g$^{-1}$ from an average of KAX and LaavX. This may be partly explained by difference in extraction methods used between this study (nitric acid digestion) and the two published sources (nitric/perchloric acid digestion). It is believed that the nitric/perchloric acids method gives a more complete digestion for some metals, for example, lead, with approximately 5% difference between the two methods in favour of the nitric/perchloric acid method. Lead is probably removed at about 95% from mineral soils by a hot, concentrated nitric acid digest alone. For other elements, for example, copper, perchloric acid does not release the total amount of the lattice bound fraction (James, 1986; pers. comm.). Therefore, it may be expected that nitric/perchloric acid digests will give higher initial concentrations provided there is no interference with the

method of determination in solution and the calibration of the instruments is equal. A second possible cause of discrepancy is the difference in sampling intervals. The published sources use mainly the 'live' layer incorporating approximately one year's growth. The slice interval used in this chapter is much thicker, incorporating 7.1±5.31 years growth. Such a comparatively large increment is most probably affected by the leaching gradient within the peat profile. The lower limit of the timescale over which the elements become mobile and are translocated through the profile is not known, although almost certainly seasonally. A further consideration is the method of calculation used to determine the annual flux of elements. None of the published sources used report the method of calculation for comparison. It may reasonably be assumed that any errors, over-estimates or under-estimates, for example in the chronology, that are present within the initial stages of the calculation will be multiplied through, markedly affecting the final answer. Despite this, the deposition values given for the elements are all consistently within the range of estimates given within the literature for the various sites in northern and southern Finland. By using the mean values from several sites it is hoped that some of the errors are reduced.

4.6.4 Spatial and Temporal Variation in Magnetic Particulate Deposition

The post-1900 cumulative magnetic particulate deposition is summarised in fig. 4.13, the area of each circle (A) being proportional to the amount of magnetic particulate deposition estimated at each site. Within each proportional circle the segments represent post-1973 deposition, post-1945 deposition (including post-1973) and pre-1945 deposition. These are compared against the 'expected' proportion given a theoretically constant rate of deposition since 1900. It is clear that none of the sites, with the possible exception of Laaviosuo, approximate to the

same expected proportions.

The regional variation in the sites from the northern part of Finland display an apparent southeast-northwest decreasing gradient, although this is partly a function of the large post-1900 cumulative deposition at Liikanen, mentioned with regard to the heavy metals in sub-section 4.6.2. The total cumulative post-1900 deposition for the sites in southern Finland is very similar, however, in comparison with the northern sites they do not reflect the same north-south gradient previously inferred from the chemical deposition (section 4.5).

It would appear that with such a limited sample set any site specific anomalies tend to be depicted in preference to any overall regional trend. This is probably true in a temporal as well as spatial framework.

## 4.7 Conclusions

The main conclusions from this chapter may be broadly defined within two frames of reference. The first deals with observations made from the chemical and magnetic profiles obtained at the sites used within northern Scandinavia, whilst the second deals with estimates of chemical and magnetic particulate deposition into the sites, and the spatial and temporal variations associated with that deposition.

There are three main conclusions within the first framework. The first is that within the cores available from the northern Scandinavian sites there is a noticeable increase in the influence of the zone of water table fluctuation nearer the surface, progressing northwards. The main evidence for this is the exponential increase in iron concentrations at distinct points down-profile. This has precluded estimates of iron deposition over time, and cumulatively above dated horizons at some sites, for example, Norja, northern Norway (Table 4.1). Furthermore, variations noted in the previous

chapter (sub-section 3.9.2) regarding fluctuations around the water table are less obvious as a result.

The second conclusion about the chemical profiles is a product of the enrichment ratios given in Table 4.2. The ranking produced:

Mn > Cu > Zn > Fe, Pb > Ni

for all the elements used. Manganese at the top of the scale represents the most depleted element, whilst nickel at the other extreme appears to be stored at greater depths. This conclusion approximates with the results of Pakarinen et al. (1983), despite the variations in the calculation of the ratio (sub-section 4.4.1). The enrichment ratios also appear to confirm that the estimation of accumulation rates for all elements in all but the surface sample might be inappropriate. Even the surface samples are likely to be affected to some unquantifiable extent by leaching and mobility of elements and this must be taken into account when interpreting the accuracy of the results (sub-section 4.6.3).

The third conclusion is that at sites where there is more than one core available, there is a strong similarity between the respective chemical and magnetic profiles, both in terms of actual values and down-profile trends. For the magnetic measurements, the similarity is predominantly between the SIRM profiles, although at Pousujärvi and Norja the similarity extends to other parametric ratios and also the interparametric ratios including the backfield ratios. Unlike the previous sites from southern Finland (Chapter 3) a distinct take-off point was not evident within all the SIRM profiles. Concentrations for each slice increment tended to increase on a gradual, linear scale towards a surface or sub-surface peak.

The availability of a recent chronology in the form of moss increment dated horizons allowed the use of a base date, 1900, from which to assess cumulative SIRM and heavy metal deposition. These dates form the basis of

the second set of conclusions, based on estimated deposition rates. As a result all the following conclusions are made tentatively, based on the reliabilty of the moss increment dating method, as outlined in sub-section 4.2.2.

Cumulative SIRM above 1900 varies between 57.5 (Utsjoki) and 375 (Liikanen) for the northern Scandinavian sites. These are lower than the post-1950 cumulative deposition at Harpar Lilltrask, near an iron and steel works on the south coast of Finland by 21 and 3.2 times respectively. The cumulative values are also lower than the cumulative deposition over approximately comparable time periods at Rotmell Moss in Scotland and substantially lower than the deposition at Ringinglow Bog in industrial South Yorkshire.

Temporal variation in the deposition rate at the sites is evident by comparing the A/B ratios presented in Table 4.4 (section 4.5). The highest ratios (eg. VAX and Liikanen) are interpreted as being a function of the increased deposition at those sites in recent times, compared with the deposition ca.1945. This is also evident in fig. 4.13.

Regional variations in chemical concentrations are noted within the surface sample (0-2.5cm). Mean concentrations for the northern Scandinavian sites are substantially less than those of the southern Finnish sites in all elements. Furthermore, the values given for the former group in Table 4.5 for the respective elements are within the regional limits quoted in published sources (eg. Rühling & Tyler, 1973; Tolonen, 1974; Pakarinen & Tolonen, 1976; Pakarinen, 1978, 1981a). Concentrations of elements within surface samples of the southern Finnish sites are up to 1.5 times smaller than the equivalents in the same published sources. This has been interpreted partly as a function of the decreases within the deposition within heavy metals (Rühling & Tyler, 1984), and partly due to the

differences in metal retention capacity between the mosses Hylocomium splendens and Sphagnum fuscum.

The decreasing values from south to north are also evident within the deposition estimates. When the mean values for all sites in northern Scandinavia, with the exception of Liikanen, are compared with the mean value from Kaurastensuo and Laaviosuo, a decrease in SIRM, iron, lead and zinc is again obvious. This is in agreement with the general trend of deposition over Finland, noted in published sources (eg. Pakarinen, 1978; Pakarinen et al., 1983). The actual deposition rates calculated are however, consistently lower than those quoted by the two published sources (op. cit.) most probably due to differences in initial concentrations and also the difference in sampling intervals, for example, 0-1 years growth (Pakarinen, op. cit.) compared with 0-7.1±5.31 years growth used in this chapter.

The influence of site specific factors leading to anomalously high SIRM and chemical concentrations must always be considered. The two prime examples are Varrassuo, in the south of Finland, and Liikanen in the north. The influence of these two sites in regional trends has been noted in section 4.6 and where possible the values of these sites have been ignored in the calculation of regional mean values. The effect of the anomalous sites upon the mean values for a given region is most noticeable in southern Finland where the mean difference between the means calculated with and without Varrassuo may be seen in Table 4.6. The influence of Varrassuo is primarily a function of the number of sites available for the calculation of the mean for southern Finland. The smaller the number of sites the greater the influence. In southern Finland only three sites with any recent chronologies were available.

## 5. Two Further Scandinavian Sites

### 5.1 Introduction

Having focussed attention almost entirely on Finnish mires, the two remaining sites are located in northwest Scandinavia (Mo-I-Rana) and southwest Scandinavia (Draved Moss). In terms of site location and proximity to major industrial sources, it might be expected that Draved Moss in southern Denmark will receive a greater contribution of anthropogenic deposition in comparison with the 'remote' site, Mo-I-Rana in northern Norway. Unlike the two previous chapters, emphasis is placed on the magnetic measurements and a number of supportive techniques outlined below.

In addition to the techniques used in previous chapters emphasis is placed on the following two supportive techniques. Magnetic particle extracts from the peat samples have been prepared and examined by Scanning Electron Microscopy (SEM). The method used, is outlined in sub-section 5.2.1. For the Mo-I-Rana site, samples of the local bedrock, a garnet mica-schist, are examined by X-Ray Diffraction (XRD) techniques outlined in sub-section 5.2.2. Finally, at Draved Moss a 210-lead ($^{210}Pb$) profile has been determined from a hollow core and is compared with results published by Aaby et al. (1979). A $^{210}Pb$ profile is also presented for Mo-I-Rana in sub-section 5.5.6.

#### 5.1.1 Draved Moss

The raised bog, Draved Moss (55°02'N 08°57'E), lies 3km south of Løgumkloster and 10km north of Tønder in southwest Jutland at a distance of about 20km from the North Sea and an altitude of 19.6m.a.s.l.. Geologically the bog is located on a 'hill island' which is covered by aeolian sands blown up from the surrounding outwash plains in late-glacial times (Andersen, 1966). The original area of the bog was approximately 500

hectares (fig. 5.1). Peat cutting has occurred in the marginal areas for centuries, although this expanded toward the centre of the bog plane at the beginning of the Twentieth Century (Hansen, 1966). By 1957 only 5 hectares of the central bog plane remained as virgin peatland. This figure had declined to 3.5 hectares by 1961 which is approximately the same area remaining today due to a preservation order by the Danish government in the 1960's.

South of the bog plane lies a rectangular 'Russerfennen' of about 7.5 hectares in area. During the First World War (about 1917) the occupying German forces attempted to cultivate the peat soil with the help of Russian prisoners-of-war. Drainage ditches were initiated in this part of the bog although this was not particularly successful. Grasses and Trifolium were sown and for a short while, according to local sources, cattle were grazed on the area. As a result of the disturbance many new species were introduced to the bog surface within the 'Russerfennen'. Only 6 of the 34 phanerogams and pteridophytes could possibly have originated from the former bog vegetation, these include Empetrum nigrum, Molinia caerulea and Erica tetralix (Hansen, op. cit.).

At the eastern border of the bog, close to Draved Skov (fig. 5.1), a small part of the original lagg is still intact. The altitude here is about 17m.a.s.l. indicating a quite substantial rise from the lagg to the ombrotrophic crown, despite some shrinkage due to drainage from peat cutting. Some 52 phanerogam and pteridophyte species are known to be preserved in this area, along with 38 different bryophyte species (Hansen, op. cit.). The latter includes 10 species of Sphagnum moss including pool-forming and hummock-forming species.

According to Hansen (op. cit.) the central bog plane of Draved Kongsmosse represents a typical west-Danish raised bog, the only apparent

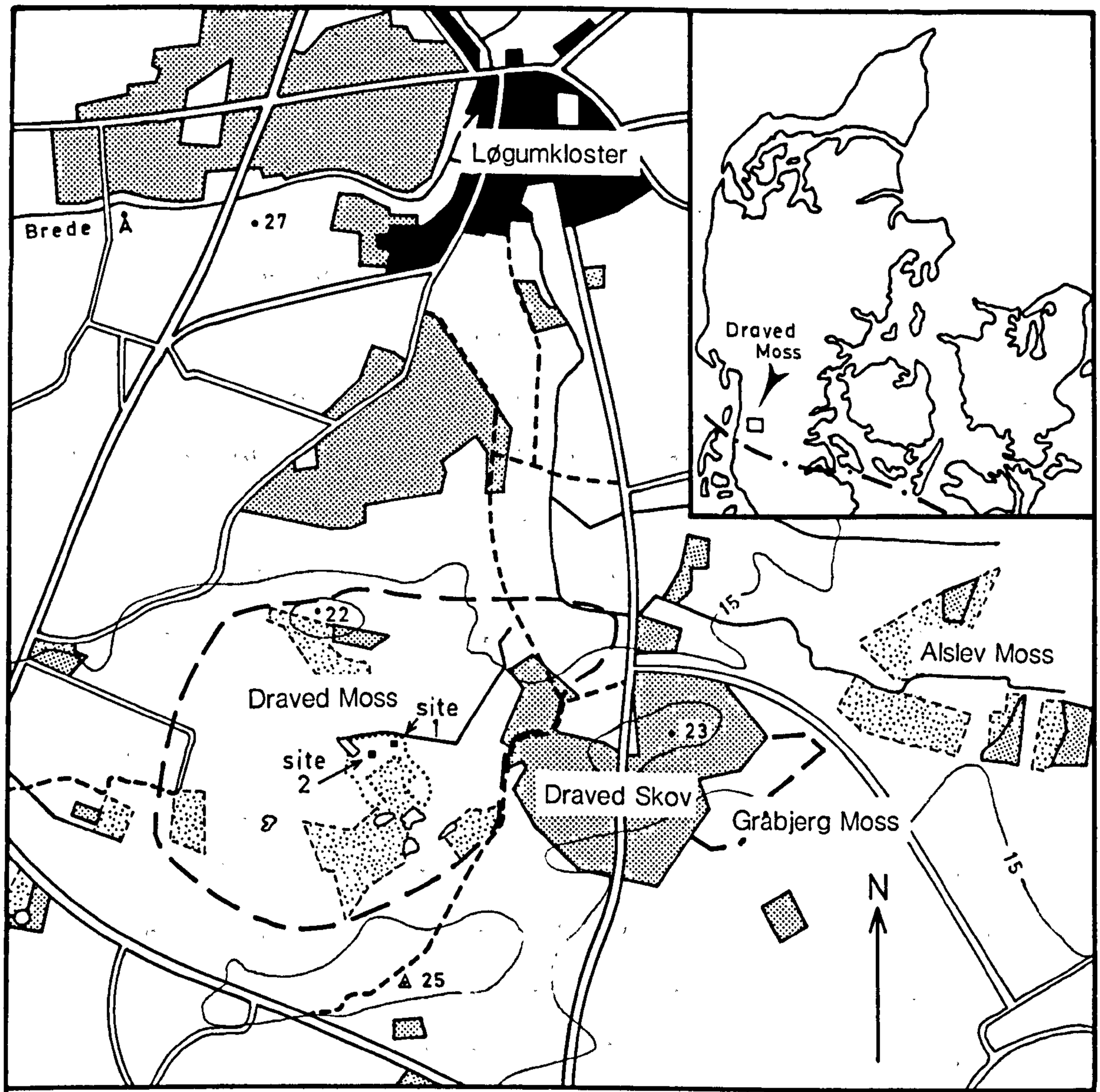


**Figure 5.1** Location of Draved Moss, southern Denmark

example in that part of the country. In 1966 only 10 sociations were evident on the bog, compared with 164 found on nearby Komosse (Hansen, op. cit.). These are summarised in fig. 5.2.

The literature pertaining to Draved is centred almost exclusively on the work of the Geological Survey of Denmark. In 1959 a large section was cut into the central part of the bog for macroscopic analyses. In 1973 a further section was cut in order to determine the rate of humification and of peat formation. Aaby & Tauber (1975) calculated accumulation rates during the past 6500 years to be of the order of 0.16-0.8mm.yr$^{-1}$ based on 59 $C^{14}$ dates. Cyclic climatic variations with a periodicity of ca.260 years were also inferred, based on the relationship between degree of humification and humidity at the time of peat formation (Aaby & Tauber, 1976). Aaby & Jacobsen (1979) attempted a reconstruction of palaeobotanical change over the past millenium. The extinction of a S. imbricatum sociation dominant during the Middle Ages is closely related to the formation of hummock-hollow microtopographical features. The storage of some trace elements (A.D. 1300-1973) is also calculated. A further study by Aaby et al. (1979) attempted to calculate the recent lead deposition into Draved Moss, based on $^{210}Pb$ dating of a hollow core. These results are discussed more fully within the context of the present study in sub-section 5.3.6.

5.1.2 Mo-I-Rana

Mo-I-Rana (66°20'N 13°40'E) lies about 30km south of the arctic circle between the small icecaps of Svartissen, to the north and Okstindan, to the south (fig. 5.3). The area around Mo-I-Rana comprises mainly mica-schists, phyllites and shales, including limestones, dolomites, quartzites and sandstones of Cambrian to Mid-Silurian age, rich in iron ore deposits. These ore deposits are centred on Ørtfjell in the Dunderland

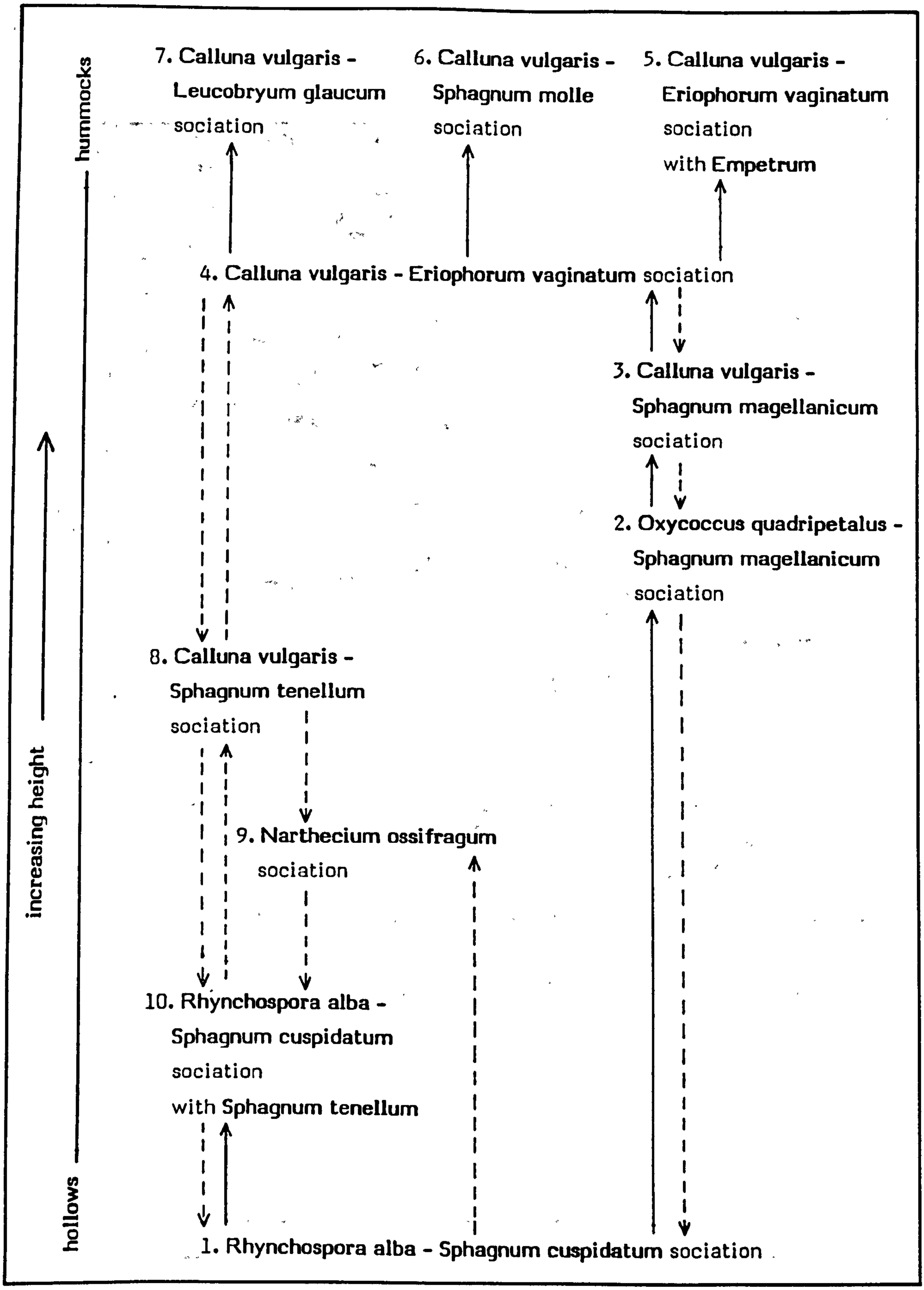


**Figure 5.2** Zonation- and succession diagram for Draved Moss. The succession shown by full-drawn arrows is almost certain. Broken arrows show possible tendencies of succession (adapted from Hansen, 1966).

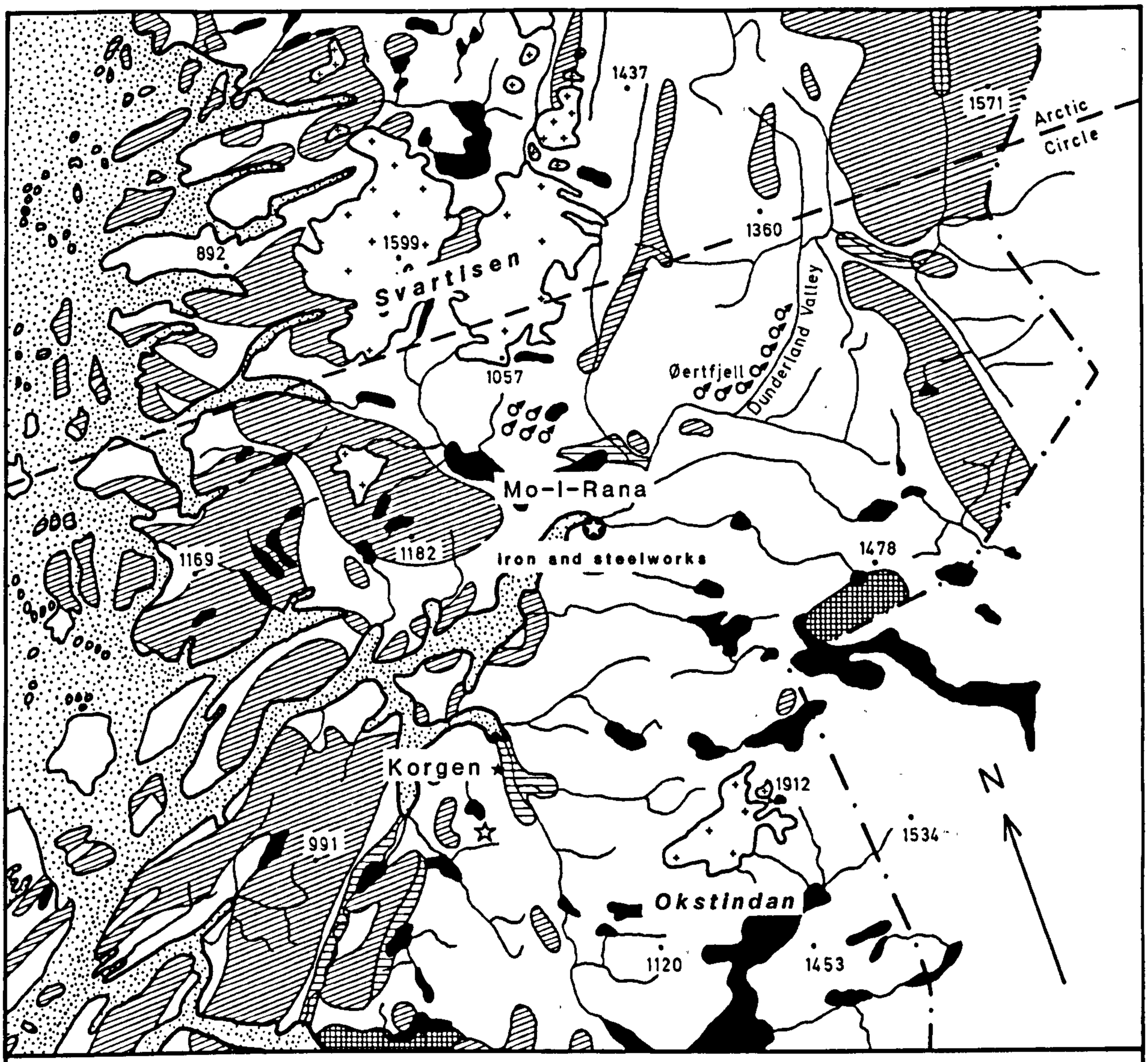


**Figure 5.3** Geology of Hemnes and Rana, northern Norway. With Mo-I-Rana peat core location.

Valley, about 30km northeast of Mo-I-Rana. The iron ore deposits in Rana were discovered, and have been partially mined, since the beginning of the Seventeenth Century. At the turn of the century the British Dunderland Iron Ore Company Ltd. (DIOC) began mining operations. Production began in 1906 and had three short operational periods before closing down in 1939.

In 1947 the Norwegian government purchased equipment and mineral rights from DIOC and formed AS Norsk Jernverk. Iron production began in 1955. The mining division (Rana Gruber) was purchased in 1961 and normal open cast mining operations were started up in 1964. The history of AS Norsk Jernverk is summarised in Table 5.1.

The ore in the Dunderland Valley contains about 37 per cent iron, a mixture of haematite and magnetite. The ore is ground to a concentrate (ca.68% iron) at Gullsmedvik 35km to the southwest. The concentrate is then processed into sinter and pellets at the iron and steel works in Mo-I-Rana. In 1982 the production of iron concentrate was in the region of 1,115,000 tons, inclusive of sinter, pellets and pig iron.

The peat core (0-55cm) from this region was taken from a site (66°04'N 13°40'E) some 40km southwest of the town of Mo-I-Rana, in the approximate direction of the prevailing summer winds (northwesterly). Using the mineral magnetic measurements it was hoped that the impact of the mining and production of iron ore in the region could be assessed in the context of local particulate deposition onto surrounding areas. In order to assess the impact of such deposition, samples of the local bedrock, a garnet mica-shist, were taken and analysed (sub-section 5.4.4) to assess the contribution of the local weathering product to the magnetic record.

**Table 5.1** History of AS Norsk Jernverk

| | | |
|---|---|---|
| **1946:** | 10 July: | Parliament adopts the resolution to build Jernverket in Mo-I-Rana |
| **1949:** | | Norsk Jernverk takes over Blikkvalseverket in Bergen |
| **1955:** | | Production at Jernverket begins: |
| | 19 April: | First charge in the furnace |
| | 22 April: | Electric current to the first pig iron furnace |
| | 16 May: | First tap of the pig iron furnace |
| | 10 June: | The first Bessemer converter starts in the steelworks |
| **1961:** | | LD-converters replace the Bessemer converters. Norsk Jernverk takes over Rana Gruber |
| **1962:** | | New cold rolling mill at Blikkvalseverket |
| **1964:** | | Ordinary operations begin at Rana Gruber |
| **1974:** | | Norsk Jernverk takes over AS Norsk Ståltau. The machining plant for ship sections becomes operational |
| **1978:** | | AS Norsk Ståltau's new production plant at Lade near Trondheim becomes operational |
| **1981:** | | The Ørtfjell open cast mine is opened |
| **1982:** | | A new ore dressing plant becomes operational. A new continuous casting machine for billets in the steelworks and a modernised bar and rod mill are made operational during the summer |
| **1983:** | | Ørtfjell open cast mine in full operation. New crusher is operational |

**Source:** AS Norsk Jernverk Company Information (1983)

## 5.2 Methods

### 5.2.1 Scanning Electron Microscopy

The micrographs obtained by Scanning Electron Microscopy (SEM) comprise the magnetic extracts from selected slice samples at Draved Moss and Mo-I-Rana. In addition, micrographs are also presented from the extract of the garnet mica-schist sample. The micrographs were obtained using a Philips 501 scanning electron microscope with FP4 film.

To extract the magnetic phase of a given sample, homogenised peat (about 1.0g) was placed in methanol and dispersed ultrasonically using a few drops of Coulter dispersant. The strongly magnetic phases were then removed from suspension using a large conventional horseshoe magnetic with an approximate field of 300mT. The efficiency of extraction is dependent upon the field gradient (Jones, 1985). It is important to note that any antiferromagnetic component (e.g. haematite) present as individual grains are not likely to be extracted by this method. In samples where the ferrimagnetic and antiferromagnetic components are found together in the same particle, some extraction of the antiferromagnetic would be achieved. Once extracted, sub-samples of the strongly magnetic extract were pipetted onto a carbon stub. The stub is subsequently coated in a thin gold layer, approximately 200Å thick, which improves the quality of the micrograph by reducing the tendency of the sample to charge under the electron beam.

### 5.2.2 X-Ray Diffraction

The garnet mica-schist sample used in sub-section 5.4.4 was analysed by X-Ray diffraction (XRD), using a Siemens D500 X-Ray diffractometer. The diffractometer follows the conventional Bragg theories of diffraction (cf. Milner, 1962), with the sample being rotated through 2° to 46° to maintain a constant $\theta$ setting. The garnet mica-schist samples were

rotated at either 1° 2θ/minute or 2° 2θ/minute (sub-section 5.4.4) using copper K-alpha radiation at $2x10^2$ counts/minute, using a power source of 20kv 6mA. It is important to note that the addition of a monochromator allows the analysis of iron-bearing minerals. Since the monochromator reduces the effect of scatter due to the iron minerals fluorescing.

The samples were prepared by crushing to a powder matrix and mounting on aluminium unorientated mounts. The powder has to be packed tightly enough to maintain its structure within the mount, but loosely enough to avoid any orientation of the mineral grains.

5.2.3 Chronology

There is a lack of any recent chronological control on the samples from Draved Moss and Mo-I-Rana. Aaby & Jacobsen (op. cit.) used a series of 59 $C^{14}$ dates from their peat sections at Draved Moss. However, the lack of any precise location details and a reference surface (cf. Chapter 3, sub- section 3.2.1) precludes the possibility of using these dates. The nature of the cores (ie. surface cores, less than 55cm long) also precludes the use of $C^{14}$ dates due to the dilution of $^{14}CO_2$ in the atmosphere by increased fossil fuel burning, a phenomenon noted by Suess (1955). Aaby et al. (op. cit.) attempted to date recent peats by $^{210}Pb$ dating, reporting the results from a hollow core taken at Draved Moss.

Using the recently developed short-lived radioisotope dating facility in the Department of Physics at Liverpool University, similar $^{210}Pb$ chronologies have been attempted on the hollow core, DMHol2 (sub-section 5.3.5) and the Mo-I-Rana peat core (sub-section 5.5.6). Ashed peat samples are measured on a low-background planar hyper-pure germanium detector and computer processing unit. Age-depth curves are based on the constant rate of supply model (CRS) described in Appleby & Oldfield (1978) and Oldfield et al. (1979) summarised in sub-section 5.4.1. As the dating

procedure is on a relative timescale, the curve is fixed by means of the sampling date, in this case, 1983. The rationale for using hollow cores is based on results presented by Oldfield et al. (op. cit.). The accumulation of up to 4 times as much **unsupported** $^{210}Pb$ in pools as opposed to hummocks is attributed to significant amounts of downward mobility of **unsupported** $^{210}Pb$ within the hummock profile. Evidence for downward mobility of total lead in hummock cores is available directly from Pakarinen & Tolonen (1977a) and this study (Chapter 3, sub-section 3.9.2), and indirectly from Aaby et al. (op. cit.).

The samples are ashed in order to obtain the maximum pre-ashed weight of the peat sample being measured. An optimum temperature of 450°C for about three hours is used to obtain a complete combustion without the loss of significant amounts of lead or radioisotopes by volatilisation.

## 5.3 Draved Moss

### 5.3.1 Core Location and Stratigraphy

The two coring sites on Draved Moss are marked in fig. 5.1. Site 1 is located on the northern edge of the remaining virgin bog plane. The hummock and hollow cores extruded were 26cm and 22.5cm long respectively. The variation in surface height (amplitude) between the two cores was 24cm and the distance between them, 30cm. The hummock core (DMHum1) was extracted from a Calluna vulgaris-Sphagnum magellanicum sociation with Empetrum (fig. 5.2). The adjacent hollow core (DMHol1) was extracted from a Rhynchospora alba-Sphagnum cuspidatum sociation with Sphagnum tenellum (fig. 5.2).

Site 2 is located in the centre of the remaining virgin peatland (fig. 5.1). The hummock and hollow cores extruded were 52cm and 47cm long

respectively. The variation in amplitude between the two cores was 22cm and the distance between them 45cm. The hummock core (DMHum2) was extracted from a Calluna vulgaris-Eriophorum vaginatum sociation (fig. 5.2), whilst the hollow core (DMHol2) was extracted from a Rhynchospora alba-S. cuspidatum sociation with S. tenellum. No data areavailable for the location of the water table at either site at the time of sampling.

Bulk density and ash residue profiles for the four cores are presented in fig. 5.4. Both cores from site 1 and DMHol2 from site 2 display a decrease from sub-surface maximum bulk density values towards the surface. In DMHum2, the profile is essentially the same as the other three, with the exception of a small increase in value for the surface sample. The ash residue profiles all display a decrease from sub-surface peaks, predominantly 2.5-5cm, towards the surface. The maximum percentage values of the ash residues are high, ranging from 6.7% (DMHum1) to 9.3% (DMHum2). Sub-samples of the ashed peat from DMHum2 (2.5-5cm) and DMHol1 (7.5-10cm) were examined using a conventional pollen microscope (Reichert-Jung Microstar 110) at magnifications of 40/.66 and 100/1.25. The microscopic analyses revealed two main observations. First, in both sub-samples the presence of perfectly spherical opaque particles was noticed. The size range of these particles was predominantly around 10µm. Second, the sub-samples comprised mainly transluscent/semi-opaque quartz-silica grains in the size range 50-100µm. These grains were usually square or rectangular shaped and displayed sub-rounded edges.

Water content profiles for the four cores are presented in fig. 5.5. The two hummock profiles display a decrease towards the surface from peak values of 90-91%. The surface slice displays the minimum values in the respective profiles, 77% (DMHum1) and 83% (DMHum2). The two hollow cores also display decreases in values towards the surface with a

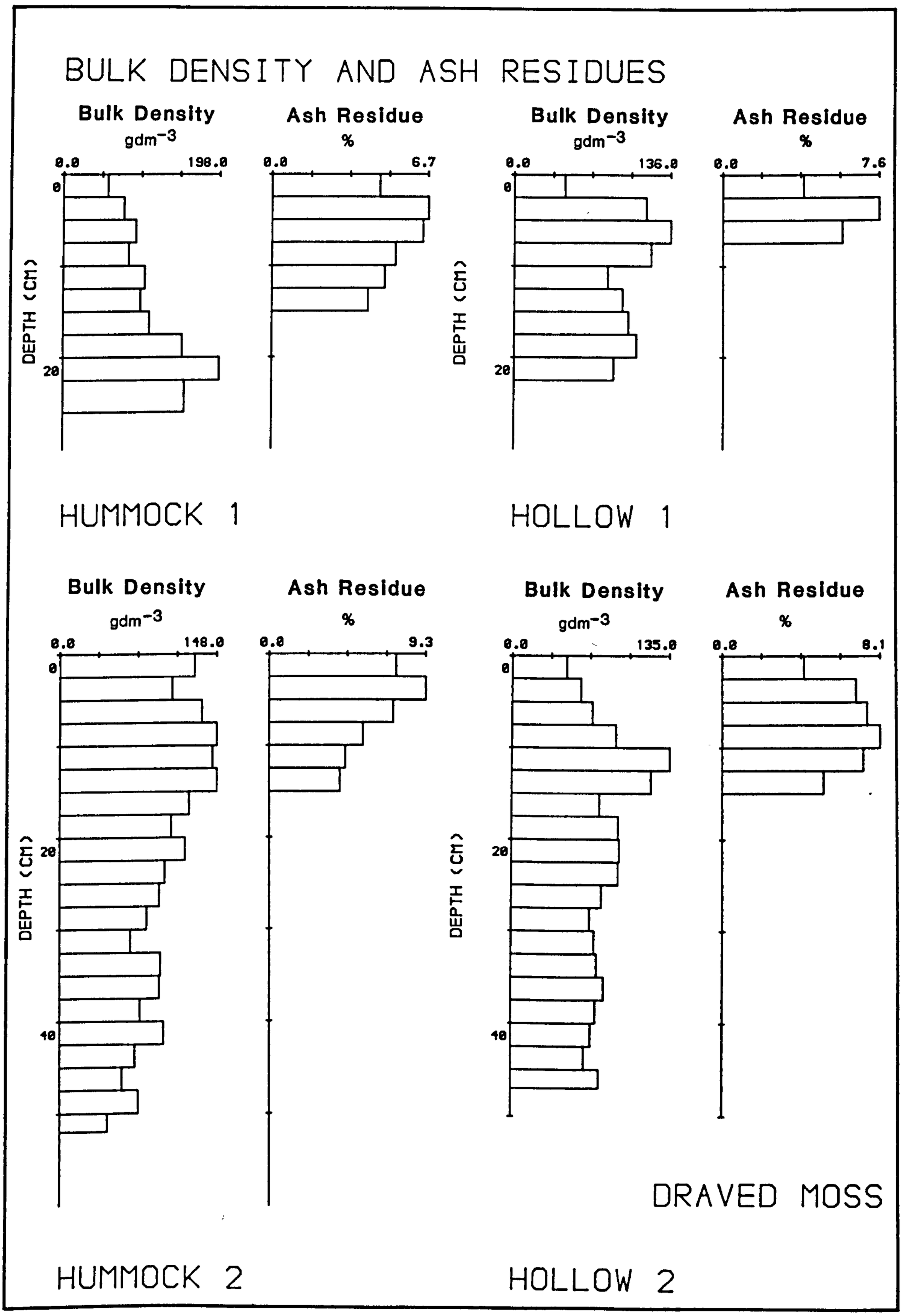


**Figure 5.4** Bulk density and ash residues of cores from Draved Moss

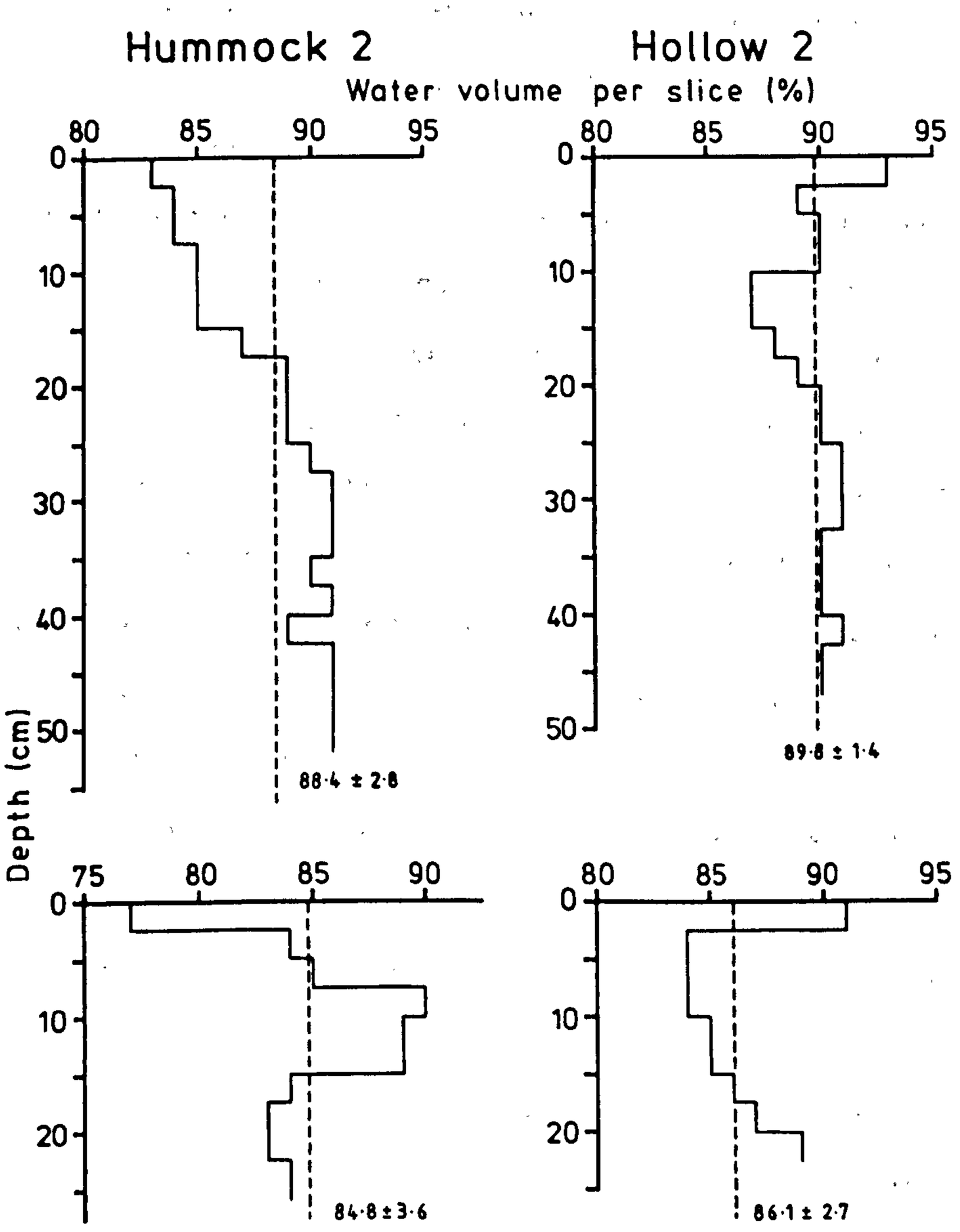


**Figure 5.5** Water content of cores from Draved Moss. With the mean and standard deviation for each core.

sharp increase within the topmost sample, representing the maximum value for each respective core, 91.5% (DMHol1) and 93.5% (DMHol2). The mean values for each core were slightly lower in the hummocks, which also displayed the largest standard deviations as might be expected.

The cumulative dry mass against depth curves for Draved Moss are presented in fig. 5.6. At site 1 the hummock core (DMHum1) curve is noticeably concave between 0-22.5cm. In contrast the hollow core for site 1 (DMHol1) is slightly convex. Between 0-15cm the curve is slightly concave, whilst between 15-52cm it is markedly convex. At site 2 the hummock core curve (DMHum2) is concavo-convex. Between 0-15cm the curve is slightly concave, whilst between 15-52cm it is markedly convex. The hollow core curve (DMHol2) appears to display a similar shape although the concavity (0-15cm) and convexity (15-47cm) are far less pronounced. Contrasts between the two sites are limited slightly by the difference in length of the respective cores from each site. However, between 0-20cm the two hummock cores display similar concave curve shapes, whilst the hollow cores display contrasting curve shapes. The rate of peat accumulation throughout the top 20cm at site 1 is slowest in the hummock core, taken from the C. vulgaris-S. magellanicum sociation. In relative terms, this is denoted by a steeper gradient. The hummock core from site 2 (Calluna-Eriophorum sociation) displays the shallowest gradient throughout its length and therefore the fastest rate of peat accumulation of all four cores.

### 5.3.2 Chemical Results

Five elements: iron, lead, copper, zinc and nickel have been determined for each of the cores at Draved Moss. The profiles are presented in figs. 5.7-5.10 for DMHum1, DMHol1, DMHum2 and DMHol2 respectively.

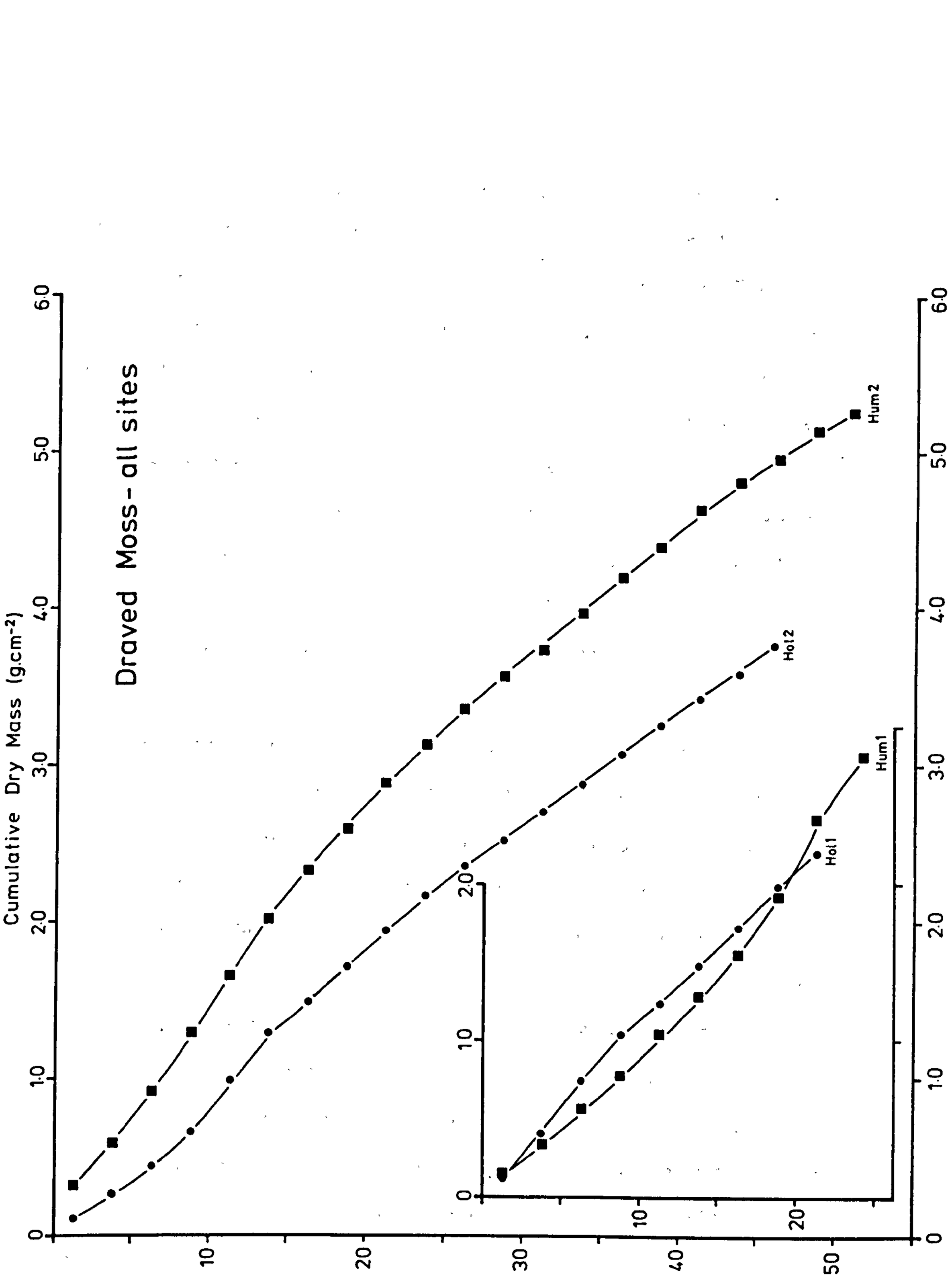


**Figure 5.6** Cumulative dry mass curves for Draved Moss

The iron profiles for site 1 in fig. 5.7 (DMHum1) and fig. 5.8 (DMHol1) both display a contrast between low concentrations at the base of the core and higher concentrations near the surface. The low concentrations for both cores are between 371$\mu g.g^{-1}$ and 797$\mu g.g^{-1}$. In DMHum1 the inflection point is at 10cm with an increase of over 5 times. In DMHol1 the inflection point is closer to the surface, at 5cm, with an increase of just over 3 times. In both cases the concentrations decrease from the peak concentration towards the surface, linearly in the case of DMHum1. The peak concentration of iron, as well as being 5cm lower down in the hummock, is also 3.5 times higher (4285$\mu g.g^{-1}$). The surface concentration is, however, higher in the hollow, 1038$\mu g.g^{-1}$ compared with 883$\mu g.g^{-1}$.

The lead profiles in both cores display sub-surface peaks, at 5-7.5cm in DMHum1 and 2.5-5cm in DMHol1. Below these depths the concentrations decrease in an approximately linear manner in both cores. The maximum slice concentration of lead is 1.6 times higher in the hummock core, and the surface sample 1.35 times higher. The copper profiles both display increasing concentrations towards the surface culminating in a sub-surface peak in the hollow core (2.5-5cm) and a surface peak in the hummock. The concentrations in the hummock start to increase at 15-17.5cm in contrast to the hollow (5-7.5cm). Maximum copper concentrations are 1.8 times higher in the hummock, and 1.9 times higher in the surface sample. The zinc profiles display some similarity between the hummock and the hollow and also with the copper profiles. Concentrations increase in an approximately linear manner, toward a sub-surface peak in the hummock (2.5-5cm) and a surface peak in the hollow. As with all the other elements, the peak value is slightly higher in the hummock compared with the hollow.

The nickel profiles are contrasted mainly by detectable and undetectable

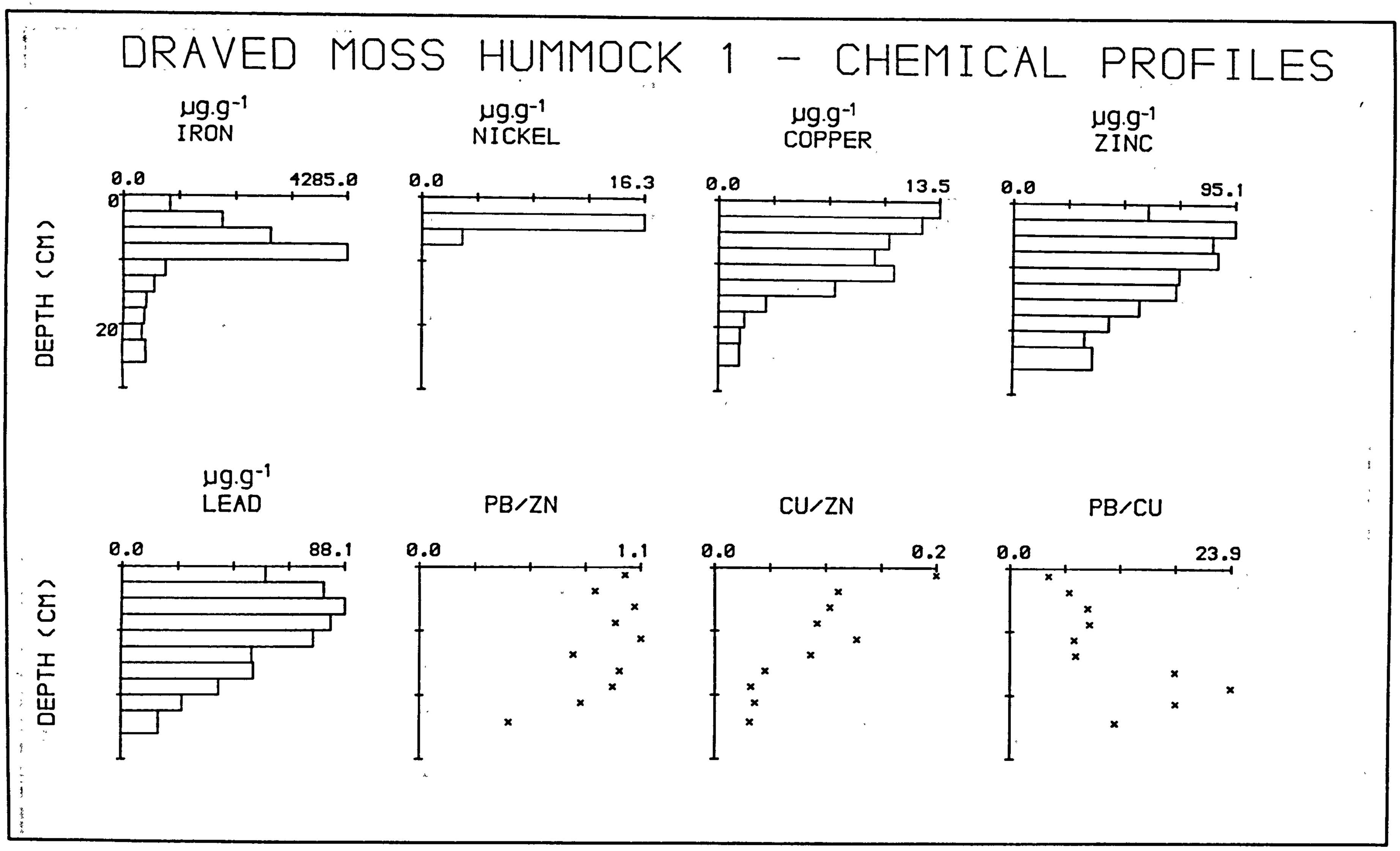


**Figure 5.7** Chemical profiles for DMHum1, Draved Moss

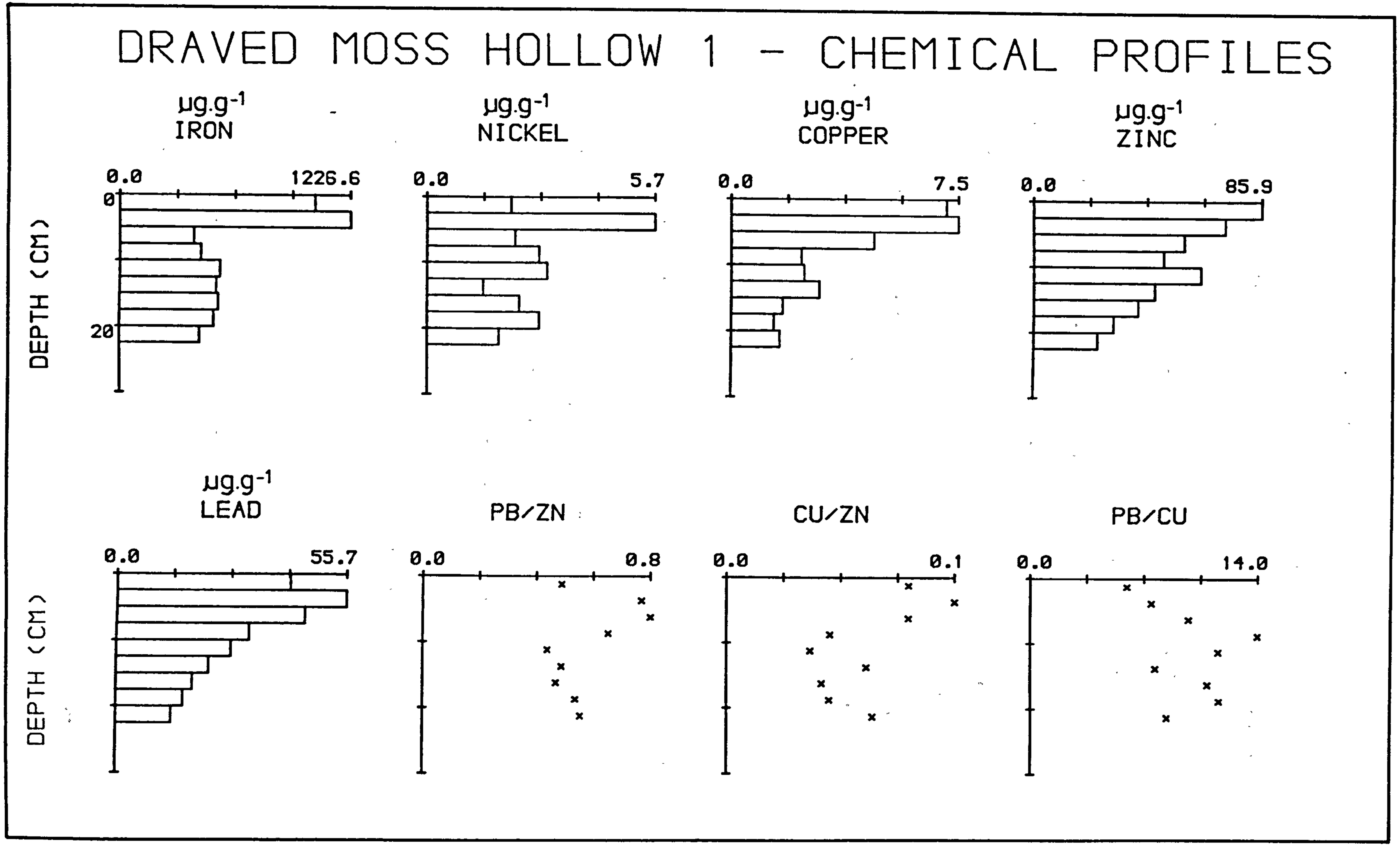


**Figure 5.8** Chemical profiles for DMHol1, Draved Moss

concentrations. In the hummock core there are only two detectable concentrations, between 2.5cm and 7.5cm. This is in contrast to the hollow profile which displays low but consistently detectable concentrations.

The inter-metal ratios presented for site 1 are for lead and copper normalised to zinc and Pb/Cu (figs. 5.7 and 5.8). In both cores the ratios distinguish between two sets of samples within the profiles: upper profile samples and lower profile samples. In the hummock, both the Cu/Zn and Pb/Cu profiles divide the samples into two groups: those above 15cm (relatively larger Cu/Zn values and lower Pb/Cu values), and those below 15cm (lower Cu/Zn values and higher Pb/Cu values). In the hollow core, all three ratios distinguish between samples above 10cm with relatively high Pb/Zn and Cu/Zn values and decreasing Pb/Cu values, and samples below 10cm with low Pb/Zn and Cu/Zn values and intermediate Pb/Cu values.

At site 2 the iron profiles for DMHum2 (fig. 5.9) and DMHol2 (fig. 5.10) display similar, low concentrations below 10cm (192-520$\mu g.g^{-1}$). Above 10cm in both cores the concentrations increase exponentially to a peak of 2265$\mu g.g^{-1}$ between 2.5-7.5cm in DMHum2 and 3277$\mu g.g^{-1}$ at 2.5-5cm in DMHol2. The peak iron concentration in the hollow is 1.45 times higher than in the hummock. The surface concentrations of iron are the reverse, being 1.14 times higher in the hummock.

The lead profiles at site 2 display similar trends throughout their length, as with the iron profiles. Below 17.5cm the lead concentration in both cores is between 16.9$\mu g.g^{-1}$ and 7.4$\mu g.g^{-1}$. Above 17.5cm the lead concentrations increase in both cores in a linear manner to sub-surface peaks at 5-7.5cm (140$\mu g.g^{-1}$) in DMHol2 and at 2.5-5cm (116$\mu g.g^{-1}$) in DMHum2. The peak lead concentration is 1.2 times higher in the hollow core, and 1.3 times higher in the surface sample.

Both cores at site 2 display copper profiles with undetectable

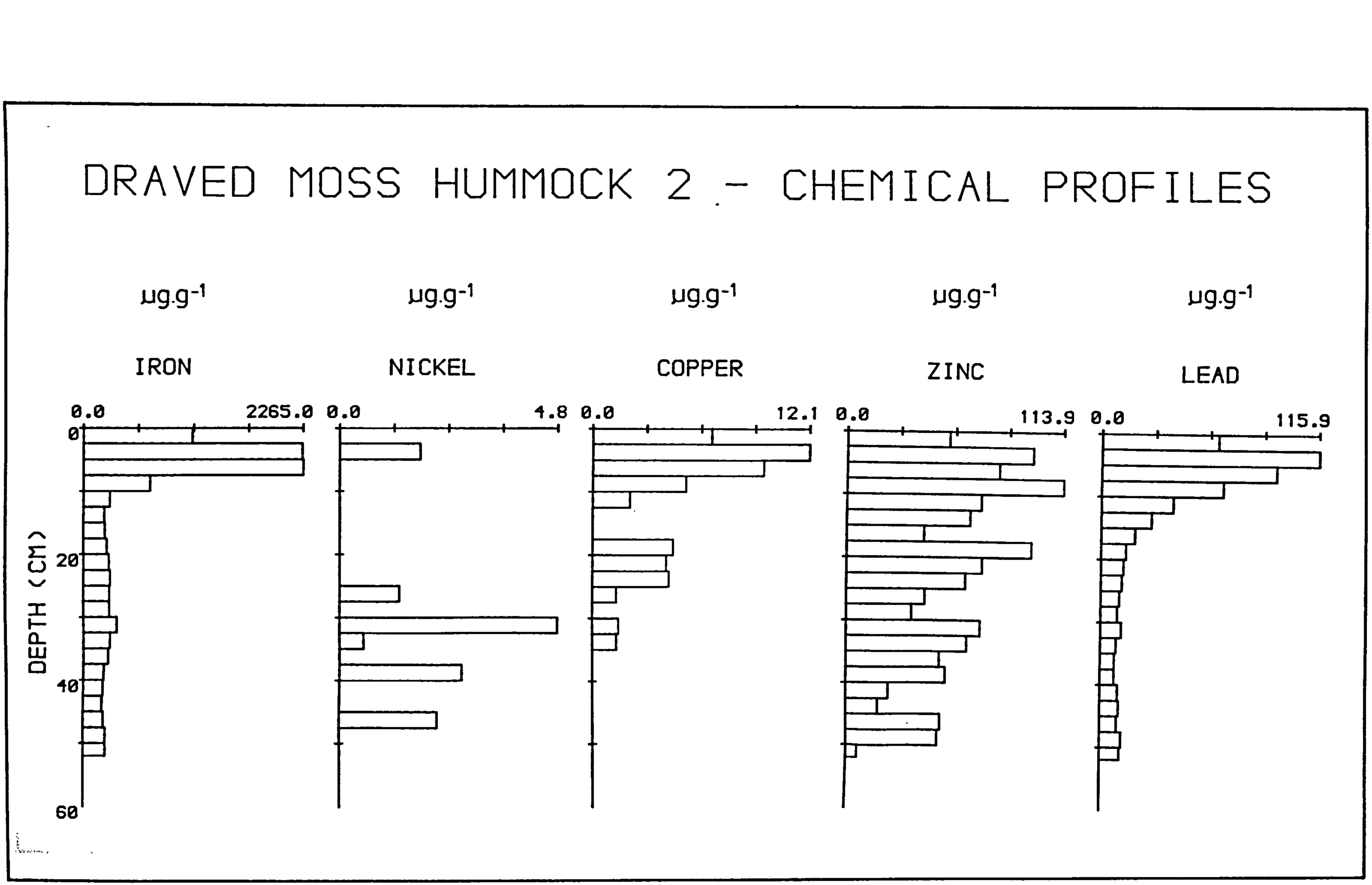


**Figure 5.9** Chemical profiles for DMHum2, Draved Moss

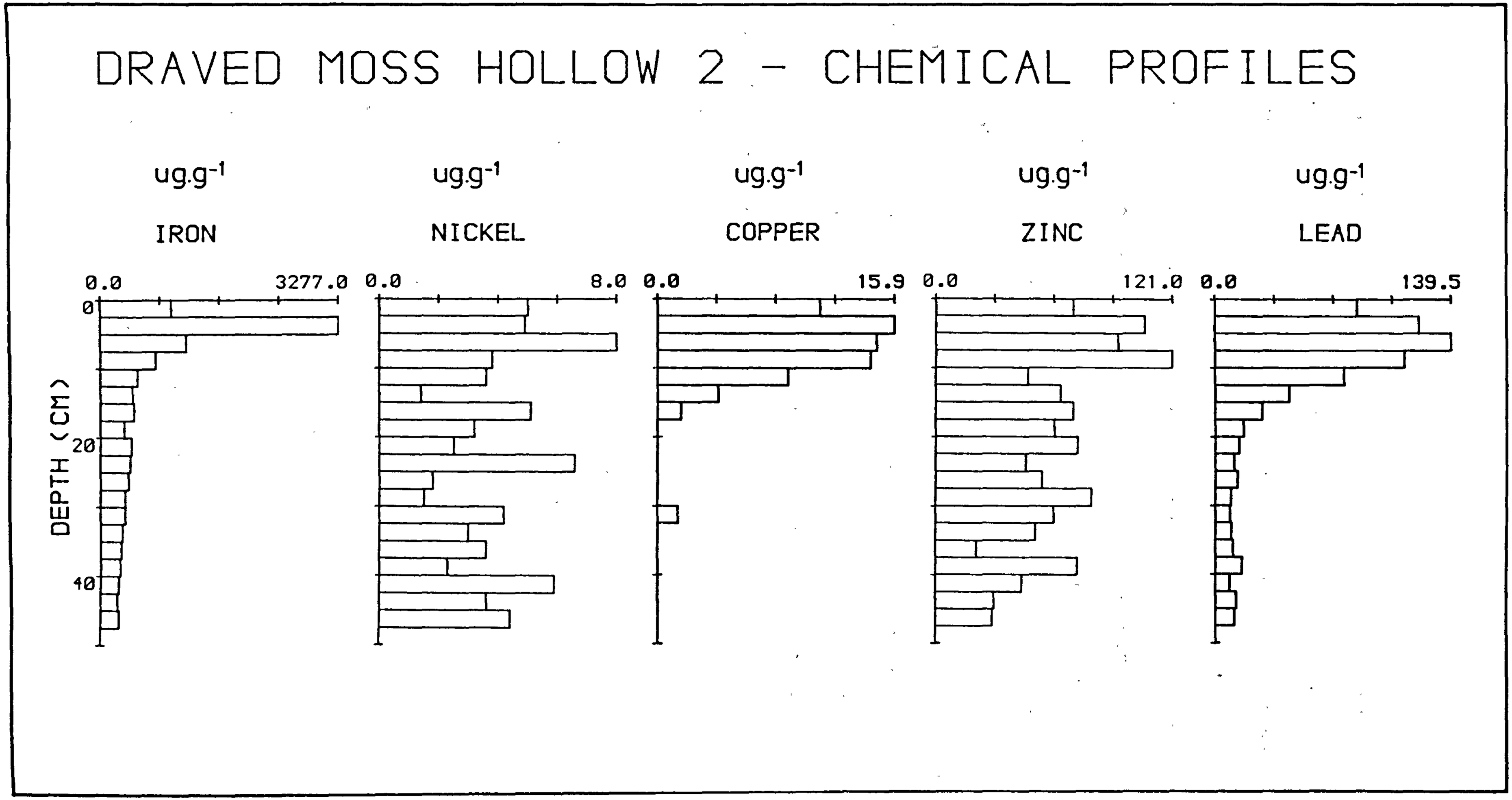


**Figure 5.10** Chemical profiles for DMHol2, Draved Moss

concentrations at lower depths. In the hummock core there are detectable concentrations between 35-17.5cm and above 12.5cm where values increase linearly to a sub-surface peak at 2.5-5cm (hummock and hollow). The peak copper concentration is 1.3 times higher in the hollow and the surface concentration is 1.7 times higher. The zinc concentrations do not appear to display any regular pattern throughout the profile, although there are several peaks and troughs at irregular intervals throughout both profiles. Within the top 10cm the pattern in the hummock core corresponds closely to that of the hollow. The peak concentration is at 5-7.5cm, being marginally higher in the hollow, 121$\mu g.g^{-1}$ (DMHol2) in contrast to 114$\mu g.g^{-1}$ (DMHum2). The suface concentration of zinc is 1.3 times higher in the hollow. The contrast between the hummock and hollow nickel profiles is again mainly one of presence and absence. The hummock profile comprises mainly undetectable amounts of nickel. This contrasts with the hollow profile which displays consistently detectable concentrations although there is no apparent regular pattern within the profile.

The inter-metal ratios Pb/Zn, Cu/Zn and Pb/Cu for site 2 are presented in fig. 5.11. In the hummock core several distinct steps are obvious in all three ratios. At 22.5-25cm there is an increase in the Cu/Zn and Pb/Cu ratios. An increase in the Pb/Zn ratio is noticeable at 15-17.5cm, which corresponds to decreases in the Cu/Zn and Pb/Cu profiles. All three ratios also appear to distinguish between the two samples at 7.5-12.5cm (increasing Pb/Zn and Cu/Zn, and decreasing Pb/Cu) and the samples above, up to the surface (relatively high Pb/Zn, Cu/Zn and low Pb/Cu). The hollow core displays similar trends in the Pb/Zn and Cu/Zn ratios above 20cm. The ratio values increase upwards towards the surface, corresponding to a decrease in the Pb/Cu ratio.

There are a number of inter-site variations within the chemical

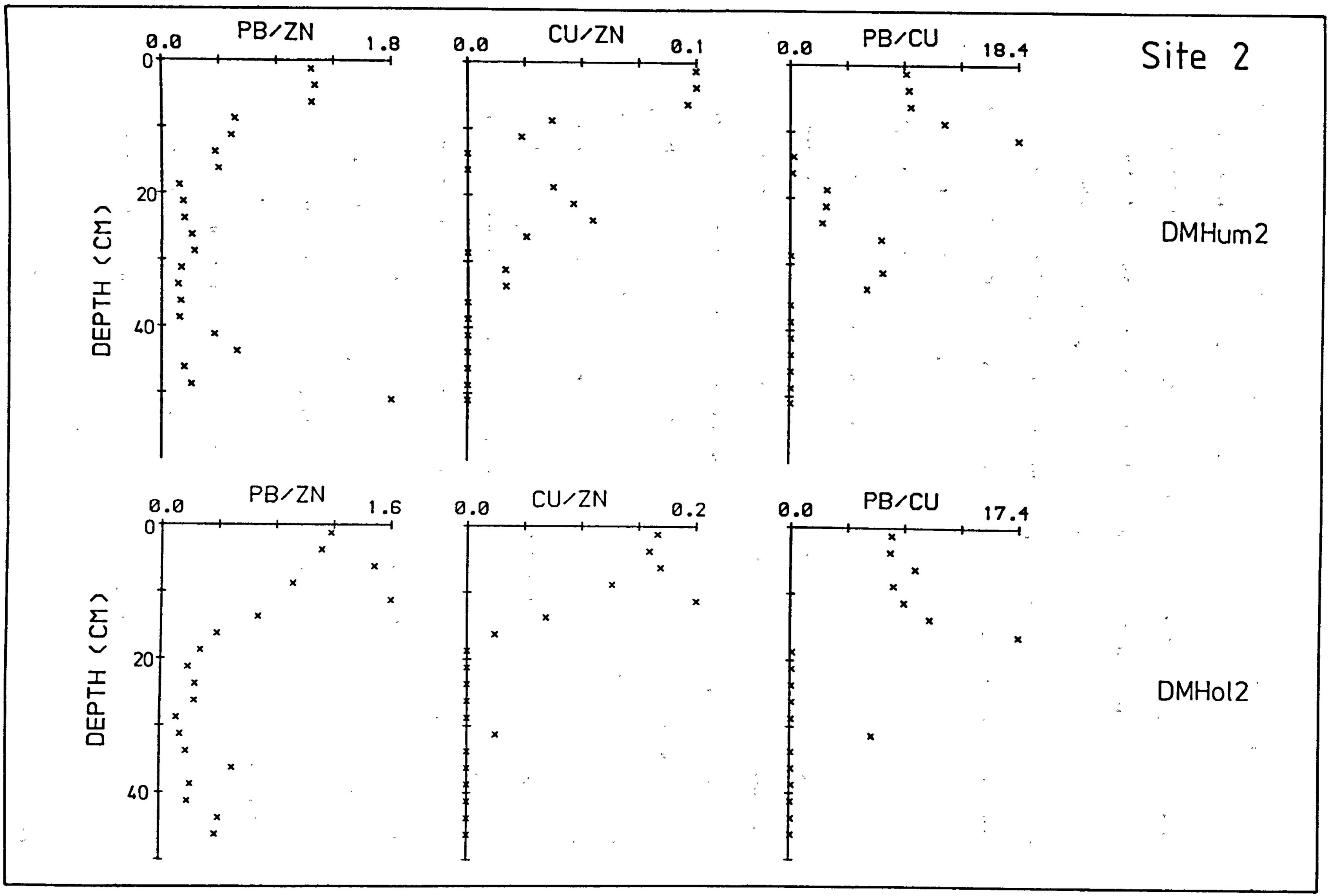


**Figure 5.11** Inter-metal ratios for site 2, Draved Moss

profiles from Draved Moss, mainly related to the peak and surface concentrations of the elements. Regarding the peak concentrations, an important point to note is that for site 1 peak iron, lead, copper and zinc concentrations are all higher in the hummock core. The reverse is true for site 2 where the hollow concentrations are consistently higher than the hummock. A similar pattern exists for surface concentrations of iron, lead and zinc, where the hollow values are higher at site 1, whilst the hummock values are higher at site 2.

5.3.3 Magnetic Results

The magnetic profiles for DMHum1 and DMHol1 (site 1) are presented in figs. 5.12 and 5.13 respectively. In addition to the concentration dependent parameters and interparametric ratios are two further types of magnetic measurement. The first, frequency dependent susceptibility ($X_{fd}$) is a percentage ratio of the difference between low frequency susceptibility ($X_{LF}$) and high frequency susceptibility ($X_{HF}$). Magnetic minerals spanning the superparamagnetic/stable single domain boundary are known to exhibit a time-dependent magnetic phenomenon termed **viscosity** (Chapter 1, sub-section 1.6.1). The frequency dependent susceptibility ratio ($X_{fd}$) is a more precise definition where the percentage value is cited. The second additional profile is $IRM_{300mT}$, the remanent magnetisation resulting from a field of 300mT as opposed to 850mT (SIRM). In both diagrams (figs. 5.12 and 5.13) the lower core samples displaying very low ARM and SIRM values have been plotted on an enlarged scale adjacent to the main ARM and SIRM profiles.

In the hummock core, DMHum1 (fig. 5.12), the take-off point is evident in all three concentration dependent parameters at 10cm below the surface. Below 10cm the X profile displays diamagnetic X values (see below) and low ARM and SIRM values. Above 10cm all three concentration

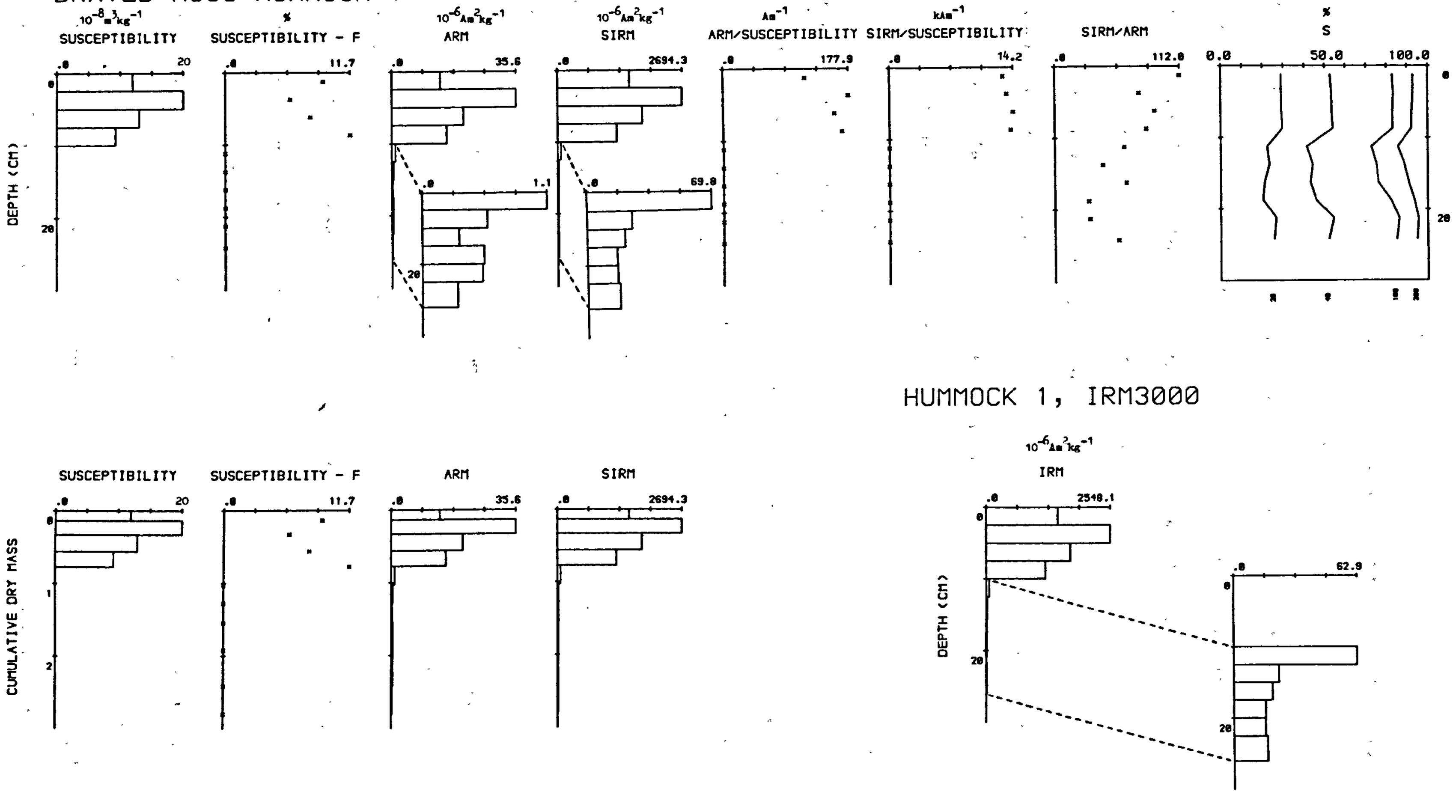


**Figure 5.12** Magnetic measurements for DMHum1, Draved Moss

dependent parameters increase linearly to a peak at 2.5-5cm below the surface. The peak SIRM value is 2694 $10^{-6}Am^2kg^{-1}$, decreasing to 1548 $10^{-6}Am^2kg^{-1}$ at the surface. This decrease within the surface sample value is also evident in the X and ARM profiles, corresponding to an increase in $X_{fd}$. The $IRM_{300mT}$ profile displays a similar pattern to the SIRM profile. All the $IRM_{300mT}$/SIRM ratios are between 0.9-0.96 indicating the proportion of remanent magnetisation aquired at $IRM_{300mT}$ compared with that acquired at the SIRM (850mT). The interparametric ratios, where available, display consistent values for post-take-off samples, with the exception of the surface sample which displays a decrease in the proportion of fine-grain minerals present (low ARM/X) and an increase in the proportion of coarse, multidomain minerals present (increased SIRM/ARM). The backfield ratios for the post-take-off samples show very little variation. One point to note regarding the backfield ratios is that the ratio $IRM_{-200mT}$/SIRM is plotted instead of $IRM_{-300mT}$/SIRM used in previous chapters. This is simply an attempt to improve the discriminatory power of the backfield ratios as a whole.

The hollow core DMHol1 (fig. 5.13), displays similar down-profile trends to the hummock, regarding the magnetic parameters. A take-off point at 5cm below the surface is clearly discernible within the concentration dependent parameters. Samples below 5cm display diamagnetic X values (see below) and low ARM and SIRM values. The X values change from negative (diamagnetic) below 5cm to positive above, $X_{fd}$ ratios are available for both the post-take-off samples. Above the take-off point SIRM values increase by a factor of 25 compared with 18 for the hummock core. All the concentration dependent parameters peak within the surface sample, in the case of SIRM the peak value is 680 $10^{-6}Am^2kg^{-1}$. The $IRM_{300mT}$/SIRM ratio discriminates between the three

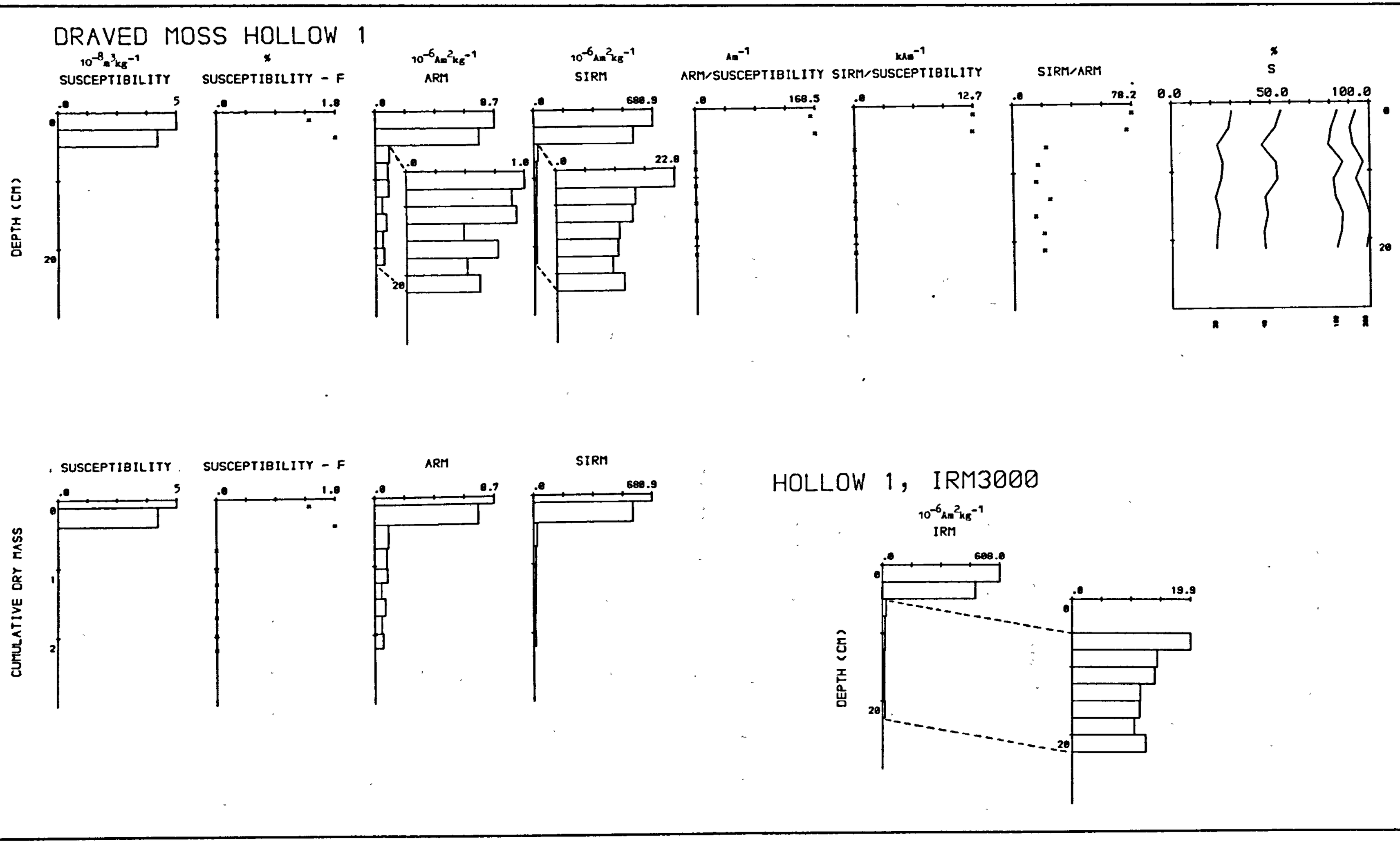


**Figure 5.13** Magnetic measurements for DMholl, Draved Moss

surface samples (0-7.5cm), with ratios of 0.85 to 0.89 and the remainder of the core samples with ratios of 0.94 to 0.97. The interparametric ratios all show a strong similarity between the two post-take-off samples. in the case of the SIRM/ARM ratio there is a 3.6 times increase from pre- to post-take-off samples. The backfield ratios again show little variation between the post-take-off samples.

A comparison of the magnetic profiles from the hummock and hollow cores at site 1 reveals that the take-off point, as at previous sites, is lower down the profile in the hummock core. The peak SIRM value in the hummock (2.5-5cm) is approximately 4 times higher than the hollow (0-2.5cm), whilst the surface sample in the hummock is 2.3 times higher. Both the hummock and the hollow cores display a 'hardness' feature within the backfield ratios immediately below the take-off point. In the hummock core this feature extends over 10cm compared with only 2.5cm, or one sample, in the hollow (5-7.5cm).

The coercivity of remanence curves for DMHum1 and DMHol1 are presented in figs. 5.14 and 5.15. The coercivity of remanence curves for the top 10cm of DMHum1 show very little variation, with consistent $(B_0)_{CR}$ values (37-39mT). These are in contrast to the wide range of curve shapes for samples below 10cm, evident in the wide range of $(B_0)_{CR}$ values (37-51mT). The 'hardness' feature mentioned above is also evident within the coercivity curves for samples between 10cm and 20cm, with $(B_0)_{CR}$ values between 43-51mT. The coercivity of remanence curves for DMHol1 (fig. 5.15) display less variance down-core in contrast to DMHum1. The $(B_0)_{CR}$ values vary between 37mT and 44mT.

The magnetic profiles for the hummock and hollow cores at site 2 are presented in figs. 5.16 and 5.17 respectively. In the hummock core (fig. 5.16) the concentration dependent parameters show the same distinctive

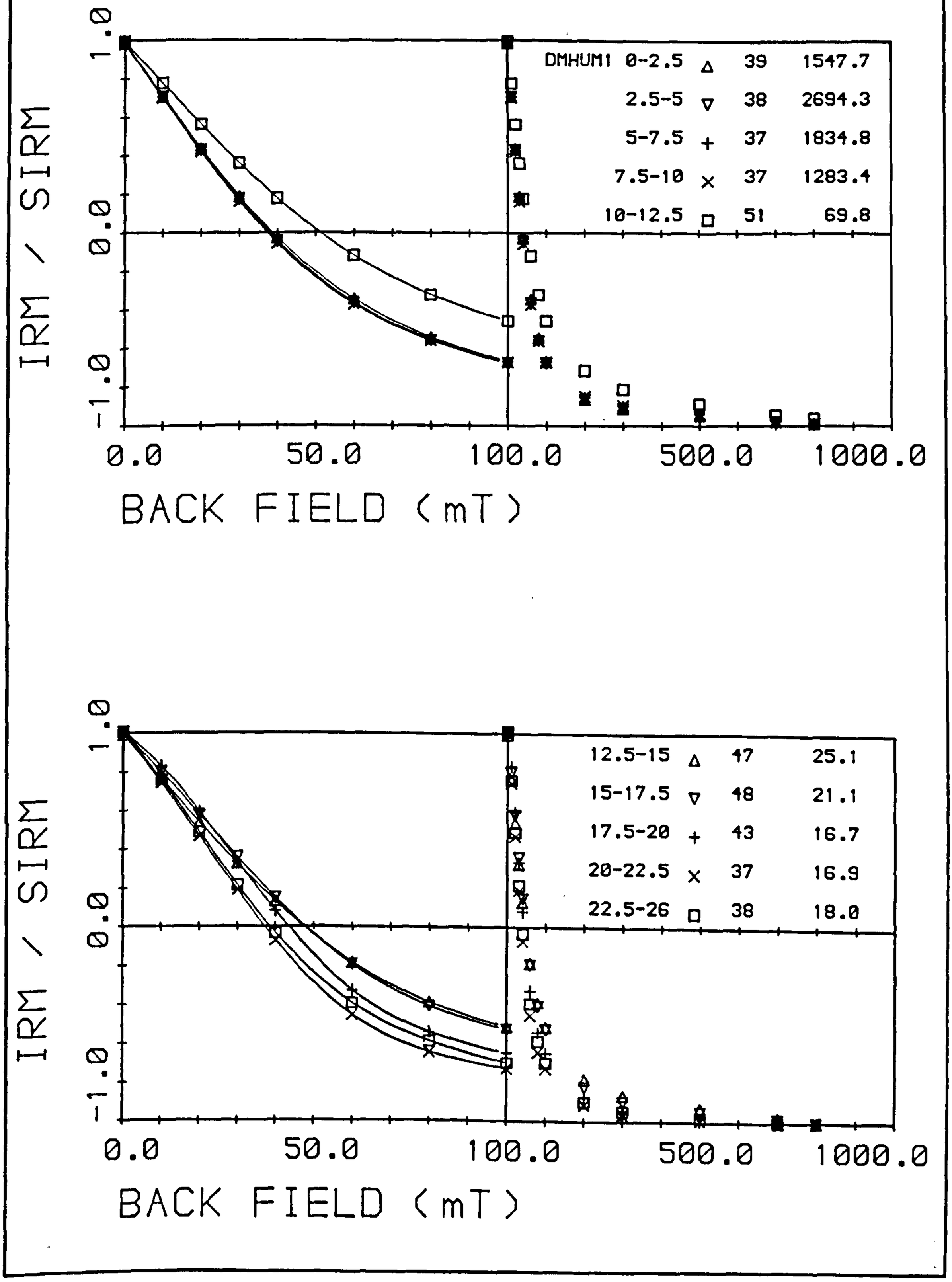


**Figure 5.14** Coercivity of remanence curves for DMHum1, Draved Moss

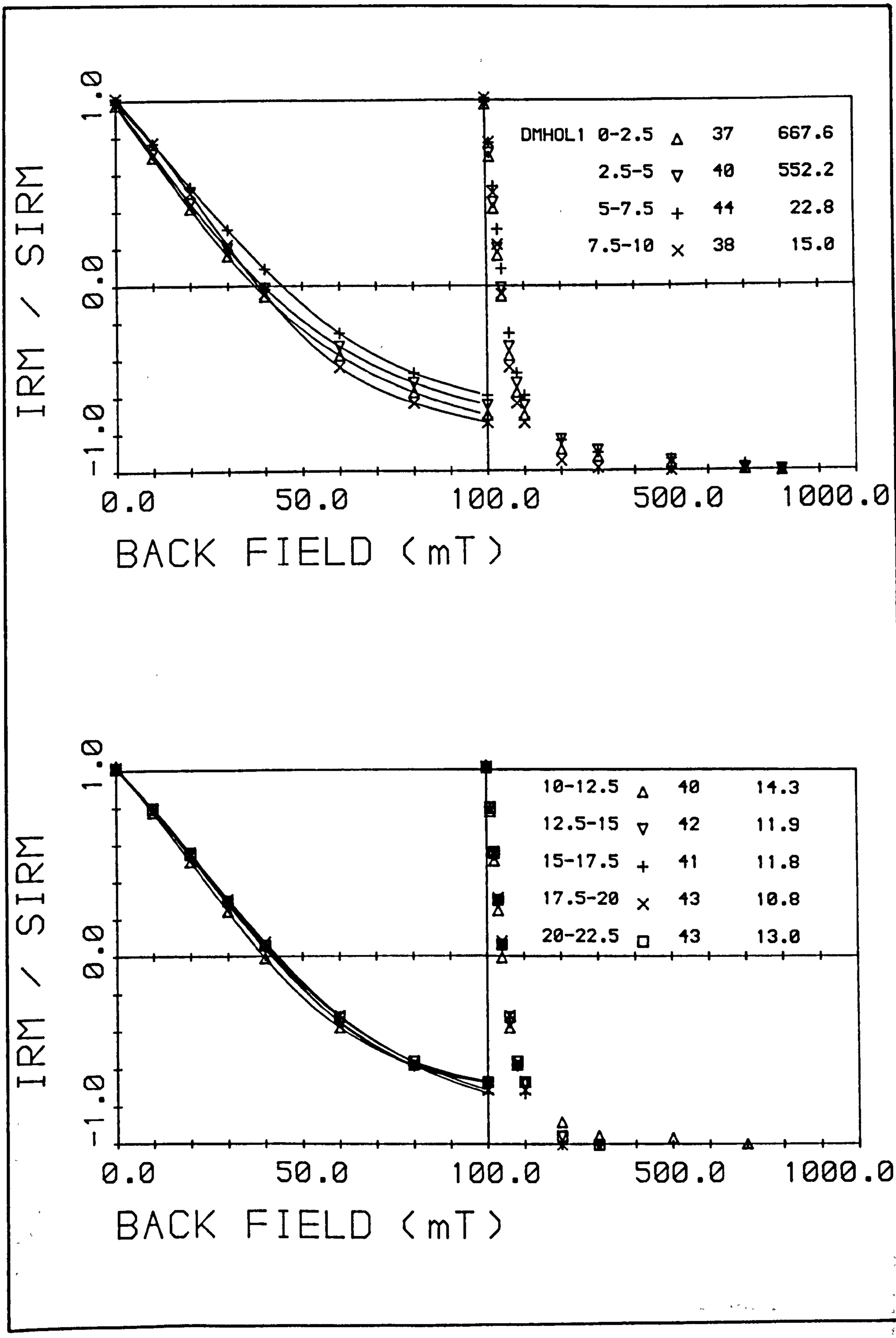


**Figure 5.15** Coercivity of remanence curves for DMHoll; Draved Moss

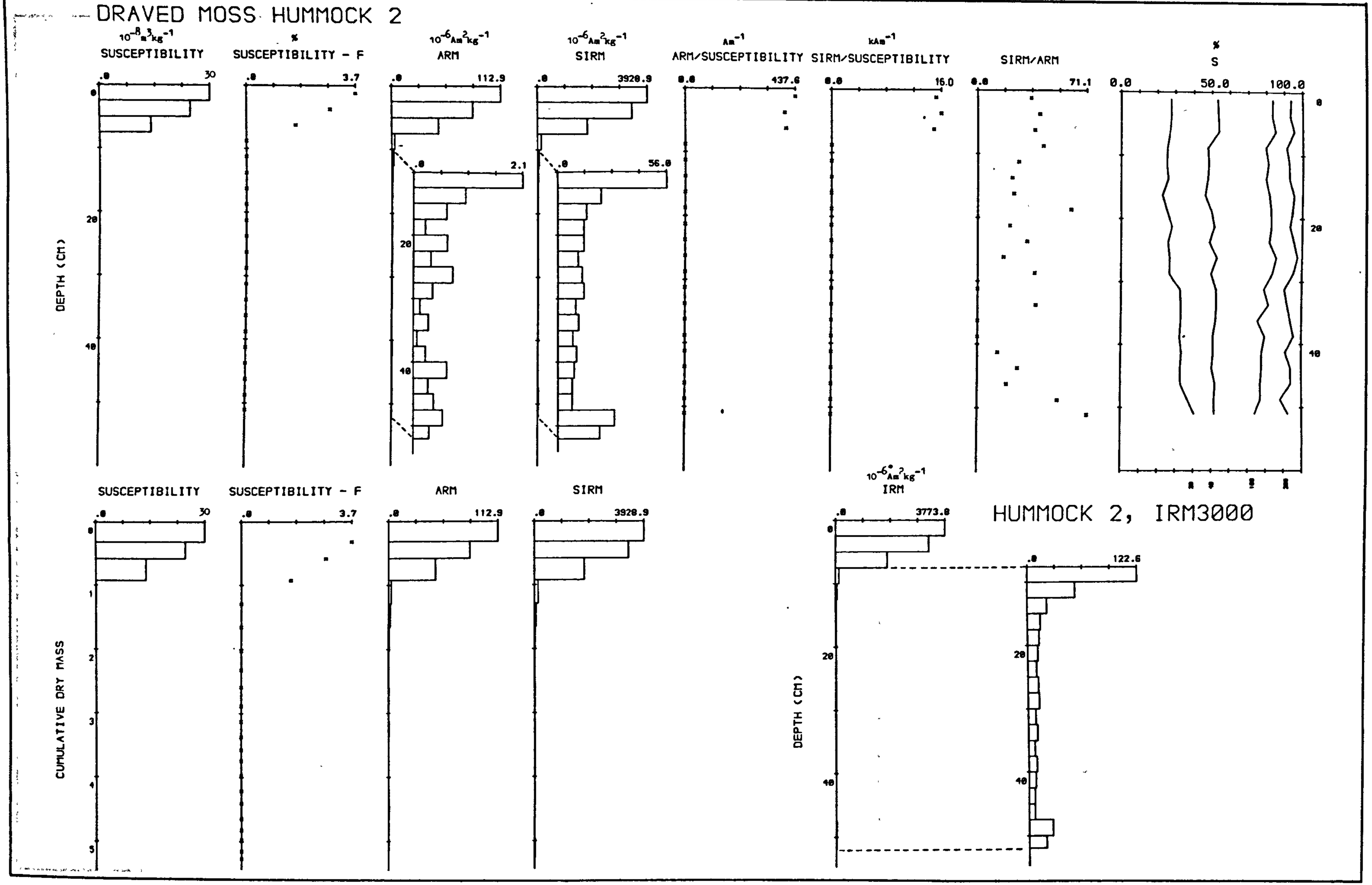


**Figure 5.16** Magnetic measurements for DMHum2, Draved Moss

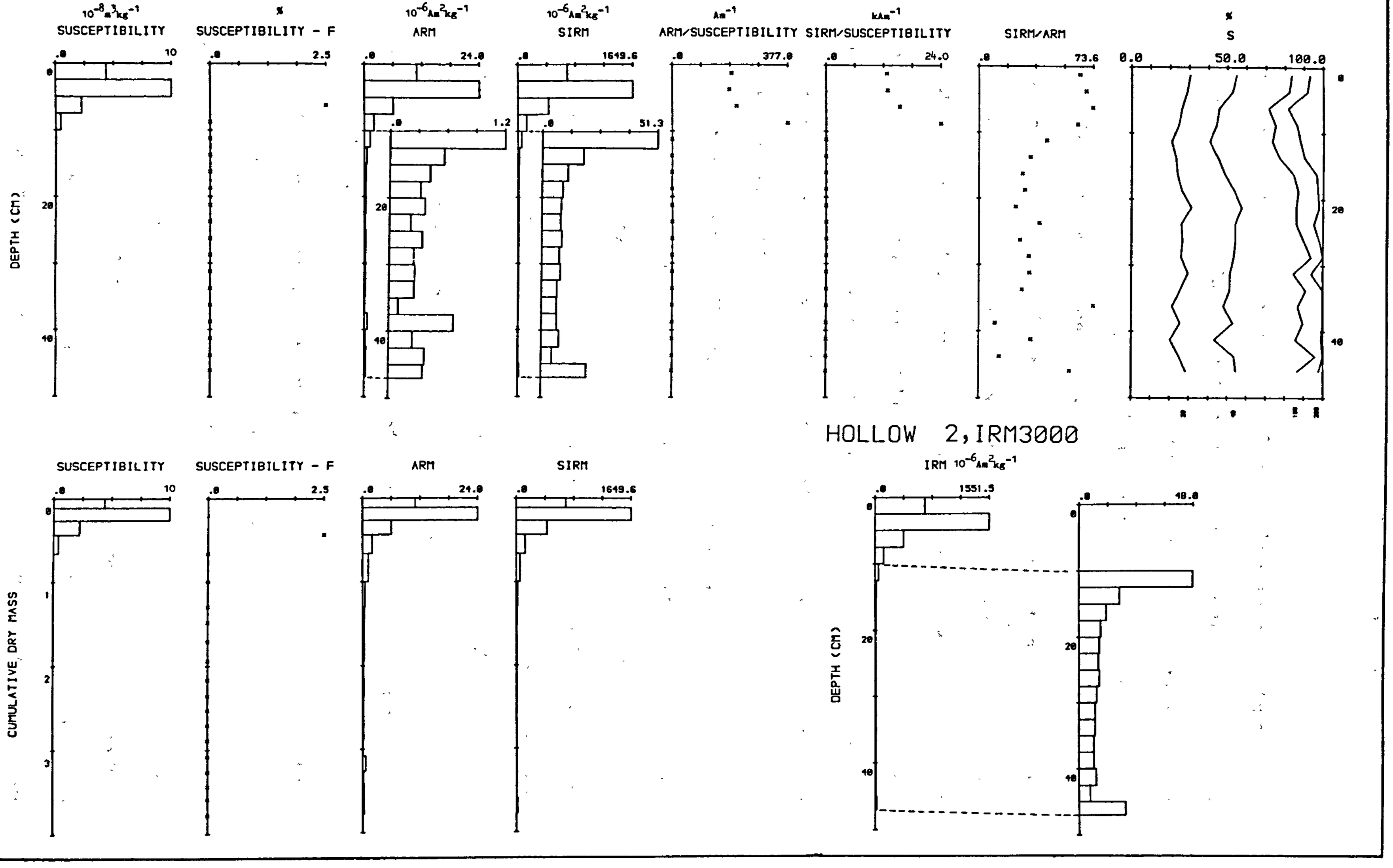


**Figure 5.17** Magnetic measurements for DMHol2, Draved Moss

increase in values above the take-off point, located at 5-7.5cm. SIRM values increase by 13.6 times from 7.5-10cm depth to 5-7.5cm depth. Above this the SIRM values increase toward a surface maximum of 3929 $10^{-6}Am^2kg^{-1}$. The $IRM_{300mT}$/SIRM ratio is predominantly between 0.95 and unity, although it occasionally drops as low as 0.92 (7.5-10cm). The interparametric ratios display similar values for the post-take-off samples, conspicuous by their high ARM/X values (384-438 $Am^{-1}$), intermediate SIRM/X values (ca. 16.0 $kAm^{-1}$) and low SIRM/ARM values (35-40.3). The backfield ratios again show little variation between the post-take-off samples. The presence of a 'hardness' feature is also noticeable immediately below the take-off point, within all the backfield ratios with the exception of $IRM_{-20mT}$/SIRM.

In the hollow core (fig. 5.17), the same down-core trends are evident in the magnetic profiles. The X profile is dominated by positive values above 10cm. Below this level the peat exhibits diamagnetic behaviour, corresponding to low concentrations of magnetic minerals. An average value of the diamagnetic component within the peat at both sites has been estimated at $0.42\pm0.02\ 10^{-8}m^3kg^{-1}$. Only the sample at 5-7.5cm within the hollow core displayed any viscosity, the $X_{fd}$ ratio being 2.5%. The ARM and SIRM profiles display more of a gradual increase within their respective profiles, in contrast to the marked variation in values noted within the previous cores. The increase begins about 10-12.5cm in the SIRM profile, with the take-off probably occurring at around 5-7.5cm. All the concentration dependent parameters display a sub-surface peak at 2.5-5cm, the SIRM value being 1650 $10^{-6}Am^2kg^{-1}$ and 711 $10^{-6}Am^2kg^{-1}$ for the surface sample. The $IRM_{300mT}$/SIRM ratio is predominantly between 0.94 and unity although it occasionally drops as low as 0.83 (30-32.5cm). The interparametric ratios display a reasonable consistency for the post-take-

off samples, with low ARM/X (186-210 $Am^{-1}$), intermediate SIRM/X (11.9-14.6 $kAm^{-1}$) and relatively high SIRM/ARM (65-73.6) compared with the hummock core, DMHum2. The backfield ratios again display the 'hardness' feature around the take-off point, predominantly within the upper backfield ratios ($IRM_{-100mT}$/SIRM and $IRM_{-200mT}$/SIRM).

A comparison of the hummock and hollow cores at site 2 reveals that the take-off point is at approximately the same depth in both cores (5-7.5cm). The peak SIRM value is again greater within the hummock compared with the hollow (2.4 times) and the surface value is also greater (5.5 times). Within the interparametric ratios, the ARM/X and to a lesser extent SIRM/X are all higher in the hummock core, within the post-take-off samples. As at site 1 both cores display the 'hardness' feature in some, or all of the backfield ratios.

The coercivity of remanence curves for DMHum2 and DMHol2 are presented in figs. 5.18 and 5.19 respectively. In DMHum2 (fig. 5.18) individual curves are presented for the top five samples (0-12.5cm). The post-take-off samples display very similar curve shapes and $(B_0)_{CR}$ values (38-39mT). Similarly, the two preceeding samples (7.5-12.5cm) display similar curve shapes with slightly higher $(B_0)_{CR}$ values (42-43mT). Below 12.5cm the remaining samples are grouped to form an envelope of values based on the broadest limits of the curve shapes and widest range of $(B_0)_{CR}$ values. In DMHum2 two envelopes of values are evident within the pre-take-off samples. The first, between 1.2-30cm and 40-47cm displays slightly concave curve shapes and $(B_0)_{CR}$ values in the range of 37-48mT. The second envelope of values (30-40cm) in contrast, displays concave curves, especially between 1.0-0 IRM/SIRM (fig. 5.18). The range of $(B_0)_{CR}$ values for this group of samples is slightly lower at 33-38mT.

In DMHol2 (fig. 5.19), the remanence curves for the top four samples

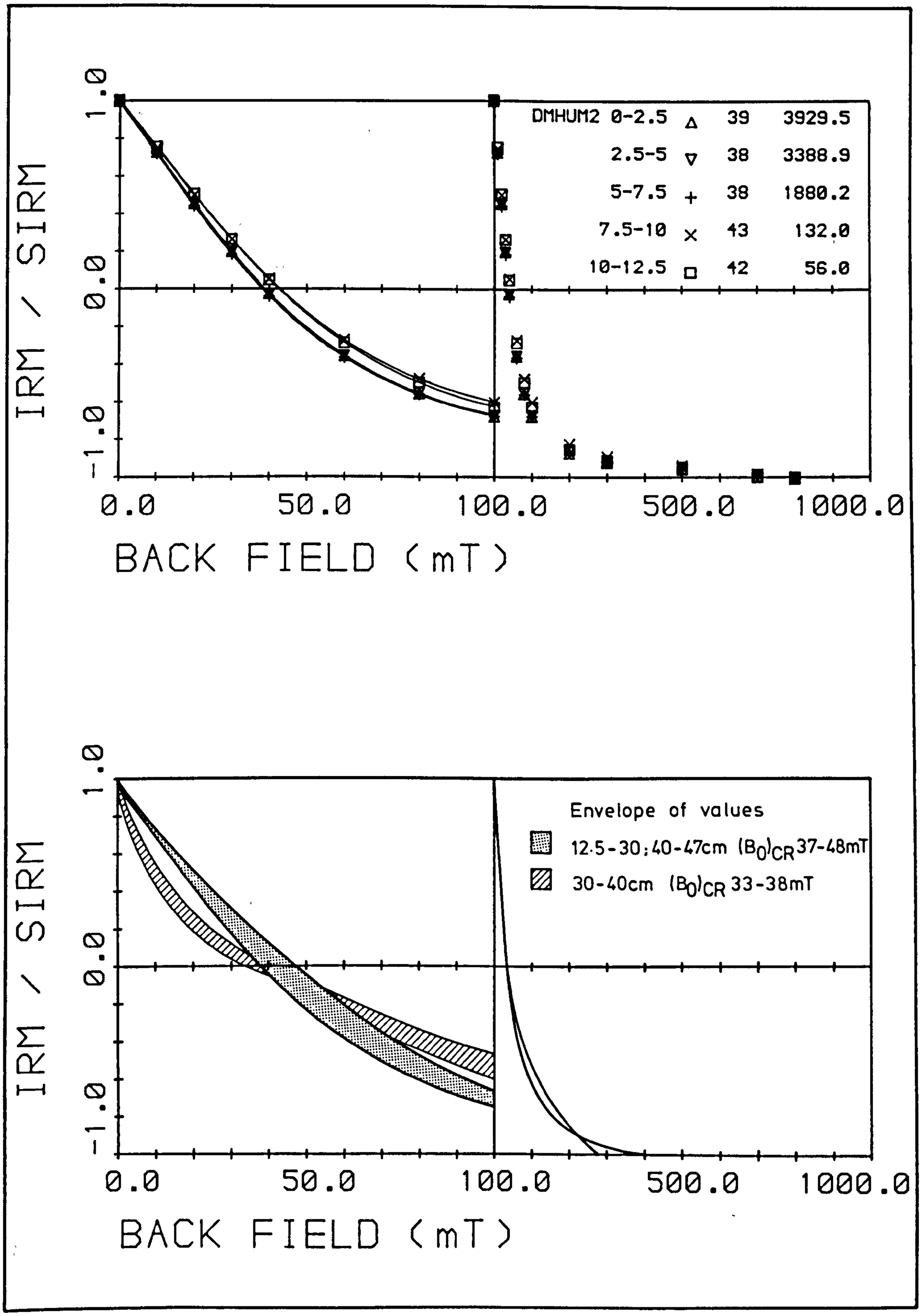


**Figure 5.18** Coercivity of remanence curves for DMHum2, Draved Moss

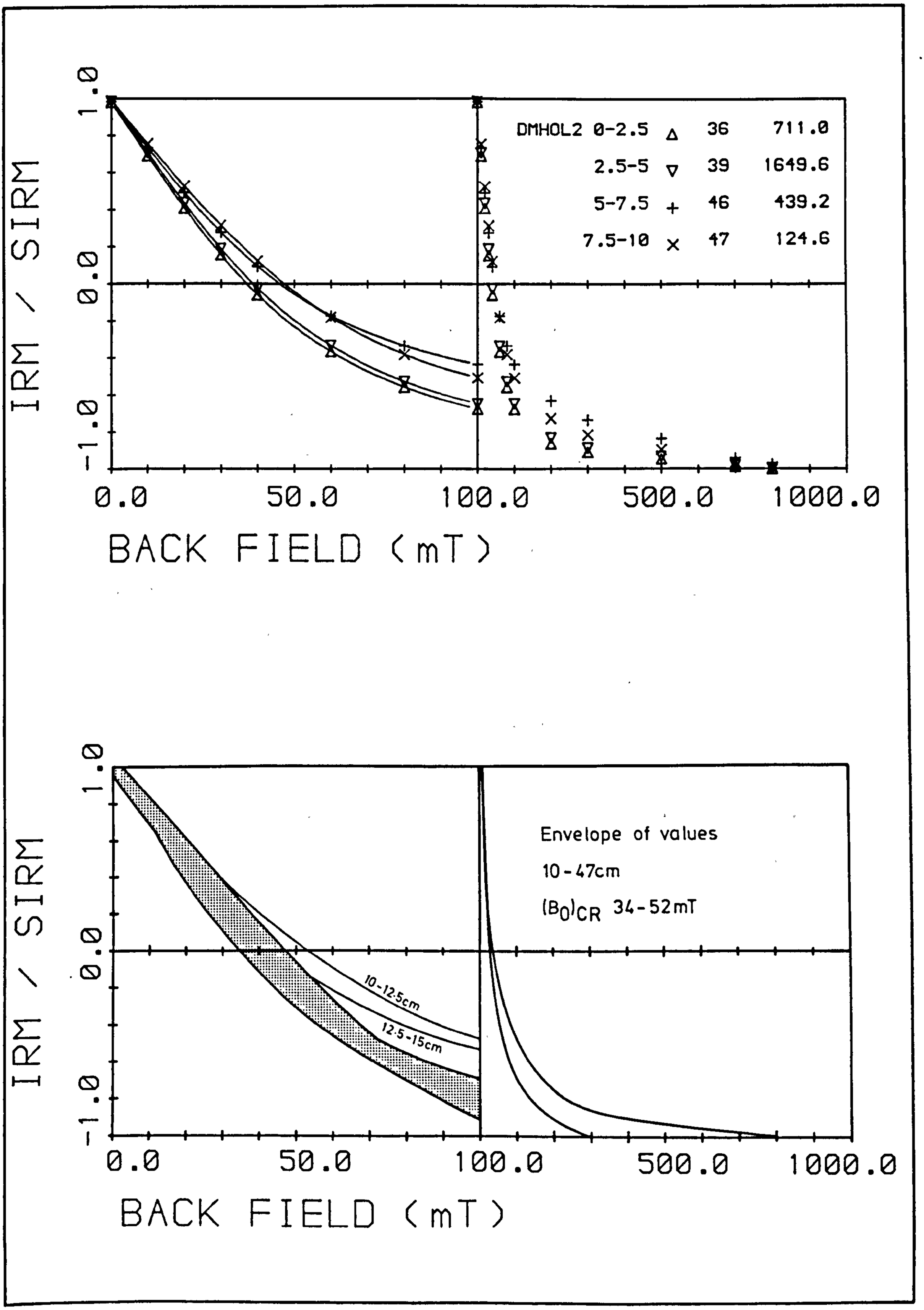


**Figure 5.19** Coercivity of remanence curves for DMHol2, Draved Moss

are plotted individually, and an envelope of values encompasses the range of curves exhibited by samples between 10-47cm. The curve shapes of 0-5cm differ from those of the preceeding 5cm, being slightly more concave and exhibiting lower $(B_0)_{CR}$ values, 36-39mT compared with 46-47mT for 5-10cm. The envelope of values for samples below 10cm encompasses both of the curve shapes mentioned above. The $(B_0)_{CR}$ values vary between 34mT and 52mT.

An overall comparison of the magnetic measurements at the two sites shows that the SIRM values at site 2 display consistently higher values for both peak samples and surface samples respectively. Within the hollows, peak SIRM values are 2.4 times higher at site 2 and marginally higher for the surface sample. Another observation is that the take-off point varies within the hummock and hollow cores at site 1 in contrast to site 2, where the take-off probably occurs at around the same depth in both cores (5-7.5cm). The SIRM/ARM ratios also display inter-site variance, being consistently higher in both the hummock and hollow cores at site 1 compared with the respective cores at site 2. A final observation is that regardless of hummock-hollow microtopography or site location on the bog plane, all four cores display the 'hardness' feature within the backfield ratios, for samples immediately below the take-off point.

5.3.4 Scanning Electron Micrographs

Plates 5.1-5.3 are scanning electron micrographs of magnetic extracts taken from the surface sample (0-2.5cm) of DMHum2. The extraction method has been outlined previously in sub-section 5.2.1. The most distinguishing feature of the micrographs is the paucity of magnetic material extracted, in contrast with other sites, for example in England (see below). The micrographs show two broad groups within the magnetic extracts. The first group comprises opaque spherical particles or spherules.

**Plate 5.1** Scanning electron micrograph (x2500) of the magnetic extract from the surface sample (0-2.5cm) of core DMHum2, Draved Moss, southern Denmark.

**Plate 5.2** Scanning electron micrograph (x2500) of the magnetic extract from the surface sample of DMHum2. The micrograph depicts a clearer view of a spherule.

**Plate 5.3** Scanning electron micrograph (x1250) of the magnetic extract (spherules and non-spherules) from the surface sample of DMHum2.

**N.B.** The dark grey areas in the upper and lower corners of each plate are the carbon stub surface.

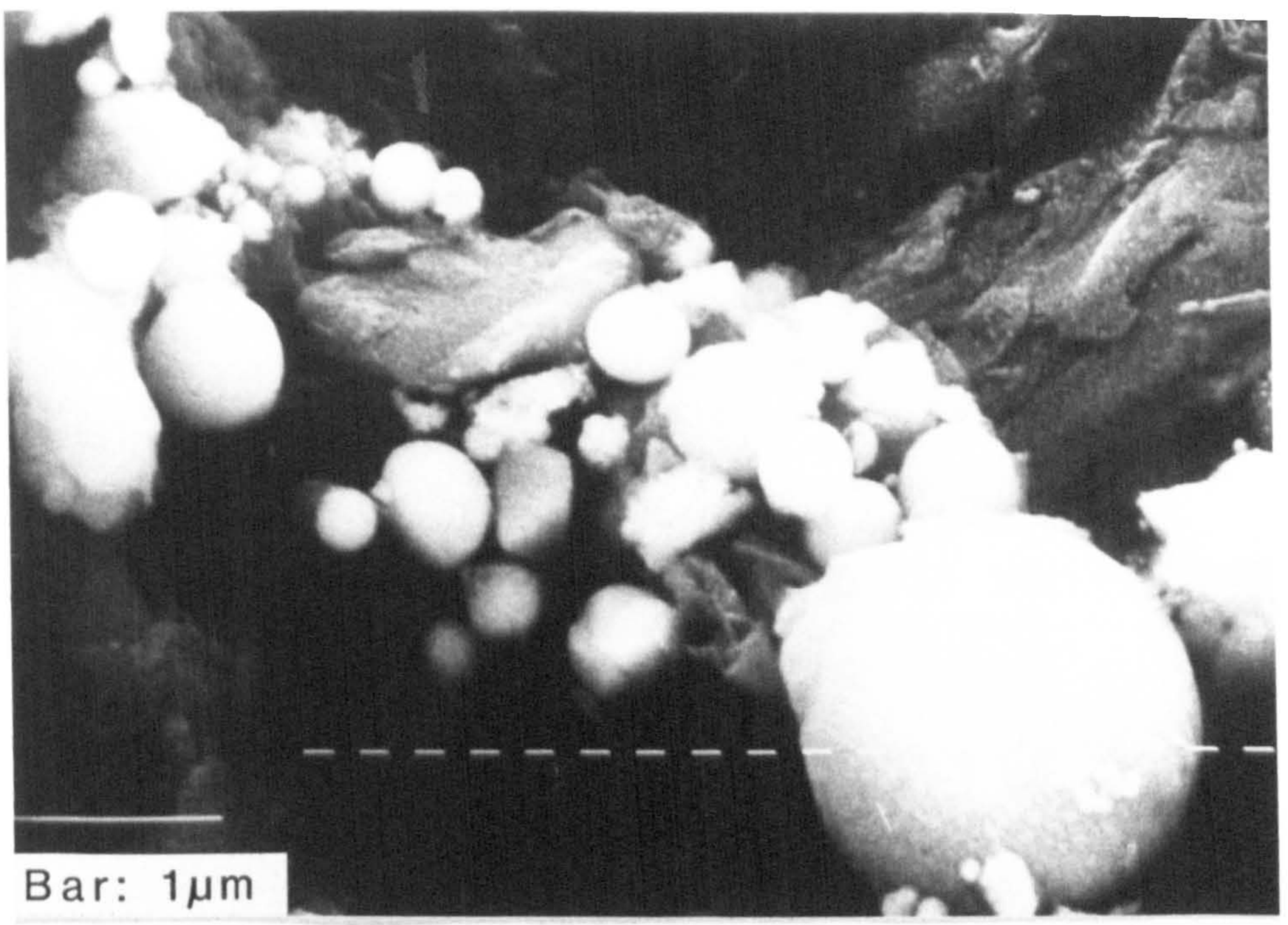
Bar: 1µm

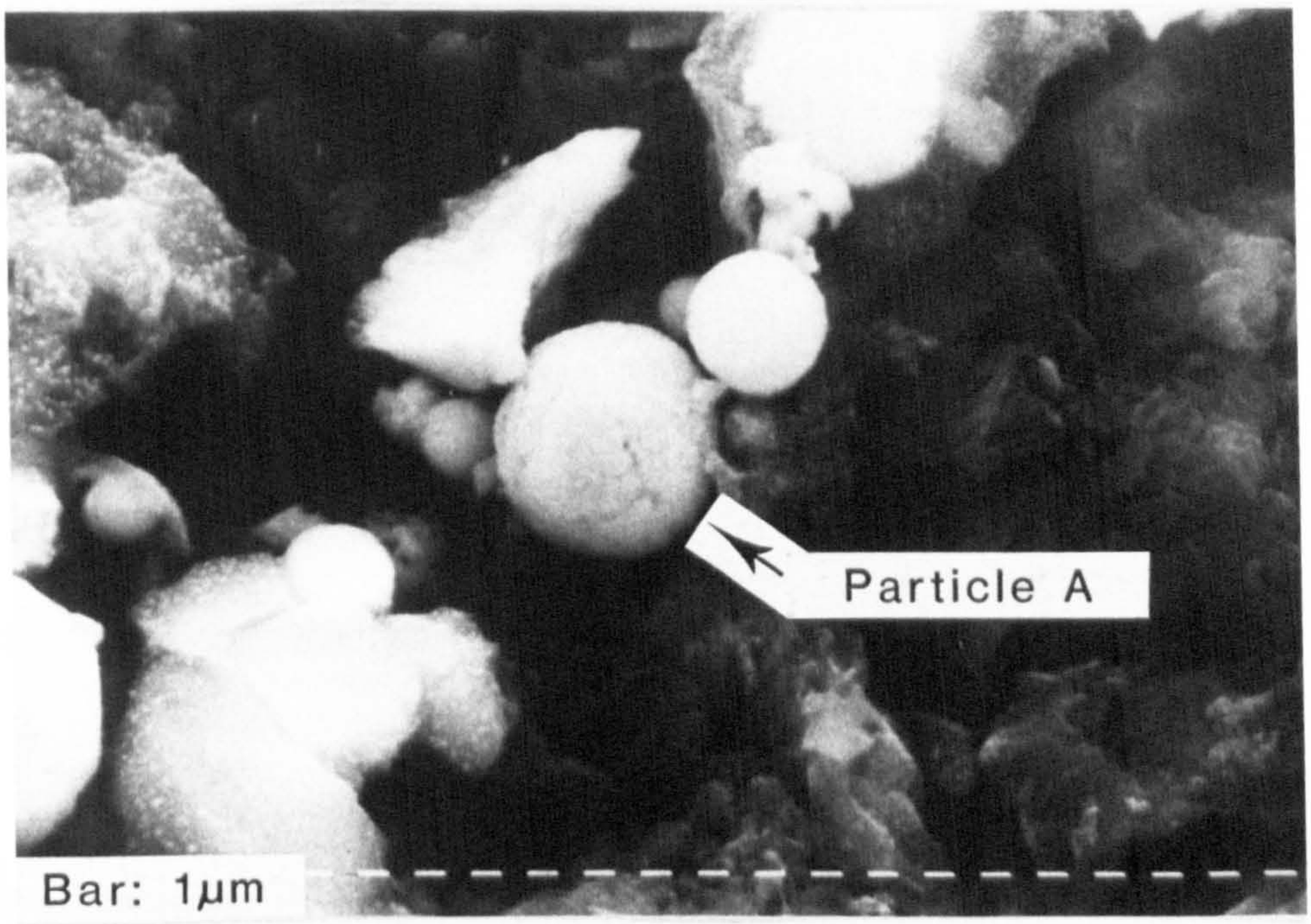
Particle A
Bar: 1µm

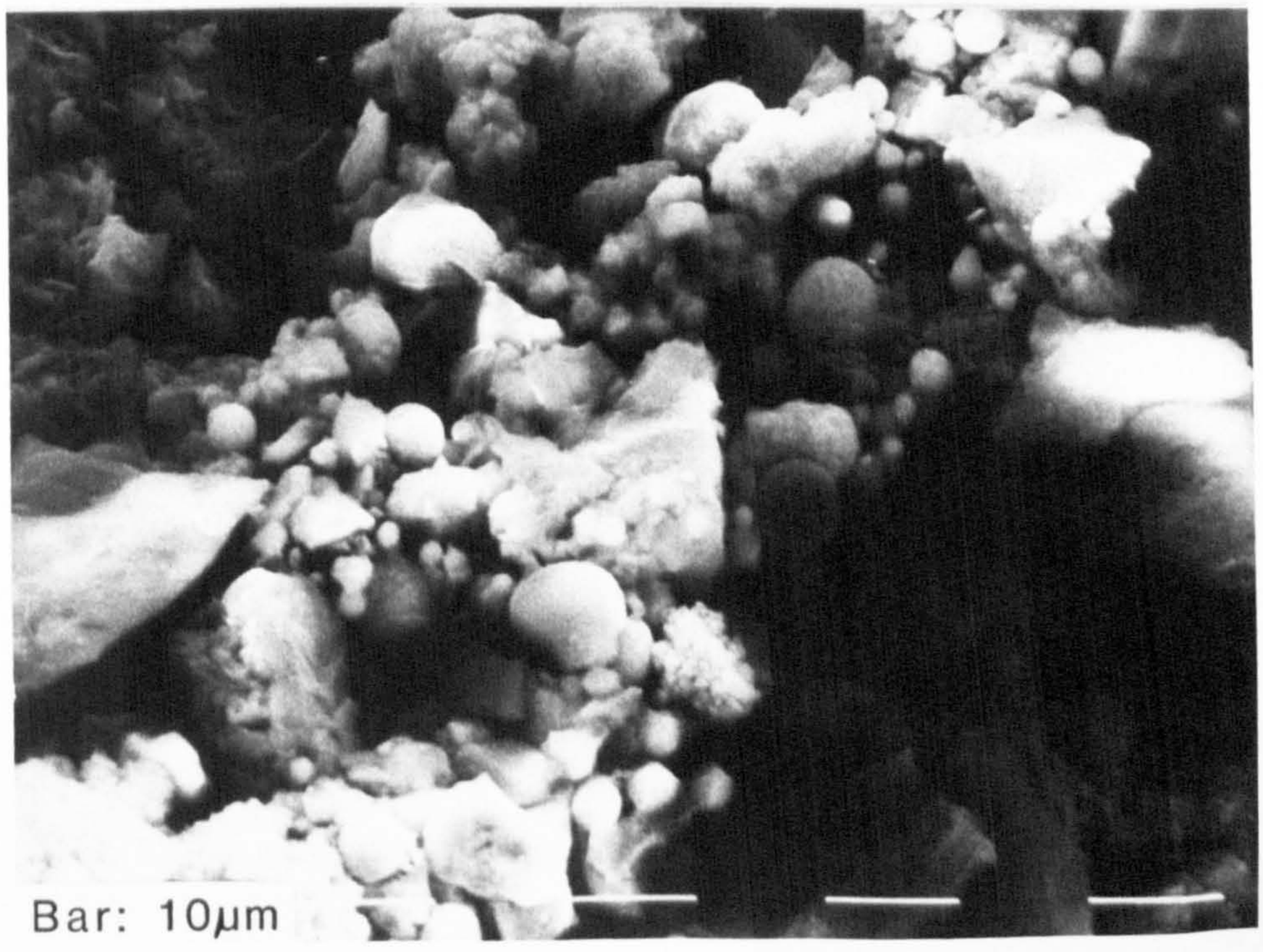
Bar: 10µm

**Plate 5.4** Scanning electron micrograph (x2500) of the magnetic extract from the surface layer (0-1cm) of Mo-I-Rana peat core, northern Norway (inset). With EDX spectrum taken from Spherule A.

**Plate 5.5** Scanning electron micrograph (x1250) of the magnetic extract from the surface layer of Mo-I-Rana peat core (inset). With EDX spectrum of Particle A.

**N.B.** Note the size of Particle A in relation to the surrounding spherules.

**Plate 5.6** Scanning electron micrograph (x1250) of the magnetic extract from the surface sample of Mo-I-Rana peat core (inset: left). With EDX spectra of Particle B (inset: right) and Particle C.

**Plate 5.7** Scanning electron micrograph (x2500) of an elongated particle (Particle D), within the magnetic extract from the surface sample of Mo-I-Rana peat core (inset). With EDX spectrum of Particle D.

**Plate 5.8** Scanning electron micrograph (x640) of the magnetic extract from garnet mica-schist, northern Norway. With EDX spectrum of Particle A.

**Plate 5.9** Scanning electron micrograph (x1250) of magnetically extracted particles from 3-4cm, core RB5, Ringinglow Bog, England. Bar equals 10µm. (source: J. Jones, 1985)

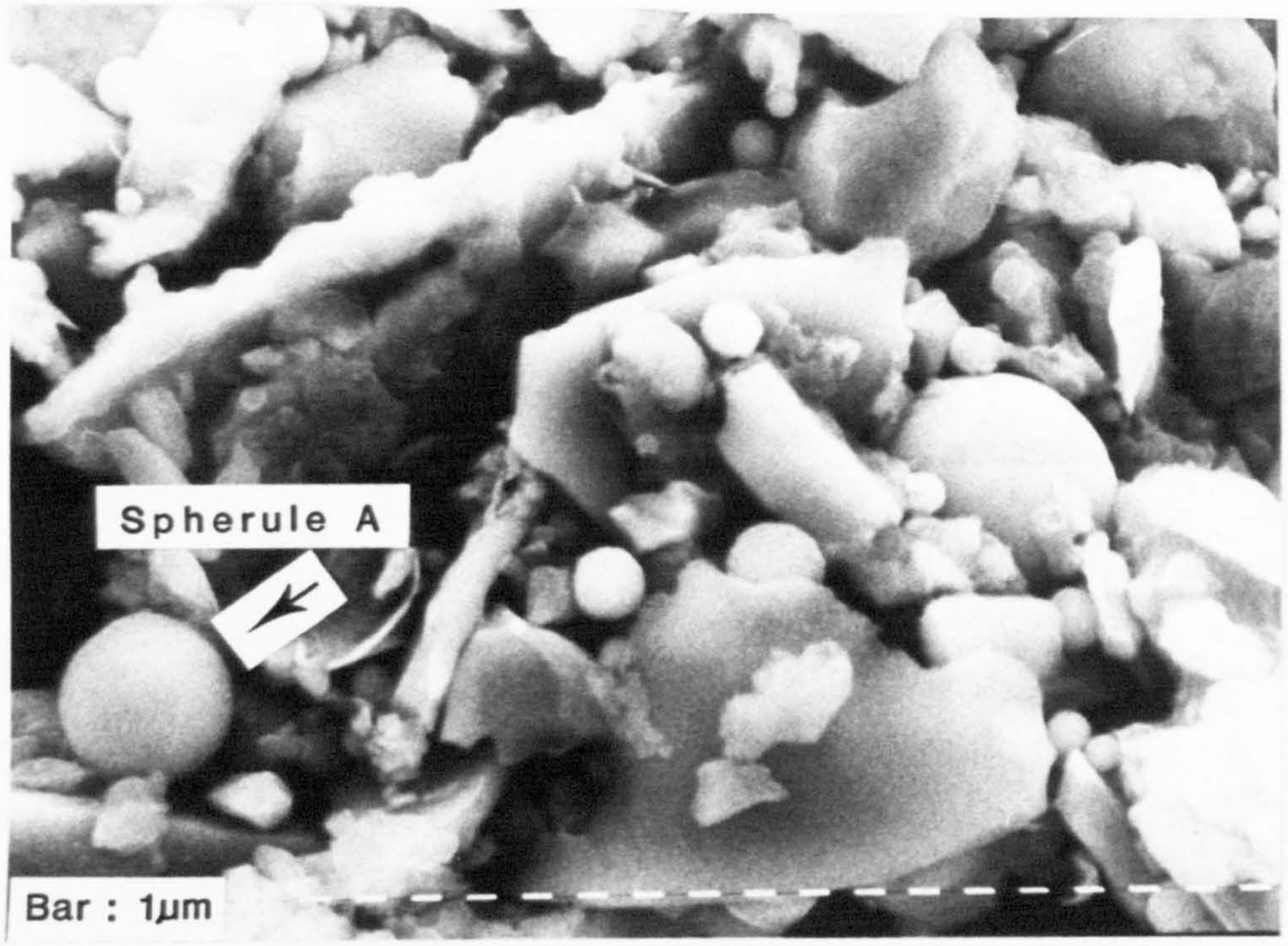


EDX spectrum of
Spherule A

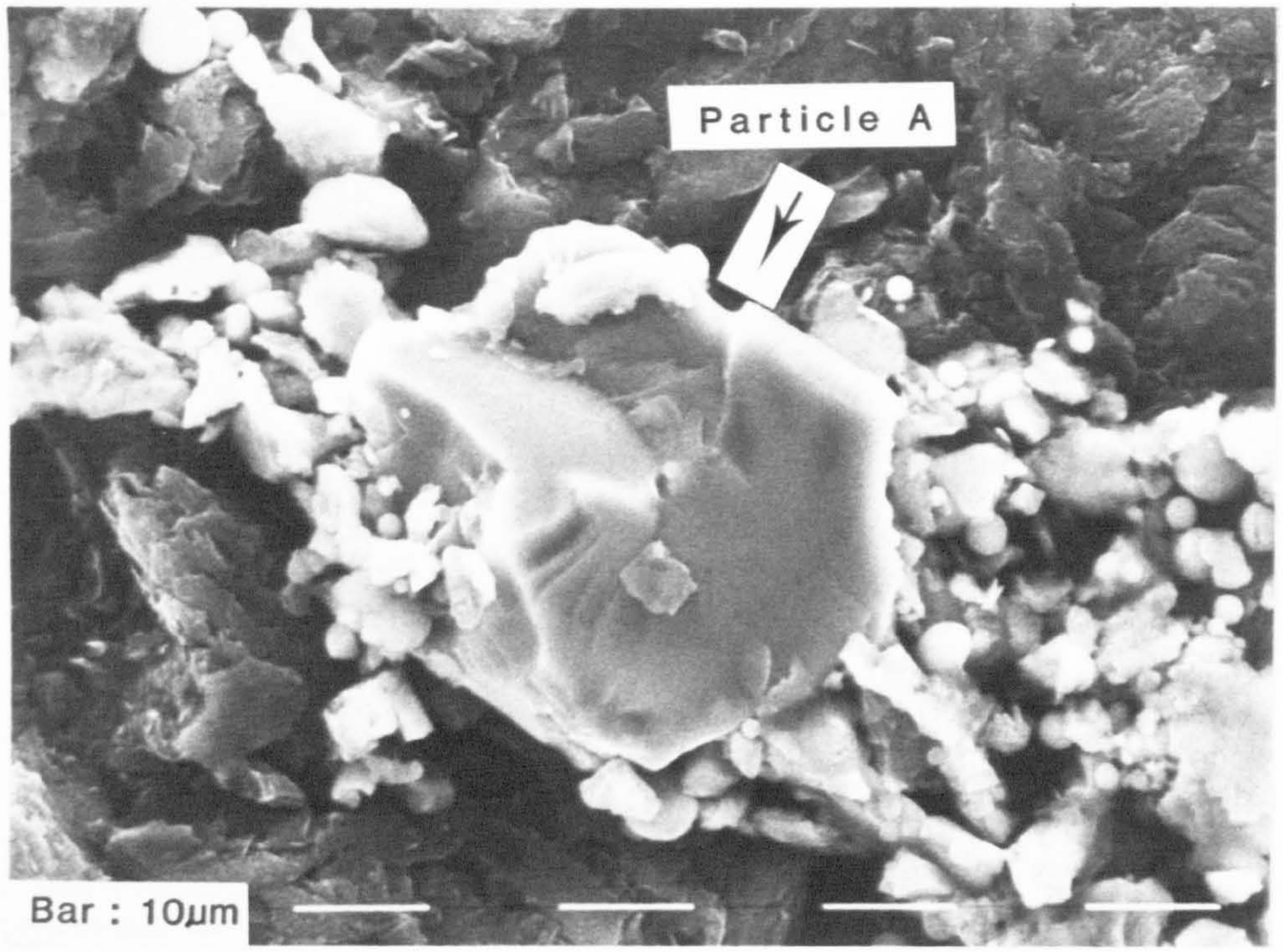


EDX spectrum
of Particle A

Fe

Fe

0

2

4

6

8

keV

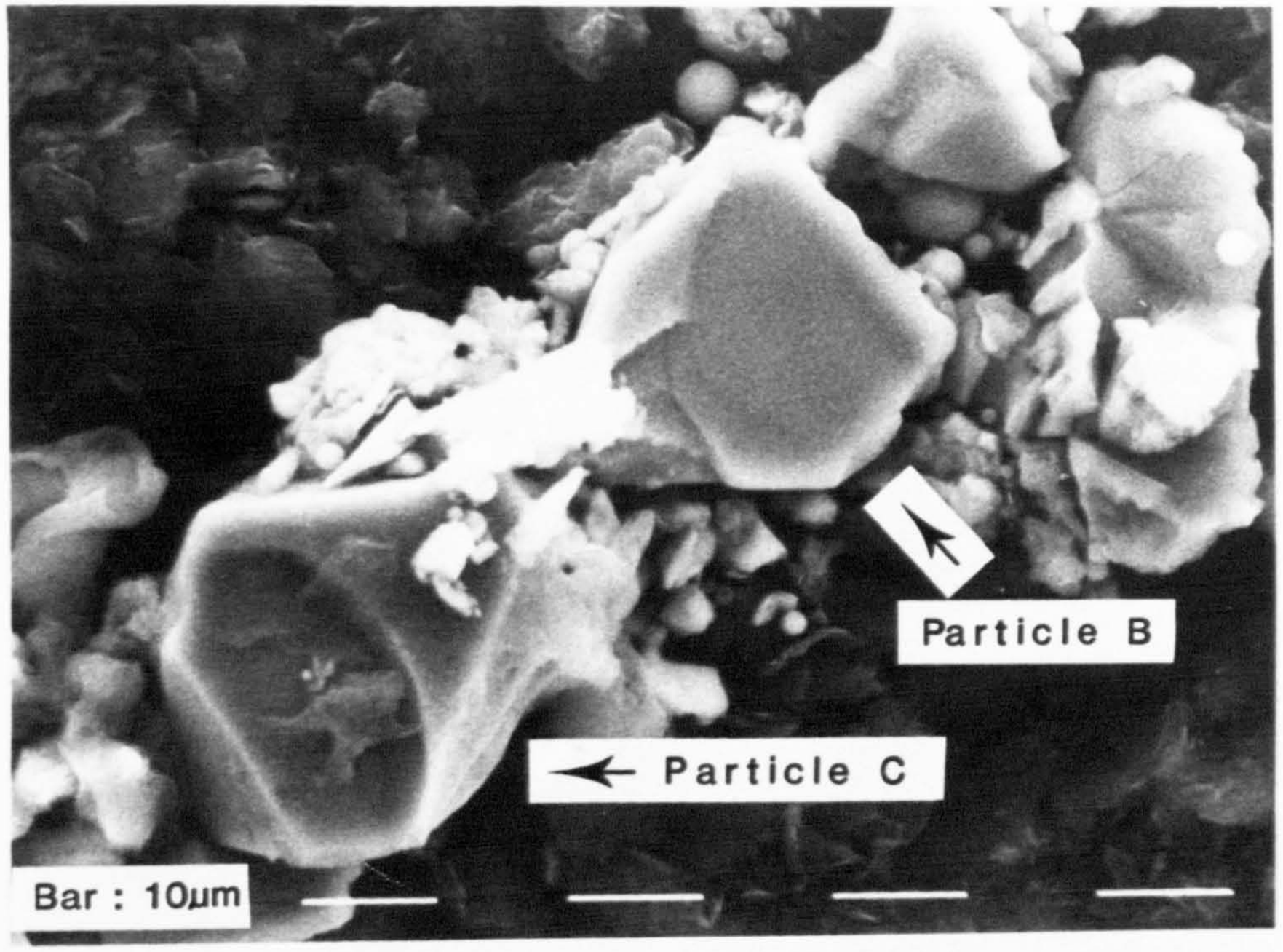


EDX spectrum of Particle C

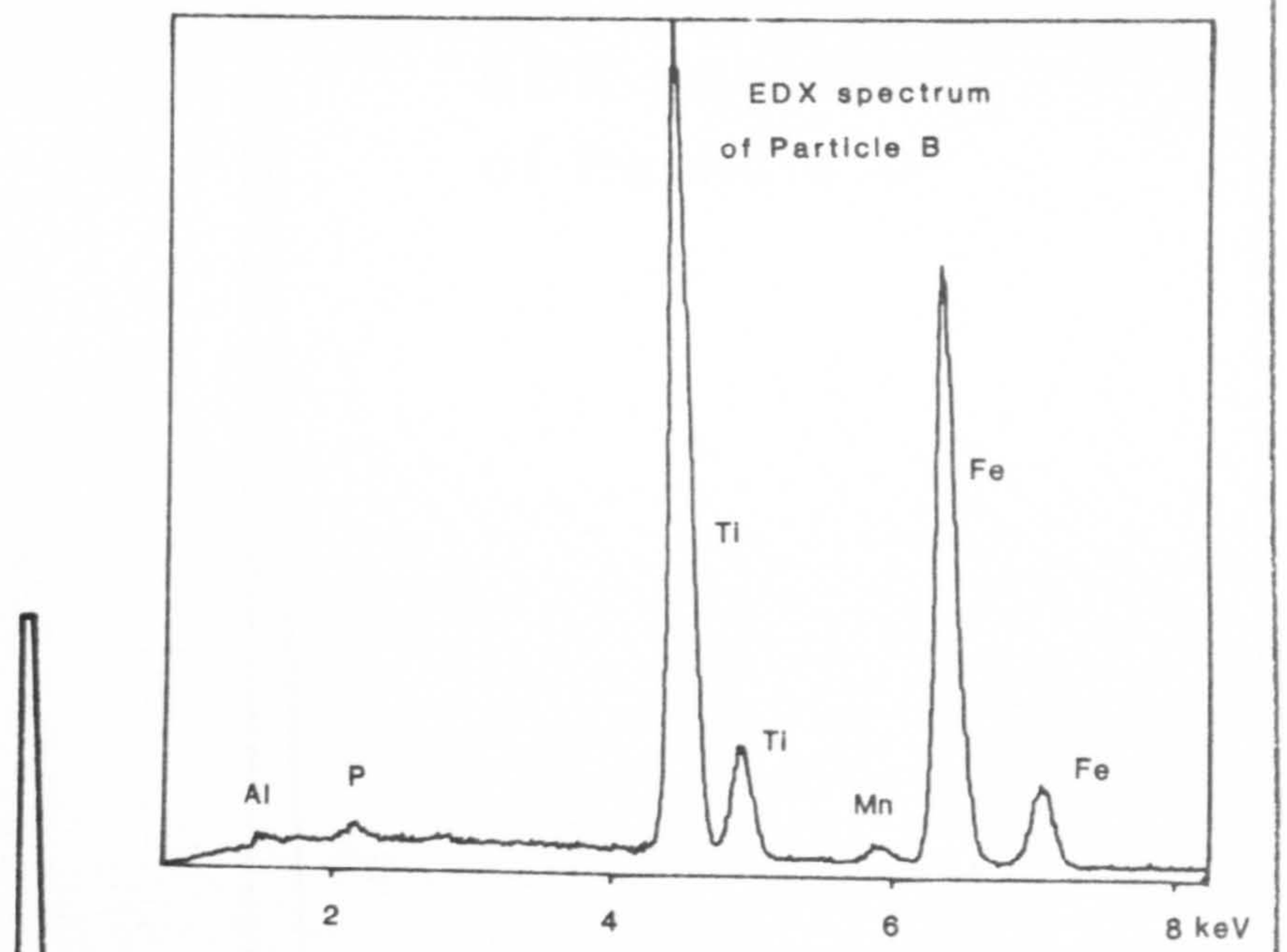

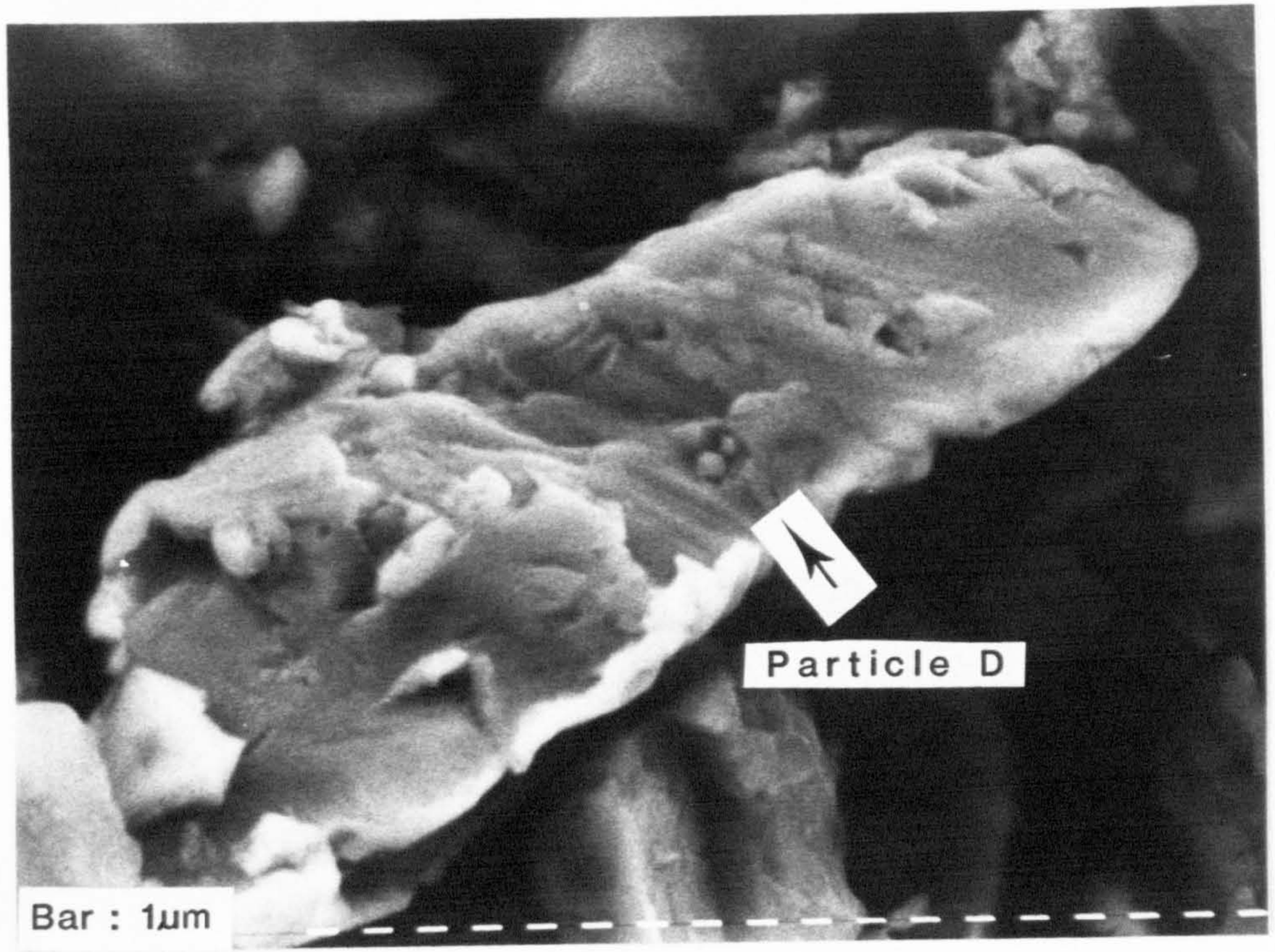


EDX spectrum
of Particle D

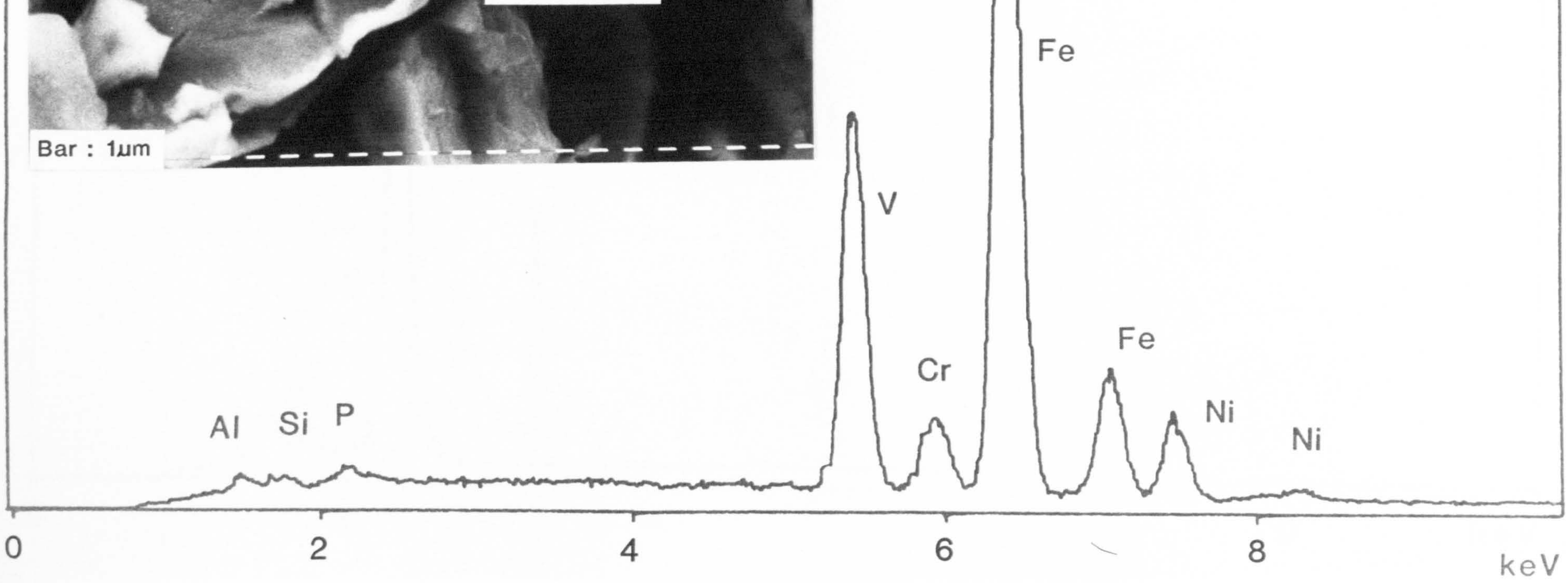

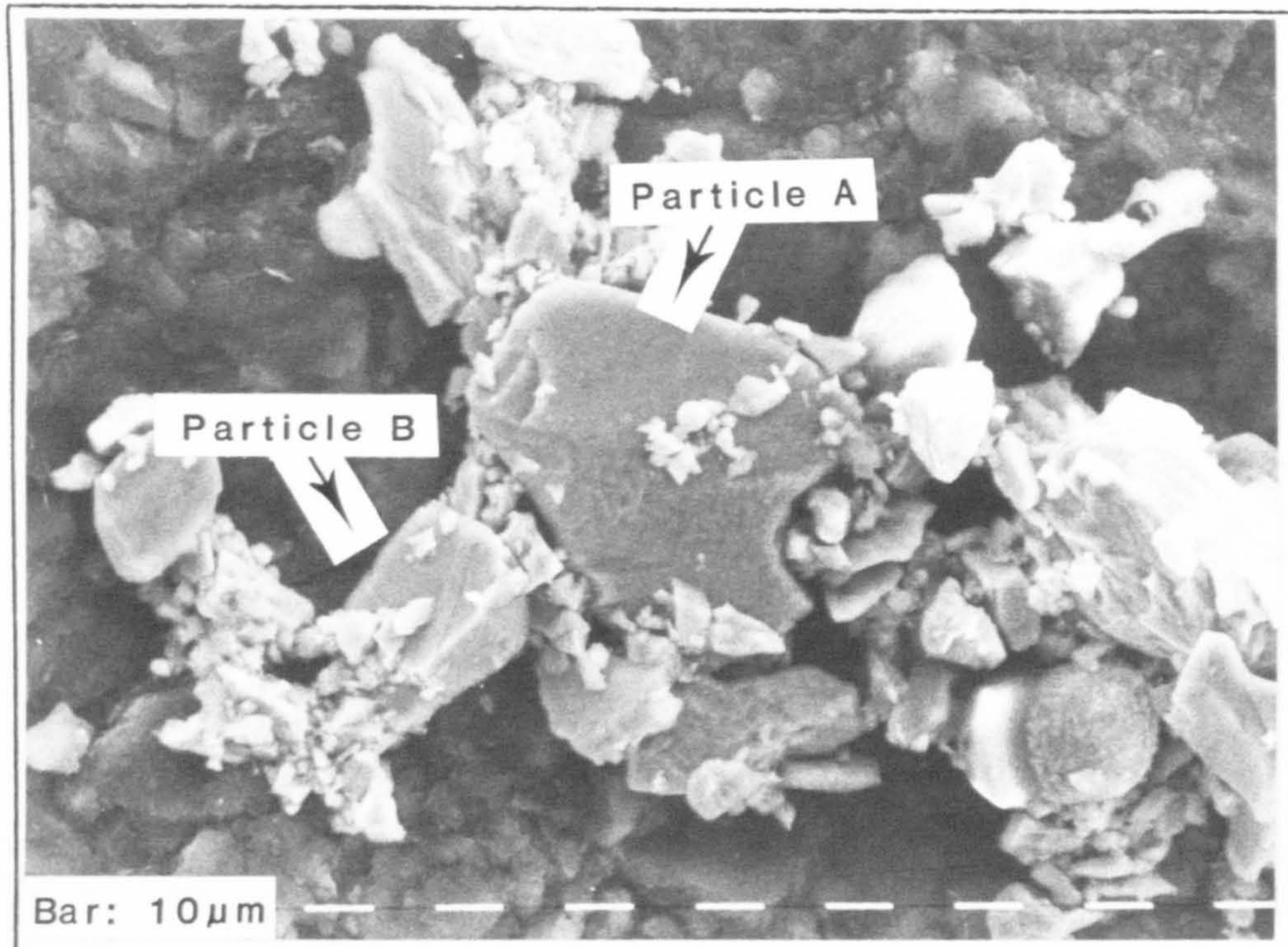


EDX spectrum
of Particle A

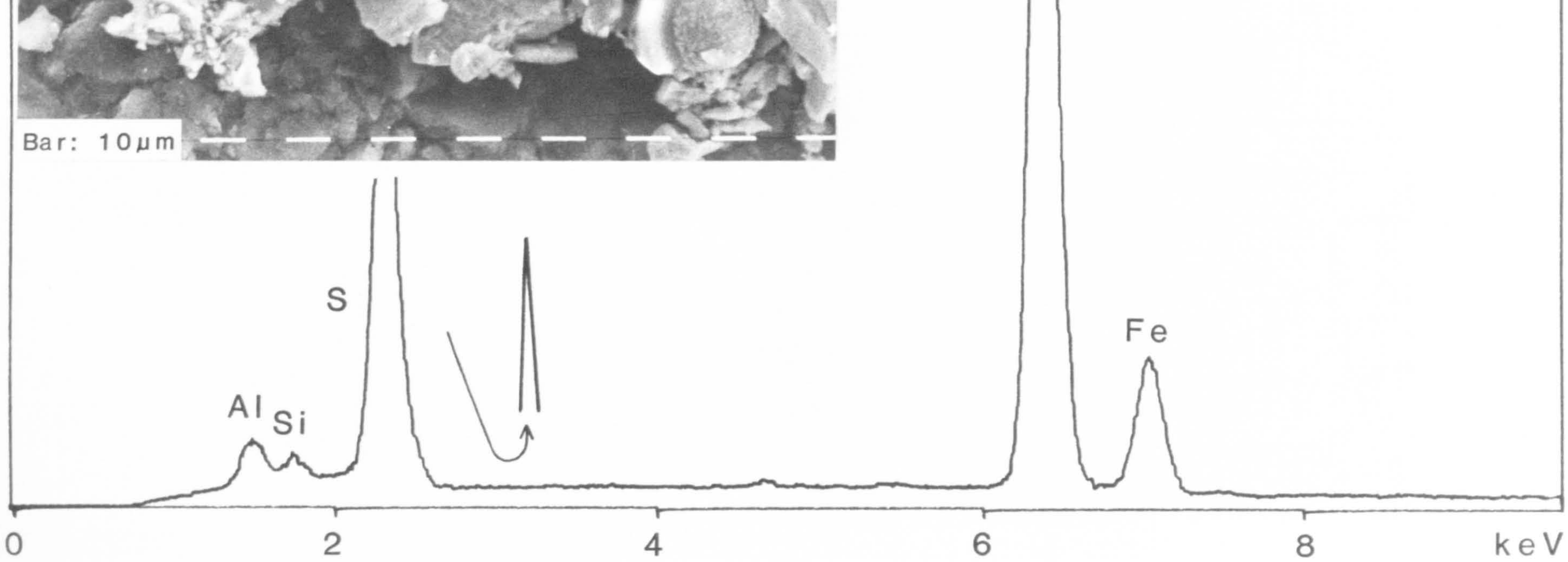

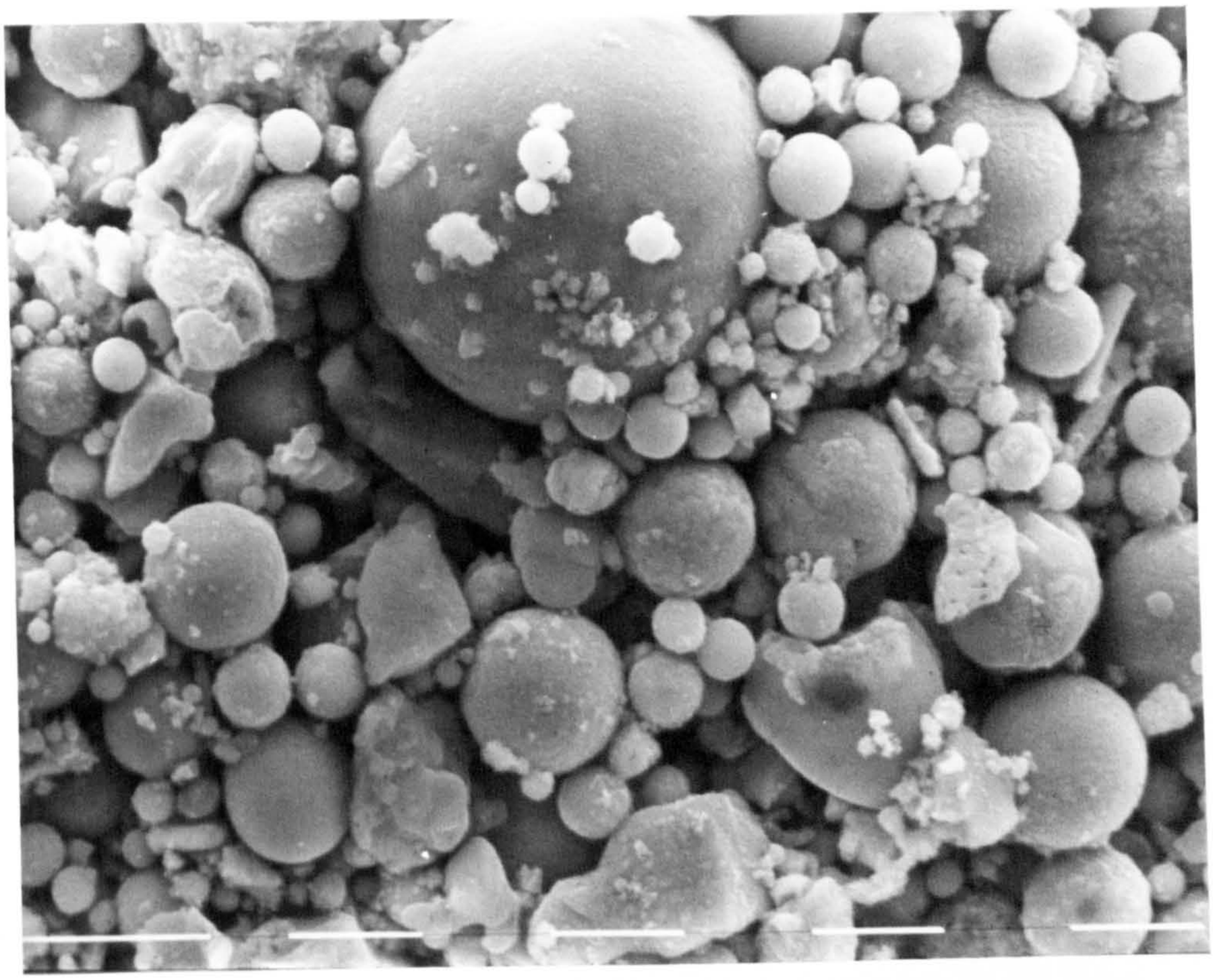

These spherules range in size from micron and probably sub-micron sizes to about 7μm. The smaller particles within the size range tend to predominate. According to Griffin & Goldberg (1981), sphericity is symptomatic of particles derived from high temperature fossil fuel combustion processes. A more detailed and thorough account of these fossil fuel combustion processes is given by Jones (1985). There is little evidence of any distinct surface morphology on any of the spherules present in the extracts. Particle A (Plate 5.2) possibly shows some surface relief although nothing as evident as the particle morphologies noted by, for example Del Monte & Sabbioni (1984a, 1984b) on fly ash material, or by Jones (op. cit.) on particles extracted from peat layers associated with post-industrial times in South Yorkshire, England.

The second group of particulates comprises angular and sub-angular particles, possibly in greater abundance than the spherules. Many of these particles are much larger than the biggest spherule, being up to 20-30μm along the long axis or a-axis and probably larger, given the distortion caused by depth. These particles are most probably a soil-derived component, the product of wind-blown field erosion as noted previously and by Vuorela (1983) and Tolonen (1984).

5.3.5 Discussion

The interpretation of the data relating to Draved Moss is discussed within the context of two main themes. The first involves a discussion of the heavy metal data in the context of previous work, for example Aaby & Jacobsen (1979). The second theme involves an interpretation of the magnetic data.

The chemical composition of the surface layers of the four cores is summarised in Table 5.2. The mean concentrations for the hummock and hollows are compared with mean concentrations from five hummocks and

**Table 5.2** Concentrations of Heavy Metals in the Surface Layers of Hummock and Hollow Peat. A comparison of the mean hummock and hollow element concentrations in the surface sample of this study with those of Aaby & Jacobsen (1979). The older date of 1978-1966 gives the concentrations from the 2.5-5cm layer which encompass the age of the surface sample from the published source.

| | Fe $\mu g.g^{-1}$ | Pb $\mu g.g^{-1}$ | Cu $\mu g.g^{-1}$ | Zn $\mu g.g^{-1}$ | Ni $\mu g.g^{-1}$ |
|---|---|---|---|---|---|
| **Hummock** | | | | | |
| 1983 | 1000 | 59.5 | 10.1 | 55.8 | - |
| 1973-1970* | 1082 | 51.3 | 6.1 | 58.4 | 3.0 |
| 1978-1966 | 2066 | 97.9 | 12.3 | 96.4 | 11.0 |
| **Hollow** | | | | | |
| 1983 | 1010 | 62.8 | 9.0 | 78.2 | 3.6 |
| 1973-1972* | 1925 | 123.5 | 5.6 | 93.5 | 2.6 |
| 1978-1966 | 2252 | 88.0 | 11.7 | 89.7 | 5.3 |

* Aaby & Jacobsen (1979)

two hollows presented in Aaby & Jacobsen (op. cit.). The published data come from S. magellanicum-S. rubellum sociations (hummocks) sampled between 1970-1973, and S. cuspidatum sociations (hollows) sampled between 1972-1973. In contrast, the data presented from this study come from S. magellanicum/C. vulgaris-E. vaginatum sociations (hummocks) and S. cuspidatum sociations (hollows) sampled in 1983. Although the variation in concentrations is marked, due to differences in the time of sampling and sociations amongst other factors, the concentrations of each element are within the same order of magnitude.

The difference between hummock and hollow sociations is not particularly marked except in the case of lead and zinc. Homogeneity of metal concentrations in surface samples from hummocks and hollows, respectively, is therefore demonstrated over the last 10-14 years, similar to the conclusions of Aaby & Jacobsen (op. cit.). Using the $^{210}Pb$ chronology given in section 5.4 for DMHol2, the age of the 2.5-5cm slice is between 5.5 years (2.5cm) and 16.5 years (5cm) before 1983. This time interval encompasses the time-span used by Aaby & Jacobsen (op. cit.), in comparison with the present study, namely 10-14 years before 1983. Therefore, a comparison of element concentrations from the 2.5-5cm slice in the four cores, assuming the rate of peat growth to be approximately comparable in all four cores, and the surface concentrations of Aaby & Jacobsen (op. cit.) might serve to indicate any possible vertical mobility of the elements within the peat cores. A comparison of the data (Table 5.2) shows that mobility is likely over the timescale of approximately 10 years in the case of iron, lead, zinc and nickel within the hummocks, and iron and nickel within the hollows. The difference between vertical mobility between the hummocks and hollows in, for example lead, has previously been observed by Pakarinen & Tolonen (1977a). In the cases of iron, lead,

zinc and nickel which all appear to show some form of vertical mobility, this always leads to storage at lower depths, based on samples within the top 5cm of the peat cores within this study. The results from Aaby & Jacobsen (op. cit.) also suggest that copper, nickel, lead, zinc and probably iron are retained in surface layers in quantities reflecting the actual deposition. However, the evidence given above would appear to preclude the use of annual storage of elements in discrete peat layers as a record of actual deposition in the past, as suggested by Aaby & Jacobsen (op. cit.). The use of depositional data from contiguous slices above a given date or dated horizon would appear to be more appropriate.

A comparison between the ash residue profiles in fig. 5.4 and those presented in Aaby & Jacobsen (op. cit.) shows good agreement for both the hummock and hollow cores. The ash residue values are highest in the top 10cm in the hummock profiles and in the top 20cm of the hollow profiles, the majority of values being between 5-12%.

Regarding the composition of the inorganic fraction within the surface ombrotrophic peat layers, Aaby & Jacobsen (op. cit.) have assumed that the iron component within the inorganic fraction is derived solely from wind-blown field erosion. The evidence from the magnetic data given in sub-section 5.3.3 and more specifically from the micrographs presented in sub-section 5.3.4 suggests that this is not entirely accurate.

The concentration parameters in the magnetic profiles (figs. 5.12, 5.13, 5.16 and 5.17) notably the SIRM profiles for all the cores, regardless of site location and hummock-hollow microtopography, display a marked increase or take-off in values from about 10cm depth in all the cores, towards the surface. The take-off point, like that noted in previous cores is deeper on average in the hummock cores, for example at site 1, the take-off point is at 10cm in the hummock compared with 5-7.5cm in the hollow.

The increase noted within the concentration dependent parameters is associated with qualitative shifts in the interparametric ratios. For example, the ratio of $IRM_{300mT}$/SIRM compares the values obtained when a sample is magnetised in a forward field of 300mT and subsequently in a forward field of 850mT (SIRM). In pre-take-off samples from all cores, the ratio is either equal to, or approaching unity (0.96-1.0). However, in post-take-off samples, the ratio is lower, between 0.94-0.85 indicating that some percentage of magnetic minerals are not acquiring a remanence until higher backfields are applied. This appears to indicate that although a strong ferrimagnetic component still dominates the magnetic characteristics of the post-take-off samples, there is also an antiferromagnetic component characterised within the magnetic measurements of these samples, relative to the pre-take-off samples.

The difference between the pre- and post-take-off samples is also evident in the shape of the coercivity of remanence curves (figs. 5.14, 5.15, 5.18 and 5.19). The similarity of the post-take-off curves, regardless of site location or hummock-hollow microtopography, is apparent in the $(B_0)_{CR}$ values which lie between 36-40mT for all cores. It would appear from this that not only do the magnetic minerals present within the post-take-off have a common source, but also that there is a uniform deposition on the central bog plane in terms of magnetic mineral type. An estimate of the uniformity in concentration terms is a little less obvious.

## 5.4 Radiometric Data

### 5.4.1 Introduction

Since the beginning of the last decade, the use of short-lived radioisotopes, notably 210-Lead ($^{210}Pb$), in the construction of recent (ca.150 years) chronologies has increased markedly. In the majority of the

early papers on $^{210}Pb$ chronology, for example Krishnaswamy et al. (1971), Koide et al. (1973) and Robbins & Edgington (1975), the methods used assumed a constant rate of sediment accumulation, and that the **unsupported** $^{210}Pb$ or 'excess' $^{210}Pb$ activity declines exponentially down through the core. There is still some doubt surrounding the precise nature of the process by which $^{210}Pb$ is deposited in lake sediments, therefore, $^{210}Pb$ data from different sites with varying sedimentation rates are interpreted by different authors in different ways. The two main models used in the determination of $^{210}Pb$ chronologies are the **constant initial concentration** of **unsupported** $^{210}Pb$ (CIC model) and the **constant rate of supply** of **unsupported** $^{210}Pb$ (CRS model). Both models are outlined briefly below.

Even more recently, the $^{210}Pb$ technique has been applied to surface peats, for example Oldfield et al. (1979b), Aaby et al. (1979), El-Daoushy et al. (1982), El-Daoushy & Tolonen (1982) and Malmer & Holm (1984). The majority of this work is based on the CRS model using the assumptions outlined below.

210-Lead, with a half-life ($t_{\frac{1}{2}}$) of 22.26 years, is a member of the 238-Uranium ($^{238}U$) decay series. Disintegration of the intermediate isotope, 226-Radium ($^{226}Ra$), with a half-life of 1622 years, yields the inert gas 222-Radon ($^{222}Rn$) with a half-life of 3.83 days. This then decays through a series of short-lived isotopes to $^{210}Pb$. 226-Radium is supplied to the lake sediments and peat bogs by in situ decay and in the case of lake sediments, erosive input. The $^{210}Pb$ formed by the in situ decay of $^{226}Ra$ is termed **supported** $^{210}Pb$ and is normally assumed to be in radioactive equilibrium with the radium. This equilibrium is disturbed by the supply of **unsupported** $^{210}Pb$ from other sources. Three main pathways have been outlined for the deposition of **unsupported** $^{210}Pb$ in lake sediments: direct

atmospheric fall-out by dry or wet deposition, indirect atmospheric fall-out via the catchment, and $^{222}Rn$ decay in the water column (Oldfield & Appleby, 1984a). The indirect atmospheric component may further be sub-divided into two components, one with a short residence time in the catchment soils due to drainage, and the other with a longer residence time. In ombrotrophic peat bogs, the last two pathways are not valid for the deposition of $^{210}Pb$ onto the bog surface. However, additional factors such as the mobility of lead within the hummock-hollow microenvironment (Pakarinen & Tolonen, 1977a), have to be taken into consideration. The principal source is, however, taken to be direct atmospheric fall-out, although the importance of the other sources has not been extensively evaluated (Oldfield & Appleby, op. cit.).

In dating by $^{210}Pb$, only the **unsupported $^{210}Pb$** component is used, since once incorporated into the sediment it decays exponentially with time in accordance with its radioactive half-life:

$$k = \frac{\ln 2}{22.26} = 0.03114 \qquad [5.1]$$

The total residual **unsupported $^{210}Pb$** beneath depth x (A(x)) is calculated by numerical integration of the **unsupported $^{210}Pb$** concentration with respect to the cumulated dry mass (sub-section 5.2.3).

When the $^{210}Pb$ activity is plotted against depth in the core, as distinct from cumulative dry mass, non-linearities in the profile may appear near the surface, ranging from depressed $^{210}Pb$ concentrations in the top few centimetres to strongly 'kinked' profiles exhibiting non-monotonic behaviour (cf. Koide et al., 1973; Oldfield et al., 1978b). One approach is to interpret the non-linearities by assuming that there is a constant net rate of supply (CRS) of $^{210}Pb$ to the bog surface, irrespective

of changes which may have occurred in the net dry mass sedimentation rate. The procedure for calculating $^{210}Pb$ dates using the CRS model was first outlined by Goldberg (1963) and is set out in detail in Appleby & Oldfield (1978). Although inflected and non-monotonic profiles may be expected if there is a varying sedimentation rate but a constant supply of $^{210}Pb$, as in the CRS model, other possible causes include post-depositional redistribution of lead (Oldfield et al., 1979b), hence the use of hollow or pool cores, and loss of organic matter via respiration in the 'live' layer.

An alternative to the CRS model, more specifically in terms of lake sediments, is the constant initial concentration model (CIC) or constant initial specific activity model (Robbins, 1978) used by earlier authors, for example Pennington et al. (1976). It is based on the assumption that all sediments have the same initial **unsupported** $^{210}Pb$ concentration and that the present **unsupported** $^{210}Pb$ concentration (C) in a sediment column will vary exponentially with age (t). There are a number of hypotheses under which the CIC calculations are feasible. The model assumes, in environments where sedimentation is dominated by allocthonous particle input, that the main delivery pathway for **unsupported** $^{210}Pb$ is inwash from the catchment ($C_2$). The **unsupported** $^{210}Pb$ reaches the sediment in particle-associated form and the initial **unsupported** $^{210}Pb$ concentration of the sediment is constant for all depths. The second hypothesis assumes, especially in environments where sedimentation is dominated by autochthonous material derived from primary production within the lake waters, that increased flux of sedimentary particulates from the water column will remove proportionally increased amounts of $^{210}Pb$ from the water to the sediment surface. Finally, a third hypothesis assumes a constant sedimentation rate and constant $^{210}Pb$ supply to the lake, whereby sediments have the same initial concentration, and that varying

sedimentation rates in different parts of the lake and at different times simply reflect varying patterns of sediment deposition.

An important point to note is that when the dry mass sedimentation rate in a lake has, in reality, been constant or nearly so, the CIC and CRS $^{210}Pb$ chronologies will be similar and the precise nature of the $^{210}Pb$ supply mechanism is immaterial. However, where the sedimentation rate may have varied, the choice of model is critical (Oldfield & Appleby, 1984b). In the case of ombrotrophic peat bogs that choice appears to be limited to the CRS model, given the assumptions of the CIC model. At present the CRS model appears to be the only credible method of dating recent ombrotrophic peat given the assumptions above (Oldfield, pers. comm.). The integrity of the model and its potential in dating peat, are still being investigated.

A more thorough and detailed account of the alternative assumptions of the $^{210}Pb$ models and their critique is given in Appleby & Oldfield (1978) and Oldfield & Appleby (op. cit.). The $^{210}Pb$ chronology of DMHol2 is presented in sub-section 5.4.2 and discussed in sub-section 5.4.6. Using the $^{210}Pb$ dates, estimated deposition rates of lead, iron and copper are calculated from the formula given in Appleby & Oldfield (1979):

$$F(t) = r(t)c(x) \qquad [5.2]$$

where $F(t)$ = Total flux rate to the sediment of age t and depth x

$r(t)$ = Sedimentation rate at time t

$c(x)$ = Total concentration ($\mu g.g^{-1}$) at depth x

The estimated deposition rates are presented in sub-section 5.4.5. The $^{210}Pb$ chronology for Mo-I-Rana is presented in sub-section 5.5.6 along with $^{137}Cs$ data.

5.4.2 <u>210-Lead Results</u>

The **unsupported** $^{210}Pb$ and **supported** $^{210}Pb$ ($^{226}Ra$) are presented in

fig. 5.20a. The peak concentration of **unsupported** $^{210}Pb$ lies between 2.5-5 cm (11.4±0.49 $pCi.g^{-1}$). The $^{210}Pb$ concentrations below the peak decrease exponentially to a value of 0.16±0.05 $pCi.g^{-1}$ between 17.5-20cm. The percentage error of the $^{210}Pb$ concentrations increases from 4% at the surface to 30% at 20cm. In contrast, the **supported** $^{210}Pb$ component, as approximated by $^{226}Ra$, displays no regular pattern within the profile above 17.5cm. Below 17.5cm the $^{226}Ra$ count is too low for an accurate measurement. An important point to note is that the $^{210}Pb$ and $^{226}Ra$ are not quite in equilibrium at 20cm, although the $^{210}Pb$ count from the next slice (20-22.5cm) would be too low to measure accurately. The difference is taken account of within the calculation of the age-depth curve and $^{210}Pb$ chronology, and is significant enough to make the oldest date for the core some 45 years younger when accounted for (sub-section 5.4.4).

5.4.3 137-Caesium Results

The concentrations of $^{137}Cs$ and $^{241}Am$ are plotted in fig. 5.20b. The $^{137}Cs$ peak, similar to $^{210}Pb$ is between 2.5cm and 5cm (7.73±0.62 $pCi.g^{-1}$). Concentrations decrease down-profile to a minimum value of 0.57±0.05 $pCi.g^{-1}$ between 17.5cm and 20cm. The error bars are consistently below 10% throughout the profile.

The core also contains a small, but significant amount of $^{241}Am$ between 2.5cm and 10cm. The peak concentration is at 5-7.5cm (0.12±0.01 $pCi.g^{-1}$) with concentrations of 0.04 $pCi.g^{-1}$ and 0.06 $pCi.g^{-1}$ above and below it respectively.

5.4.4 210-Lead Chronology

Using both the CRS and CIC models the age-depth curves for DMHol2 are plotted in fig. 5.21. The age-depth curve using the CRS model is transposed upwards in order to present the error bars for each point which might otherwise have been masked by those from the CIC curve. From 0-

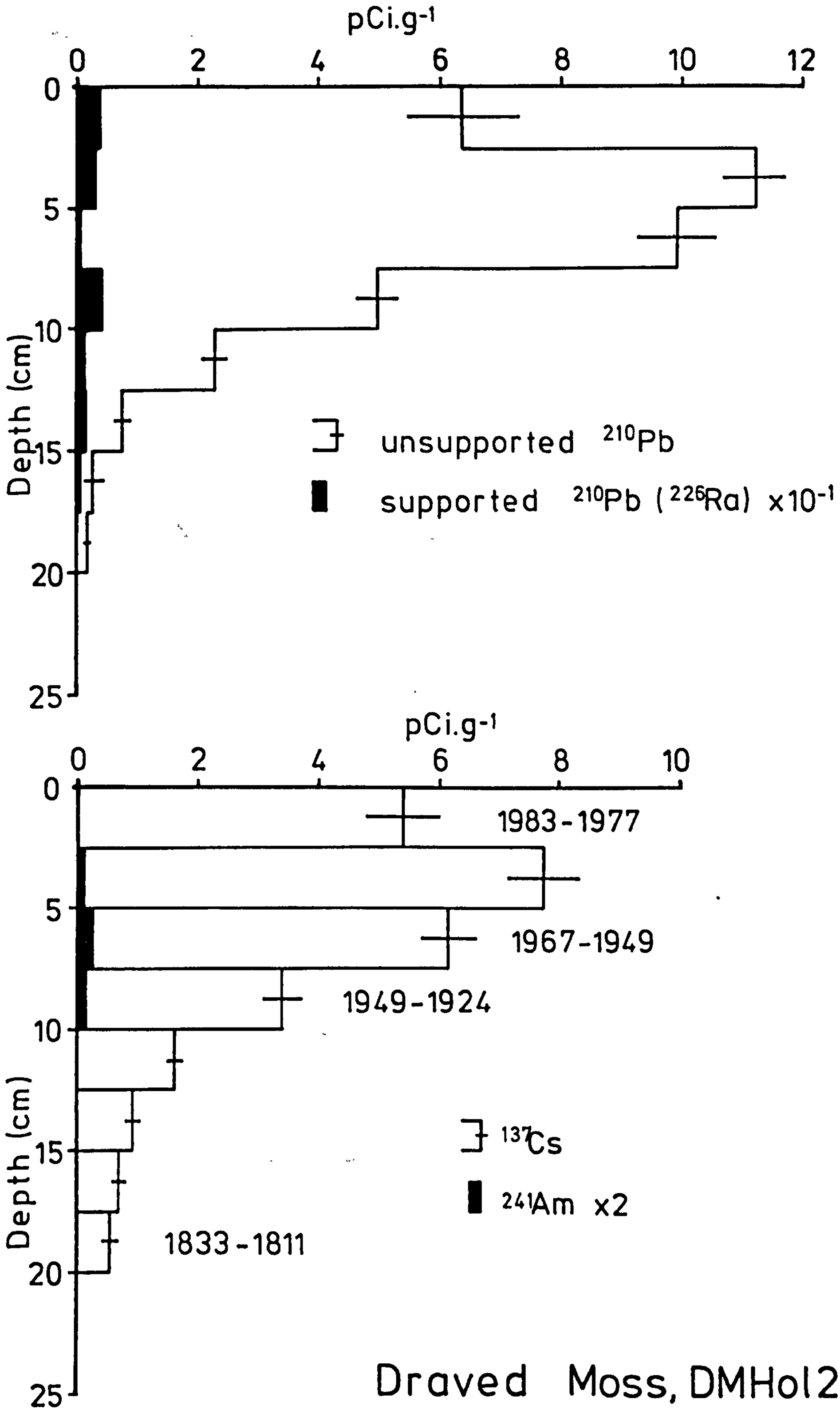


**Figure 5.20** Radioisotope profiles for DMHol2, Draved Moss
a) $^{210}Pb$ and $^{226}Ra$ concentration profiles
b) $^{137}Cs$ and $^{241}Am$ concentration profiles. With $^{210}Pb$ dates at selected intervals.
Both $^{210}Pb$ and $^{137}Cs$ are shown with error bars.

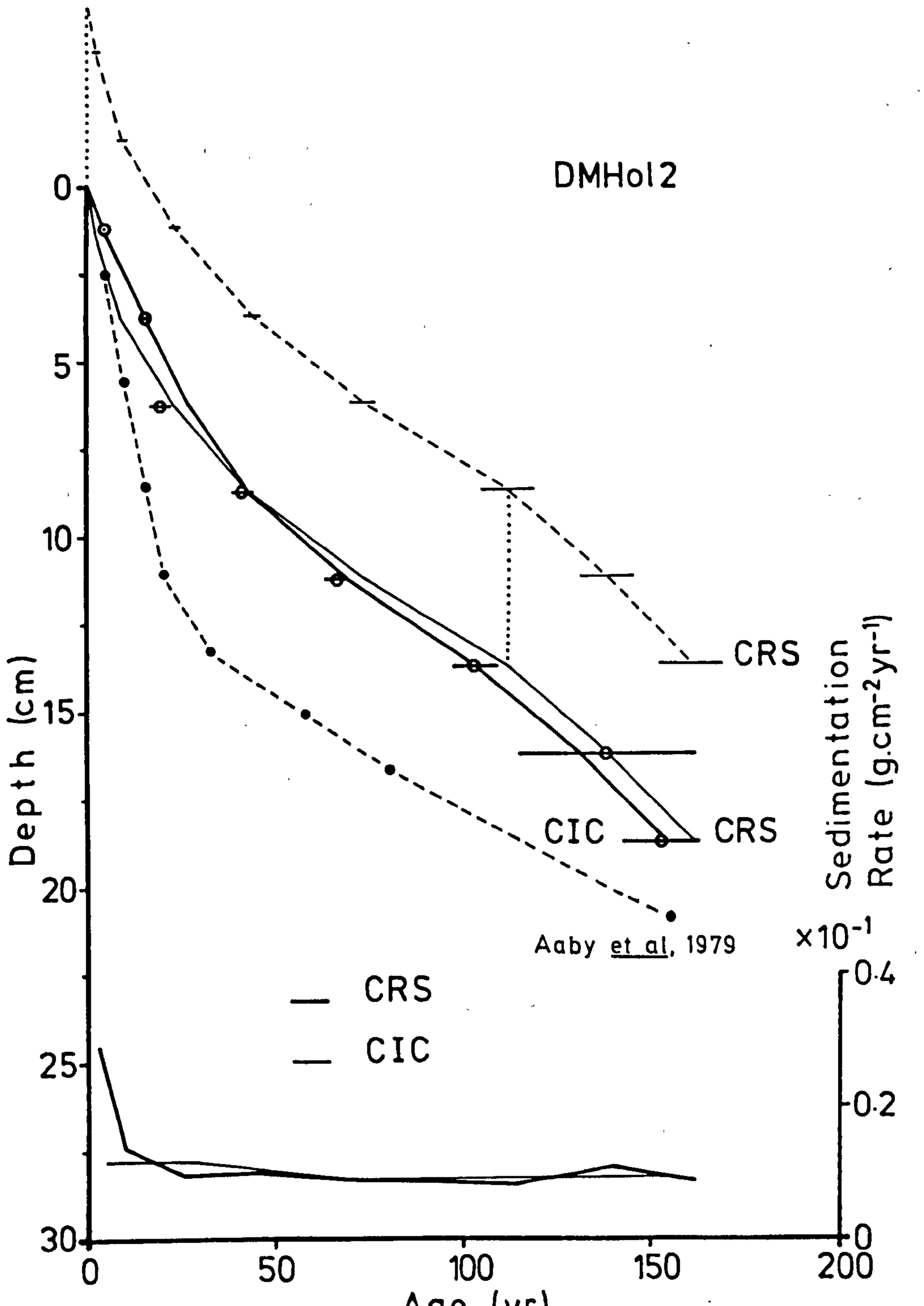


**Figure 5.21** Age/depth curves of CRS and CIC models for DMHol2, Draved Moss. With $^{210}Pb$ sedimentation rate for both models. The CRS curve is also shown displaced upwards in order to display the error bars. The broken line with solid dots is the age/depth curve from Aaby et al.(1979).

8.25cm the CRS curve gives a consistently younger age for each point, whereas below 8.25cm to a depth of 20cm, the CRS curve gives consistently older dates when compared with the CIC curve. The sedimentation curves of both models are very similar below 3.75cm with an average value of 0.0091 $g.cm^{-2}yr^{-1}$. Above 3.75cm the sedimentation rate differs markedly between the two models. In the CIC model, sedimentation remains constant at 0.0119 $g.cm^{-2}yr^{-1}$, whilst for the CRS model the rate increases from 0.0131 $g.cm^{-2}yr^{-1}$ at 3.75cm to 0.0286 $g.cm^{-2}yr^{-1}$ at the surface. The latter is probably an over-estimate given the possible loss of organic matter, and hence mass, within the 'live' layer by $CO_2$ respiration (Appleby & Oldfield, pers. comm.). The percentage standard error of the top sample is 13.8% which could potentially reduce the rate to as low as 0.0247 $g.cm^{-2}yr^{-1}$ at the surface. Using the curvilinear relationship of the CRS age-depth curve, the number of years represented by each slice is calculated by the computer software and the results are presented in Table 5.3. From the number of years represented by each slice (CRS Model) the growth rate of the peat is calculated and the results are also presented in Table 5.3. Using the growth rates and sedimentation rates, the deposition of SIRM, iron, lead and copper may therefore be estimated.

5.4.5 Estimated Deposition Rates

The estimated deposition rates of SIRM, iron, lead and copper are presented in fig. 5.22 (SIRM and iron) and 5.23 (lead and copper). The SIRM and iron deposition profiles are very similar, with background (pre-1811) deposition in both cores being low in comparison with the rest of the respective cores, 0.07 $10^{-6}Am^2yr^{-1}$ for SIRM and 29.2 $mg.m^{-2}yr^{-1}$ for iron. Between 1811 and 1924 the values for both profiles barely increase from 0.08 $10^{-6}Am^2yr^{-1}$ to 0.47 $10^{-6}Am^2yr^{-1}$ for SIRM and from 30.5 $mg.m^{-2}yr^{-1}$ to 47.3 $mg.m^{-2}yr^{-1}$ for iron. From 1924 to 1977 there is an

**Table 5.3** 210-Lead Dating of DMHol2, Draved Moss, Southern Finland and Mo-I-Rana, Northern Norway. Growth rates are based on the CRS dates. The data for Mo-I-Rana is discussed in sub-section 5.5.6.

| Depth (cm) | CRS Age Range (years) | CRS (years) | CIC (years) | Growth Rate ($mm.yr^{-1}$) |
|---|---|---|---|---|
| **DMHol2** | | | | |
| 0-2.5 | 0-5.5 | 5.5 | 10.5 | 4.55±1.7 |
| 2.5-5 | 5.5-16 | 10.5 | 11 | 2.38±1.1 |
| 5-7.5 | 16-33.5 | 17.5 | 13.5 | 1.43±0.04 |
| 7.5-10 | 33.5-59 | 25.5 | 21 | 0.98±0.02 |
| 10-12.5 | 59-93 | 34 | 30 | 0.74±0.05 |
| 12.5-15 | 93-125.5 | 32.5 | 31 | 0.77±0.27 |
| 15-17.5 | 125.5-150 | 24.5 | 25.5 | 1.02±0.44 |
| 17.5-20 | 150-172 | 22 | 23 | 1.14±0.5 |
| **Mo-I-Rana** | | | | |
| 0-1 | 0-8.2 | 8.2 | 11 | 1.22±0.2 |
| 1-2.5 | 8.2-20.5 | 12.3 | 16.5 | |
| 2.5-5 | 20.5-47 | 26.5 | 32 | 0.94±0.18 |
| 5-7.5 | 47-83.5 | 36.5 | 27.5 | 0.68±0.02 |
| 7.5-10 | 83.5-118.5 | 35 | 46 | 0.71±0.27 |
| 10-13 | 118.5-209 | 90.5 | 62 | 0.33±0.04 |

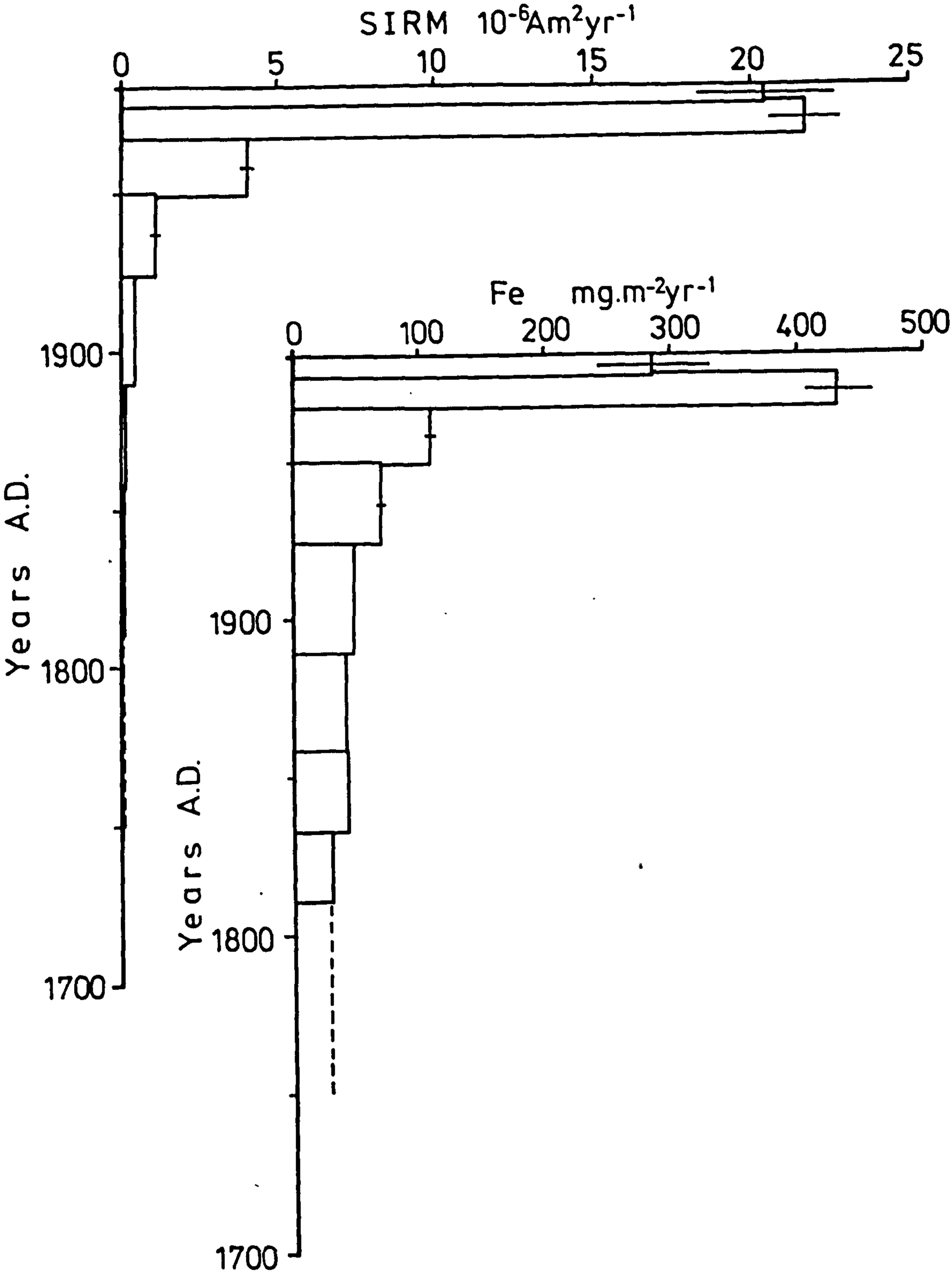


# Draved Moss, DMHol2

**Figure 5.22** SIRM and iron deposition profiles (with error bars) for DMHol2, Draved Moss

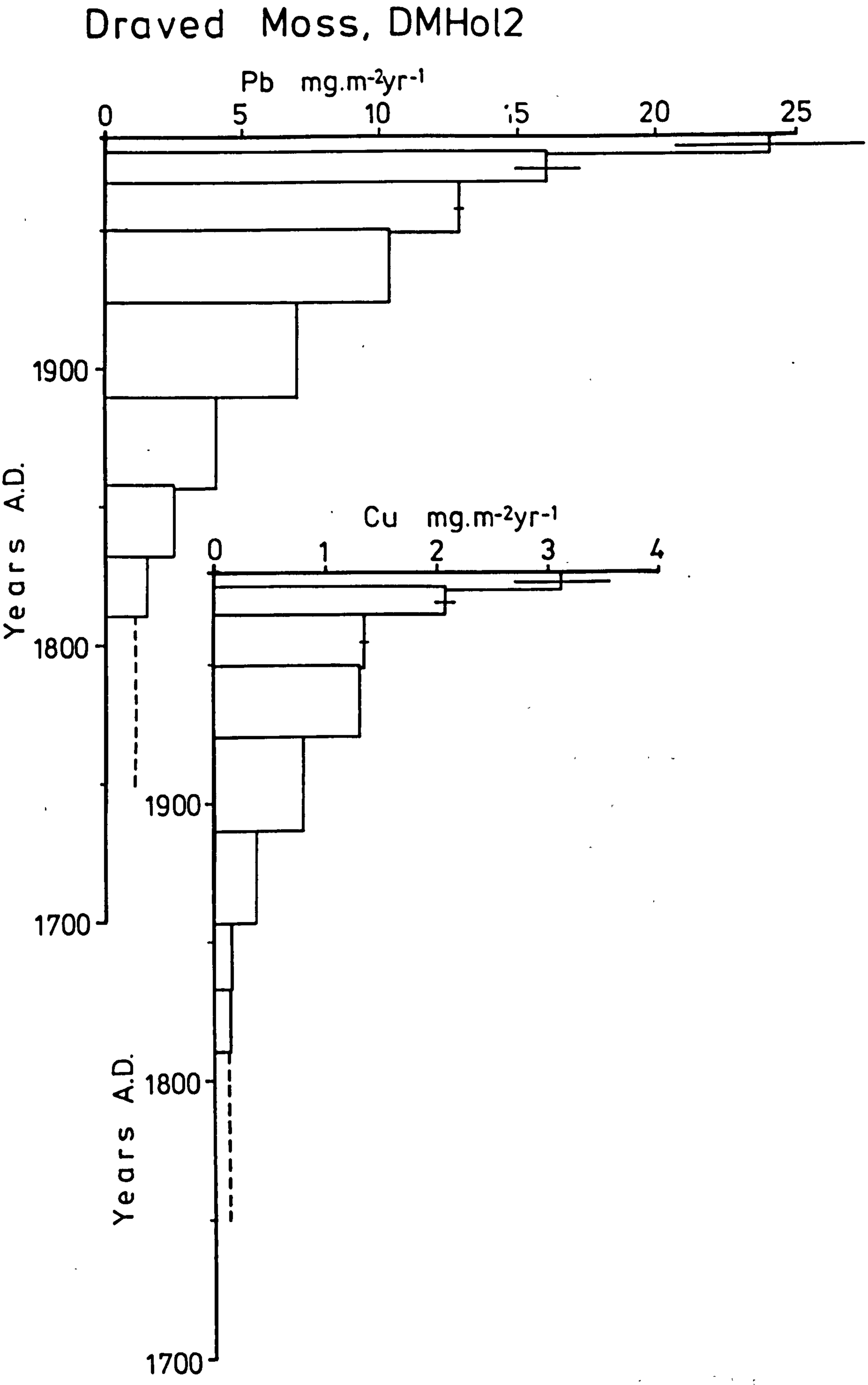


**Figure 5.23** Lead and copper deposition profiles (with error bars) for DMHol2, Draved Moss

exponential increase in deposition within both profiles, an increase of 46 times up to 21.6 $10^{-6}Am^2yr^{-1}$ for SIRM and an increase of 9 times for iron up to 429 $mg.m^{-2}yr^{-1}$. Both profiles display a decrease in deposition between 1977-1983, down to 20.3 $10^{-6}Am^2yr^{-1}$ for SIRM and to 281 $mg.m^{-2}yr^{-1}$ for iron.

In contrast, the lead and copper profiles peak at the surface, between 1977 and 1983 (fig. 5.23). Below 1811 the background deposition of lead is estimated to be 1.02 $mg.m^{-2}yr^{-1}$ whilst for copper it is less than or equal to 0.13 $mg.m^{-2}yr^{-1}$. Both cores display an approximately linear increase from 1811 up to 1977, 1.5 $mg.m^{-2}yr^{-1}$ to 15.8 $mg.m^{-2}yr^{-1}$ for lead and from 0.14 $mg.m^{-2}yr^{-1}$ to 2.08 $mg.m^{-2}yr^{-1}$ for copper. The surface peak of lead is 23.9 $mg.m^{-2}yr^{-1}$, an increase of 1.5 times from the preceeding sample, similarly for copper the increase is 1.5 times, to 3.12 $mg.m^{-2}yr^{-1}$.

In the case of SIRM and iron, the peak deposition between 1967 and 1978 was over 300 times and 14.7 times higher than the background or pre-1811 estimated deposition rates. The difference between the surface sample deposition and background deposition was 290 times for SIRM and 9.6 times for iron. For lead and copper the increase between the pre-1811 deposition and peak surface deposition rates is 23 times and 22 times respectively.

5.4.6 Discussion

The discussion is based on three themes: first, a discussion of the $^{210}Pb$ chronology in the context of previously published material; second, an interpretation and discussion of the $^{137}Cs$ data; and third, a discussion of the estimated deposition rates in the context of pre-existing material.

Oldfield et al. (1979b) suggested that in British peats the total unsupported $^{210}Pb$ accumulation was 4 times greater in the hollows compared with neighbouring hummocks. This was interpreted as evidence

of sub-lateral mobility between hummock and pool, either as a result of surface run-off, sub-surface diffusion or both. The downward mobility of lead accords with the indirect evidence of total lead concentrations noted in Pakarinen & Tolonen (1977a) and this study (sub-section 5.3.2, figs. 5.7-5.10). The use of hummock profiles for $^{210}Pb$ dating is noted in Aaby et al. (1979), El-Daoushy et al. (1982) and El-Daoushy & Tolonen (1982). The latter two papers present $^{210}Pb$ in comparison with moss increment dates whilst the results of Aaby et al. (op. cit.) are not published. The results of El-Daoushy et al. (op. cit.) show the $^{210}Pb$ dates (CRS model) to be in strong agreement with comparable moss increment dates. However, more recent results from a Sphagnum hummock at Varrassuo, southern Finland show that the $^{210}Pb$ dates (CRS model) are consistently and increasingly younger than comparable moss increment dates (fig. 5.24). The difference at the oldest comparable depth is 52 years, with the $^{210}Pb$ date giving an age of 67 years before 1983 and the moss increment date giving an age of 119 years before 1983.

Figure 5.22 displays a good agreement between the CRS and CIC models in terms of age-depth relationships. This suggests that the sedimentation rate with the peat core has been fairly constant over the time-span involved. The cumulative dry mass curve for DMHol2, presented in fig. 5.6, appears to confirm this observation.

The $^{137}Cs$ profile presented in fig. 5.20b fails to display the profile characteristic of many lake sediments which appear to parallel the monitored fall-out of $^{137}Cs$ since 1954. This 'typical' $^{137}Cs$ profile includes a sub-surface peak around 1963 corresponding to the peak fall-out years (Cambray et al., 1971). The profile does however display a sub-surface peak, dispaced upwards to between 1978 and 1967, which contrast with the surface peaks in $^{137}Cs$ from Lough Fea Bog, Northern Ireland and Bolton

# Varrassuo Bog, Southern Finland

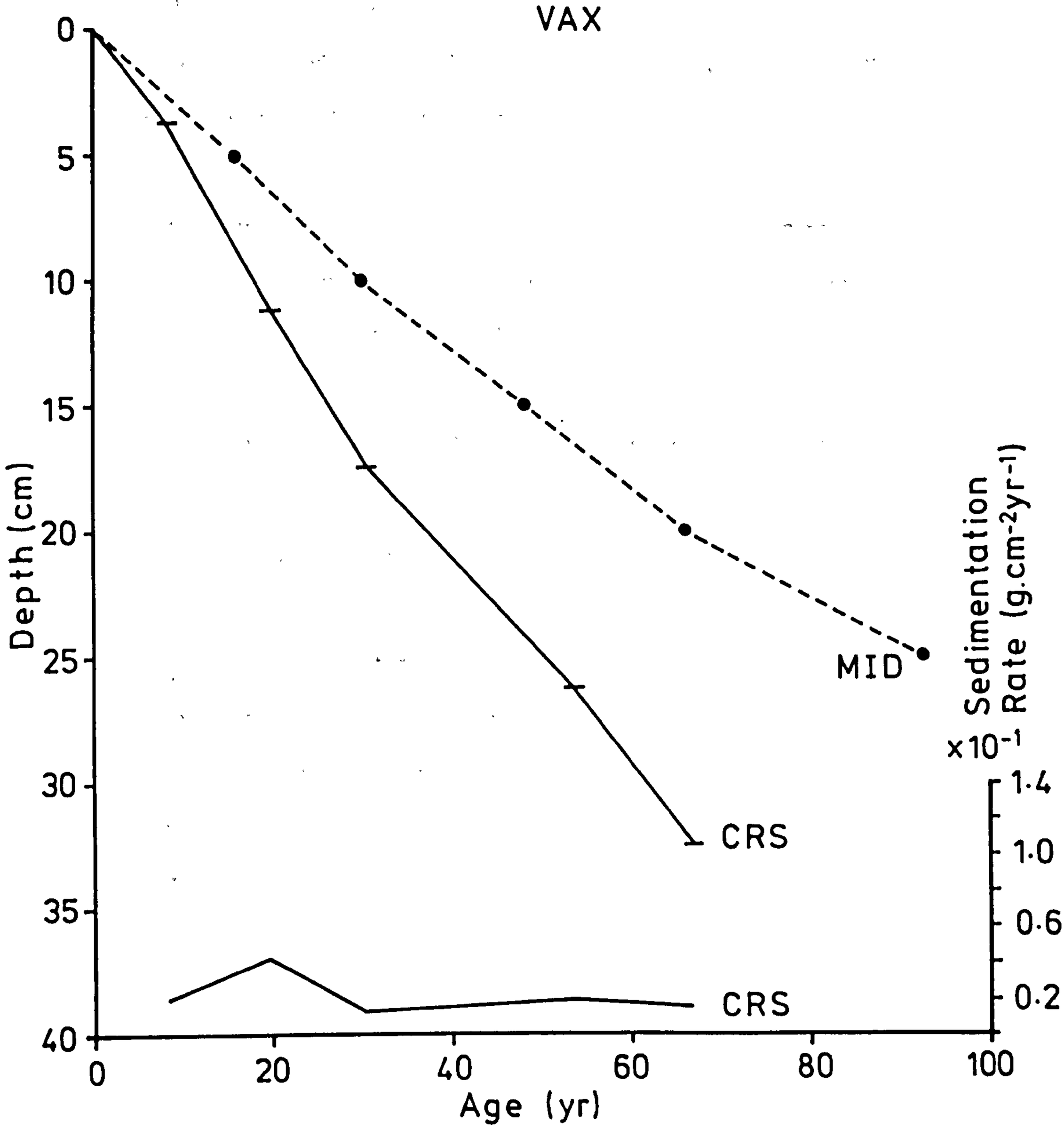


**Figure 5.24** $^{210}Pb$ dates and moss increment dates for Varrassuo, southern Finland. With the $^{210}Pb$ sedimentation rate shown below.

Fell Moss, England, noted by Oldfield et al. (op. cit.). It is important to note that the profiles displayed in Oldfield et al. (op. cit.) come from Sphagnum hummocks, whereas DMHol2 is a Sphagnum hollow.

The presence of detectable $^{137}Cs$ well below 1954 in DMHol2 indicates downward diffusion in addition to any inferred active uptake at the surface, assuming the displaced peak to be evidence of uptake by the living component of the peat (Oldfield et al., op. cit.). The presence of $^{137}Cs$ down to at least 20cm (between 1833 and 1811) supports the conclusion of Oldfield et al. (op. cit.) that $^{137}Cs$ assay does not provide a valid dating method in ombrotrophic peat.

The presence of $^{241}Am$, derived from nuclear power generation, within the peat core DMHol2, may possibly be explained by the close proximity of Draved Moss to the coast, 20km from the North Sea. Cambray & Eakins (1982) established a relationship between marine-derived sodium and certain radionuclides, for example $^{238}Pu$ and $^{241}Am$. Of the possible transfer mechanisms noted by Cambray & Eakins (op. cit.), direct suspension of the sea by the wind in the form of spray, and re-suspension from inter-tidal sediments by the wind appear to be the most likely causes of excess deposition on the bog surface.

In order to fully assess the significance of a comparison between the deposition rates of lead presented by Aaby et al. (op. cit.) and those presented above, a comparison of the age-depth profiles for the two sets of data is given in fig. 5.21. Above 12.5cm the age-depth profile from Aaby et al (op. cit.) is consistently and increasingly younger than either the CRS or CIC profiles. Below 12.5cm the age remains younger for the Aaby et al. profile although the difference in age between the curves becomes increasingly smaller towards the base of the profiles. If both curves are extrapolated beyond the lowest point, the intersection is at approximately

21.5cm or around 1809. The difference in dates from the two curves may be explained by the strong concave curvilinear relationship noted within both the CRS and CIC curves of the present data set, presented in fig. 5.21.

When the lead deposition rates are compared between the two studies, the patterns of deposition below 1950 are found to be in good agreement with each other, whilst those above 1950 are in marked contrast to each other. Before 1800 Aaby et al. (op. cit.) estimate a constant rate of 0.5mg Pb $m^{-2}yr^{-1}$ compared with 1.02mg Pb $m^{-2}yr^{-1}$ in the present study. Between 1800 and 1900 deposition increases to around 5mg Pb $m^{-2}yr^{-1}$ in the published material compared with the present estimated mean of 3.73mg Pb $m^{-2}yr^{-1}$ between 1811 and 1900. From 1900 to 1950 the estimated deposition from the published source increases by a factor of 3 to about 15mg Pb $m^{-2}yr^{-1}$, which compares with an increase from 6.9mg Pb $m^{-2}yr^{-1}$ to 12.8mg Pb $m^{-2}yr^{-1}$ between 1900 and 1950 for the present study. Above 1950 Aaby et al. (op. cit.) estimate that deposition increases exponentially up to a peak of ca.60mg Pb $m^{-2}yr^{-1}$ in the late 1960's before decreasing to less than 50mg Pb $m^{-2}yr^{-1}$ by 1978. This contrasts markedly with the profile presented in fig. 5.23 which displays lead deposition increasing rapidly above 1950 to a peak of 23.9mg Pb $m^{-2}yr^{-1}$ at the surface. A possible explanation for this marked contrast in post-1950 deposition levels is given by the marked difference in sedimentation rates for that period (fig. 5.23) and hinted at by the age-depth curves (fig. 5.23). The period of divergence between the age-depth curves of the two studies is between 1950 and 1978, with the greatest divergence being towards the older date. Therefore, the sedimentation rates at the surface of the hollow core used by Aaby et al. (op. cit.) would have been estimated to be double that noted in the present study, given that total lead concentrations are

comparable, which the evidence from Table 5.2 and from DMHol2 2.5-5cm suggests is the case. It must also be remembered that Aaby et al. (op. cit.) do not present their $^{210}Pb$ dating model, which could well account for some of the variations, especially at the surface.

## 5.5 Mo-I-Rana

### 5.5.1 Core Location and Stratigraphy

Norway currently has some 3 million hectares of bogland, with 2.1 million hectares below the treeline, in lowland and upland areas which comprise some 50 per cent of the total area of the country. Of this, 61.5% is moss-bog, with the remaining 38.5% comprising mainly grass-bog with forest-, heather- and brushwood-bog. Nordland, the county in which Mo-I-Rana is situated, has 4.62% of its total area covered by bogland and 13.4% of the total area below the treeline (Hornburg, 1972).

The peat core, taken from a bog within the zone of main aapa mires (Eurola & Rühijarvi, 1961) was extracted by means of a Damman corer and spans the top 55cm of the bog. The total depth of peat at the site is undetermined. The site (66°04'N 13°40'E) is 5km east of Korgen and about 36km southeast of Mo-I-Rana (fig. 5.3). The stratigraphic indicators: humification, bulk density, ash residue and colour are presented in fig. 5.25. The bulk density profile decreases from high values ($263gdm^{-3}$) to a minimum at 1-2.5cm ($41.9gdm^{-3}$), immediately below the surface. The surface bulk density value (0-1cm) increases to $110gdm^{-3}$. The ash residue profile is restricted to the top 12.5cm. Within this depth range the percentage ash increases from 2.2% (13cm) to a sub-surface peak of 4.96% (5-7.5cm), before decreasing towards the surface. The surface sample, 0-1cm, displays the highest percentage value at 6.2%.

A cumulative dry mass against depth curve for the peat core is

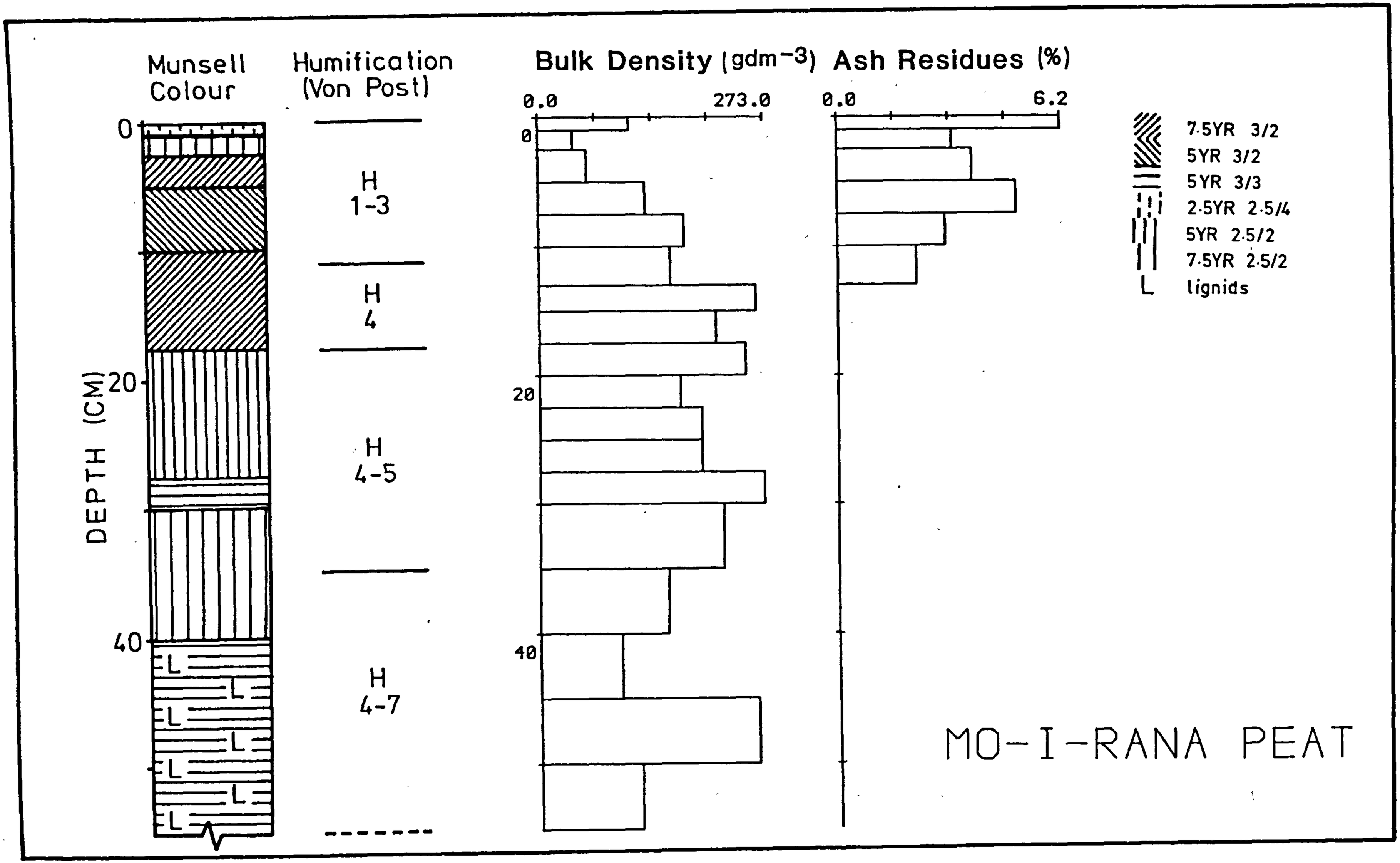


**Figure 5.25** Stratigraphy of Mo-I-Rana peat core

plotted in fig. 5.26. Within the top 10cm the curve is noticeably concave. Compared with previously plotted profiles, for example Draved Moss (fig. 5.6), the peat has accumulated much more rapidly against depth within the Mo-I-Rana peat core, 1.8 times faster than in DMHum2 over 50cm and 2.35 times faster than DMHol2 over 45cm.

5.5.2 Chemical Results

Profiles of the elements: iron, nickel, copper, zinc and lead are presented in fig. 5.27. The iron profile displays high concentrations below 35cm (2100-2377$\mu g.g^{-1}$) with two further peaks higher up the profile. The lower of the two peaks, at 7.5-13cm displays the highest iron concentrations within the core, 2781-2943$\mu g.g^{-1}$. The other peak is within the surface sample, 0-1cm, with a concentration of 1798$\mu g.g^{-1}$.

Total lead concentrations within the peat core are predominantly undetectable below 15cm. Above 15cm the lead concentrations rise steadily to 18.3$\mu g.g^{-1}$ at 1-2.5cm, before increasing by a factor of 2.3 at the surface. In contrast, the copper profile exhibits detectable concentrations throughout the profile with a diffuse peak between 7.5-20cm. A surface peak is also evident within the copper profile (6.6$\mu g.g^{-1}$), 1.5 times higher than the preceeding sample. The zinc profile displays what is perhaps the most regular and readily definable profile. Below 13cm, zinc concentrations are low, between 1.5-2.9$\mu g.g^{-1}$. Above 13cm the concentrations begin to rise gradually to 5cm before increasing exponentially to a surface peak of 36.4$\mu g.g^{-1}$. The nickel profile displays two areas of interest: the first being a peak between 20-30cm (26.0-32.4$\mu g.g^{-1}$), and the second being a peak in the surface sample representing an increase of 4.5 times from the preceeding sample.

A noticeable feature in all the element profiles is the surface sample

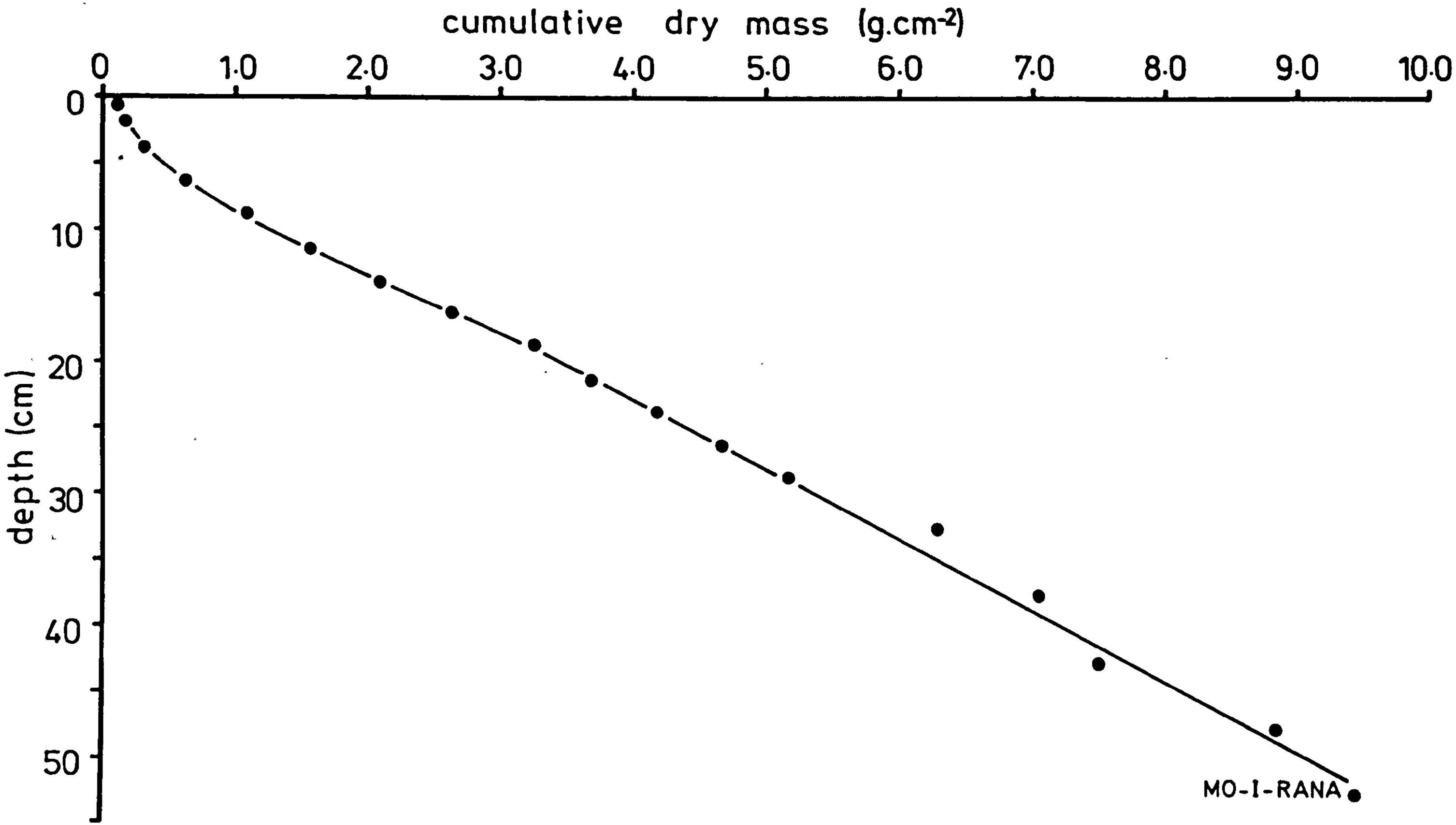


**Figure 5.26** Cumulative dry mass curve for Mo-I-Rana peat core

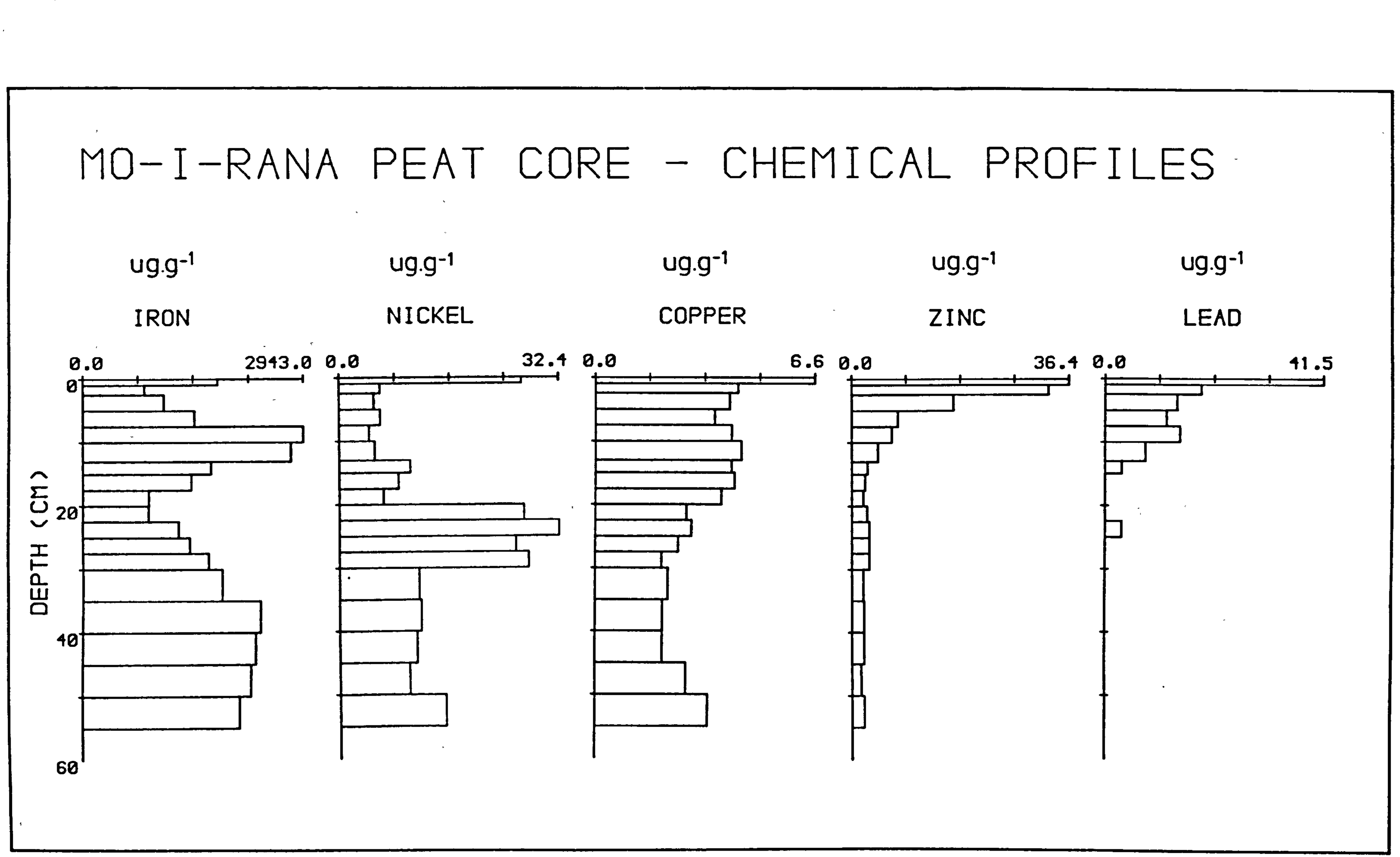


**Figure 5.27** Chemical profiles for Mo-I-Rana peat core

peak concentration. For some elements, such as zinc, the surface sample peak has been noted in the majority of zinc profiles from other Scandinavian sites. However, for other elements such as nickel and lead, this peak is contrary to the majority of profiles noted in other Scandinavian sites. This feature is, however, consistent with sites such as Varrassuo, which are in close proximity to a source of anthropogenic emissions.

5.5.3 Magnetic Results

The magnetic profiles of the Mo-I-Rana peat core are presented in fig. 5.28. These include X, $X_{fd}$ (for the top two surface samples, 0-2.5cm), ARM, $IRM_{300mT}$, SIRM, interparametric ratios and the four backfield ratios, $IRM_{-20mT}/SIRM$, $IRM_{-40mT}/SIRM$, $IRM_{-100mT}/SIRM$ and $IRM_{-300mT}/SIRM$. Below 25cm the scale of the SIRM profile has been increased in order to display variations within the SIRM values of low concentration samples.

The X profile displays positive values above 13cm, gradually increasing towards the surface. There is a 4.8 times increase in concentrations at the surface compared with the preceeding sample. The $X_{fd}$ ratio of the surface samples (0-2.5cm) is low, between 1.1-1.5%. ARM measurements below 30cm are close to the lower limits of detection for the magnetometer (0.34-0.73 $10^{-6}Am^2kg^{-1}$) and are therefore omitted from the profile in order to avoid spurious points in the relevant interparametric ratios. The ARM profile displays the same exponential increase in values at the surface as the other concentration dependent parameters. The $IRM_{300mT}$ and SIRM profiles both display consistently low values below 10cm, in the case of SIRM the lower profile values are between 6.8-54.3 $10^{-6}Am^2kg^{-1}$. Above 10cm the SIRM values increase linearly to 1-2.5cm before increasing again, by a factor of 3.2 at the surface (1395 $10^{-6}Am^2kg^{-1}$). The take-off point within the SIRM profile is

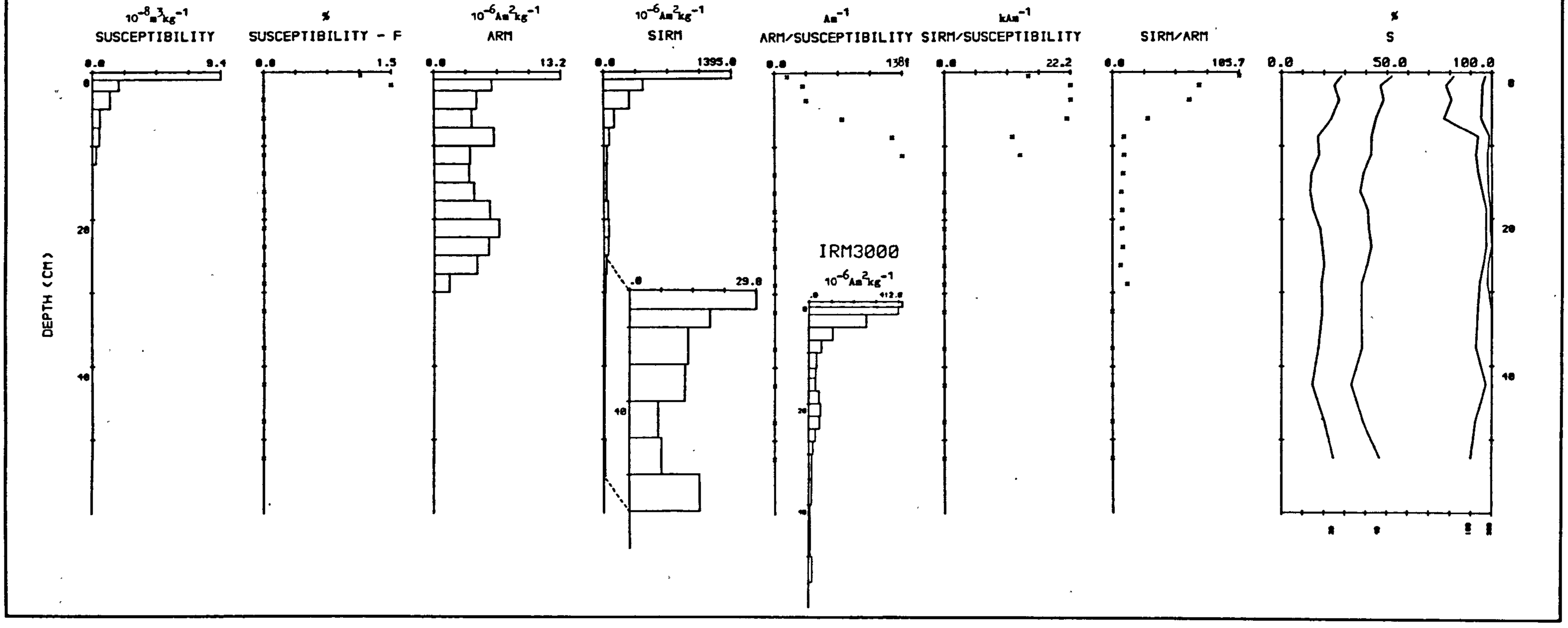


**Figure 5.28** Magnetic measurements for Mo-I-Rana peat core

probably at 5-7.5cm. The $IRM_{300mT}$ profile also displays a surface peak (419 $10^{-6}Am^2kg^{-1}$) although this is not nearly as large as the SIRM peak. The difference in the two profiles is reflected in the $IRM_{300mT}$/SIRM ratio which below 17.5cm is equal to unity. Between 1cm and 17.5cm the ratio varies between 0.94 and unity, however, in the surface sample the ratio decreases dramatically, to 0.3, the lowest value encountered for any peat sample measured within the context of the present study.

The interparametric ratios display decreasing ARM/X values and increasing SIRM/ARM values towards the surface, for samples above 10cm. The ARM/X values decrease from high values of $1381Am^{-1}$ at 10cm down to $140Am^{-1}$ at the surface, whilst the SIRM/ARM values increase from low values between 6.8-12.3 (below 10cm) to a surface peak of 106. The upper backfield ratios, $IRM_{-300mT}$/SIRM and especially $IRM_{-100mT}$/SIRM ('S' ratio) are distinctively harder above 10cm. The surface sample shows a distinct softening in all of the backfield ratios, though in the upper backfield ratios, $IRM_{-100mT}$/SIRM and $IRM_{-300mT}$/SIRM, this is relative to the hardness displayed by the other samples above 10cm

The coercivity of remanence curves for the Mo-I-Rana peat core have been divided into three groups (fig. 5.29). The first group consists of the top four samples (0-7.5cm), which are portrayed by individual curves, as is the preceeding sample, 7.5-10cm. The curve shape between 0-100mT of the top four samples is very similar, consisting of a shallow concave slope. The $(B_0)_{CR}$ values of these samples range from 39-47mT. The $(B_0)_{CR}$ values of the following group (7.5-35cm) are of a similar although slightly higher range, 44-51mT, although the curve shape is noticeably different. The individual curve of the sample from 7.5-10cm is concavo-convex, and the envelope of sample values within the second group encompasses curve shapes of this nature. From 35cm to 55cm the

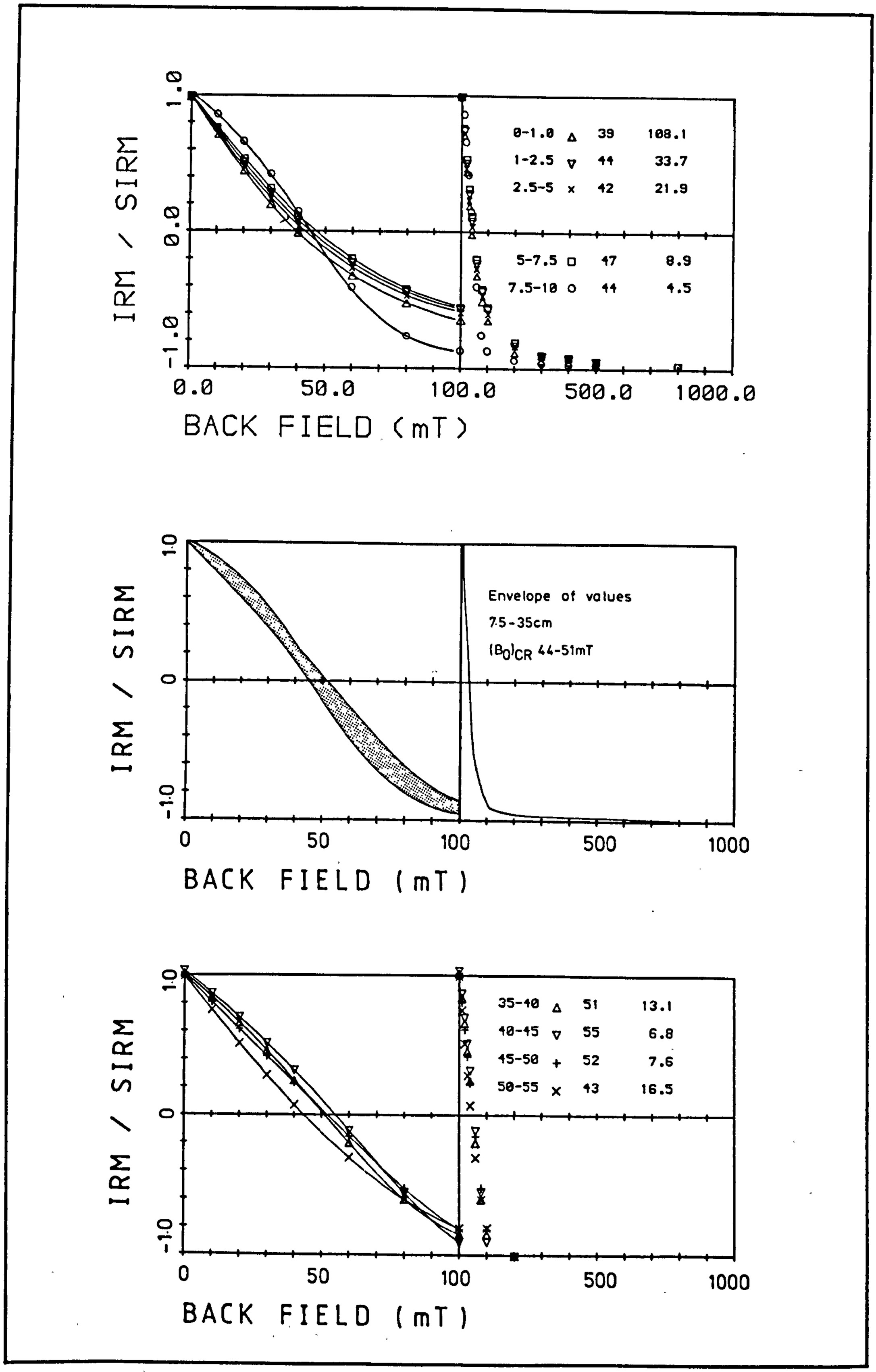


**Figure 5.29** Coercivity of remanence curves for Mo-I-Rana peat core

remanence curves alter shape again, with the curve between 0-100mT becoming almost linear in these samples. The $(B_0)_{CR}$ values are higher for this group than for the two previous groups, being between 51mT and 55mT, with the exception of the last sample, 50-55cm, which has a $(B_0)_{CR}$ value of 43mT.

5.5.4 Garnet Mica-Schist

In order to try and assess the influence of the local weathering product on the magnetic fraction of the inorganic component within the peat layers, a sample of the local bedrock, a garnet mica-schist, has been measured. The complete range of magnetic measurements, including backfields, were performed and the results tabulated in Table 5.4 (magnetic data) and plotted in fig. 5.30 (coercivity of remanence curves). The rock sample was crushed before measuring as a bulk sample, and subsequently powdered and separated into 'magnetic' and 'non-magnetic' fractions. Separation of the rock sample was achieved by a Frantz Isodynamic Magnetic Separator (model L1), which divides the sample into two components: more magnetic and less magnetic (Hutchinson, 1974). The separator was operated with a forward slope of 25° and a side tilt of 15° at increasingly higher amperage (0.1amps for magnetite through to 0.7amps for hornblendes and feldspars).

The 'magnetic' fraction (GMSmag) was then subjected to the same mineral magnetic characterisation as the bulk sample. The magnetic data for the 'magnetic' fraction (GMSmag) are presented in Table 5.4, and the coercivity of remanence curve is plotted in fig. 5.30. The mineral magnetic characterisation of the rock samples are in marked contrast to those of the peat samples (cf. fig. 5.28 and Table 5.4). The variance in the interparametric ratios, low SIRM/X and ARM/X and SIRM/ARM, is due to the higher than normal (relative to peat samples) X values and low ARM

**Table 5.4** Summary of Magnetic Data for Garnet Mica-Schist. GMS refers to the bulk sample, GMSmag to the 'magnetic' fraction.

| Parameter | GMS | GMSmag |
|---|---|---|
| **Susceptibility** $10^{-8}m^3kg^{-1}$ | 20.5 | 44.4 |
| $X_{fd}$ % | - | 0.45 |
| $IRM_{300mT}$/SIRM | 0.95 | 0.95 |
| ARM $10^{-6}Am^2kg^{-1}$ | 1.27 | 0.40 |
| SIRM $10^{-6}Am^2kg^{-1}$ | 734 | 190 |
| SIRM/X $kAm^{-1}$ | 3.58 | 0.43 |
| ARM/X $Am^{-1}$ | 62.0 | 0.90 |
| **SIRM/ARM** dimensionless | 578 | 476 |
| **'S'** % | 0.79 | 0.71 |

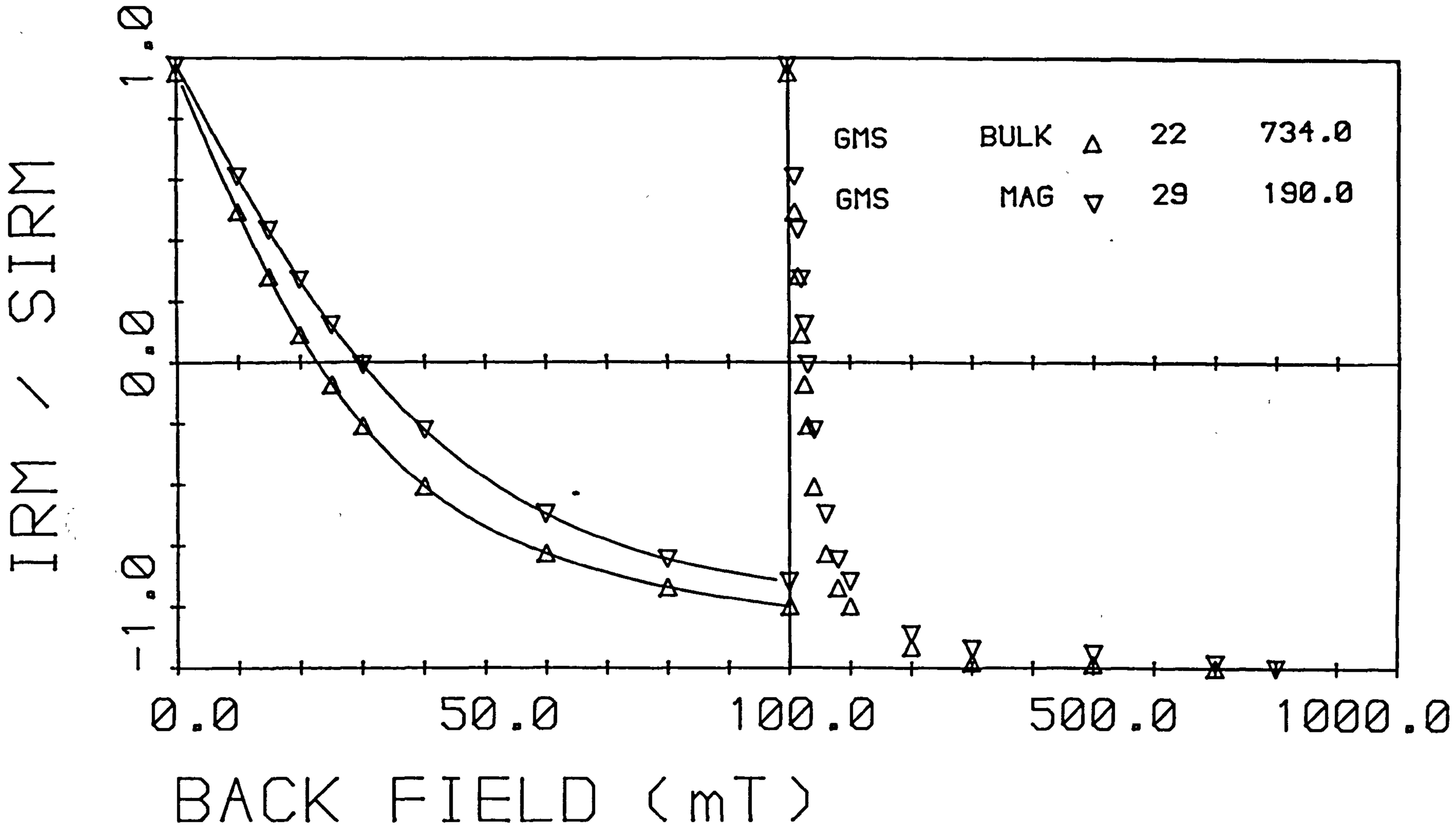


**Figure 5.30** Coercivity of remanence curves for garnet mica-shist. Showing the remanence curve for both the bulk rock sample and magnetic fraction.

and SIRM values. The coercivity of remanence curves (fig. 5.30) display strongly concave curve shapes between 0-100mT and low $(B_0)_{CR}$ values, 22mT for the bulk sample and 29mT for the 'magnetic' fraction.

The magnetic data presented in Table 5.4 suggest that the separation was less than complete. In order to test this, and examine the mineralogical composition of the rock samples, powdered extracts of both the bulk and 'magnetic' fractions of the garnet mica-schist were subjected to X-Ray diffraction (XRD). The results are presented in fig. 5.31 and suggest empirically, that the 'magnetic' fraction has retained the magnetite-maghemite minerals and considerably reduced the presence of micas (phlogopite, biotite and muscovite). The overall effect of the separation has been to give a clearer view of the main constituent minerals with the garnet mica-schist.

Finally, the powdered extract of garnet mica-schist was separated by means of a conventional horseshoe magnet with an approximate field of 300mT. The magnetic fraction was then examined along with the magnetic extract from the surface peat sample (0-1cm), by means of scanning electron microscopy. The results are presented in the following sub-section.

5.5.5 Scanning Electron Microscopy

Plates 5.4-5.8 consist of reproductions of scanning electron micrographs and Energy Dispersive X-Ray (EDX) analysis spectra relating to specific particles displayed by the micrographs. Three of the Plates, Plates 5.4-5.7, are from the surface sample of the peat core, whilst Plate 5.8 depicts a micrograph and EDX spectrum of the garnet mica-schist sample.

The particles observed on the micrograph of magnetic extract from the peat may be divided into two simple groups: spherules and non-

# XRD Spectra of Garnet Mica-Schist

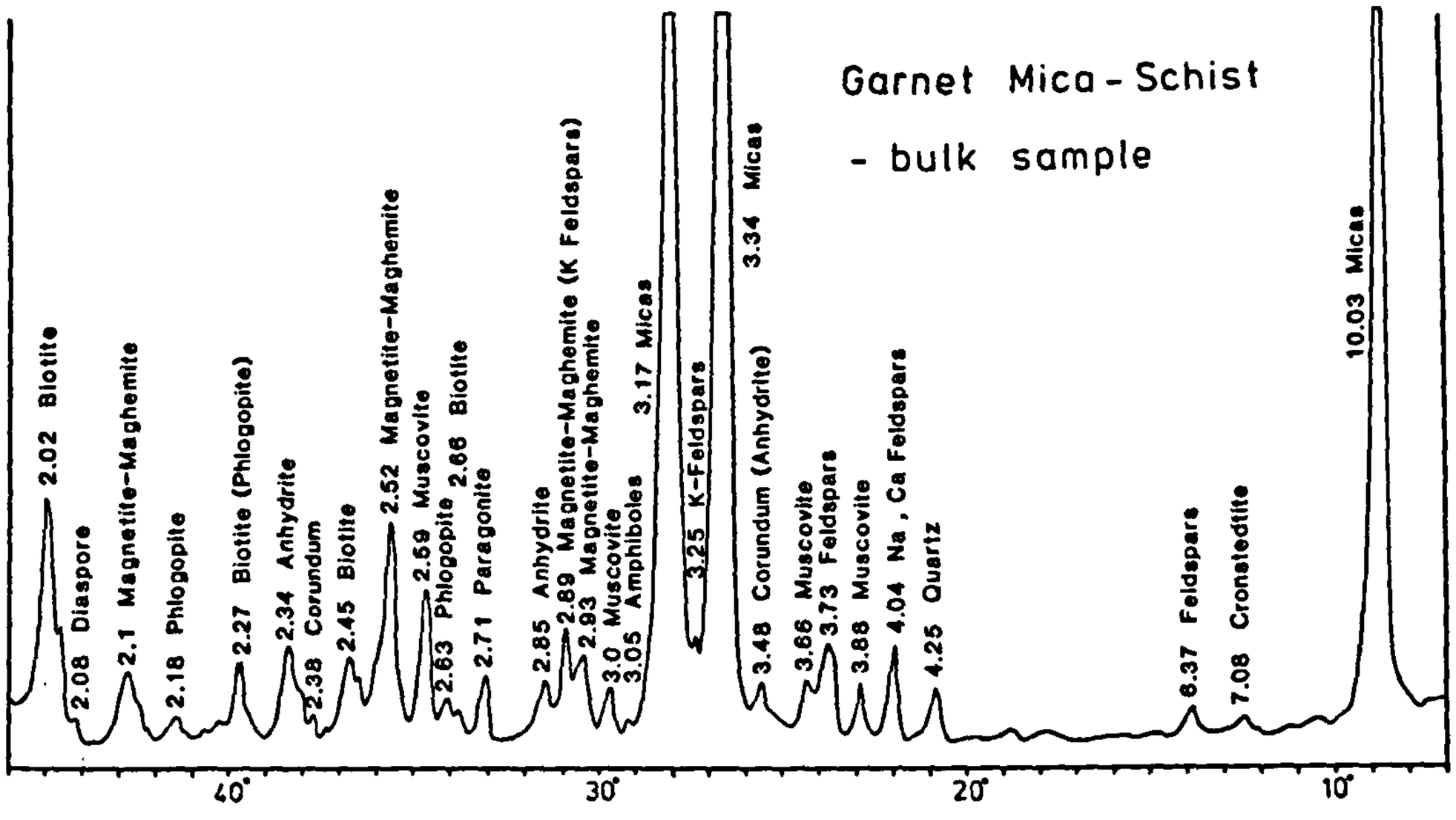


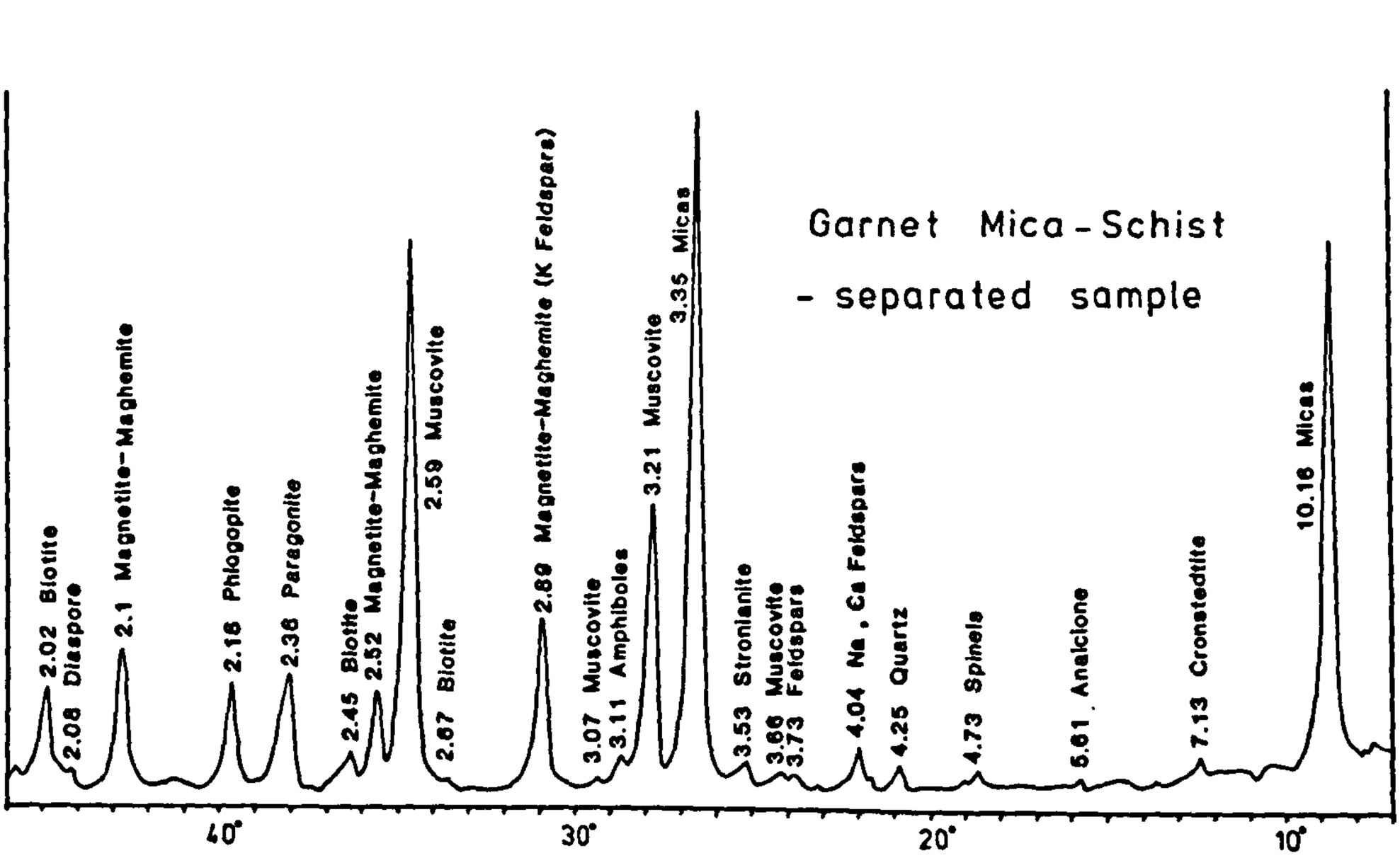


**Figure 5.31** XRD spectra of garnet mica-schist.
a) XRD spectrum of the bulk sample
b) XRD spectrum of the magnetic fraction

spherules. The quantity of magnetic extract was low, as noticed by the large areas of the carbon stub surface visible in, for example Plate 5.5 (lower left and upper right of the micrograph). The quantity of spherules was also small, although significant, in contrast to British peats (section 5.6, Plate 5.9). All the spherules observed were less than 10μm in diameter, predominantly in the range of 2-7μm, perfectly spherical and opaque. Plate 5.4 contains the EDX spectrum of Particle A displayed in the lower left hand corner of the micrograph. The element composition is dominated by iron. All the subsequent evidence indicated a dominance of iron in the spherules, and the micrographs revealed a lack of any distinctive surface morphology.

The second group or non-spherules, comprised the majority of particles observed. The non-spherules were also more distinctly heterogeneous in character, for example the size range, shape and element composition. The size range varied from small 1μm diameter particles up to the largest particles observed, for example Particle A, Plate 5.5 with a length of 45μm along the a-axis.

The particle shapes were irregular and sub-angular (smallest particles) and irregular and angular particles with sharply defined edges (larger particles). The shapes of Particle A (Plate 5.5) and Particle C (Plate 5.6) are indicative of fracturing, with the creation of irregular multi-faceted planes. Evidence from other micrographs (Plate 5.7) also show bar-shaped platelets, with an extended a-axis, for example Particle D (a-axis <36μm given the distortion of depth on the 2-dimensional image).

The element composition (as shown by the EDX spectrum) of the specifc particles depicted in the micrographs, also show little homogeneity. Particle composition ranges from that of predominantly iron in Particle A (Plate 5.5), through the more complex composition comprising iron,

titanium, manganese and aluminium, like Particle B (Plate 5.6), to the complex composition of Particle D (Plate 5.7) comprising iron, vanadium, silicon, aluminium and nickel.

The micrograph of garnet mica-schist (Plate 5.8) comprises particles relating to the non-spherule group mentioned above. Particle size and shape are also similar to those of the irregular particles mentioned above, being between 5μm and 50μm. The particles display the irregular and angular planes and edges characteristic of fractured material. An important note is that the magnetic extract came from powdered garnet mica-schist, crushed and pulverised under laboratory conditions, the magnetic particles in Plates 5.4-5.7 came from the undisturbed peat. The EDX spectra from Particle A (Plate 5.8) and Particle B (not shown), reveal identical element compositions of the two particles comprising iron, sulphur, silicon and aluminium.

5.5.6 210-Lead Results

A $^{210}Pb$ chronology has also been estimated for the Mo-I-Rana peat core. Based on the **unsupported** $^{210}Pb$ and **supported** $^{210}Pb$ concentrations in fig. 5.32a, the slice ages have been determined by both the CRS and CIC models. A comparison of the slice ages for each model, along with an estimate of the growth rate of peat is given in Table 5.3. The results show little difference between the two models in terms of age, with the maximum CRS age being 209 years at 13cm and the maximum CIC age being 195 years at 13cm. The equilibrium depth between the **unsupported** $^{210}Pb$ and **supported** $^{210}Pb$ for the CRS and CIC models is 10.9cm and 10.1cm respectively with 99% certainty.

The $^{137}Cs$ and $^{241}Am$ profiles are presented in fig. 5.32b. Both profiles display similar features with a large surface peak, 4 times higher than the preceeding value for $^{137}Cs$, and little variation in concentrations

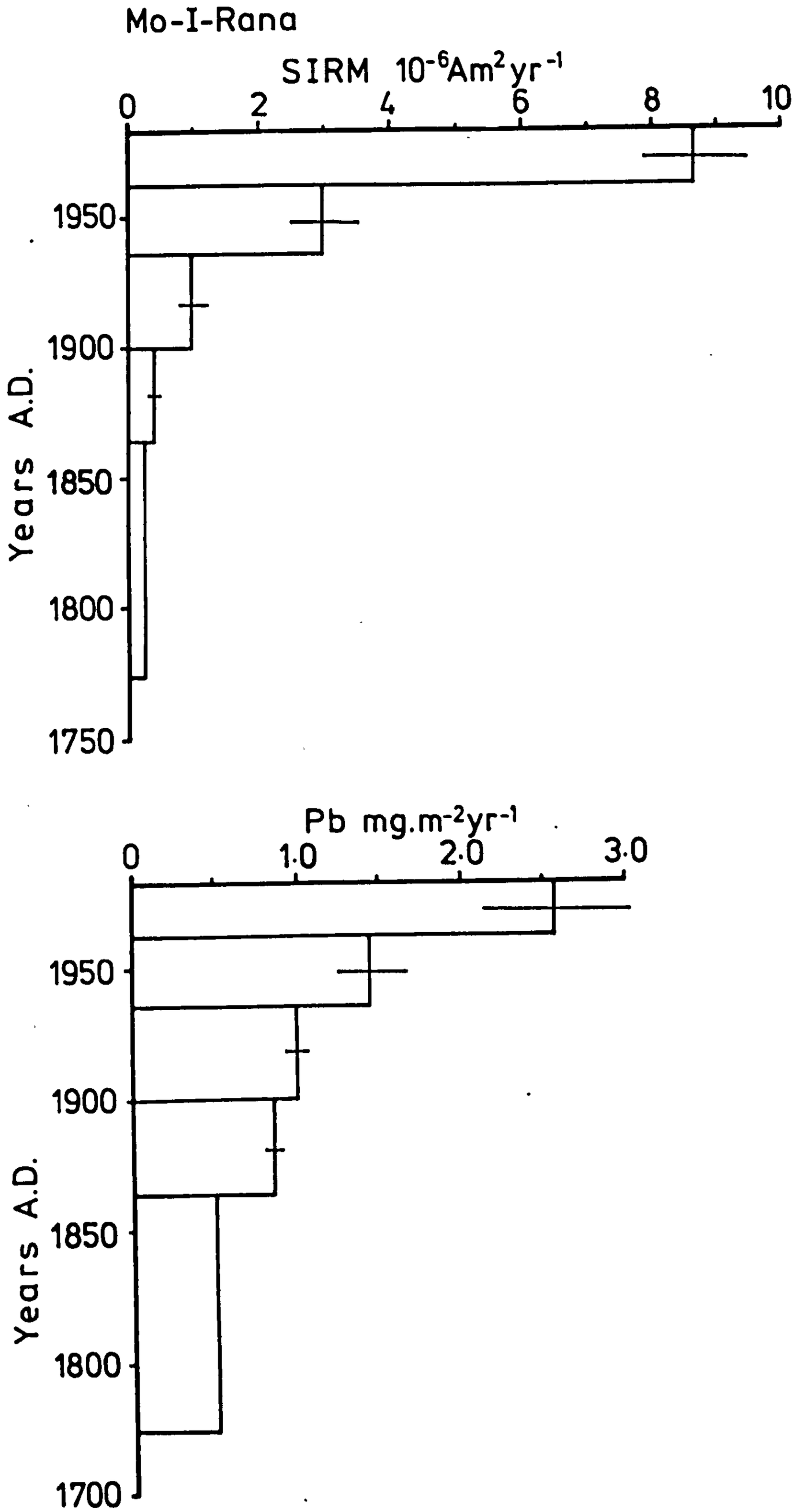


**Figure 5.33** SIRM and lead deposition profiles (with error bars) for Mo-I-Rana peat core

between 2.5-5cm. The $^{137}Cs$ profile extends down to at least 15cm, well below the base date of 1954 if the $^{210}Pb$ dating is correct. This aspect of the profile is discussed in the following sub-section.

When dates are applied to the SIRM profile in fig. 5.28, it is apparent that the increase in SIRM concentrations above 7.5cm has occurred since the beginning of the century. This is discussed with respect to the history of the iron and steel works in the area in the following sub-section.

SIRM and lead deposition profiles for the Mo-I-Rana peat core are presented in fig. 5.33. In both the SIRM and lead profiles, the deposition increases from low values of 0.236 $10^{-6}Am^2yr^{-1}$ and 0.508 $mg.m^{-2}yr^{-1}$ respectively, between 1774 and 1864/5, up to marked surface peaks of 8.65 $10^{-6}Am^2yr^{-1}$ and 2.57 $mg.m^2yr^{-1}$ respectively, between 1962/3 and 1983. The bulking up of the top two slices, 0-1cm and 1-2.5cm has precluded the possibility of greater resolution within the depositional timescale. These surface values are 2.9 times (SIRM) and 1.8 times (lead) higher than the preceeding values which are dated between 1936 and 1962/3.

5.5.7 Discussion

The chemical and magnetic data presented in figs. 5.27 and 5.28 respectively, suggest that the surface sample (0-1cm) in terms of concentration dependent parameters may be distinct from the rest of the core samples. The backfield curves (fig. 5.28) and coercivity of remanence curves suggest however, that the top four samples (0-7.5cm) may be separated from the remainder of the core in terms of qualitative mineral magnetic variation. The basic difference appears to be in the antiferromagnetic component. This component is strongly in evidence within the top four samples (0-7.5cm) as shown by the upper backfield ratios, $IRM_{-100mT}/SIRM$ and $IRM_{-300mT}/SIRM$, in fig. 5.28 and the inabiltiy of the samples to fully reverse saturate until the application of

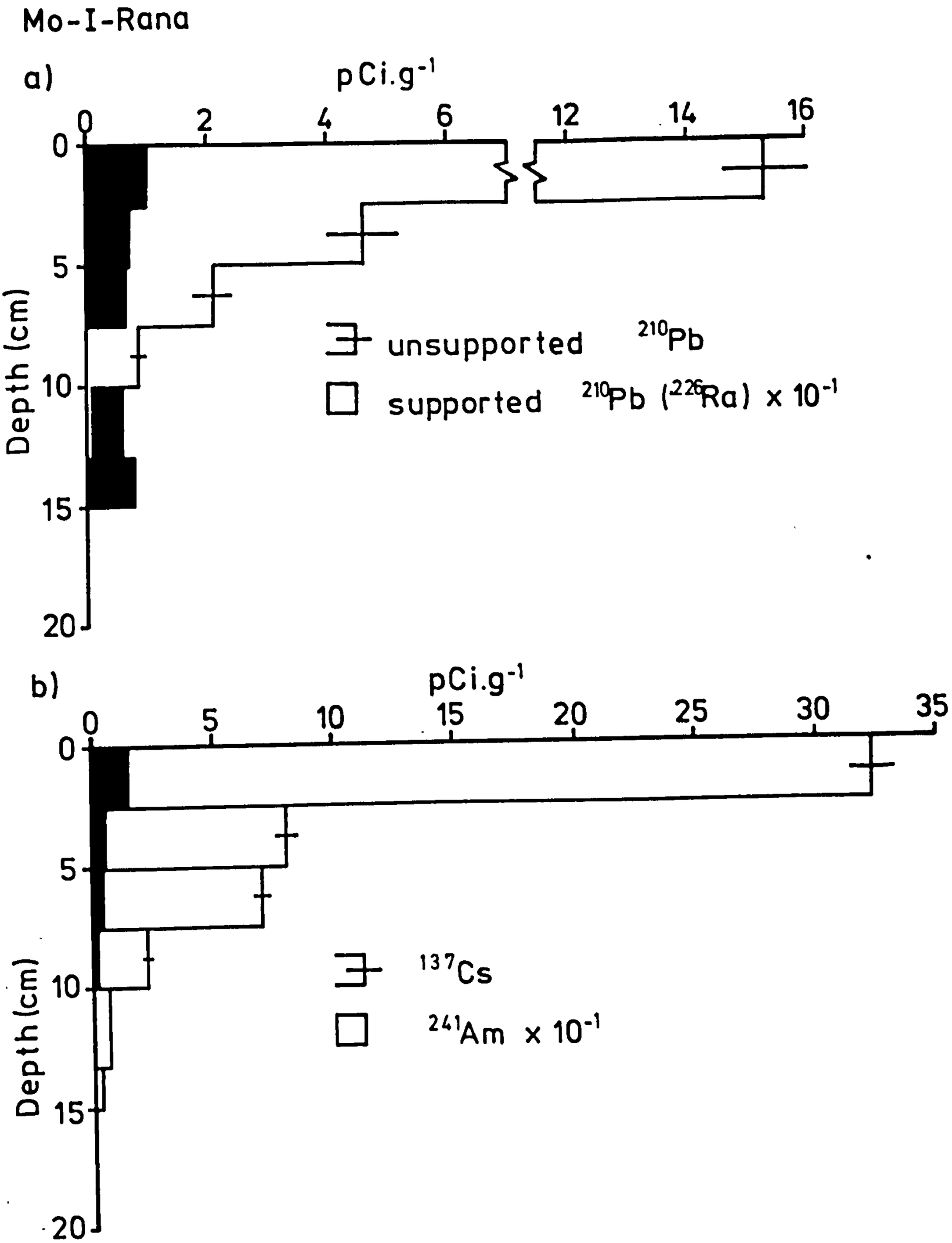


**Figure 5.32** Radioisotope profiles for Mo-I-Rana peat core.
a) $^{210}Pb$ and $^{226}Ra$ concentration profiles
b) $^{137}Cs$ and $^{241}Am$ concentration profiles
Both $^{210}Pb$ and $^{137}Cs$ are shown with error bars.

the highest backfield, -850mT (fig. 5.29). The influence of the antiferromagnetic component on the remanence curve shapes is reduced for samples between 7.5-35cm and non-existent for samples between 35cm and 55cm, as seen by the reverse saturation of all the samples at -200mT.

The remanence curve shapes for the garnet mica-schist samples (fig. 5.30) are similar to those of the surface samples (0-7.5cm), being concave, although the antiferromagnetic component appears to have the same influence as samples between 7.5-35cm. This suggests that if the presence of garnet mica-schist within the peat samples has any influence on the magnetic characteristics of the peat samples, then it appears to be strongest on the four surface samples. Assuming that the weathering of the local bedrock has been constant throughout the time-span represented by the 55cm of peat, then the influence on the magnetic characteristics of the surface samples may represent an increase in the deposition of the local weathering product. The $^{210}Pb$ dates from sub-section 5.5.6 provide a chronology which may be supported, in part, by the written history of the iron and steel works (Table 5.1).

The SIRM profile in fig. 5.28 displays the take-off point at 5-7.5cm. These depths are dated to 1936 and 1899/1900 respectively, which corresponds with to the operational period of the Dunderland Iron Ore Company (1906-1939). The increase in SIRM concentrations from 5cm up to the surface corresponds to the period over which the iron and steel works began, and increased its production to the present capacity of 1.15 million tons of iron concentrate a year. The micrographs in Plates 5.4-5.6 display evidence that the surface sample at least contains the strongly magnetic products of combustion processes (Griffin & Goldberg, 1981). Hansen (1981) observed magnetic oxides (magnetite and haematite fractions) within fly ash samples (spherules) and concluded that they must have their genesis in

the combustion process. Similarly, McCrone & Delly (1973) also revealed that particulate emissions from a variety of industrial processes, including iron and steel production, possessed magnetic components.

A second plausible source leading to deposition of non-spherule particles within the peat is Rana Gruber. The open cast mining division of AS Norsk Jernverk, Rana Gruber began operations in 1964, to the northeast of Mo-I-Rana in the Dunderland Valley and at Ørtfjell from 1981 (Table 5.1, fig. 5.3). The production of iron concentrates from the open cast mines is at present 1.4-1.5 million tons per annum. The timing of these events corresponds approximately to 1-2.5cm and 0-1cm respectively. During the mining phase, a quantity of the ore is released into the atmosphere and deposited onto surrounding regions, including those in the path of the prevailing northerly winds.

A third possible contribution is a specific event, and not a source of continued deposition. This relates to the construction of the unmetalled highway, E6, running from Trondheim to Mo-I-Rana. The road passes about 1km west of the peat core location. Construction of the road occurred at some time between 1964 and 1983, which corresponds to the top 2.5cm of peat and peak SIRM concentrations.

The EDX spectra presented in Plates 5.5-5.7 present a complex picture of the elemental composition of particles within the non-spherule group. Apart from just an identification of the elemental composition, a crude quantitative estimate of the minerals present may be made since the peak heights of major elements, for example silicon, aluminium, potassium and calcium are roughly proportional to their concentration (Welton, 1984). Particles A (Plate 5.5) and B (Plate 5.6) are probably magnetite. The EDX spectrum of Particle C (inset, Plate 5.6) is similar to that of ilmenite depicted in Welton (op. cit.). The EDX spectrum of Particle D (Plate 5.7)

contains vanadium, chromium and nickel. The first two are rare elements in naturally occurring minerals, however, vanadium is used in the production of vanadium steel, whilst nickel and chromium are products of smelting processes (section 5.6), strongly suggesting an anthropogenic origin for this particle, probably from the iron and steel works. Finally, the EDX of the garnet mica-schist sample (Plate 5.8) gives an elemental composition of iron, sulphur, aluminium and silica in decreasing proportions. A similar EDX spectrum, with a substantially larger peak, is obtained from Particle B (Plate 5.8) suggesting a similar origin or rock-forming mineral, probably from the Fe-S system (sulphides group).

The $^{137}Cs$ profile in fig. 5.32b suggests that downward diffusion has probably occurred, as at Draved Moss. The fourfold increase at the surface suggests that at some stage the preceeding samples have been of a similar concentration but now, due to the diffusion process, are now largely depleted. The similarity in concentrations between for the two samples between 2.5-7.5cm also suggests that that there has been a variation in accumulation rates within one of these samples, most probably the lower 5-7.5cm sample which has accumulated more slowly, producing a concentrating effect on the Cs ions. This is partially supported by the increased $^{210}Pb$ age for the slice (Table 5.3) and the slower growth rate of peat, $0.68\pm0.02 mm.yr^{-1}$. The bulk density values of the peat also show a substantial increase from $58.5 gdm^{-3}$ at 2.5-5cm to $129 gdm^{-3}$ at 5-7.5cm.

## 5.6 General Discussion

As envisaged in section 5.1, a comparison of the two sites, Draved Moss and Mo-I-Rana, reveals that the mainland European site appears to have received considerably more magnetic particulate deposition than the 'remote' Norwegian site. However, the evidence from section 5.5 also

suggests that a direct comparison is misleading since the peat core site is located within an area of iron-bearing formations (fig. 5.3). Furthermore, these formations are being actively mined (Table 5.1) and the ore smelted at the nearby Mo-I-Rana iron and steel works.

The discussion below centres on relationship between heavy metals and magnetic minerals. This links in with the evidence of spherules of anthropogenic origin (Griffin & Goldberg, 1981) noted in the micrographs from both sites.

Jones (1985) notes the three main types of human activity which accelerate the emission of heavy metals to the atmosphere: fossil fuel combustion (coal and oil) for power generation and automobiles; iron and steel manufacture; and non-ferrous metal smelting. Davison et al. (1974) noted that coal-fired power generation results in the emission of significant quantities of iron, copper, cadmium, chromium, nickel, lead and zinc. The most significant metal emission from oil-fired processes is vanadium (cf. Plate 5.7). Alar y et al. (1983) and Van Craen et al. (1983) noted the emission of significant quantities of copper, lead, zinc, chromium and manganese from electric powered steel furnaces. Lead smelting is a source of cadmium, lead, copper and zinc (Dorn et al., 1976). The chemical profiles from Draved Moss (figs. 5.7-5.10) display surface increases in copper, iron, zinc and lead, whilst the chemical profiles for Mo-I-Rana display surface increases in iron, nickel, copper, zinc and lead.

The same three anthropogenic sources responsible for heavy metal emissions are also linked with the emission of magnetic minerals (Jones, op cit). Preliminary results of some fly ash emissions from power stations are summarised in Hunt et al. (1984). Generally, the fly ash appears to display a significant antiferromagnetic (viz. haematite) component (cf. figs. 5.14, 5.15, 5.18, 5.19). At Mo-I-Rana however, the nearest industrial source is

the steelworks and not a power station. Puffer et al. (1980) identified spherules of magnetic composition (cf. Plate 5.4) in the magnetic fraction of samples removed from the scrubber of a scrap iron foundry. McCrone & Delly (1973) reported similar findings for emissions from open hearth and Bessemer steel manufacturing processes. The steelworks at Mo-I-Rana had furnaces of the latter type from 1955 to 1961 (Table 5.1).

In the context of magnetic measurements, Scoullos et al. (1979) observed a distance decay effect on the SIRM of filter samples obtained from a transect across the Gulf of Elefsis, away from coastal iron and steelworks. Similar point source dominance has been revealed for the Mesabi Iron Range, Minnesota (Thompson & Oldfield, in press). There is also some limited evidence which suggests that non-ferrous smelting processes can also contribute to the magnetic particulate loading of the atmosphere. Magnetic measurements of peat profiles taken from within the proximal zone of the Sudbury nickel smelter, USA, have revealed marked increases in magnetic deposition coincident with the development of the complex along with a marked distance decay effect (Thompson & Oldfield, op. cit.).

The evidence of spherules in Draved Moss and to a lesser extent, Mo-I-Rana, is consistent with evidence from industrial areas, for example Ringinglow Bog, England (Jones, op. cit.). Plate 5.9 is a micrograph of the magnetic fraction extracted under identical conditions (cf. sub-section 5.2.1). Whereas the analysis of magnetic particles by SEM cannot be undertaken on a quantitative basis at present (Hunt, 1986, pers. comm.), it is evident from Plate 5.9 that the magnetic fraction extracted from peats in heavily industrialised locations is probably an order of magnitude greater than at either Draved Moss or Mo-I-Rana, as well as being dominated almost exclusively by the spherule group.

## 5.7 Conclusions

The conclusions fall broadly into two categories. The first category is centred around the $^{210}Pb$ chronology and subsequent estimates of elemental deposition, whilst the second category focusses on the evidence of the SEM, XRD and EDX data.

It would appear from the close similarity between the CRS and CIC age-depth curves that the sedimentation rates at Draved Moss and Mo-I-Rana have been relatively constant. The calculated growth rate of peat at Draved Moss shows increasing growth rates towards the surface (Table 5.3), in agreement with the results presented in Aaby & Jacobsen (1979). The explanation given by the latter is one of autocompaction within the peat layers at depth. The chronologies calculated from the two models are in close agreement, although for the purposes of this study only the CRS dates are used, since the assumptions as laid out in sub-section 5.4.1 appear to be most applicable to ombrotrophic peat environments. The chronology produced is extremely tentative given the limited knowledge at present of radiometric dating controls within peat environments. No independent chronologies are available to calibrate or substantiate any of the dates upon the curve. The deposition rates calculated for lead (fig. 5.23) are, however, in good agreement with those presented by Aaby et al. (1979) for Draved Moss, between 1800 and 1950. The increased rates noted by Aaby et al. (op. cit.) post-1950, 50-60mg Pb $m^{-2}yr^{-1}$ are between 2 and 2.5 times higher than the present calculations. The difference is tentatively explained by the premise that the earlier, published calculations, failed to take account of variations in the growth rate at the top of the core. The present estimate of 23.9mg Pb $m^{-2}yr^{-1}$ (see above) for 1977 to 1983 (CRS model), is close to the values obtained by Hovmand (1973, 1976) for bulk precipitation trapped by rain gauges (7-20mg Pb $m^{-2}yr^{-1}$). The deposition

of magnetic particulates, as approximated by SIRM, is slightly different, displaying a sub-surface peak of 21.6 $10^{-6}Am^2yr^{-1}$ between 1978 and 1967 (fig. 5.24).

The mobility observed within the $^{137}Cs$ profile (figs. 5.20b and 5.32b) appears to show upward mobility of the univalent Cs-ion near the surface, and significant downward diffusion below the 1954 level associated with the beginning of significant increases in the production of $^{137}Cs$ from test nuclear weapons (Cambray et al., op. cit.). The pattern noted in DMHol2 profile accords closely with that described by Aaby & Jacobsen (1979). The recycling and leaching indicated by the $^{137}Cs$ measurements are probably important for other cations, especially those of similar electric potential.

The evidence from the scanning electron micrographs (Plates 5.1-5.9) at both sites, indicates the presence of two groups of magnetic particles: spherules and non-spherules. The non-spherules appear to be the product of localised factors, being varied in size range up to 50µm with a short atmospheric residence time. At Draved Moss these are attributed to local field erosion, in the absence of any EDX spectra to suggest anthropogenic sources. The evidence from earlier chapters (cf. Chapter 3) and published work (Vuorela, 1983; Tolonen, 1984), points to this as being a likely source. The deposition of non-spherules in the Norwegian peat core is also attributed in part to the erosion product of the local bedrock, although this appears to have been accelerated by the mining operations in the Dunderland valley to the north (Table 5.1). There is however, limited evidence from the EDX spectrum in Plate 5.7 which suggests that some non-spherule particles are of anthropogenic origin, given their elemental composition. The most likely source of these particles is probably the iron and steel works at Mo-I-Rana to the north of the peat site, or even deposition from the nearby unmetalled highway (E6) to the west.

The spherules from both Draved Moss and Mo-I-Rana have a common form with no distinct surface morphology. Evidence from published sources (cf. section 5.6) strongly suggests that these particles probably provide the link between heavy metal deposition and the deposition of magnetic particulates. Jones (1985) provides similar evidence from heavily industrialised sites in South Yorkshire.

In order to assess the data presented in the four chapters (see above), the final chapter concentrates on a general perspective of peat deposition studies. More specifically, evidence from Great Britain and North America is summarised both in qualitative and semi-quantitative terms.

# 6. Summary and Conclusions

## 6.1 The Magnetic Primary Deposition Record in Peat

### 6.1.1 General Characteristics

The input of magnetic particulates in one form or another is common to all the Scandinavian sites studied. Variation in input, as indicated by the range of magnetic measurements conducted on the samples, is seen to occur both spatially and temporally. The variations may be discriminated further into variations in volume and quality. On the timescales involved, <200 years, the magnetic record may also be divided into **'pre-industrial'** and **'post-industrial'** samples. The results from Chapter 2 show that at some sites, these two groups may be divided by a marked transition, or **take-off,** from low background mineral magnetic concentrations ('pre-industrial') to relatively high 'post-industrial' values. At other sites, for example in northern Scandinavia (eg. Ahmajänkä) there is merely a gradual increase in X, ARM and SIRM with no discernible take-off.

Table 6.1 provides a general summary of the magnetic characteristics of surface peats (<50cm) from Scandinavia. The range of measurements corroborates the conclusions of Chapters 2 and 5 which differentiated between the pre- and post-industrial samples on both qualitative and quantitative criteria. Irrespective of location, the pre-industrial samples are characterised by low but measurable concentrations of magnetic particulates, as indicated by the range of low ARM and SIRM values and predominantly diamagnetic susceptibility values. The diamagnetic component of these 'clean' peats has already been estimated in Chapter 1 (Table 1.1), ranging between $-0.79\ 10^{-8}m^3kg^{-1}$ and $-0.16\ 10^{-8}m^3kg^{-1}$ for all the Scandinavian sites. The maximum SIRM values, 1393-3929 $10^{-6}Am^2kg^{-1}$ represent intermediate values between 'remote' British and North American sites and the heavily polluted sites close to major

**Table 6.1** Summary of Magnetic Characteristics in Scandinavian Peats. The units of measurement for the respective parameters and interparametric ratios are presented in Table 1.3. The pre-industrial characteristics are derived from peat samples to a depth of 50cm.

| Site | X | ARM | SIRM | ARM/X | SIRM/X | SIRM/ARM | 'S' | $(B_0)_{CR}$ |
|---|---|---|---|---|---|---|---|---|
| **S. Finland** | | | | | | | | |
| Post-Industrial | 0.53-12.7 | 1.15-19.3 | 36.9-1393 | 83-625 | 11.0-17.8 | 23.1-133 | 44-82 | 24-48 |
| Pre-Industrial | diamagnetic | 0-6.8 | 10-123 | - | - | 14.8-44.1 | 29-83 | 32-56 |
| **N. Scandinavia** (mainly N. Finland) | diamagnetic to 9.34 | 1.02 to 8.2 | 10.2 to 2430 | 356 to 1021 | 0.35 to 27.7 | 22.2 to 88.2 | 50 to 97 | 29 to 52 |
| **N. Norway** | | | | | | | | |
| Post-Industrial | 0.5-9.41 | 6.0-13.2 | 115-1395 | 140-1381 | 11.9-22.2 | 30-106 | 54-64 | 40-47 |
| Pre-Industrial | diamagnetic | 1.54-6.7 | 6.8-58.4 | - | - | 6.8-16.5 | 80-94 | 44-52 |
| **S. Denmark** | | | | | | | | |
| Post-Industrial | 1.0-25.8 | 6.0-113 | 568-3929 | 158-608 | 11.9-25.9 | 34.8-112 | 81-100 | 36-46 |
| Pre-Industrial | diamagnetic | 0-3.1 | 6.9-132 | - | - | 14.7-62.5 | 75-100 | 33-52 |

industrial sources. These spatial perspectives are discussed in sub-sections 6.1.2 and 6.1.3.

The variations within the mineral assemblages of pre- and post-industrial samples are evident in key parameters, for example the 'S' ratio ($IRM_{-100mT}$/SIRM) and $(B_0)_{CR}$ values (Table 6.1). The post-industrial samples all appear to be of a homogeneous type, in contrast to the heterogeneous mix of pre-industrial samples. Qualitative variations within the peats are assessed in the context of the much wider range of mineral assemblages outlined in Chapter 1, sub-section 6.1.4.

6.1.2 Spatial Perspectives in the PDR- North American Peats

In both spatial and stratigraphical terms the patterns of variation in eastern and central North America appear to be markedly different. At Regent Street Bog, Fredericton, New Brunswick for example, profiles displayed a sharp decline in concentration towards the surface. The SIRM deposition rate peaked between 1900 and 1930, paralleling the history of the local iron and steel industry almost perfectly. Further North American sites display similar trends, for example, curves constructed from the combined results from eight sites across eastern and central North America showed peak accumulations between 1950 and 1965, followed by a decline over the last two decades (Tolonen & Oldfield, in prep.).

Spatial variations in North American magnetic deposition, similar to the conclusions based on Scandinavian peats, appear to be dominated by point sources, for example the Mesabi Iron Range and the Sudbury copper smelter (Thompson & Oldfield, in press). The results from Scandinavian bogs indicated the dominance of point sources at Varrassuo, southern Finland and Mo-I-Rana, northern Norway, with the possibility of a further proximal source at Liikanen, northern Finland. The sharp increases in magnetic deposition within the peat profiles near each site give good

chronological markers in both quantitative and qualitative terms.

In quantitative terms the variations in magnetic deposition from North America are up to 2 orders of magnitude higher than their Scandinavian counterparts, being between 247-122,175 $10^{-6}Am^2kg^{-1}$. The larger value is from point source samples at Sudbury (Sahota, pers. comm.). In qualitative terms, the $(B_0)_{CR}$ values (27-62mT) are within the same range as the Scandinavian sites.

6.1.3 Spatial Perspectives in the PDR- British Peats

Until recently, the majority of works investigating the deposition of magnetic particulates in peat have been carried out on British peats . The spatial relationships in Britain are inevitably complex, given the high populations and industrialisation of specific regions such as northern England. A proliferation of foci for pollutant emissions have combined to camouflage any distance decay effect evident at the regional scale (Jones, 1985).

A comparison of the results obtained by Oldfield et al. (1978a, 1979a) from Cumbria and northern England, and the results of Jones (op. cit.) from Sheffield, Shropshire and eastern Central Scotland, give some indication of the spatial variation existing within the British Isles. The Scottish sites from the Lunan Burn catchment record peak SIRM values of between 1000-2000 $10^{-6}Am^2kg^{-1}$, whilst the Cumbrian sites record lower values of 100-1500 $10^{-6}Am^2kg^{-1}$. The latter values are strongly influenced by variations in the hummock-hollow microtopography with hummocks trapping an order of magnitude more deposition in volume magnetic terms (Oldfield et al., 1979a). This is in contrast to the results from Kaurastensuo, southern Finland (Chapter 2) and Draved Moss, southern Denmark (Chapter 5), where although the magnetic deposition appeared to favour the hummocks, the variation between hummocks and hollows was very small in comparison to

British sites. Magnetic deposition at 'remote' sites in Scotland is in marked contrast to the deposition at sites in Shropshire (Whixall Moss) and near Sheffield (Ringinglow Bog), which in terms of cumulative post-industrial values are more than six times greater (Jones, op. cit.).

The accumulating circumstantial evidence from European, North American and Scandinavian sites suggests that the hypothesis of a distance decay effect being reflected in the magnetic deposition record within ombrotrophic peat, with respect to point source studies, appears probable. The evidence for post-industrial increases in magnetic deposition is at the very least, consistent between sites of differing nature and composition, at differing spatial scales.

### 6.1.4 Qualitative Aspects of the PDR

Qualitative variations between the pre-industrial and post-industrial groups are summarised by the range of interparametric ratios in Table 6.1. The diamagnetic component evident in the pre-industrial samples precludes a comparison of ARM/X and SIRM/X between the two groups. However, the 'S' ratio ($IRM_{-100mT}$/SIRM), $(B_0)_{CR}$ values and SIRM/ARM ratio are available.

The 'S' ratio and $(B_0)_{CR}$ values may be used to indicate shifts within the mineral assemblages of pre- and post-industrial samples. Collectively, in terms of the predominantly concave shape of the coercivity of remanence curves and the relatively small range of $(B_0)_{CR}$ values, 24-56mT, the general conclusion for the peats studied is that the SIRM is carried predominantly by medium to fine grained ferrimagnetic assemblages. However, within this range there is a distinct variation at all sites, between the two groups. The post-industrial samples are predominantly characterised by a narrow range of $(B_0)_{CR}$ values, varying from site to site and region to region, although always representing the

lower $(B_0)_{CR}$ values, 24-48mT being the maximum extremes. The concave curve shape for these samples suggests their remanence is carried by the relatively coarser grained ferrimagnetic assemblages ie. the medium grain sizes. These samples respond relatively quickly to the initial demagnetisation at lower backfields (<100mT). In almost every post-industrial sample, the incomplete reverse saturation at -300mT suggests the presence of a significant canted antiferromagnetic content. This component is almost always subdued or missing in the curves for pre-industrial samples (cf. fig. 5.29). The coercivity of remanence curves from Draved Moss show clearly at that site that there is no apparent influence of the microtopography on the mineral assemblage, as depicted by coercivity curves or $(B_0)_{CR}$ values (cf. figs. 5.14, 5.15, 5.18, 5.19). The range of 'S' ratio variation for the two groups describes a very similar pattern to the $(B_0)_{CR}$ values, supporting the conclusions drawn from the hysteresis parameters (Table 6.1).

The SIRM/ARM ratio, indicative of multidomain/single domain shifts in ferrimagnetic assemblages, shows consistent variation between the two groups from one region to another. In all cases, the SIRM/ARM band for post-industrial peats was higher than the equivalent band for pre-industrial peats. The overlap at the top end of the pre-industrial band and the lower end of the post-industrial band was small but evident in all regions. The variations in SIRM/ARM reinforce the conclusions drawn that the remanence for the post-industrial samples is carried by the relatively coarser grains within the magnetic assemblages. The wider variety of the qualitative data for the pre-industrial samples suggests that the mineral assemblages cannot be collectively described as anything more than medium-fine grained ferrimagnetic types.

Chapter 1 outlined the various magnetic mineral types from ultrafine

canted antiferromagnets to the coarse multidomain ferrimagnets. In the context of samples incorporating these extremes, the mineral assemblages contained within the surface peats are narrowly defined. For example, Maher (1984) observed very 'soft' remanence curves for gleyed soils, with $(B_0)_{CR}$ values between 27-43mT. These samples paralleled the curve shapes of maghaemite samples which reverse saturated at low backfields of between -200mT and -350mT. Magnetite samples displayed an even softer remanence, with markedly concave curve shapes and reverse saturation at backfields of less than -200mT. The $(B_0)_{CR}$ samples for these curves varied between 16mT and 46mT. At the other end of the extreme, and in contrast to the assemblages noted within the surface layers of peat, are the magnetic results obtained from a well developed Exmoor stagnapodsol (G. Yates, unpub. data.). The surface soils (0-24cm) dipslay some resistance to demagnetisation, with $(B_0)_{CR}$ values of between 47-61mT. Below 28cm, resistance to demagnetisation increases enormously with the underlying parent material, a slate bedrock, recording $(B_0)_{CR}$ values of 442mT to 466mT.

## 6.2 The Chemical Primary Deposition Record

This section provides a general summary of the characteristics of iron, manganese, nickel, copper, lead and zinc, noted in detail in previous chapters. The first two elements have common properties such as high mobility in the divalent form and are therefore discussed together. Nickel is discussed in the context of natural (lithospheric) and anthropogenic sources, whilst copper, lead and zinc, all derived predominantly from industrial/combustion processes, are discussed last. Where applicable, observations are made on regional and microtopographical variations.

Iron concentrations in the surface layers of peat derive from both

natural and anthropogenic sources. The evidence from the Scandinavian sites suggests that the iron content in surface layers is derived partly from local deflation products and partly from combustion sources (cf. Chapter 5). The iron concentrations noted in the southern Finnish profiles all appear to be sensitive indicators of the water table level at the time of sampling. These observations comply with the results of Damman (1978) who noted that in anaerobic peat, iron becomes mobile as ferrous iron — accumulates in the zone of water table fluctuation. It is important to note, however, that within the acrotelm in aerated conditions, the iron is in the immobile trivalent $Fe^{3+}$ form.

Manganese profiles are available only from Sphagnum fuscum hummocks sampled at northern Scandinavian sites. The profiles are remarkably consistent, displaying minimal concentrations at depth, increasing along a smooth exponential curve and culminating in peak surface concentrations. Like iron, the element is highly mobile in the divalent form and influenced strongly by the redox potential. Manganese is reduced from the tetravalent to the divalent state under anaerobic conditions ie. from immobile to mobile form. The consistently high enrichment ratios (Table 4.2), greater than any of the other elements studied, has been observed at other Scandinavian sites in Sweden (Damman, op. cit.), Denmark (Aaby & Jacobsen, 1979) and Finland (Sillanpää, 1972; Pakarinen et al., 1983). As only hummock profiles are available for manganese, it has precluded the possibility of observations on the variation of manganese concentrations in hummock-hollow microtopography. For example, Damman (op. cit.) noted that due to the mobility of manganese and the pH and redox controls, it occurred in much lower concentrations in the hollows than in the hummocks.

Nickel has both natural and anthropogenic sources as its possible

origin in the surface layers of peat. It may be emitted as a direct or indirect product of combustion processes, both of which are probably the likely cause of the surface enrichment noted at Mo-I-Rana (cf. fig. 5.27). Fossil fuel combustion is the major anthropogenic source, with fuel oil being a significant contributor.

Regional studies of nickel in Scandinavian peats have concluded that in Finland (Pakarinen & Tolonen, 1976) and Norway (Hvatum et al., 1983) at least, there are no obvious regional trends. Pakarinen & Tolonen (op. cit.) recorded concentrations of 0.55-2.22$\mu g.g^{-1}$ significantly higher than the 'background' global base-line concentrations of 0.24-0.33$\mu g.g^{-1}$ they had estimated. The nickel data from this study for sites in northern Norway, southern Finland and Denmark show marked variations in concentrations for sites in close proximity to each other. For example, Laaviosuo has mean nickel concentrations of 3.1$\mu g.g^{-1}$ whilst Kaurastensuo, some 3km to the north west has mean concentrations of 4.35$\mu g.g^{-1}$ for the top 10cm of peat.

The only site with data on microtopographical variations in peat is Draved Moss. (section 5.3) The nickel profiles from the two sites show distinct variations. The two hummock cores are characterised by low concentrations near the surface, preceeded by undetectable (<0.05$\mu g.g^{-1}$) concentrations between ca.5-25cm. DMHum2 has a number of sporadically measurable samples below 25cm, which may or may not also be present at site 1 since the profile terminates at 25cm. In contrast, the hollow cores display consistently measurable concentrations throughout their lengths. The limited data pose a number of problems in interpretation, but it would appear that, given uniform deposition, the nickel is being preferentially removed from the hummocks and probably stored within the hollows. The absence of any water table or Eh data from Draved Moss precludes a more

detailed explanation.

The general characteristics of lead, copper and zinc may be summarised by their behaviour within the surface profiles, bearing in mind the probability that these elements are derived predominantly from industrial/combustion sources. The lead profiles from all sites exhibit predominantly sub-surface peaks, except at sites where local industrial sources are evident, for example, at Varrassuo (fig. 3.14) and Mo-I-Rana (fig. 5.27). Further down in the lead profiles at the southern Finnish sites, increases in lead appear to be sensitive to changes in the level of the water table. Once in the zone of water table fluctuation the lead forms PbS (insoluble) and $PbSO_4$ (slightly soluble) under alternating reducing (wet) and oxidising (dry) conditions. The slightly soluble $PbSO_4$ is removed from the peat layers before entering the permanently anaerobic zone, leaving accumulations of lead in the zone of water table fluctuation (Damman, op. cit.).

The distribution and behaviour of zinc within the profiles is similar to iron and lead, being a sensitive indicator of the water table level in southern Finnish sites. The mechanism of removal for zinc is also similar to lead, being reduced to ZnS and oxidised to $ZnSO_4$, whereupon it is almost entirely removed from the peat (Damman, op. cit.). The hummock-hollow paired profiles from Draved Moss show little variation for either zinc or lead. However, at both sites, both the element concentrations are slightly higher in the hollows. However, when the data for zinc and lead at Draved Moss are plotted on a volume basis, the hummocks display values 1.7 and 1.4 times greater than the hollows respectively.

The copper concentrations, with a high solubility (50-75%), based on observations on British peats, appear to be removed almost entirely below the water table level in the hummock cores from southern Finland. Most of

the sites from Scandinavia in general display increased copper concentrations near the surface. There is also a strong correspondence with industrial sources, with strongly pronounced surface peaks at Varrassuo Bog and Mo-I-Rana. Sequential extractions of copper in peat presented in Jones (1985) suggest that the deposition record is confined to the relatively insoluble fractions extracted by nitric/perchloric acids and nitric/ hydrogen peroxide, with the more soluble species extracted by magnesium chloride and hydroxylamine hydrochloride with acetic acid, being insignificant.

According to the classification given in Livett et al., (1979), all the Scandinavian sites observed, contain 'low-background' concentrations of lead, zinc and copper. The maximum values of the low-background sites in Scotland recorded by Livett et al. (op. cit.) ranged from 32-155$\mu g.g^{-1}$ for lead, 100-184$\mu g.g^{-1}$ for zinc and 6-160$\mu g.g^{-1}$ for copper. A significant point to note is that at sites where proximal industrial sources have apparently dominated the chemical deposition record such as at Varrassuo Bog and Mo-I-Rana, maximum values for lead, zinc and copper are 51.2$\mu g.g^{-1}$, 68.6$\mu g.g^{-1}$ and 8.1$\mu g.g^{-1}$ respectively at Varrassuo and 41.5$\mu g.g^{-1}$, 36.4$\mu g.g^{-1}$ and 6.6$\mu g.g^{-1}$ at Mo-I-Rana.

## 6.3 Quantification of Deposition

### 6.3.1 Magnetic Mineral Deposition

The deposition of magnetic particulates, onto Finnish raised bogs as approximated by SIRM, is summarised in Table 4.6. The only other site with an available chronology is Draved Moss, for which estimated SIRM deposition is given in fig. 5.22. Using only the surface slice (0-2.5cm) to indicate the most recent deposition trends, it is apparent that the Finnish sites (with notable exceptions) have received lower SIRM fluxes in the years immediately preceeding 1983. The average for northern Finnish sites

is $2.1x10^{-6}Am^2kg^{-1}$ whilst for southern Finnish sites the average is slightly higher, $2.7x10^{-6}Am^2kg^{-1}$. The surface SIRM deposition at Draved Moss is $20.4x10^{-6}Am^2kg^{-1}$, which is between 7 and 10 times higher than the majority of Finnish sites studied. However, a significant feature is that the flux rates from Varrassuo Bog (southern Finland) and Liikanen (northern Finland) are comparable with Draved Moss, being $15.5x10^{-6}Am^2kg^{-1}$ and $22.6x10^{-6}Am^2kg^{-1}$. Therefore, given the data available, the most heavily polluted Finnish sites are only comparable with a rural mainland European site. This is either a function of the high values in rural mainland European sites, low values from the 'heavily polluted' Finnish sites or a combination of both. The evidence from other known polluted sites such as Harpar Lilltrask (Oldfield et al., 1981) and from work on heavily polluted British sites (eg. Oldfield et al., 1978a) suggests that the levels of magnetic deposition observed from sites in this study are low in comparison with sites in close proximity to major industrial regions or sources.

The general conclusions for all sites where a chronology is available, are threefold. First, SIRM deposition has gradually increased at most sites since the turn of the century. Second, at key sites such as Kaurastensuo and Draved Moss, there have been distinct increases in the level of deposition during this century. At Kaurastensuo, the increase occurred around 1930 whilst at Draved Moss a sharp post-1950 increase is observed. Third, the increases observed, although significant, are by no means comparable with the deposition that has taken place at heavily industrialised sites, which in some cases, for example Ringinglow Bog, has been more than an order of magnitude greater.

### 6.3.2 Chemical Deposition

Estimates of depositional fluxes are made for selected elements at sites in Finland and Denmark, where both total chemistries and

chronologies are available. The calculation of element fluxes has been restricted to the surface layer (0-2.5cm) in the majority of cases, in order to minimise any possible effects from mobility and translocation. Any influence from the active uptake by living tissue is envisaged to have a minimal effect given the relatively coarse thickness of the slice, 2.5cm. However, at Draved Moss the deposition has been estimated over the time-span available from the $^{210}Pb$ chronology (ca.175 years), in order to compare the results with those of Aaby et al. (1979).

The surface elemental deposition apparently shows more regional variation than the magnetic mineral deposition. For example, the iron deposition at Draved Moss is 6 times higher than the average deposition for southern Finland (exlcuding Varrassuo), which in turn is 1.5 times higher than the northern Finnish sites. The influence of pollutant point sources does not appear to be as marked for the elements, as for the magnetic minerals. At Varrassuo Bog, the iron and lead deposition fluxes show the greatest contrast, each being 2.4 times greater than the regional average. These values are, however, 2.4 and 6.3 times lower respectively than the fluxes of iron and lead at Draved Moss.

## 6.4 Magnetic Mineral-Heavy Metal Linkages

Table 6.2 summarises the relationships between magnetic minerals, as approximated by SIRM deposition, and the deposition of the various metals. The summary takes the form of correlation coefficients (Pearson's Product Moment, r), which have been broken down into three categories: significant at the 0.01 level, significant at the 0.05 level and insignificant at the 0.05 level. The sites are grouped according to their regional locations.

Perhaps the most obvious relationship to discuss is that of SIRM and

iron. It is apparent from the correlation coefficients that the relationship between these two variables, at the different sites is not as strong as might have been expected. Sites such as Pousujärvi (PA) and Utsjoki have negative correlations as a result of low surface iron deposition and relatively higher SIRM deposition. At greater depths the iron 'deposition' increases and SIRM decreases. The increase in iron is seen more as a function of water table influences rather than true 'deposition'. Where the iron appears to have increased as a result of water table influences it is important to note that the SIRM values do not respond as sensitively to this particular influence. This is probably due to the fact that the SIRM remanence appears to be carried in the insoluble iron fractions.

On closer inspection it is also apparent that the sites with the weakest SIRM and iron relationships are those with the lowest SIRM deposition. Again, these sites also tend to show the greatest relative response to water table influences. In contrast, the sites with the strongest correlations between SIRM and iron are those linked with anthropogenic sources, for example at Liikanen, Varrassuo and Draved Moss.

If the other metals are considered individually, it is apparent that lead, copper and manganese all display significant correlations with SIRM at the majority of sites from which they are available. If the correlations are viewed on a site specific basis, it is again apparent that sites linked with anthropogenic sources, such as at Liikanen, Varrassuo and Draved Moss, all display significant correlations between SIRM and most, if not all the elements available.

The evidence presented in the Introduction (Chapter 1, section 1.4), for the production of magnetic spherules and heavy metal particulates form industrial/combustion sources is widely recognised. This evidence is supported by significant correlations noted between aluminium, copper,

**Table 6.2** Mineral Magnetic-Heavy Metal Linkages. Pearson's product moment, r, for SIRM and heavy metals, post-1900.

| Site | n | SIRM v. Fe | SIRM v. Pb | SIRM v. Cu | SIRM v. Zn | SIRM v. Ni | SIRM v. Mn |
|---|---|---|---|---|---|---|---|
| **N. Scandinavia** | | | | | | | |
| Liikanen | 8 | 0.966** | 0.715* | 0.962** | 0.976** | - | 0.715* |
| Jänkivuopajanaapa, JD | 8 | 0.597 | - | 0.802** | 0.770* | - | 0.842 |
| Pousujärvi, PA | 5 | -0.414 | 0.771 | 0.174 | 0.008 | - | 0.545 |
| PB | 6 | 0.794* | 0.818* | 0.284 | 0.120 | - | 0.925** |
| Ahmajänkä | 6 | 0.753 | - | 0.836* | 0.855* | - | 0.817* |
| Utsjoki | 7 | -0.503 | 0.915** | 0.961** | 0.708* | - | 0.571 |
| **N. Norway** | | | | | | | |
| Norja, ND | 5 | 0.829* | 0.576 | - | 0.511 | - | 0.866* |
| NE | 5 | 0.576 | 0.716 | - | 0.460 | - | 0.415 |
| **S. Finland** | | | | | | | |
| Kaurastensuo, KAX[1] | 7 | 0.981** | 0.774* | 0.995** | 0.648 | 0.207 | - |
| Laaviosuo, LaavX | 5 | 0.446 | - | 0.460 | 0.315 | 0.767 | - |
| Varrassuo, VAX[1] | 6 | 0.983** | 0.984** | - | 0.58 | - | - |
| **S. Denmark** | | | | | | | |
| Draved Moss, DMHol2 | 5 | 0.965** | 0.873* | 0.926** | 0.860* | 0.642 | - |

* Significant at 0.05 level

** Significant at 0.01 level

1. Post-1935

iron manganese, nickel and zinc from automotive emissions in the Mersey Tunnel (Hunt, unpubl. data). The results summarised within this thesis, supported by the relationships outlined in Table 6.2 suggest that at the sites studied, the linkages inferred at the combustion stage appear to persist through to deposition. These linkages appear to persist within the post-depositional environment at least over the timescale encompassing the increase in industrial deposition. One of the major controlling influences on the relationship between magnetic minerals and heavy metals appears to be the water table and its seasonal adjustments. The primary effect is the partial mobilisation of elements such as iron and manganese, which according to the results presented above, do not appear to be the carriers of magnetic remanence.

Jones (1985) points out another possible cause of the link between magnetic minerals and heavy metals, apart from the anthropogenic sources. The process of metal occlusion by hydrous iron and manganese oxides, may provide a control on a number of heavy metals. The process of occlusion is a function of Eh, pH and metal concentration among others. Sequential extractions presented in Jones (op. cit.), however, show little relationship between hydroxylamine hydrochloride with acetic acid extractable iron and SIRM. It was concluded that this process is of little significance in peat, bearing in mind the overall importance of organic matter which exerts a major control on heavy metal availability in highly organic soils or in environments conducive to hydrous oxide dissolution.

The circumstantial evidence presented is not strong enough to establish a causal relationship between magnetic minerals and heavy metals in peat. It does, however, support observations made by other workers (see above) that such a relationship i) exists and ii) is causal. The prospects for developing magnetic techniques in a complementary or even

'surrogate' role for heavy metal analyses is potentially very promising.

## 6.5 Conclusions

The major conclusions presented below are based on the aims of the study presented in Chapter 1 (section 1.8). An examination of the reproducibility of the primary magnetic deposition record in the raised bog, Kaurastensuo, was undertaken in Chapter 2. This examination involved an appraisal of the effects of hummock-hollow microtopography on the magnetic record. The basic conclusion from the results at Kaurastensuo is that the magnetic record in this bog appears to show an acceptable level of reproducibility, both spatially and temporally. The spatial reproducibility is, however, limited to the sampling sites on the ombrotrophic crown, whilst the temporal reproducibility is limited to about the last 150 years. The temporal variation, notably the identification of a magnetic 'take-off' point is consistent with the published results of Oldfield et al. (1981). The hummock cores received marginally higher deposition in comparison with the hollows, although this was significantly lower than the order of magnitude difference noted by Oldfield et al. (1979a).

Chapter 2 looked at the period corresponding to approximately the last 150 years. The temporal variation, notably the identification of a magnetic 'take-off' point is consistent with the published results of Oldfield et al. (1981). The hummock cores received marginally higher deposition in comparison with the hollows, although this was significantly lower than the order of magnitude difference noted by Oldfield et al. (1979a).

Chapters 2 and 3 looked at the persistence of the magnetic record over timescales of $10^1$-$10^3$ years. The examination of heavy metal-magnetic mineral linkages was approached in two separate ways. Chapter 3 examined the links between the long term magnetic and chemical records

at two sites overlying contrasting mineral soils. The second, and most important observations centred on the linkages in surface peats (0-50cm) and more specifically post-1900 peat. The latter involved the use of a variety of dating methods ranging from the growth rates of surface peats to $^{210}Pb$ dating. Regarding the first approach, there is good agreement between the magnetic parameters and chemical profiles, especially iron, in the minerotrophic basal peats at Kaurastensuo, overlying limnic sediments, and at Varrassuo, overlying post-glacial sands. The influence of the underlying mineral soils on the overlying peat, as a result of the persistence of minerotrophic conditions, are in marked contrast at the two sites. At Varrassuo, the influence of the post-glacial sands is extremely limited, both in terms of the magnetic parameters and the chemical profiles. In contrast, at Kaurastensuo the influence of the underlying limnic sediments extends upwards for about 60cm, gradually decreasing all the time. Both the magnetics and heavy metals appear to be extremely sensitive to the transition between the mineral soils and the organic-rich basal peats at both sites.

Chapters 4, 5 and 6 (section 6.4) have examined the deposition of magnetic minerals, as approximated by SIRM, and heavy metals at various sites throughout Scandinavia using available chronologies. The magnetic deposition has increased significantly in the majority of cases since 1900. At some sites, for example Kaurastensuo and Draved Moss, the increase in deposition may be narrowed down to a discrete point in time or 'take-off'. At Kauraarstensuo, the take-off point is dated by growth rate data at about 1931, whereas $^{210}Pb$ dating at Draved Moss indicates the take-off there to be between 1924 and 1950. Northern Scandinavian sites, in contrast showed no strong evidence of discrete increases in deposition, generally displaying a gradual rise in deposition from about the turn of the

century.

Chapter 6, section 6.4 showed a significant association between SIRM and lead, copper and manganese concentrations in post-1900 samples. This association is strengthened, and extended to iron and zinc, at sites linked with deposition from anthropogenic sources, for example at Liikanen, Varrassuo and Draved Moss.

In quantitative terms the estimated deposition at Draved Moss is approximately the same order as that at Liikanen and Varrassuo, between 15.5-22.6x$10^{-6}Am^2kg^{-1}$. These fluxes are between 7 and 10 times higher than the estimated deposition from Finnish sites studied. The variation in deposition has prompted an approximation of regional trends, again within the limitations of the sites available. The trends are masked to some extent by site-specific features in some cases. However, it appears that the magnetic and chemical deposition in northern Scandinavian sites is slightly lower than that in southern Finnish sites. The latter, in turn, are significantly lower than the deposition at Draved Moss, a mainland European site, by about 8 times for the magnetics and between 3.5-15 times for the heavy metals, dependent on the metal in question.

Finally, supportive techniques such as scanning electron microscopy (SEM) and energy dispersive X-ray analysis (EDX) have been used at Draved Moss and Mo-I-Rana to identify and characterise the inorganic fraction in magnetic extracts of surface peat. The micrographs from both sites identify two main types of particulate: spherules and non-spherules. EDX analysis of the spherule particles has characterised them as being solely composed of iron. The larger non-spherule particulates have element compositions consistent with the local bedrock at Mo-I-Rana. This latter group of particulates are interpreted as locally derived products of deflation processes. This component has been tentatively identified in

earlier chapters (eg. Chapter 2, section 2.7) as 'field erosion' from the surrounding cultivated land. The spherules have been linked in published work (cf. Chapter 1, section 1.3) with industrial/combustion processes.

In conclusion, the evidence from Chapters 2-5 appears to corroborate the findings of published work from sites in Scandinavia and to some extent Britain. The results also suggest that mineral magnetic techniques may play an important role in the characterisation of atmospheric particulates within the peat and identification of the various sources of these particulates.

# 7. Appendices

## 7.1 Sample Preparation for Magnetic Analyses

1. The 10cc polythene (plastic) sample holders were acid washed (10% hydrochloric acid) and rinsed (distilled water), before initial measurement at a field strength of 300mT. Pots with a total remanent magnetisation of $1x10^{-6}Am^2$ were rejected.

2. Samples from homogenised contiguous core slices were compressed in a purpose built peat press (Appendix 2), in order to maximise sample weight. Compression increased the weight by up to a factor of 5. The compressed sample was then extruded directly into a pre-measured, pre-weighed 10cc pot.

3. The sample mass was calculated from the total mass and the packed sample measured in the sequence:

   i. Susceptibility

   ii. ARM

   iii. ($IRM_{300mT}$), SIRM

   iv. Demagnetisation through 4-12 backfields

## 7.2 A Peat Press

Due to the low ferrimagnetic content commonly found within 'remote' or deep peat samples, the measurement of magnetic parameters had been, to a large extent, precluded by 'noise' levels of the instruments. Despite the sensitivity of the fluxgate magnetometer ($0.2 \times 10^{-6} Am^2 kg^{-1}$), a combination of the low ferrimagnetic content and small sample weights proved to be a major limiting factor in measurement. A solution to the problem was to increase the sample weight, given that the 10cc volume could not be increased. An increase in sample weight increased the volume concentration of ferrimagnetic minerals, allowing for more accurate readings to be made. This was achieved by the design and construction of a small, hand-operated peat press (Plate 7.1). The author is indebted to Mr. R. Tennant for his technical expertise and advice.

All the parts of the press in direct contact with the peat sample were fashioned from non-metallic materials. A PTFE material was used for the body and composite nylon for the base. The location of four drainage holes in the nylon base served to relieve pressure in the chamber and to enable wet peats and sediments to be compressed. The piston, also composite nylon, was sealed to the chamber by a rubber 'O'-ring. The torque plate contained a detachable nylon inner thread to prevent the possibility of shavings from metal-metal contact. The torque plate, piston screw bolt and collars were made from steel and the locking nuts from brass.

In terms of increased sample weight, the peat press increased the efficiency of packing by 2.4 times for dried samples, 1.8 times for dried and pulverised samples, and 1.9 times for wet samples. The comparisons were made from nine samples of homogenised peat from a monolith taken at Holland's Moss, South West Lancashire. At around the noise level of the magnetometer, this increase in sample weight gave significantly higher

**Plate 7.1** A Peat Press. Annotated plate of the peat press showing the components of the press and their composition.

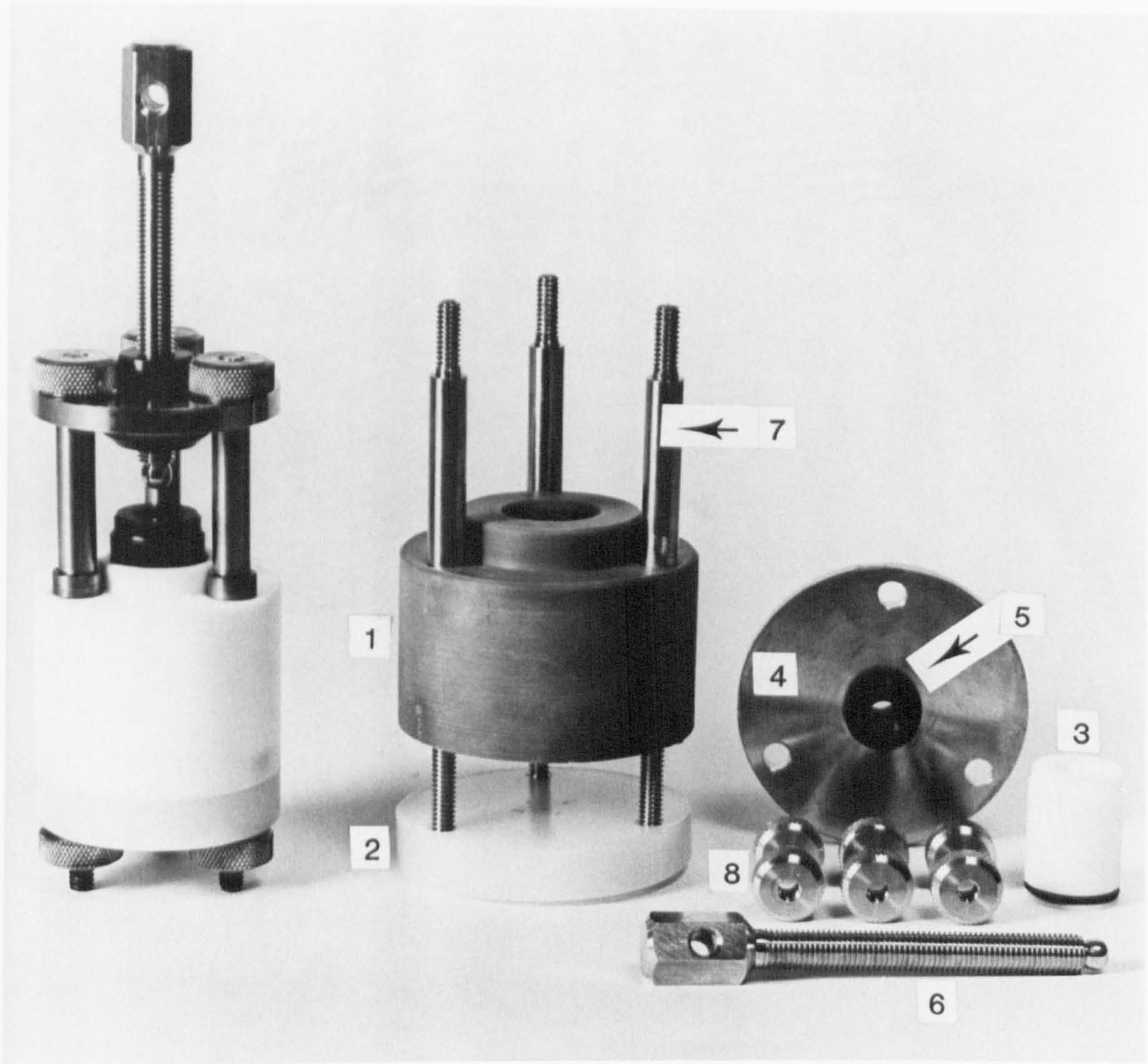


1. PTFE body

2. Composite nylon base

3. Composite nylon piston and rubber 'O'-ring

4. Steel torque plate

5. Composite nylon thread (1mm)

6. Steel piston screw bolt

7. Steel collars

8. Brass locking nuts

magnetometer readings (by a factor of 2), before the values were made mass specific. The variation in mass specific $IRM_{300mT}$ was very low, being 0.035 $10^{-6}Am^2kg^{-1}$.

## 7.3 Laboratory Methods

1. Atomic Absorption Spectroscopy

a) Sample Digestion

i. 10ml of nitric acid ($HNO_3$) were added to approximately 1.5g of ground peat.

ii. The samples were digested initially at 50°C for an hour and subsequently at 130°C for 3 hours or until complete digestion was achieved.

iii. The samples were then filtered through Whatman 42 filters and made up to 50ml volume with distilled water.

iv. Two blanks were made up in every batch of 40 digestions.

v. Two sample replicates were made up throughout.

b) Standard Solutions

i. Standard solutions were made up from stock solutions of 1000ppm Fe, Cu, Ni, Zn and Pb (Analar quality).

ii. The range of standards produced: 0.5ppm, 1.0ppm, 2ppm, 3ppm, 5ppm, 10ppm, 20ppm, 50ppm and 100ppm were made up from serial dilutions of stock solutions.

iii. Over-range samples (eg. basal iron) were serially diluted until within the standard range.

iv. Standards were made up to volume (50ml) with the same acid:distilled water ratio used in digestion ie. 20% nitric acid.

c) Detection Limits

The following detection limits ($ug.g^{-1}$) apply to element concentrations measured on the Varian AA1275 series spectrophotometer:

| Fe | Cu | Pb | Ni | Zn |
|---|---|---|---|---|
| 0.05 | 0.05 | 0.05 | 0.05 | 0.01 |

d) Replicates

Replicates of samples were made-up throughout the runs. The automatic sampler was programmed to take an average of two readings per sample. The sample blanks were automatically deducted from the spectrophotometer reading.

2. Ash residues

Samples of approximately 1.0g were ground and ashed in a Griffin muffle furnace at 550°C for approximately 3 hours. Samples were weighed to an accuracy of 0.0001g. After cooling in a dessicator, the samples were re-weighed and the inorganic component determined as a percentage.

## 7.4 Radiocarbon Dates From Southern Finland

All radiocarbon dates have been supplied by Dr. K. Tolonen, to whom the author is indebted. Analyses were made at the Helsinki Radiocarbon Laboratory by Högne Jungner based on the half-life (5568 years) of the radioisotope, $^{14}C$ (1979). All dates are given as years before 1950, a standard $^{14}C$ baseline.

| Laboratory Code | Depth 1979 (cm) | Adjusted Depth 1983 (cm) | Years (BP) |
|---|---|---|---|
| 1. Laaviosuo, Site X | | | |
| Hel-1151 | 50-60 | 43-53 | 110±90 |
| Hel-1152 | 90-100 | 83-93 | 600±90 |
| Hel-1153 | 110-120 | 103-113 | 690±130 |
| Hel-1154 | 150-160 | 143-153 | 1280±90 |
| Hel-1155 | 190-200 | 183-193 | 1870±110 |
| Hel-1156 | 210-220 | 203-213 | 2320±100 |
| Hel-1157 | 250-260 | 243-253 | 2400±140 |
| Hel-1158 | 330-340 | 323-333 | 3100±150 |
| Hel-1159 | 400-410 | 393-403 | 4420±130 |
| Hel-1160 | 445-455 | 438-448 | 5620±100 |
| Hel-1161 | 485-495 | 478-488 | 6580±150 |
| Hel-1162 | 505-515 | 498-508 | 7690±160 |
| Hel-1163 | 535-545 | 528-538 | 8780±120 |
| 2. Kaurastensuo. Site X | | | |
| Hel-1649 | 70-75 | 45-50 | 140±130 |
| Hel-1650 | 160-170 | 135-145 | 1540±120 |
| Hel-1651 | 200-210 | 175-185 | 1810±130 |
| Hel-1652 | 250-260 | 225-235 | 2110±130 |
| Hel-1653 | 330-340 | 305-315 | 3040±120 |
| Hel-1654 | 360-370 | 335-345 | 3780±110 |
| Hel-1655 | 380-390 | 355-365 | 3960±130 |
| Hel-1656 | 430-440 | 405-415 | 5770±120 |
| Hel-1660 | 460-470 | 435-445 | 6480±100 |
| Hel-1661 | 488-500 | 463-575 | 8120±110 |
| Hel-1662 | 510-520 | 485-495 | 8950±120 |
| 3. Varrassuo, Site X | | | |
| Hel-1132 | 45-55 | 31-41 | 370±110 |
| Hel-1133 | 65-75 | 51-61 | 860±120 |
| Hel-1134 | 85-95 | 71-81 | 880±100 |
| Hel-1135 | 105-115 | 91-100 | 1200±100 |

## 7.5 Translation

Translation of the riddle entitled 'The Raised Bog', with thanks to Ulrich Kockel:

**The Raised Bog**

Its trunk is of tremendous thickness;

The longest Spruce does not achieve the same;

But the crown is short, incredibly short;

Even the thornbush looks out over it.

Grown only from the rain and dew of heaven.

Not nurtured by the Earth.

And if the water rushes down the slope, -

Here you see it rest on light and slope!

## 8. References


**Aaby, B. & H. Tauber,** 1974 Rates of peat formation in relation to degree of humification and local environment, as shown by studies of a raised bog in Denmark
Boreas 4: 1-17

**Aaby, B.,** 1976 Cyclic climatic variations in climate over the past 5500yr reflected in raised bogs
Nature 263: 281-284

**Aaby, B. & J. Jacobsen,** 1979 Changes in biotic conditions and metal deposition in the last millenium as reflected in ombrotrophic peat in Draved Mose, Denmark
Danm. Geol. Unders. Arbog: 5-43

**Aaby, B., J. Jacobsen & O.S. Jacobsen,** 1979 $^{210}Pb$ dating and deposition in the ombrotrophic peat bog, Draved Mose, Denmark
Danm. Geol. Unders. Arbog: 45-68

**Alary, J., P. Bourbon, J. Esclassan, J-C. Lepert, J. Vandaele & F. Klein,** 1983 Zinc, lead and molybdenum contamination in the vicinity of an electric steelworks and environmental response to pollution abatement by bag filter
Water Air & Soil Poll. 20: 137-145

**Alhonen, P., J.J. Donner, H. Jungner & I. Vuorela,** 1977 Comparison between the Holocene biostratigraphy and radiocarbon dates of a lake and a raised bog in southern Finland
X INQUA Congress, Abs. 11

**Andersen, A.,** 1966 Geologi og arkaeologi i Draved Mose
Medd. Dan. Geol. Foren. 16: 255-258

**Appleby P.G. & F. Oldfield,** 1978 The calculation of 210-Lead dates assuming a constant rate of supply of unsupported $^{210}Pb$ to the sediment
Catena 5: 1-8

**Appleby, P.G. & F. Oldfield,** 1979 Correspondence
In: Environ. Sci. Technol. 13:4: 478-480

**Appleby. P.G. & F. Oldfield,** 1983 The assessment of $^{210}Pb$ data from sites with varying sediment accumulation rates
Hydrobiologia 103: 29-35

**Bache, B.W.,** 1984 Soil-water interactions
Phil. Trans. R. Soc. Lond. 305: 393-407

**Banerjee, S.K., J. King & J. Marvin,** 1981 A rapid method for magnetic granulometry with applications to environmental studies
Geophys. Res. Let. 8:4: 333-336

**Barber, K.E.,** 1978 A palaeoecological test of the theory of cyclic peat bog regeneration
Unpubl. Ph.D., University of Southampton

**Barclay-Estrup, P. & R.J.K. Rinne,** 1978 Lead and zinc accumulation in two feather mosses in northwestern Ontario, Canada
Oikos 30:1: 106-108

**Bellamy, D.J. & J. Rieley,** 1967 Some ecological statistics of a "miniature bog"
Oikos 18: 33-40

**Berner, R.A.,** 1970 Sedimentary pyrite formation
Am. J. Science 268: 1-23

**Berner, R.A.,** 1984 Sedimentary pyrite formation: An update
Geochim. Cosmochim. Acta 48: 605-615

**Bloemendal, J.,** 1982 The quantification of rates of total sediment influx to Llyn Goddionduon, Gwynedd
Unpubl. Ph.D., University of Liverpool

**Burgeff, H.,** 1961 Mikrobiologie des Hochmoores
Stuttgart: Fischer

**Cambray, R.S., E.M.R. Fisher, W.L. Brooks & D.H. Peirson,** 1971 Radioactive fall-out in air and rain. Results to the middle of 1971
AERE-R6923, HMSO London

**Cambray, R.S. & J.D. Eakins,** 1982 Pu, $^{241}$Am and $^{137}$Cs in soil in West Cumbria and a maritime effect
Nature 300: 46-48

**Carmichael, R.S.,** 1982 Magnetic properties of minerals and rocks
In: Handbook of Physical Properties of Rocks Vol. II: 229-287
Ed. R.S. Carmichael

**Chamberlain, A.C.,** 1953 Aspects of travel and deposition of aerosol and vapour clouds
AERE HP/R 1261. AERE, Harwell

**Chamberlain, A.C.,** 1966 Transport of Lycopodium spores and other small particles to rough surfaces
Proc. R. Soc. Series A: 45-70

**Chapman, S.B.,** 1964a The ecology of Coom Rigg Moss, Northumberland I. Stratigraphy and present vegetation
J. Ecol. 52: 299-313

**Chapman, S.B.,** 1964b The ecology of Coom Rigg Moss, Northumberland II. The chemistry of peat profiles and the development of the bog system
J. Ecol. 52: 315-321

**Clough, W.S.,** 1975 The deposition of particles on moss and grass surfaces
Atmos. Environ. 9: 1113-1119

**Clymo, R.S.,** 1963 Ion exchange in Sphagnum and its relation to bog ecology
Ann. Bot. 27:106: 309-324

**Clymo, R.S.,** 1965 Experiments on breakdown of Sphagnum in two bogs
J. Ecol. 53: 747-758

**Clymo, R.S.,** 1970 The growth of Sphagnum: Methods of measurement
J. Ecol. 58: 13-49

**Clymo, R.S.,** 1973 The growth of Shagnum: Some effects of environment
J. Ecol. 61: 849-869

**Clymo R.S.,** 1978 A model of peat bog growth
In: Production Ecology of British Moors and Montane Grasslands: 187-223
Ed. **O.W. Heal & D.F. Perkins with W.M. Brown**

**Clymo, R.S.,** 1983 Peat
In: Ecosystems of the World 4A
Mires: Swamp, Bog, Fen, and Moor. General Studies: 159-224
Ed. **A.J.P. Gore**

**Clymo, R.S.,** 1984a The limits to peat bog growth
Phil. Trans. R. Soc. Lond. Series B 303: 605-654

**Clymo, R.S.,** 1984b Sphagnum-dominated peat bog: A naturally acidic ecosystem
Phil. Trans. R. Soc. Lond. Series B 305: 487-499

**Damman, A.W.H.,** 1978 Distribution and movement of elements in ombrotrophic peat bogs
Oikos 30:1: 480-495

**Damman, A.W.H.,** 1979 Geographic patterns in peatland development in Eastern North America
In: Classification of Peat and Peatlands
Proc. Int. Peat Symp.: 42-57

**Davis, J.C.,** 1973 Statistics in Geology
New York: Wiley & Sons

**Davison, R.L., D.F.S Natusch, J.R. Wallace & C.A. Evans,** 1974 Trace elements in fly ash: dependence of concentration on particle size
Environ. Sci. Technol 8: 1107-1113

**Day, R., M. Fuller & V.A. Schmidt,** 1977 Hysteresis properties of titanomagnetites: Grain-size and compositional dependence
Phys. Earth & Plan. Int. 13: 260-267

**Dearing, J.A.,** 1979 The application of magnetic measurements to studies of particulate flux in lake-watershed ecosystems
Unpubl. Ph.D., University of Liverpool

**Del Monte, M. & C. Sabbioni,** 1984a Morphology and mineralogy of fly-ash from a coal-fuelled power plant
Arch. Met. Geoph. Biocl. B35: 93-104

**Del Monte, M. & C. Sabbioni** 1984b Gypsum crusts and fly-ash particles on carbonatic outcrops
Arch. Met. Geoph. Biocl. B35: 105-111

**Donner, J.J.,** 1951 Pollen analytical studies of late-glacial deposits in Finland
Bull. Comm. Geol. Finlande 24:154: 1-92

**Donner, J.J.,** 1965 The Quaternary of Finland
In: The Quaternary, Vol. 1: 199-272
Ed. K. Rankama

**Donner, J.J.,** 1966 The late-glacial and early post-glacial pollen stratigraphy of southern and eastern Finland
Comm. Biol. 29:9: 1-24

**Donner, J.J.,** 1971 Towards a stratigraphical division of the Finnish Quaternary
Comm. Phys.-Math. 41: 281-305

**Donner, J.J. & H. Jungner,** 1974 Errors in the radiocarbon dating of deposits in Finland from the time of deglaciation
Bull. Geol. Soc. Finland 46: 139-144

**Donner, J.J., P. Alhonen, M. Eronen, H. Jungner & I. Vuorela,** 1978 Biostratigraphy and radiocarbon dating of the Holocene lake sediments of Tyotjärvi and the peats in the adjoining bog Varrassuo, west of Lahti in southern Finland
Ann. Bot. Fennici 15: 258-280

**Dorn, C.R., J.O. Pierce, P.E. Phillips & G.R. Chase,** 1976 Airborne lead, cadmium, zinc and copper concentration by particle size near a smelter
Atmos. Environ. 10: 443-446

**Dunlop, D.J.,** 1969 Hysteresis properties of synthetic and natural monodomain grains
Phil. Mag. 19:158: 329-338

**Dunlop, D.J.,** 1972 Magnetite: Behaviour near the single domain threshold
Science 176: 41-43

**Dunlop, D.J.,** 1973 Superparamagnetic and single domain threshold sizes in Magnetite
J. Geophys. Res. 78:11: 1780-1793

**Dunlop, D.J.,** 1981 The rock magnetism of fine particles
Phys. Earth & Plan. Int. 26: 1-26

**Edgington, D.N. & J.A. Robbins,** 1975 Records of lead deposition in Lake Michigan sediments since 1800
Environ. Sci. Technol. 10: 266-274

**Edgington, D.N. & J.A. Robbins,** 1979 Correspondence
In: Environ. Sci. Technol. 13: 480-482

**El-Daoushy, F. & K. Tolonen,** 1982 $^{210}Pb$ and heavy metal contents in dated ombrotrophic peat-hummocks from Finland
ICRM, UK AEA, Harwell 26pp

**El-Daoushy, F., K. Tolonen & R. Rosenberg,** 1982 $^{210}Pb$ and moss increment dating of two Finnish Sphagnum hummocks
Nature 296: 429-431

**Eurola, S. & R. Ruuhijärvi,** 1961 Uber die regionale Einteilung der Finnischen moore
Arch. Soc. "Vanamo" 16 suppl.: 49-63

**Eurola, S.,** 1962 Uber die regionale Einteilung der sudfinnischen Moore
Ann. Bot. Soc. "Vanamo" 33:2: 1-243

**Ferguson, P., J.A. Lee & J.N.B. Bell,** 1978 Effects of sulphur pollutants on the growth of Sphagnum species
Environ. Pollut. 16: 151-162

**Ferguson, P. & J.A. Lee,** 1983 Past and present sulphur pollution in the southern Pennines
Atmos. Environ. 17:6: 1131-1137

**Firbas, F.,** 1949 Waldgeschichte Mitteleuropas nordlich der Alpen
Bd. 1. Jenna, 480pp

**Foster, I.D.L., J.A. Dearing, A.D. Simpson & P.G. Appleby,** 1985 Lake-catchment studies of erosion and denudation:
II Estimates of contemporary and historic sediment yields in the Merevale catchment, Warwicks, UK
Earth Surface Processes and Landforms 10: 45-68

**Fowler, D.,** 1984 Transfer to terrestrial surfaces
Phil. Trans. R. Soc. Lond. Series B 305: 281-297

**Frenzel, B.,** 1983 Mires-Repositories of climatic information or self-perpetuating ecosystems?
In: Ecosystems of the World 4A
Mires: Swamp, Bog, Fen, and Moor. General Studies: 35-65
Ed. A.J.P. Gore

**Gallagher, K.J., W. Feitknecht & V. Mannweiler,** 1968 Mechanism of oxidation of magnetite to $Fe_2O_3$
Nature 217: 1118-1121

**Gregory, P.H.,** 1961 The microbiology of the atmosphere
London: L. Hill

**Griffin J.J. & E.D. Goldberg,** 1981 Sphericity as a characteristic of solids from fossil fuel burning in a Lake Michigan sediment
Geochim. Cosmochim. Acta 45: 763-769

**Goodman, G. & T.M. Taylor,** 1971 Plants and soils as indicators of metals in the air
Nature 231: 287-292

**Gore, A.J.P.,** 1983 Introduction
In: Ecosystems of the World 4A
Mires: Swamp, Bog, Fen and Moor. General Studies: 1-34
Ed. **A.J.P. Gore**

**Haavisto, V.F.,** 1974 Effects of a heavy rainfall on redox potential acidity of a waterlogged peat
Can. J. Soil Sci. 54: 133-135

**Hagerup, O. & V. Petersson,** 1960 Botanisk Atlas. II. Mosser. Bregner. Padderokker.
Ulvefødder. Naaletraeer. Nedstamning
København

**Hailwood, E.A. & L. Molyneux,** 1974 Anhysteretic Remanent Magnetisation due to asymmetrical alternating fields
Geophys. J. R. Astr. Soc. 39: 421-434

**Hales, J.M.,** 1983 Precipitation chemistry: Its behaviour and its calculation
In: Air pollutants and their effects on the terrestrial ecosystem
Ed. **S.V. Krupa & A.H. Legge**

**Hansen, B.,** 1966 The raised bog Draved Kongsmose
Bot. Tids. 62: 146-185

**Hansen, L.D., D. Silberman & G.L. Fisher,** 1981 Crystalline components of stack-collected, size-fractionated coal fly ash
Environ. Sci. Tecnol. 15: 1057-1062

**Hasler, A.,** 1943 Lebensm. Hyg., Bern 34: 79pp.
In: Rühling & Tyler, 1983
*2

**Hovmand, M.F.,** 1973 Atmosfaerisk nedfald i Danmark 1972-73
Prelim. Rep. Inst. Bot. Ecol., Copenhagen University
In: **Aaby et al, 1979**

**Hovmand, M.F.,** 1976 Fall-out and rain-out of nutrients
Rep. Inst. Bot. Ecol., Copenhagen University
In: **Aaby et al, 1979**

**Hughes, M.K., N.W. Lepp & D.A. Phipps,** 1980 Aerial heavy metal pollution and terrestrial ecosystems
Adv. Ecol. Res. 11: 218-327

**Hulett, L.D. Jr., A.J. Weinberger, K.J. Northcutt & M. Ferguson,** 1980 Chemical species in fly ash from coal-burning power plants
Science 210: 1356-1358

**Hunt, A., J. Jones & F. Oldfield,** 1984 Magnetic measurements and heavy metals in atmospheric particulates of anthropogenic origin
Sci. Tot. Environ. 33: 129-139

**Hunt, A.,** in prep. Atmospheric magnetic studies
Unpubl. Ph.D., University of Liverpool

**Hutchinson, C.S.,** 1974 Laboratory handbook of petrographic techniques
Wiley & Sons 527pp

**Hvatum, O. Ø., B. Bølviken & E. Steinnes,** 1983 Heavy metals in Norwegian ombrotrophic bogs
In: Environmental Biogeochemistry
Ecol. Bull. 35: 351-356
Ed. R. Hallberg

**Ingram, H.A.P.,** 1983 Hydrology
In: Ecosystems of the World 4A
Mires: Swamp, Bog, Fen and Moor. General Studies: 67-158
Ed. A.J.P. Gore

**Ivanov, K.E.,** 1981 Water movement in mirelands
Translated by A. Thompson & H.A.P. Ingram from:
**Ivanov, K.E.,** 1975 Vodoobmen v bolotnykh landshaftkh
London: Academic Press

**Jacobsen, O.S.,** 1981 The historical development of air pollution as reflected in ombrotrophic peat bogs in Denmark
Proc. Int. UNEP-SCOPE: 21pp

**Jessen, K.,** 1935 Archaeological dating in the history of North Jutland's vegetation
Acta Archaeol. 5: 185-214

**Johnson, H.P., W. Lowrie & D.V. Kent,** 1975 Stability of ARM in fine and coarse magnetite and maghemite particles
Geophys. J. R. Astr. Soc. 41: 1-10

**Jones, J.M.,** 1985 Magnetic minerals and heavy metals in ombrotrophic peat
Unpubl. Ph.D., University of Liverpool

**Jones, M.D.H.,** 1982 Magnetic measurements of Barbados dusts
Unpubl. Report, University of Liverpool, Dept. of Geography

**King, J., S.K. Banerjee, J. Marvin & O. Ozdemir,** 1982 A comparison of different methods for determining the relative grain size of magnetite in natural materials: some results from lake sediments
Earth & Plan. Sci. Lett.59: 404-419

**Koide, M., K.W. Bruland & E.D. Goldberg,** 1973 Th-228/Th-232 and Pb-210 geochronologies in marine and lake sediments
Geochim. Cosmochchim. Acta 37: 1171-1187

**Krishnaswamy, S., D. Lal, J.M. Martin & M. Meyerbeck,** 1971 Geochronology of lake sediments
Earth & Plan. Sci. Lett. 11: 407-414

**Lamb, H.H.,** 1970 Volcanic dust in the atmosphere: with a chronology and assessment of its meteorological significance
Roy. Soc. Phil. Trans. 266: 425-533

**Le Borgne, E.,** 1955 Susceptibilitie magnetique anormale du sol superficiel
Ann. Geophys. 11: 399-419

**Le Borgne, E.,** 1960 Influence du feu sur les propietes magnetique du sol et du granite
Ann. Geophys. 16: 159-195

**Levi, S. & R.T. Merrill,** 1976 A comparison of ARM and TRM in magnetite
Earth & Plan. Sci. Lett. 32: 171-184

**Lindholm, T.,** 1981 Growth rhythm of Sphagnum fuscum (Schimp.) Klinggr. in the Laaviosuo Bog, southern Finland
Suo 32:4-5: 115-118

**Linton, R.W., D.F.S. Natusch, R.L. Solomon & C.A. Evans Jr.,** 1980 Physicochemical characterisation of lead in urban dusts: A microanalytical approach to lead tracing
Environ. Sci Technol. 14: 159-164

**Livett, E.A., J.A. Lee & J.H. Tallis,** 1979 Lead, zinc and copper analyses of British blanket peats
J. Ecol. 67: 865-891

**Longton, R.E.,** 1972 Growth and reproduction in northern and southern hemisphere populations of the peat-forming moss Polytrichum alpestre with reference to the estimation of productivity
Proc. 4th Int. Peat Congress Vol 1: 259-275

**Longworth, G. & M.S. Tite,** 1977 Mössbauer and magnetic susceptibility studies of iron oxides in soils from archaeological sites
Archaeometry 19: 3-14

**Maher, B.A.,** 1984 Origins and transformations of magnetic minerals in soils
Unpubl. Ph.D., University of Liverpool

**Malmer, N.,** 1962 Studies on the mire vegetation in the Archaean area of southwestern Götaland (southern Sweden)
2. Distribution and seasonal variation in elementary constituents on some mire types
Op. Bot. Soc. Bot. Lund. 7:2: 1-67

**Malmer, N. & E. Holm,** 1984 Variation in the C/N quotient of peat in relation to decomposition rate and age determination with $^{210}Pb$
Oikos 43: 171-182

**McCrone, W.C. & J.G. Delly,** 1973 The Particle Atlas
Vol. II The Light Microscopy Atlas
Ann Arbor Science Publishers, Michigan

**Mellor, D.P. & L. Maley,** 1947 Stability constants of internal complexes
Nature 159: 370

**Mellor, D.P. & L. Maley,** 1948 Order and stablity of metal complexes
Nature 161: 436-437

**Milner, H.B.,** 1962 Sedimentary Petrography Vol. 1
George Allen & Unwin

**Molyneux, L. & R. Thompson,** 1973 Rapid measurement of the magnetic susceptibility of long cores of sediment
Geophys. J. R. Astr. Soc. 32: 479-481

**Mullins, C.E. & M.S. Tite,** 1973 Magnetic viscosity, quadrature susceptibility, and frequency dependence of susceptibility in single domain assemblies of magnetite and maghemite
J. Geophys. Res. 78:5: 804-809

**Mullins, C.E.,** 1974 The magnetic properties of the soil and their application to archaeological prospecting
Archaeo-Physika 5: 143-347

**Mullins, C.E.,** 1977 Magnetic susceptibility of the soil and its significance in soil science: A review
J. Soil Sci. 28: 223-246

**Niiranen, A.,** 1973 Palaeobotanical studies on Kaurastensuo, Lammi
M.Sc. thesis, University of Helsinki: 87p

**Nordø, J.,** 1976 Long range transport of air pollutants in Europe and acid precipitation in Norway
Water Air & Soil Poll. 6: 199-217

**Nriagu, J.O.,** 1978 The Biogeochemistry of Lead in the Environment
Elsevier

**Oldfield, F.,** 1977 Lakes and their drainage basins as units of sediment based ecological study
Prog. Phys. Geog. 1:3: 460-504

**Oldfield, F., R. Thompson & K.E. Barber,** 1978a Changing atmospheric fallout of magnetic particles recorded in recent ombrotrophic peat sections
Science 199: 679-680

**Oldfield, F., P.G. Appleby & R.W. Battarbee,** 1978b Alternative $^{210}Pb$ dating: results from the New Guinea Highlands & Lough Erne
Nature 271: 339-342

**Oldfield, F., A. Brown & R. Thompson,** 1979a The effect of microtopography and vegetation on the catchment of airborne particles measured by remanent magnetism
Quat. Res. 12: 326-332

**Oldfield, F., P.G. Appleby, R.S. Cambray, J.D. Eakins, K.E. Barber, R.W. Battarbee, G.R. Pearson & J.M. Williams,** 1979b $^{210}Pb$, $^{137}Cs$ and $^{239}Pu$ profiles in ombrotrophic peat
Oikos 33:1: 40-45

**Oldfield, F., T.A. Rummery, R. Thompson & D.E. Walling,** 1979c Identification of suspended sediment sources by areas of magnetic measurements: some preliminary results
Water Resources Res. 15: 211-218

**Oldfield, F., P.G. Appleby & D. Petit,** 1980 A re-evaluation of lead-210 chronology and the history of total lead influx in a small South Belgian pond
Ambio 9: 97-99

**Oldfield, F., K. Tolonen & R. Thompson,** 1981 History of particulate atmospheric pollution from magnetic measurements in dated Finnish peat profiles
Ambio 10:4: 185-188

**Oldfield, F.,** 1981 Peats and lake sediments: Formation, stratigraphy, description and nomenclature
In: Geomorphological Techniques: 306-326
Ed. A. Goudie

**Oldfield, F. & P.G. Appleby,** 1984a A combined radiometric and mineral magnetic approach to recent chronology in lakes affected by catchment disturbance and sediment redistribution
Chemical Geology 44: 67-83

**Oldfield, F. & P.G. Appleby,** 1984b Empirical testing of $^{210}Pb$ dating models for lake sediments
In: Lake Sediments and Environmental History
Ed. E.Y. Haworth & J.W.G. Lund

**Oldfield, F., A. Krawiecki, B. Maher, J.J. Taylor & S. Twigger,** 1984 The role of mineral magnetics in archaeology
In: Palaeoenvironmental Techniques, Design and Interpretation
Ed. N.G.R Fieller, D.D. Gilbertson & N.G.A. Ralph

**Oldfield, F., A. Hunt, M.D.H. Jones, R Chester, J.A. Dearing, L. Olsson & J.M. Prospero,** 1985 Magnetic differentiation of atmospheric dusts
Nature 317: 516-518

**O'Reilly, W.,** 1976 Magnetic minerals in the crust of the Earth
Rep. Prog. Phys 39: 857-908

**Overbeck, F. & H. Happach,** 1957 Ueber das wachstum und den Wasserhaushalt einiger Hochmoorsphagnen
Flora 144. Jenna

**Pakarinen, P. & K. Tolonen,** 1971 Comparison between some methods of determining the degree of decomposition of Sphagnum peat
Suo 22: 48-50

**Pakarinen, P. & K. Tolonen,** 1976 Regional survey of heavy metals in peat mosses (Sphagnum)
Ambio 5:1: 38-40

**Pakarinen, P. & K. Tolonen,** 1977a Distribution of lead in Sphagnum fuscum profiles in Finland
Oikos 28:1: 69-73

**Pakarinen, P. & K. Tolonen,** 1977b On the growth rate and dating of surface peat
Suo 28: 19-24

**Pakarinen, P.,** 1978 Distribution of heavy metals in the Sphagnum layer of bog hummocks and hollows
Ann. Bot. Fennici 15: 287-292

**Pakarinen, P.,** 1981a Metal content of ombrotrophic Sphagnum mosses in North West Europe
Ann. Bot. Fennici 18: 281-292

**Pakarinen, P.,** 1981b Regional variation of sulphur concentrations in Sphagnum mosses and Cladonia lichens in Finnish bogs
Ann. Bot. Fennici 18: 275-279

**Pakarinen, P., K. Tolonen, S. Heikkinen & A. Nurmi,** 1983 Accumulation of metals in Finnish raised bogs
In: Environmental Biogeochemistry
Ecol. Bull. 35: 377-382
Ed. R. Hallberg

**Pakarinen, P. & E. Gorham,** 1983 Mineral element composition of Sphagnum fuscum peats collected from Minnesota, Manitoba and Ontario
Proc. Int. Peat Symp. 18pp

**Pennington, W., R.S. Cambray, J.D. Eakins & D.D. Harkness,** 1976 Radionuclide dating of the recent sediments of Blelham Tarn
Freshwater Biol. 6: 317-331

**Peterson, P.J.,** 1978 Lead and vegetation
In: The Biogeochemistry of Lead in the Environment
Ed. J.O. Nriagu

**Ponnamperuma, F.N.,** 1972 The Chemistry of submerged soils
Adv. Agron. 24: 29-96

**Pruppacher, H.R. & J.K. Klett,** 1978 Microphysics of clouds and precipitation
Reidel Publishers

**Puffer, J.H., E.W.B. Russell & M.R. Rampino,** 1980 Distribution and origin of magnetite spherules in air, waters and sediments of the Greater New York city area and the North Atlantic ocean
J. Sed. Pet. 50:1: 247-256

**Puustjärvi, V.,** 1955 On colloidal nature of peat forming mosses
Arch. Soc. "Vanamo" 9 (suppl.): 257-272

**Rasmussen, L.,** 1977 Epiphytic Bryophytes as indicators of the changes in the background levels of airborne metals from 1951-75
Environ. Poll. 14: 37-45

**Reinikainen, A., T. Lindholm & H. Vasander,** 1984 Ecological variation of mire site types in the small kettle-hole mire Heininsuo, southern Finland
Ann. Bot. Fennici 21: 79-101

**Renberg, I. & M. Wik,** 1984 Dating recent lake sediments by soot particle counting
Verh. Internat. Verein. Limnol. 22: 712-718

**Renberg, I. & M. Wik,** 1985 Carbonaceous particles in lake sediments - Pollutants from fossil fuel combustion
Ambio 14:3: 161-163

**Richardson, D.H.S., P.J. Beckett & E. Nieboer,** 1980 Nickel in Lichens, Bryophytes, Fungi and Algae
In: Nickel in the Environment: 367-406
Ed. J. Nriagu

**Richardson, N.,** 1986 The mineral magnetic record in recent ombrotrophic peat synchronised by fine resolution pollen analysis
Phys. Earth & Plan. Int. 42: 48-56

**Robbins, J.A. & D.N. Edgington,** 1975 Determination of recent sedimentation rates in Lake michigan using $^{210}Pb$ and $^{137}Cs$
Geochim. Cosmochim. Acta 39: 285-304

**Rühling, Å. & G. Tyler,** 1968 An ecological approach to the lead problem
Bot. Notiser. 121: 321-342

**Rühling, Å. & G. Tyler,** 1970 Sorption and retention of heavy metals in the woodland moss Hylocomium splendens (Hedw.) Br. et Sch.
Oikos 21: 92-97

**Rühling, Å. & G. Tyler,** 1971 Regional differences in the deposition of heavy metals over Scandinavia
J. Appl. Ecol. 8: 497-507

**Rühling, Å. & G. Tyler,** 1973 Heavy metal deposition in Scandinavia
Water Air & Soil Poll. 2: 445-455

**Rühling, Å. & G. Tyler,** 1984 Recent changes in the deposition of heavy metals in northern Europe
Water Air & Soil Poll. 22: 173-180

**Rummery, T.A.,** 1981 The effects of fire on soil and sediment magnetism
Unpubl. Ph.D., University of Liverpool

**Ruuhijärvi, R.,** 1974 A general description of the oligotrophic lake Pääjärvi, southern Finland, and the ecological studies on it
Ann. Bot. Fennici 11: 95-104

**Salmi, M.,** 1955 Prospecting for bog-covered ore by means of peat investigations
Bull. Comm. Geol. Finlande 169: 5-34

**Sauramo, M.,** 1949 Das dritte Scharnier der fennoskandischen Landhebung
Soc. Sci. Fennici, Arsbok-Vuosikirja 27:4 26pp

**Sauramo, M.,** 1958 Die Geschichte der Oste
Ann. Acad. Sci. Fennicae AIII 51 522pp

**Scoullos, M., F. Oldfield & R. Thompson,** 1979 Magnetic monitoring of marine particulate pollution in the Elefsis Gulf, Greece
Marine Poll. Bull. 10: 287-292

**Sehmel, G.A.,** 1971 Particle diffusivities and deposition velocities over a horizontal smooth surface
J. Colloid. Interface Science 37: 891-906

**Sikora, D.J. & D.R. Keeney,** 1983 Further aspects of soil chemistry under anaerobic conditions
In: Ecosystems of the World 4A
Mires: Swamps, Bog, Fen and Moor. General Studies: 247-256
Ed. A.J.P. Gore

**Sillanpää, M.,** 1972 Distribution of trace elements in peat profiles
Proc. 4th Int. Peat Congress Vol. 5: 185-191

**Stacey, F.D. & S.K. Banerjee,** 1974 The Physical Principles of Rock Magnetism
New York: Elsevier

**Suess, H.E.,** 1955 Radicarbon concentrations in modern wood
Science 122: 415-417

**Swaine, D.J. & R.L. Mitchell,** 1960 Trace-element distribution in soil profiles
J. Soil Sci. 11:2: 347-368

**Takai, Y. & T. Kamura** 1966 The mechanism of reduction in waterlogged paddy soil
Folia Microbiol. 11: 304-313

**Tallis, J.H.,** 1983 Changes in wetland communities
In: Ecosystems of the world 4A
Mires: Swamps, Bog, Fen and Moor. General Studies: 311-347
Ed. A.J.P. Gore

**Tamm, C.O.,** 1953 Growth, yield and nutrition in carpets of a forest moss (Hylocomium splendens)
Meddn St. SkogsforskInst. 43:1: 1-140

**Tanskanen, H.,** 1972 On the vertical distribution of microelements in peat soils
Suo 23: 63-69

**Taylor, F.G. & J.P. Witherspoon,** 1972 Retention of simulated particles by lichens and mosses
Health Phys. 23: 867-869

**Thompson, R., J. Bloemendal, J.A. Dearing, F. Oldfield, T.A. Rummery, J.C. Stober & G.M. Turner,** 1980 Environmental applications of magnetic measurements
Science 207: 481-486

**Thompson, R., R.W. Battarbee, P. O'Sullivan & F. Oldfield,** 1975 Magnetic susceptibility of lake sediments
Limnol. Oceanog. 20: 687-698

**Thompson, R. & F. Oldfield,** (in press) Environmental Magnetism
Allen & Unwin, London

**Tolonen, K.,** 1966 Stratigraphic and rhizopod analyses on an old raised bog, Varrassuo, in Hollola, South Finland
Ann. Bot. Fennici 3: 147-166

**Tolonen, K.,** 1968 On methods used in studies of the peatland development. II. On the peat samplers
Suo 18: 86-92

**Tolonen, K.,** 1973 On the rate and pattern of peat formation during the postglacial time
Suo 24: 83-88

**Tolonen, K. & R. Ruuhijärvi,** 1976 Standard pollen diagrams from the Salpausselkä region of southern Finland
Ann. Bot. Fennici 13: 155-196

**Tolonen, K.,** 1977 On dry matter accumulation and bulk density values in three South Finnish raised bogs
Suo 28: 1-8

**Tolonen, K.,** 1979 Peat as a renewable resource: long term accumulation rates in North European mires
Proc. Int. Symp. Classific. Peat and Peatlands (IPS): 282-296

**Tolonen, K. & L. Saarenmaa,** 1979 The relationship of bulk density to three different measures of the degree of peat humification
Proc. Int. Symp. Classific. Peat and Peatlands (IPS): 227-238

**Tolonen, K.,** 1982 Usefulness of five common methods of determining the degree of decomposition in estimating the amount and energy content of fuel peats in Finland
Suo 33: 133-142

**Tolonen, K., D. Keys, & V. Klemetti,** 1982a Predicting energy content of in situ peats by means of their moisture content and bulk density
Suo 33: 17-24

**Tolonen, K., M. Tiuri, M. Toikka & M. Saarilahti,** 1982b Radiowave probe in assessing the yield of peat and energy in peat deposits in Finland
Suo 33: 105-112

**Tolonen, K.,** 1983 The post-glacial fire record
In: The Role of Fire in Northern Circumpolar Ecosystems: 21-44
Ed. R.W. Wein & D.A. Maclean

**Tolonen, K.,** 1984 Interpretation of changes in the ash content of ombrotrophic peat layers
Bull. Geol. Soc. Finland 56:1-2: 207-219

**Tolonen, K. & F. Oldfield,** in prep. Magnetic measurements from moss increment dated peat cores from Maine, U.S.A.

**Urquhart, C. & A.J.P. Gore,** 1973 The redox characteristics of four peat profiles
Soil Biol. Biochem. 5: 659-672

**Urvas, L., M. Sillanpää & R. Ervio,** 1979 The chemical properties of major peat types in Finland
In: Classification of Peat and Peatlands
Proc. Int. Peat Symp.: 184-189

**Van Craen, M.J., E.A. Denoyer, D.F.S. Natusch & F. Adams,** 1983 Surface enrichment of trace elements in electric steel furnace dust
Environ. Sci. Technol. 17: 435-439

**Vodyunitskiy, Y. N.,** 1981 Formation of ferrimagnets in sod-podsolic soil
Pochvovedeniye 5: 114-122

**Von Post, L. & E. Granlund,** 1926 Sodra sveriges torvtillgangar I.
Sven. Geol. Unders. C 335

**Vuorela, I.,** 1983 Field erosion by wind as indicated by fluctuations in the ash content of Sphagnum peat
Bull. Geol. Soc. Finland 55: 25-33

**Walling, D.E., M.R. Peart, F. Oldfield & R. Thompson,** 1979 Suspended sediment sources identified by magnetic measurements
Nature 281: 110-113

**Walton, E.K.,** 1977 Looking back through time
In: Understanding the Earth: 163-192
Ed. I.G. Gass, P.J. Smith & R.C.L. Wilson

**Weber, C.A.,** 1908 Aufbau und vegetation der moore Norddeutschlands
Englers Bot. Jahrb. 90 (suppl.): 19-34

**Welton, J.E.,** 1984 SEM Petrology Atlas
AAPG Methods in Exploration Series, Vol. 4

**Whitby, K.T.,** 1978 The physical characteristics of sulfur aerosols
Atmos. Environ 12: 135-159

**Wilde, S.A., C.T. Youngberg & J.H. David,** 1950 Changes in the composition of ground water soil fertility, and forest growth produced by the construction and removal of beaverdams
J. Wildlife Manage. 14: 123-128

**Yliroukanen, I.,** 1976 Heavy metal distributions and their significance in Finnish peat bogs
Proc 5th Int. Peat Congress 2: 276-283

## Additional References

Gelting, G. & A. Ponten, 1971 Inst. Plant Ecol., Uppsala (mimeogr. rep.)

Hornburg, P., 1972 4th Int. Peat Congress Vol 1 pp 179-190

Mornsjo, T., 1968 Bot. Not. 121 pp 343-360

Tyler, G., 1971 Proc. 2nd Int. Clean Air Congr., Wash., D.C. p 129